CRANFIELD UNIVERSITY

Nagat M G Almesmari

Natural Vegetation Cover Changes in North-East Libya

School of Water, Energy and Environment
Environment and Agrifood

PhD
Academic Year: 2018 – 2019

Supervisor: Dr Stephen Hallett
Dr Robert Simmons

CRANFIELD UNIVERSITY

School of Water, Energy and Environment

PhD

Academic Year: 2018 - 2019

Nagat M G Almesmari

Natural Vegetation Cover Changes in North-East Libya

Supervisor: Dr Stephen Hallett
Dr Robert Simmons

July-2019

This thesis is submitted in partial fulfilment of the requirements for the degree of PhD

ABSTRACT

The vegetation cover in Al Jabal Al Akhdar has been subjected to human and natural pressures that have contributed to the deterioration and shrinking of the vegetated area. Therefore, the principle goal of this dissertation was to establish and evaluate the changes in the natural vegetation of the Al Jabal Al Akhdar region in the period following the 2011 Libyan uprising. The thesis is comprised of three main objectives; the first is to provide a quantitative assessment of changes in natural vegetation cover over a period from 2004-2016, and identify the consequent impact of human activity; the second is to investigate the impact of climate on the natural vegetation cover; and the third objective is to evaluate the ability of machine learning techniques to predict the natural vegetation cover types.

GIS and remote sensing techniques and Landsat imagery, population MODIS NDVI and climate satellite-based data have been used to achieve these objectives, along with the ancillary data, across 53 sites in the study area. Six classified Landsat image scenes have been used for undertaking a post-classification comparison approach to detect the changes and the types of changes, by the use of image processing, GIS software and spreadsheet, and programme scripts used to detect LULC changes and determine human activities impact. The correlaction between the ANDVI and climate factors for each lanform, and the trends of climate factors and ANDVI for each sites in each landform have been undertaken using statistical analysis package and spreadsheet. Lastly the machine learning ‘J48’ algorithm, within the WEKA tool, was applied on ANDVI, climate data, and spatial characteristics for 53 sites and analysed statistically to test its ability to predict the natural vegetation type.

The main research findings have confirmed that from 2004-2016, natural forest and rangelands decreased by 71,543 ha or 7.10% of the total area as a result of urbanisation and agricultural expansion. Human activities have had more impact than climate impact on LULC changes. The machine learning classifier decision tree ‘J48’ algorithm was also found to have the ability to classify and predict the natural vegetation cover type.

Finally, an evaluation was undertaken of the current distribution of natural vegetation cover, and a forecast of future changes, utilising high-resolution imagery is recommended. A conclusion considers how developing action plans using tools such as those described to manage and protect the natural vegetation cover are highly recommended.

Keywords:

Post-classification comparison, Land use cover change, J48 algorithm, MODIS NDVI, Urbanisation, Al Jabal Al Akhdar

ACKNOWLEDGEMENTS

All praise and thanks are to Allah the Almighty, for giving me the health, strength, and patience to finish my study.

My great thanks go to my mother, Khairia M Ahmed, who without her Du'a (Prayers), I did not finish my studies, as her Du’a was always accepted. Also, I would like to thank my brothers and sisters for supporting my decision to study in the UK, which was an enjoyable, valuable experience for me.

I would like to express my deep and sincere gratitude to my supervisor Dr Stephen Hallett, and Dr Robert Simmons for their help, advice, and encouragement, in addition to their patience and unwavering belief in my ability to accomplish this work.

I would like to thank Mrs Elizabeth Hallett for her valuable comments those greatly improved the manuscript. Also my thanks to all my colleagues and staff member of the Faculty of Natural Resources and Environmental Science for their scientific support.

Finally, my thanks also go to Libyan Education Ministry and Omer Al-Mukhtar University for financial support to pursue my education in the UK.

TABLE OF CONTENTS

LIST OF FIGURES

LIST OF TABLES

LIST OF EQUATIONS

LIST OF ABBREVIATIONS

3rd GPP	Third-Generation Project of planning
a.s.l.	Altitude 'Above Sea Level' (m)
AA	Agricultural Areas
ACSAD	The Arab Centre for the Studies of Arid Zones
API	Application Programming Interface
ARFF	Attribute-Relation File Format
BA	Built-up Areas
B-distance	Bhattacharyya distance
BSC-L	Bureau of Statistics and Census-Libya
$CaCO_3$	Calcium Carbonate
CEC	Cation Exchange Capacity
CHRS RainSphere	Hydrometeorology and Remote Sensing University of California
CRU	Climate Research Unit
CRU-TS	Climate Research Unit Time Series
CSV	Comma-Separated Values
D	Divergence
DEM	Digital Elevation Model
EC	Electrical Conductivity (dS m^{-1})
ENVI	Environment for Visualizing Images (An image processing software)
ESP	Exchangeable Sodium Percentage
FLAASH	Fast Line-of-sight Atmospheric Analysis of Spectral Hypercubes
GCMon	Global Climate Monitor
GE	Google Earth
GEE	Google Earth Engine
GIS	Geographical Information System
IDE	Integrated Development Environment

IDW	Inverse Distance Weighting
IN	Infrastructure
JM	Jeffreys-Matusita Distance
KML	Keyhole Markup Language
L1T	level One Train Correction
LNMC	Libyan National Meteorological Centre
LSWIR	Longer Shortwave Infrared
LULC	Land Use Land Cover
LUPA	Libyan Urban Planning Agency
LWGA	Libyan Water General Authority
MCC	Mathews Correlation Coefficient
MDC	Minimum Distance Classifier
MLC	Maximum Likelihood Classifier
MLS	Mid-Latitude Summer
MODIS	The Moderate Resolution Imaging Spectroradiometer
NDVI	Normalised Difference Vegetation Index
NF	Natural Forest
NIR	Near-Infrared
NOAA	National Oceanic and Atmospheric Administration
NV	Non-Vegetated areas
OLI	Operational Land Imager
OM	Organic Matter
OMU	Omer Al-Mukhtar University
PCC	Post-classification comparison
PF	Planted Forest
PNG	Portable Network Graphic
RL	Rangelands
ROC	Receiver Operating Characteristic
ROI	Region Of Interest
RPC	Precision-Recall

SAR	Sodium Adsorption Ratio
SOTER	Soils terrain digital databases
TAMSAT	Meteorology using Satellite data and ground-based observations
TD	Transformed Divergence
TDS	Total Dissolved Solids
TIRS	Thermal Infrared Sensor
TM	Thematic Mapper
UNCCD	United Nations Convention to Combat Desertification
USDA	United States Department of Agriculture
UTM	Universal Transverse Mercator
VIs	Vegetation Indices
WEKA	Waikato Environment for Knowledge Analysis
WGS	World Geodetic System

1 INTRODUCTION

This chapter reviews the importance of this research. The sections of this chapter in sequence illustrate brief information of the changes in terrestrial ecosystems as a background and explain the issues prevalent in the study area region. It closes with the aim and objectives of this research and the thesis structure.

Natural vegetation is one of the most critical environmental components and plays a significant role in preserving the ecological balance. It includes all plants from forests, grasses, algae, large or small wild plants, trees and shrubs that have grown spontaneously without human intervention. Degradation of vegetation is one of the key environmental problems globally as a result of the imbalance between humans and the environment. With population growth and technological progress, the demand for natural environmental resources has increased, leading to depletion and destruction of ecosystems. Overgrazing, logging in a passive, random and unorganised manner in forests, over exploitation of ecosystem services, and climate change, are not only a local or regional problem but a global phenomenon that must be taken into consideration to prevent degradation. This chapter reviews the importance of this research, wherein sequence the sections will discuss, in brief, the changes in terrestrial ecosystems as a background as well as the specific problems and challenges in the study area of this research. Finally, this section concludes with a discussion of the research aim and objectives.

1.1 Background and Context

Land use and land cover (LULC) are combined units of the resource base (Di-Gregorio, 2005). Land cover is the reflection of human activities, so any changes in their activity lead to changes in it. The changes in LULC can affect the ecosystems globally or locally. Globally, when fluid system such as atmosphere, climate and sea level influenced by LULC changes leading to

degradation of biodiversity, soil, and water sources (Meyer and Turner II, 1992). Locally, occurs when land cover and land use changes are sufficient to have significant impacts on local areas (Meyer and Turner II, 1992). Land cover is a geographical feature that can be used as a reference base for several applications ranging from management techniques that are used for monitoring forest and rangeland, to biodiversity, climate change and desertification control. (Di-Gregorio, 2005). Terrestrial vegetation plays a vital role in environmental balance where it contributes to many biogeochemical cycles such as water, carbon and nitrogen cycles, climate maintenance and mitigation of climate change. It is also subject to change as a result of natural cycles and trends such as the increase in CO_2 as well as human activities (Matthews, 1983).

Human activity exerts a visible impact on global vegetation distribution (Wang et al., 2006), through conversions or degradation of 30-50% of the land surface from forest to crop cultivation and/or urban-industrial areas (Vitousek et al., 1997). Globally, vegetation is influenced by land transformation where the increase in human demand or management have generated persistent alterations in land cover (e.g., from forest to agriculture). Despite the impact of natural disturbances on vegetation such as fires, floods, drought and pests, these typically do not make any change on their vegetation community composition, and they commonly recover after the disturbance (Wang et al., 2006). This is not the case following the impact of human activities.

North Africa, on the Southern Mediterranean Basin, is located in a semi-arid, arid and hyper-arid bioclimatic zone (NIC, 2009; Price, 2017), characterised by annual and seasonal drying/warming (Niang et al., 2014), and water scarcity (rainfall < 300 mm yr^{-1} and below 1000 m^3 $capita^{-1}$ yr^{-1} for renewable surface water and groundwater resources) (Price, 2017). It also has a high population growth rate (2.9% for the period 1990-2002) (Boko et al., 2007), which contributes to increasing pressure on natural vegetation and associated ecosystems. Climate change has also become a key factor in driving vegetation cover change. The most direct and immediate consequence of climate change is wildfires, with other effects including, for example, extended periods of

drought and extreme meteorological phenomena such as heat waves and strong winds (FAO, 2011c). Therefore, monitoring the natural vegetation cover and understanding the reasons for change represents a critical requirement in its protection and conservation. For this research, a case study area is drawn from among the five countries in North Africa, from Libya, and particularly from the Al Jabal Al Akhdar region.

1.2 **Research Problem**

The coastal region of Al Jabal Al Akhdar has always been important in the development of society, not only in Libya but also in other surrounding Mediterranean countries. For example, historical evidence reveals how Al Jabal Al Akhdar flourished during the Greek and Roman eras (Apendix Figure A.1.1 and Figure A.1.2) when various foodstuffs were exported from their cities, especially during the Greek famine period (El-Barasi and Saaed, 2013). The present-day remains of the wells, cisterns, dykes, irrigation canals and olive oil mills provide evidence of the extensive human activities during those periods (Hamad, 2012). These have continued through different successive eras including the Arab, Ottoman, and Italian occupation to the second half of the 20th century, and have all influenced the land cover and land use (El-Barasi and Saaed, 2013).

The vegetation in Al Jabal Al Akhdar has been subjected to many human and natural pressures, contributing to the deterioration and shrinking of the vegetated area. Fire is an old phenomenon of change in this region and clearing land for cultivation by burning is considered to be the main reason for this. Extensive fires occurred in 1923, 1956, 1987, 2001 and 2013 in Ras'Helal, which is located northeast of the study area of the current study, (Zatout and Soliman, 2014) with consequent impacts on land cover. Furthermore, fires have eliminated some 7,500 ha of forest, as the average annual statistics reveal from 1986 to 2003 (Afhima et al., 2008).

Agriculture, grazing and charcoal production are practiced by 53%, 37% and 6% of the local communities, respectively. These are the economic activities affecting the land and natural vegetation cover in Al Jabal Al Akhdar (OMU,

2005). The important species that are affected by those activites are Arbutus pavarii Pamp. “Libyan Strawberry-tree”, Pistacia lentiscus L. “Mastic tree” and Ceratonia siliqua L. “Carob”. Besides urbanisation pressures, the collection of medicinal and aromatic plant species at a commercial scale is also significant locally, with annual sales being estimated at more than one million Libyan dinars (c. GBP £500,000). Moreover, increases in all these pressures on the natural vegetation have been occurring as the Libyan state does not exert its right to ownership of forests and grasslands in the region even though it owns 56% of the land. A significant portion of these lands was also taken illegally by tribes or clans or individuals to enlarge their farms (Afhima et al., 2008). This behaviour increased after the 2011 Libyan uprising that resulted in of the abundance of weapons and the absence of authorities (El Shatshat, 2015).

There is a need to develop applied and verifiable techniques to guide land management in this region, to conserve and protect the fragile environment, and to understand the interplay of the factors leading to change; novel tools are required to support this. In Al Jabal Al Akhdar, the application of Remote Sensing (RS) and Geographical Information System (GIS) technology which can be used to assess the status of the natural vegetation cover, can determine optimal future land cover management planning and offer valuable management tools. Methods used here can be applied for similar environments in Libya and the wider North Africa region.

1.3 **Aim and Objectives**

The overarching research aim of this study is: “*to establish and evaluate the changes in the natural vegetation of the Al Jabal Al Akhdar region following the 2011 Libyan uprising”*. This aim is achieved through the definition of the drivers and pressures, and the major effects of these exerted on the natural vegetation cover and the identification of the type and rate of the changes in the vegetation cover in the Al Jabal Al Akhdar region. The aim of this study is accomplished through the following four interlinked objectives:

1. Assess and evaluate changes in natural vegetation cover over the period from 2004 to 2016.

2. Identify and characterise the impacts of human activities on the natural vegetation cover in Al Jabal Al Akhdar.
3. To investigate and quantify the impact of climate on the natural vegetation cover in Al Jabal Al Akhdar.
4. To evaluate the ability of machine learning to predict the natural vegetation cover types in Al Jabal al Akhdar

1.4 **Research hypotheses**

These objectives are accompanied by the following explicit hypotheses that can be tested and evaluated:

1. "Natural vegetation cover has been in decline from 2004 to 2016."
2. **"**Human activities have exerted a significant effect on the changes in Al Jabal Al Akhdar natural vegetation cover."
3. **"**The natural vegetation cover in Al Jabal Al Akhdar has been affected by the climate over the period from 2004-2016."
4. "Natural vegetation cover types in Al Jabal Al Akhdar can be predicted by using "machine learning".

1.5 **Research questions**

To complement the objectives and hypotheses, the research was guided by four specific research questions;

1. Has the natural vegetation cover of the Al Jabal Al Akhdar changed over the period 2004 to 2016, and if so, how?
2. Have human activities influenced the natural vegetation cover of the Al Jabal Al Akhdar?
3. Is there any discernible impact of climate on natural vegetation cover in the Al Jabal Al Akhdar region over the period from 2004-2016?
4. Is it possible to predict the natural vegetation cover type based on location properties using machine learning?

1.6 **Thesis Structure**

This thesis contains seven chapters. Chapter One introduces the subject of the research by providing background and context, highlighting the research

problems, its aim and objectives, as well as its research hypotheses and research questions. Chapter Two presents a wide-ranging review of the relevant literature, including an overview of land degradation, and an assessment of the vegetation of the Mediterranean Basin, and specifically within the study area. The research context in Chapter Three provides a background of the Al Jabal Al Akhdar region, as well as detailed information from a botanical survey conducted by Omer Al-Mukhtar University which has been used as baseline dataset in this research. Chapter Four illustrates the research methodology, including quantitative data collection methods, the data sources, image processing and LULC image production, detection of changes, population impacts, and climate impacts. Chapter Five displays the results of images classification, change detection, NDVI trends, human activity impacts, climate element trends and climate impacts. The research results and outcomes are discussed in Chapter Six. Finally, Chapter Seven provides conclusions and recommendations

2 LITERATURE REVIEW

This chapter reviews the academic literature concerning land degradation, the vegetation of the Mediterranean-type ecosystem, the vegetation Al Jabal Al Akhdar, and the Area of interest with the provision of the common species found in the area.

This chapter presents a literature review in three thematic sections. The first section considers the definitions and causes of land degradation. The second section sheds light on the vegetation associated with Mediterranean-type ecosystems and is divided into two sub-sections; the first considers the vegetation of the Mediterranean basin, and the second considers vegetation communities associated with the study area, Al Jabal Al Akhdar.

2.1 LAND DEGRADATION

Land degradation is an environmental issue threatening the quality of a given vegetation community. Over 33% of the world's land surface is susceptible to land degradation (WMO, 2005; Ioras et al., 2014; ELD Initiative and UNEP, 2015). In natural ecosystems, plant communities are in a continual process of dynamic change, leading to the development of plant community succession. Such dynamics reveal the influence of both endogenous or exogenous factors (Penny et al., 2013). The dynamics of plant communities also occur over a range of temporal scales (Knapp, 1974). This process may also be regressive from the climax, due to some land use and management practices such as grazing, cultivating, logging or fire (Kuchler, 1988).

Natural vegetation cover can be subject to degradation, which can lead to changes in environmental equilibrium (Baartman et al., 2007), climate (Betts et al., 2008) and soil properties (Abdi et al., 2013; Masoudi and Amiri, 2013). Land degradation also has an adverse impact on the efficient use of rainwater

decreasing the portion of the rain that is used effectively by vegetation (Stroosnijder, 2003), due to the degradation of soil properties and erosion. Land degradation can lead to a decline in water infiltration, soil water holding capacity and transpiration, hence an increase in runoff and soil evaporation (Stroosnijder, 2007; Cornelis et al., 2012) and a decrease in the efficient use of green water (i.e. the ratio of transpiration to precipitation) (Stroosnijder, 2007). Bosch & Hewlett (1982) and Zhao et al. (2009) studied the relationship between the changes in water yield and vegetation cover, reporting that afforestation led to an increase in groundwater yield and a decrease in runoff. Bosch & Hewlett (1982) reviewed 94 catchment experiments conducted in different countries and across various rainfall ranges within a number of broad categories of vegetation types. The study revealed that water yield would decrease or increase annually according to a respective increase or decrease in vegetation cover, respectively. Similarly, Zhao et al. (2009) applied a dynamic water balance model to a range of spatial scale catchments selected from Australia and South Africa at a yearly time scale. The results showed an increased streamflow after deforestation and decreased streamflow following afforestation.

2.1.1 Definitions

The United Nations Convention to Combat Desertification (UNCCD) (1994) refers to land as “the terrestrial bio-productive system that comprises soil, vegetation, other biotas, as well as the ecological and hydrological processes that operate within this system”. These components (i.e. vegetation, soil, water) are subject to the world environmental issue, degradation (Foley et al., 2005). Land degradation was defined as “a decrease in the capacity of the environment as managed to meet its user demands” (Baartman et al., 2007). Bai et al., (2008) suggested that land degradation may be defined as “a long-term decline in ecosystem function and productivity caused by disturbances from which land cannot recover unaided”.

Land degradation in arid, semi-arid and dry sub-humid areas, resulting from various factors, including climatic variations and human activitiesis known as

desertification (Kassas, 1995). The definition excludes hyper-arid zones, which are the true deserts (FAO, 2011a).

Land degradation also described as “a decrease or loss of the biological or economic productivity of cropland (rain-fed, irrigated), or rangeland, pasture, forest, and woodlands, that occur because of land uses or human activities and habitation patterns or the combination of processes such as: (i) soil erosion resulting from wind and/or water; (ii) degeneration of the physical, chemical, and biological or economic properties of soil; (iii) long-term loss of natural vegetation” (UNCCD, 1994; WMO, 2005; Sivakumar, 2007; FAO, 2011a). Kassas (1995) reported that land degradation occurs widely, in drylands and humid lands; while desertification is attributed to the degradation of drylands. This statement was confirmed by Baartman et al. (2007), who noted that desertification could be considered as “a particular type of land degradation occurring mainly, but not exclusively, in dryland regions”.

The FAO (2011a) categorised three types of land degradation, namely: soil degradation; vegetation degradation; and water resources degradation. However, the same report further noted that most considerations over the previous 20 years had focused on soil and water degradation. In addition, FAO (2011a) also documented features that can be used to detect vegetation degradation using six indicators, namely: vegetation cover change; vegetation structure and plant community composition change; habitat and species diversity change; indicator species abundance change; vegetation health and biomass change; and vegetation management and the impacts of using its production.

Johnson and Lewis (2007) further defined land degradation as “the substantial decrease in either or both of an area’s biological productivity, or usefulness due to human activities”. The FAO (2013) also defined degradation as “a long term loss of ecosystem functions over time, as perceived by the land users”. In addition, a recent definition of the UNCCD describes land degradation as “any reduction or loss in the biological or economic productive capacity of the land resource base”, noting that “it is widely accepted that land degradation is

caused by human activities, exacerbated by natural processes, and often magnified by and closely intertwined with climate change and biodiversity loss" (ELD Initiative and UNEP, 2015).

For the purpose of this research, vegetation degradation as a type of land degradation is occurring when the available biomass decreases leading to a decrease in the vegetation cover (Masoudi, 2014) and its diversity and/or the economic value. According to the FAO (2011a) vegetation degradation involves "a reduction in the quantity through a decrease in vegetation ground cover and vegetation biomass; and a decline in the measurable quality of the vegetation biomass where the high-value species in terms of their economic value are replaced by the low-value species and/or the impact on their health due to overcutting specific parts of the plant (for timber, fuelwood, fodder, fruits, food, medicine)". Masoudi & Amiri (2013) and Masoudi (2014) noted the definition of vegetation degradation according to FAO/UNEP (1984) as being "either the temporary or permanent reduction in the density, structure, species composition or productivity of vegetation cover". Moreover, deforestation refers to "the clearance of forest for agriculture or other purposes." The land degradation considered in this study, therefore, refers to the decrease in natural vegetation cover which in turn could reflect the changes in vegetation community composition because of the deforestation in order to use the natural vegetation land for agriculture or development purposes.

2.1.2 The causes of land degradation

A key importance of terrestrial vegetation is its role in the radiation equilibrium of the earth and in the several biogeochemical cycles related to climate maintenance and climate change. Natural processes and trends such as global warming and wildfire, and human activities such as land use change, overgrazing, and urban expansion, could influence vegetation patterns by their modification (Matthews, 1983).

Franklin et al. (2016) reported that global alterations such as global warming, changed disturbance regimes (e.g. natural fire regimes) and that changes in

land use could be caused by increases in the % CO_2 and other gases resulting from human activities. Franklin et al. (2016) also stated that the disruption of services provided by ecosystems could be expected to result in consequent impacts and global changes on terrestrial plant communities. These impacts include ecosystem services such as the effect on climate regulation, water balance and forest products. Vitousek et al. (1997) also explained that human activities contributed to changes in 30-50% of the global land surface, biological resources (such as species and genetically distinct communities), and altering global vegetation distribution by changes in land use, through permanent changes in land cover due to human demands and management, for instance, shifts in afforested lands to agricultural production.

In the Mediterranean Basin, the spatial patterns and distribution of natural vegetation can be related to past human activities and their disturbances (Mazzoleni et al., 2005); where the land has been exposed to several processes including grazing, burning and cutting (Di-Pasquale et al., 2005). Historically, such activities have led to the composition of Mediterranean vegetation being replaced with evergreen forests and by 'anthropogenous vegetation types'. These include 'Maquis', which is a shrubland biome in the Mediterranean region, consisting typically of densely growing evergreen shrubs. These include *Arbutus unedo*, *Pistacia lentiscus* 'the lentisc', *Olea europaea* 'the wild olive', Myrtus communis 'the myrtle', or *Juniperus* 'juniper' (Sundseth, 2009) (see Section 2.2.1.2). 'Garrigue', an open shrubby vegetation of dry Mediterranean regions, consisting of spiny or aromatic dwarf shrubs interspersed with colourful ephemeral species contain mainly Rosmarinus 'rosemary, Salvia 'sage' and Thymus 'thyme' (Sundseth, 2009) (see Section 2.2.1.1), and weed-communities of annual plants on cultivated areas (Pignatti, 1978). In this section, the factors that may lead to degradation of land and vegetation are discussed in the following sub-sections.

2.1.2.1 Climate

As a result of global warming, the increase in temperature in some Mediterranean countries, from 1971 to 2000, was 1.53 ºC (FAO, 2011c). Further to this, during the 20th century, an increase in temperature of about 0.7°C was recorded over the majority of Africa (Desanker et al., 2001). Additionally, some regions located in North Africa, specifically those areas north of the Atlas Mountains comprising the coastal regions of Algeria and Tunisia, have been subject to a noted decline in the quantity of rainfall during the winter (December-February), and the beginning of spring (March-April) (Niang et al., 2014). This decrease in rainfall is estimated to be by some 5 –15% (Terink et al., 2013). Furthermore, in the mid-21st century, the majority of countries located in the Mediterranean region of the Middle East and North Africa (MENA) region, are expected to experience a decrease in annual rainfall of a further 15-20% for the future period (2020-2050). (Terink et al., 2013). An analysis of 900 years (1100-2012) of the Mediterranean drought variability shows important east-west coherence over the basin on multidecadal to centennial timescales and north-south antiphasing in the eastern Mediterranean. The centre of the recent droughts are in the western Mediterranean, Greece, and the Levant, and the driest period is recorded in the current 15-year drought (1980-2012) in the Levant (Cook et al., 2016).

Vegetation distribution and soil formation are related to the climate, being determined particularly by rainfall and temperature (WMO, 2005). These factors also affect vegetation production, particularly in rangelands, where vegetation cover becomes discontinuous with the decline in annual rainfall (WMO, 2005). Vicente-Serrano et al. (2012) studied the impact of the incremental increases in climate aridity, which is a permanent climate characteristic and limited to low rainfall areas (Mishra and Singh, 2010), on the reduction in vegetation cover in the northeast Iberian Peninsula, Spain. They noted that decreased vegetation cover occurred during the dry season, an effect found to be more pronounced in those areas suffering from water shortage. They also asserted that inappropriate land practice and management in the past, together with global warming, had contributed to accelerating this degradation.

Niang et al. (2014) noted that the future effect of climate change on the availability of water would be less than other factors (i.e. population growth, urbanisation, agricultural expansion, and land use change). Despite this fact, Niang et al. (2014) reported that North Africa would be subject to an increased water deficit and consequent drought risk. In the arid zone of Tunisia, Ben Salem et al. (2009) evaluated the effects of human activities on natural vegetation cover during autumn 2005 and spring 2006 at four locations using a quadrat-point method. The sites selected varied through their location, elevation, soil substratum and degree of disturbance. Two locations are characterised by a loamy substratum: the first one is dominated by *Stipa tenacissima* L. 'Halfah grass', *Rosmarinus officinalis* L. 'Rosemary', and *Genista microcephala '*Coss'., while the second is dominated by *Stipa tenacissima* L. The substratum of the third is gypsum and dominated by *Stipa tenacissima* L. and *Rosmarinus officinalis* L. Calcaro-gypsum is the substratum of the fourth site, being dominated by *Stipa tenacissima* L. and *Gymnocarpa decander* 'Forsk'. Total vegetation cover and plant density are used as ecological indicators to assess degradation. The main findings indicate that plant cover is affected by climatic drought, annual plants being more abundant when climate conditions were suitable (i.e. in spring). The results revealed that older plants appear to be more vulnerable to drought than the young plants.

In Libya, significant increases in the mean annual minimum temperature during the period from 1978 to 2009 were reported by Ageena et al. (2013), which were 56-67% in summer and 50-67% in autumn. Further to this, Ageena et al. (2014) reported an increase in maximum (0.017°C yr^{-1}) and mean average temperatures (0.021°C yr^{-1}) over the period (1945-2009). A statistical analysis of climatic time series concluded by Zeleňáková et al. (2014), showed that, in Libya, the trend in rainfall has declined significantly, and temperatures have risen significantly in the last 40 years (1971-2010). Therefore, the risk of drought is growing in the country, with geographical analysis illustrating that the parts most significantly affected by drought are in the south, east and the west.

Studies conducted by OMU (2005), El-Barasi and Saaed (2013) and Elshatshat and Mansour (2014) noted tree die-back, with dry branches observed on numerous trees. This phenomenon involved *Juniperus phoenicia* L. 'Phoenicean juniper' (more than 90% (Elshatshat and Mansour, 2014)), *Pinus helepensis* Mill. 'Aleppo pine', *Olea europaea* L. 'European olive' observed in the whole of Al Jabal Al Akhdar, in northeast Libya. The results of those studies attributed the reasons for this phenomenon to climate change over the last 40 years; however, El-Barasi and Saaed (2013) reported that the new generation of these species is healthy.

2.1.2.2 Fire

Terrestrial vegetation has been subject to fire since ancient eras, where some fossil coal and ash layers relevant to the Mesozoic era confirm that vegetation fires had occurred (Di-Pasquale et al., 2005). Furthermore, during dry seasons, the fire risk is increased, particularly in the Mediterranean basin, due to many factors, including land mismanagement and global warming (Barbati et al., 2010). Moreover, in the case of the management of forest fires, changes in fire regime arising from human activities could make preventing the influences of the fires on biodiversity and ecosystem more difficult (Noss et al., 2006). Fires are considered a major factor leading to disturbance of forest ecosystems (Di-Pasquale, Di Martino and Mazzoleni, 2005; Benyon and Lane, 2013), with direct impacts on plant community structure (Malkisnon et al., 2011).

The area of forest and rural lands burning every year in Europe because of wildfires is estimated to be half a million ha (Barbati et al., 2010). In the Mediterranean basin, more than 4 million ha were burned during 1995 and 2004 (Barbati et al., 2010). In Libya, El-Barasi and Saaed (2013) reported that the average of *circa* 100 fires per annum occurred in the Al Jabal Al Akhdar region during the period from 1986 to 2003, damaging 8,975 ha yr^{-1} (2.8% of the total natural vegetation in the region). They suggest that this number of fires is abnormal, referring to human activities that have been responsible for > 90% of fires in the region. Moreover, between 1986 and 2003, the number of wildfires was reported as 1,991 through several parts in Al Jabal Al Akhdar, including

Ras Al Hilal. This resulted in the burning of approximately 161,533 ha of a mixed forest of *Arbutus pavarii* Pamp. 'Libyan Strawberry-tree', *Pinus halepensis* Mill., *Quercus coccifera* L. 'Kermes oak', *Juniperus phoenicea* L., *Olea europaea* L., *Ceratonia siliqua* L. 'Carob tree' and *Pistacia lentiscus* L. 'Mastic tree' (El-Barasi and Saaed, 2013).

Zavala and Celis (2014) explained that the severe decrease in vegetation cover over a short period (hours, days or months) is attributed to the impact of fire on soils which increases soil erosion risk. As a result of fire frequency in the Mediterranean-type climates, regional flora has adapted to fire, showing different ways of re-growth, which depended on the plant morpholgy and its reproductive strategy (Bradshaw et al., 2011; Zavala and Celis, 2014). For example, Crosti et al. (2006) reported that, due to the recurrence of wildfires in the Mediterranean Basin, several species re-sprout after the fire, such as *Quercus coccifera, Pistacia lentiscus, Brachypodium , Rhamnus spp and Arbutus* (Pausas, 1999). These plants are found in the study area. In contrast, seed germination of several species, belong to the Mediterranean-type vegetation found in Western Australia, California and South Africa, is increased due to fires such as *Cistus incanus* and *C. vitalba* (Crosti et al., 2006). Pausas (1999) also reported that seeds of *Cistus* spp. and *Pinus* spp. can germinate after fire (both genera are found in the study area).

Further, in Australia, the majority of trees have the ability to sprout from stem buds and so recover from fires in a short time (Pausas, 1999). The successional phases after the fire, starting with 'short-life herbaceous plants' associated with resprouting shrubs, which have the ability to grow rapidly in the first years. After 5 years, the growth rate of the herbaceous vegetation has declined (Zavala and Celis, 2014). Since the natural vegetation in the Al Jabal Al Akhdar, (study area), belongs to the Mediterranean-Type (see Section 2.2.1.2), therefore, such successional phases can be expected to occur.

Benyon and Lane (2013) investigated the impact of wildfire on forest hydrology in a Eucalyptus forest suffering from different classes of fire severity in Australia. They found that the catchment water yields vary depending on the

density of plant regeneration 2 years after the fire, where the high seedling density results in a decline in catchment yield.

In Libya, Zatout and Soliman (2014) reported that differences in the above-ground plant diversity, between burnt and unburnt forest subjected to the 1996 fire in the Ras Al-Hila forest in Al Jabal Al Akhdar, were not observed. El-Barasi and Saaed (2013), however, highlighted the negative influences of fires, with the loss of some species, being unable to regenerate after fire damage, such as *Juniperus phoenicea*, and changes in the structure and composition of vegetation communities. In contrast, an increase in some species such as *Querecus coccifera*, *Rosmarinus officinalis*, *Arbutus pavarii* and *Pinus halepensis* was observed.

2.1.2.3 Land use/ land cover changes

Globally, vegetation has been affected through land use conversion when human pressures or management have caused persistent alterations in land cover such as the conversion of natural forest to agriculture. Data arising from Ramankutty and Foley (1999) indicated that some 13% of the global land surface had been converted to permanent crop agriculture by 1992 (Wang et al., 2006). Wang et al. (2006) reported that, based on most predictions for the global economy and population growth, land use change is tending to continue swiftly. They compared the impact of human activities on land use changes and the same effect of fire as a natural factor. They noted that significant effects on land use occurred by anthropogenic activities; while in fire events, the components of the vegetation did not change, and they restore naturally after fire disturbance. A preliminary study conducted by Kim et al. (2014) investigated changes in forest cover globally from 1990 to 2000. The study showed that the forest cover changes in temperate and tropic zones have significant impacts on the current land use and land use changes, respectively.

Niang et al. (2014) reviewed the distribution and changing of all classes of terrestrial ecosystems in Africa. The study covered deserts, grasslands, shrublands, savannas, woodlands, and forests. The findings indicate three main trends at the continental scale, as follows:

1. A small overall expansion of desert and reduction of the total vegetated area;
2. A sharp increase in the rate of human impact on the vegetated areas, associated with a decline of the natural vegetation;
3. A complex set of shifts in the spatial distribution of the remaining natural vegetation types, with net decreases in woody vegetation in western Africa and net increases in woody vegetation in central, eastern, and southern Africa.

McGregor et al. (2009) reviewed land use in North Africa, and in particular southern Morocco over the last 2000 years. The history of land degradation showed that the changes in land use in southern Morocco might have led to a decline in deciduous and evergreen oak. The historical evidence also showed that the cultivation of olives and the native argan tree had been expanded, and the Australian eucalyptus trees had been introduced.

In North-Eastern Libya, several factors have been considered by El-Barasi and Saaed (2013) as representing the key causes of land cover degradation in the Al Jabal Al Akhdar region. These factors include: population growth; overgrazing of natural vegetation, by sheep, goats, cattle, and camels; the uprooting of woody species for use as fuel or for medicinal purposes; ploughing land for cereal production; infrastructure development; disposal of solid and liquid wastes; mining, and mismanagement of forest and rangelands. Elshatshat and Mansour (2014) reported that some activities were being practised illegally, including, illegal charcoal-burning, tree felling and collection of medicinal plants at a commercial scale. Abdalrahman et al. (2010) investigated the direct effects of human activity, particularly overgrazing and agricultural practice, on land degradation. The study was undertaken in Omar Al-Mukhtar, Marawa and Gandolla, located in Al Jabal Al Akhdar region (included in the study area). The results highlight the role of human activities on vegetation degradation such a clear-cutting and loss of diversity. The results also showed that the primary traditional activities were agriculture and grazing, both of which impacted negatively on the landscape. The findings also showed

that areas of Omar Al-Mukhtar and Marawa suffered from overgrazing, while the chief factor in Gandolla was inappropriate agricultural practices of intensive cropping, improper use of irrigation water, and misuse of agrochemicals.

Several studies have been conducted by El-Barasi et al. (2013) to examine land degradation, and to classify and assess plants in an area of approximately 1,800 km^2, located in south Al Jabal Al Akhdar. Harch climatic conditions in this area reflected the degradation state and controlled land productivity. The interaction between human activities and these factors resulted iv its degraded state with regards its productivity (i.e. low biomass productivity), succession (i.e. retrogressive succession), soil erosion, and sand encroachment from the desert to the south.

Elshatshat (2015) stated that a key indicator to determine the degraded status of a botanical cover is the type of land use. Humans and their activities exert a significant negative impact on vegetation composition in an area extending from El-Bakor road to the end of Ras El Helal. The study highlighted that the seed bank of the annual species of natural vegetation was destroyed as a result of shifting the land to crops. The seed bank was also mixed with the seed of the crops that grow after rainfall leading to damage to the seedlings of native annual species.

2.1.2.4 Overgrazing

Grazing in rangeland is a natural method of accessing palatable fodder; it is also considered to be a more suitable, low-cost means of meat production (Czeglédi and Radácsi, 2005). Fernández-Lugo et al. (2013) studied the impacts of different grazing systems on vegetation structure in Anaga Rural Park, in the northeast sector of the island of Tenerife, Canary Islands. The climate of the area is the Mediterranean with mean annual temperature is ca. 15 °C, and mean annual precipitation is 425 mm. The results revealed an insignificant effect of grazing on the species composition among three grazing systems. Grazing caused an increase in species richness and insignificant changes in the frequency of bare soil or native and endemic species.

Han (2008) described overgrazing as the condition of rangeland when the livestock density is above the carrying capacity of the rangeland, which occurs when grazing rates exceed the vegetation production rates (Rowntree et al., 2004). Rangeland productivity can be explained by forage availability that can be determined through the analysis of some biophysical parameters such as rainfall distribution and land cover (Fajji et al., 2018). Therefore, overgrazing affects the flora negatively by decreasing numbers of grazing-sensitive shrubs and palatable species, which are unable to recover, or by increasing exotic species (Fernández-Lugo et al., 2013).

Wang (2014) studied the impacts of overgrazing on the properties of the soil, in eastern Hovsgol, Mongolia. They established that overgrazing led to declining soil fertility, changes in soil chemical properties, where soil organic matter, exchangeable calcium and nitrate nitrogen content are lower as compared with non-grazing areas. The results also show changes in soil water physical properties such as temperature, moisture, bulk density, and particle density, rising topsoil temperatures, and decreasing moisture content. Wang (2014) also observed increasing topsoil density due to trampling, leading to increases in bulk and particle density. On the other hand, Kairis et al. (2015) reported that changes in soil properties and moisture and decreasing in vegetation cover led to soil erosion, particularly in the dry regions of the Mediterranean. The climate is dry sub-humid with an average annual temperature is 15.4°C, the average annual precipitation is 900 mm, and annual reference evapotranspiration ranges between 1250 and 1430 mm. Such a study can be considered when comparing with the condition of the rangelands in the study area.

In Morocco, due to recorded increases in pollen from the genus of *Cichorioideae*, *Plantago*, and *Artemisia*, including various weedy species McGregor et al. (2009) noted that the vegetation structure could be changed as a result of livestock pressure. They also suggested that goats play a role in erosion and overgrazing, causing a decrease in deciduous and evergreen oaks.

In the Al Jabal Al Akhdar, Libya, (Marawa, Gandolla, and Omar Al- Mukhtar those located within the study area), overgrazing has caused a decrease and loss of vegetation composition and diversity (Abdalrahman et al., 2010). The number of livestock (sheep, goats, cows and camels), in the selected sites occupy an area of 94,900 ha, had increased from 120 thousend head in 1980 to 153 thousend head in 2008. Gebril and Saeid (2012) also studied the status of rangeland, in South Al-Abyar and South Al Jabal Al Akhdar, Libya (south of the study area); between the 200 mm and 50 mm isohyets and covers an area of approximately 9,288 km². Overgrazing or grazing in the open and irregular grazing lands in these areas throughout the year, had led to decline in palatable species such such as *Artemisia herba-alba* 'Wormwood' and *Retama raetam* 'White Broom' particularly at times during the growth cycle (March to May).

El-Barasi et al. (2013) also studied land degradation of a semi-desert grazing area located in south Al Jabal Al Akhdar (south-western of the study area), extending between the cities of Solouk and Al-Abyar, Libya. The area is described as a degraded zone of about 16,875 km^2 (Solouk plain), and the domestic animals constituted 1.23 million head (goats, camels and cows). They stated that the area sufferd from soil erosion and retrogressive succession that was caused by cutting and collecting the wood of economic and medical plants, overgrazing and overstocking, conversion to agriculture, and mining.

2.1.2.5 Urban expansion

Urban expansion (urbanisation) may be defined as “a process that leads to the growth of cities due to industrialisation and economic development, and that leads to urban-specific changes in specialisation, labour division and human behaviours” (Uttara et al., 2012).

Desanker et al. (2001), noted that by the mid-21th century, population and expansion pressures would remain as the main force of land-cover transformation in Africa, with climate change becoming an increasingly significant contributory factor. They explained that ecosystem service provision would be influenced by the resulting changes in ecosystems, which can have a significant impact on plants species regarding distribution and productivity.

Elmahdy and Mohamed (2016) investigated the factors that control Juniperus *phoenicia* L. mortality through the period from 2000 to 2015 in Al Jabal Al Akhdar district by integrating Remote Sensing (RS), using 2000 and 2015 Landsat images, and Geographical Information system (GIS). They reported a decline in *J. phoenicea* that started during the period from the year 2000 to the year 2015 and an expansion in building and infrastructures, the most obvious being in Al Bayda and Al Massah cities.

2.1.2.6 Policies and Legislation

The FAO (2010) described the meaning of the term “policy” as “a course of action adopted and pursued”, which can be explicitly stated or not; It can also be planned, or it can rise by evident behaviour. Policy, i.e. an agreement on strategic direction, requires improvement before any part of it can be made legally obligated. While legislation represents the key tool for applying a policy through the formal statement of rights and obligations, with a regulation of the rules established through primary and secondary legislation. Therefore, the purpose of the policy framework is to place clear direction and management priorities over time and is mainly expressed in policy statements (FAO and Plan Bleu, 2013). Furthermore, legislation can be amended based on the agreed policy statement to achieve the policy (FAO, 2010).

In the Mediterranean region, FAO and Plan Bleu (2013) reported that Governments appear to give higher consideration to formulating and developing policies directed, for example, particularly at forest protection. Such updated policies can provide sufficient strategic guidance for sustainable forest management. They also reported that forest legislation in most countries had been enacted or amended recently, that should confer a strong foundation for sustainable forest management in cases where legislation is applied effectively. They also noted that forest policy issues need to give more consideration to the value arising through the provision of ecosystem services, and also that national and regional public authorities are often unable to meet policy improvement due to limited economic resources.

In Libya, there are many measures and legislative instruments designed to prevent damage to the natural vegetation cover of rangelands and forests. The Libyan government, through the Ministry of Justice, has issued legislation that aims to restrict harmful activities that could affect the vegetation environment; these are listed in Table 2.1 and are available online at http://itcadel.gov.ly in the Arabic version. Table 2.1 shows the acts and decrees of the Libyan legislation that were issued to protect natural vegetation cover and indicates whether these legislations are in force. The articles covered by laws and decrees include those that guarantee to preserve, mandate inspection, force penalties, impose fines and liabilities and regulate investments. The articles also restrict plant/tree burning and cutting and the disposal of harmful materials on forests and pasture lands. They also oblige landowners to rehabilitate dunes located within their lands and to conserve the soil.

Table 2.1 Libyan legislation issued to protect natural vegetation cover

No.	Year	Title of Document	Validity
I-Act* 1	1947	Protection of Rangelands and Forest	Abolished in 1950
8	1951	Protection of Rangelands and Forest	Abolished in 1952
12	1956	Protection of Rangelands and Forest	Abolished in 1971
47	1971	Protection of Rangelands and Forest	Amended with law no 75 of 1972
75	1972	Protection of Rangelands and Forest	Abolished in 1982
5	1982	Protection of Rangelands and Forest	Amended with law No. 14 of 1992
15	1989	Protection of Animals and Trees	Article 2 that relevant to Animals was amended by law No. 22 of 2002 Still in force
14	1992	Protection of Rangelands and Forest	Still in force
II- Decree** 3	1984	Actions necessary to protect forests and pastures from fire.	In force
127	1990	Provisions on the protection of animals and trees.	In force
676	1993	Provision on the rectification of harmful acts imposed on forests lands.	In force

(Source: *Ministry of Justice /Libya, Information and Documentation Centre http://itcadel.gov.ly, and **Alsoul (2016)**).**

Although the act No. 15/1989 and 14/1994, and Decree No. 3/1984, 127/1990 and 676/1993 are still in force until now, the spread of weapons among ordinary people after the 2011 Libyan uprising (El Shatshat, 2015; Alsoul, 2016) has prevented the current government from enforcing and applying these lows and acts.

In north-west Libya, Alsoul (2016) studied the relationship between Libyan policy and desertification in the Jefara Plain. The results showed that the main causes of the desertification are: poor forest governance, corruption, political instability, unclear regulations and conflicting laws. Alsoul (2016) also concluded that a primary cause of deforestation in the area is corruption within law enforcement. Gebril and Saeid (2012) stated that the present policies and plans are insufficient to tackle desertification and rangelands issues of the area in South-eastern Libya. The study recommended the Libyan state develop a general strategy that assists in a progressive decrease in the livestock in the south Al Jabal Al Akhdar and similar regions in Libya, together with the development of a comprehensive environmental plan to preserve the vegetation cover and prevent degradation and desertification.

2.2 **Vegetation**

Description and classification of vegetation community structure provides important information that is required for recording and monitoring natural communities, mapping, and managing preservation programmes, recording the needs of single species, controlling the use of natural resources such as forest and range lands, and setting goals for rehabilitation (van der Maarel and Franklin, 2015). Hobohm (2014) documented how vascular plants have spread across the world, and now belong to particular biomes. A specific species cannot exist in all biomes. Despite this fact, some species are widespread. Hobohm (2014) placed them into three sets, namely: arctic-alpine plants, temperate plants, and pan-tropical plants. However, there are also endemic species where their presence is restricted to a specific area. Concerning the importance of identifying the vegetation and plant communities, this section will provide a detailed overview of the vegetation types that belong to the

geographic location of the study area. The study area is located in the Mediterranean climate, which belongs to the Mediterranean-type ecosystems (MTEs).

2.2.1 Vegetation associated with Mediterranean-type ecosystems (MTEs)

The MTEs comprise all regions having a climate that has a dry summer where the dry period remains for >2 or 3 and up to 11 months, and a cold rainy winter period (Zahran, 2010). There are five MTE regions around the world (Pausas, 1999), occurring between latitudes 30° and 40° north and south of the equator (Bartsch et al., 1973; Archibold, 1995; Vogiatzakis et al., 2006). These regions are: the Mediterranean Basin (MB), South Africa, California, Southern Australia, and Central Chile (Pausas, 1999). Zahran (2010) also described six "sub-climates" types in the Mediterranean climate based on the drought length of the summer. These climatic zones are hyper-arid (11-12 dry months), arid (9-10 dry months), semi-arid (7-8 dry months), sub-humid (5-6 dry months), humid (3-4 dry months) and hyper-humid (1-2 dry months).

The natural vegetation structure of MTEs is however similar, resulting from a concurrence of the environmental conditions within each region (Bartsch et al., 1973), and in particular climatic conditions, which have a robust impact on the vegetation (Sundseth, 2009). Pausas (1999) noted that the vegetation structure of the MTE comprises forest and open woodland with pines and evergreen oaks being dominant in this formation. The second formation is heathlands and dense shrublands, several types of the stemmed woody species are dominant in this formation. The third one is open scrubland, which is dominated by shrubby plants and grasses. Pausas (1999) suggested that the existence of any of these vegetation types that form the MTE arise due to the function of the environment and the disturbance regime.

The following sections focus on the vegetation of the MB and in particular on, Al Jabal Al Akhdar, the study area of interest for this research.

2.2.1.1 Mediterranean Basin Vegetation

The MB covers ca. 3,800 km east to west from Portugal to the Lebanon and ca. 1,000 km from Italy to Morocco and Libya (Sundseth, 2009). FAO and Plan Bleu (2013) identified three groups of MB countries, Northern, Southern and Eastern, shown in Figure 2.1. The southern sub-region (SMCs) has low forest cover, being composed of open woodlands with scattered trees and xerophytic shrubs, as a result of being under semi-arid to desert conditions and grazing in a degraded environment (FAO, 2011c). The dominant climatic conditions of the MB are characterised by hot (25-45°C), dry (no rain) summers, and mild (<100 mm ->2,000 mm), cold (-10-15°C) winters (Sundseth, 2009), which makes moisture a key limiting agent for plant growth. Total annual rainfall ranges from <300 up to 900 mm but is irregularly distributed within and between years (Pausas, 1999).

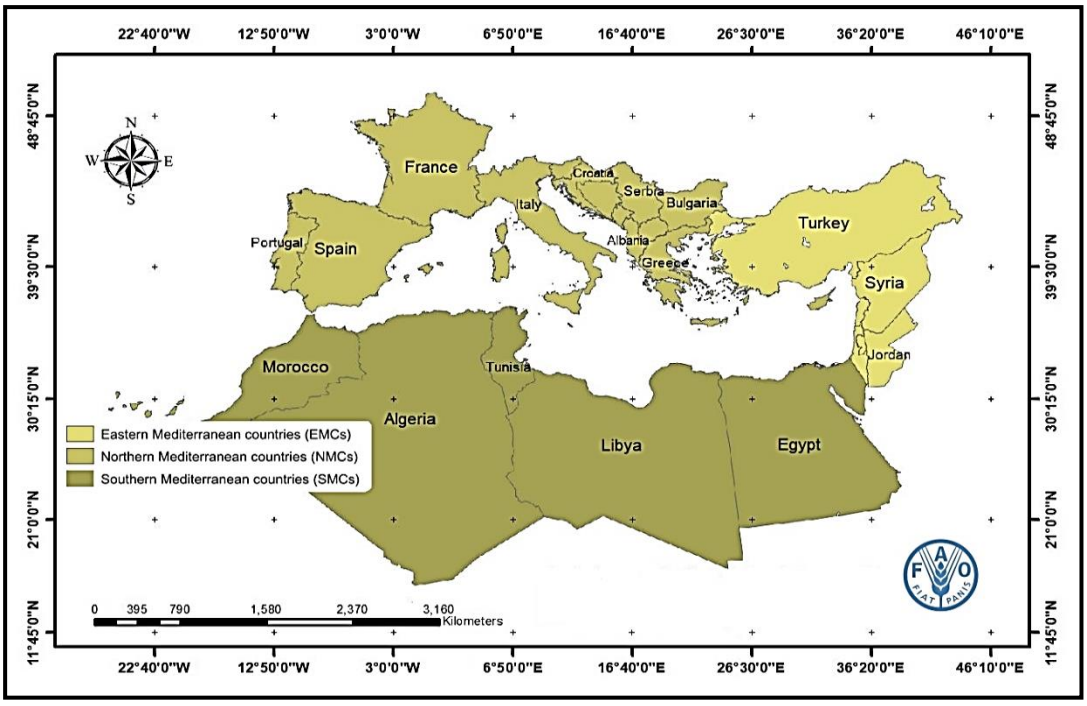

Figure 2.1 The Mediterranean sub-regions (Source: FAO and Plan Bleu (2013)**)**

The SMCs are associated with a variety of climatic conditions and topography, which have impacts on the vegetation types within the region (Sundseth, 2009; Radford et al., 2011). Therefore, the region is both rich in plant diversity, and the number of individuals per species. It also has a high percentage of endemic

species. For example, *Cicer atlanticum* ‘Atlantic chickpea’ is restricted to Morocco, and *Euphorbia postii* is restricted to Syria, *Allium qasunense* is restricted to Palestine, and *Onosma cyrenaica* and *Arbutus pavarii* ‘Libyan Strawberry-tree’ are restricted to Al Jabal Al Akdar in Libya. The SMC region (Figure 2.1) holds 25,000 plant species, which represent 10% of the vascular plants in the world, with about half of these being endemic (Vogiatzakis et al., 2006; Sundseth, 2009; Zahran, 2010; Radford et al., 2011; FAO and Plan Bleu, 2013). For Mediterranean scrubland areas, Sundseth (2009) reported that it has a different shape and size and has been given exotic names such as ‘Matorral’, ‘Maquis’ (or Mecchia), ‘Garrigue’ and ‘Phrygana’ (Batha), which form on different types of habitats with a variety of location, soil type, the degree of degradation, human usage, and species composition. Furthermore, Maquis is the first main stage in forest degradation in many counties suffering from degradation, followed by Garrigue, Phrygana or Batha, all of which are smaller and less complex than Maquis (Zahran, 2010). Zahran (2010) noted nine types of vegetation (Table 2.2) in the MB.

With regards to the plant biodiversity, the MB ranks as the third richest hotspot in the world (Mittermeier et al. 2004 in David, 2010). The original vegetation which comprised evergreen forests (Pignatti, 1978; Archibold, 1995) has now been replaced by a dense scrub, named locally as Maquis or Garrigue. Zahran (2010) mentioned that to distinguish between Garrigue and Maquis, several geographers and phytoecologists consider primarily the geological substrate. Thus Garrigue occurs chiefly on limestone, while Maquis is apparent on those formations occurring on acid, siliceous soils.

Table 2.2 The Vegetation types of the MB

Vegetation Type	Dominant species
Broad-leaved evergreen forest (High Maquis)	Evergreen *Quercus* species such as *Q. ilex*, *Q. suber* and *Q. coccifera* and associated with *Arbutus unedo*, *Erica arborea*, *Myrtus communis* and *Genista hispanica*.
Stunted and degenerate woodland (Low Maquis)	Three species of the genus Cistus, *C. salviifolius*, *C. crispus* and *C. ladanifer*. Typically associated with one of the parasitic plants, a genus of Cytinus, which grow on the roots of Cistus.
Deciduous forest	two species of Quercus (Q. *aegilops* and Q. *cerris*).
Aquatic grasses and reeds	*Phragmites australis*, *Typha domingensis* and species of Cyperus, Juncus, Panicum, Echinochloa.
Coniferous forests	*Abies pectinata*, *A. marocana*, *Pinus pinaster*, *P. sylvesiris*, *P. pyrenaica*, *P. brutia*, *P. halepensis*, *P. pinea*, *Cupressus sempervirens*, *Cedrus libani*, *Juniperus communis*, *J. thurifera* and *J. drupacea;*
Steppe vegetation	Associated with an ecosystem that has a wide seasonal variation in temperature and low precipitation between 400-100 mm. The landscape is characterised by one of the numerous species of grasses and bulbous plants and the absence of trees. The dry steppes and the semi-desert (receiving rainfall between 150 and 300 mm/year) are covered by *Stipa tenacissima* and *Lygeum spartum.*

Table 2.2 The Vegetation types of the MB (continued)

Vegetation Type	Dominant species
Desert vegetation Found in the aridest areas (the aforementioned hyper-arid and arid bioclimatic zones) in Southern and Eastern countries of the MB.	Plants of these deserts have adapted to the extreme temperature, where the with average summer temperature above 30°C with a wide daily range of about 20°C, and drought.
The alpine flora Adapted to extreme cold and may be found on islands of rock even above the snow-line of high mountains, which have altitude more than 2000 m.a.s.l. (Vargas, 2003; Radford et al., 2011).	*Erigeron alpinus*, *Azolla procumbens*, *Salix retusa*, *Juniperus nana*, *Corchus vernus*, *Colchicum alpinum*, *Erica carnea* and *Leontopodium alpinum.*

In addition, desert-like steppes that can be created by overgrazing by goats is another formation which has replaced evergreen forests (Archibold, 1995). Vogiatzakis (2006) defined Maquis as “a dense, mainly evergreen shrub community 1–3 m high” while Garrigue is defined as “open heath communities, often with low-growing thorny and aromatic shrubs”. Moreover, Maquis and Garrigue are noted by the World Wildlife Fund (WWF) in its vegetation type classification, which includes 32 eco-regions of ‘hotspot habitats’ (Derneği, 2010). This classification considered Maquis which occurs in the study area, as the dominant vegetation type in the MB region and described it as hard-leaved shrubland chiefly comprising *Cistus*, *Erica*, *Genista*, *Juniperus*, *Myrtus*, *Phillyrea*, *Pistacia* and other evergreens. Garrigue, as found in the study area, is defined as a habitat limited to the semi-arid, lowland and coastal regions of

the MB, its species are aromatic, soft-leaved and drought resistant and contain mainly *Rosmarinus*, *Salvia* and *Thymus*, and the third type is forests. In the MB region, the forest had been transformed into cropland or pasture about 8,000 years ago; however, pine and deciduous forests occur in Northern and Eastern MB and do cover significant geographical areas (Derneği, 2010).

2.2.1.2 Vegetation of Al Jabal Al Akhdar and the Area of Interest (study area)

Libya is in North Africa (SMC), occupying an area of about 1,759,540 km^2 with most of this area classified as a desert. The coastal strip and mountains of the MB coastline, being about 1,900 km long, are the most important areas for plant diversity. Radford et al*.* (2011) noted that the original coastal vegetation covers a large area quickly after winter rainfall. *Artemisia campestris* L. 'Field Wormwood' and *Retama raetam* (Forssk.) Webb 'White Broom' are the dominant species and early spring annuals such as *Senecio gallicus* Chaix 'French groundsel', *Hussonia pinnata* (Viv.) Jafri, *Eruca sativa* Mill 'Rocket', *Chrysanthemum segetum* L. 'Corn marigold', *Malva sylvestris* L. 'common mallow' and *Erodium laciniatum* (Cav.) Willd. 'Cut-leaved storkbill, and the perennial herb *Echium angustifolium* Mill. 'Narrow-leaved bugloss' are also associated with this community. In respect of the oases and valleys of the Libyan Sahara, Radford et al*.* (2011) also described the vegetation of this ecosystem as scattered vegetation characterised by its low diversity. *Phoenix dactylifera* L. (date palm), *Tamarix* spp., *Retama raetam* (Forssk.) Webb 'White Broom', *Ziziphus lotus* (L.) Lam. 'Lotus jujube'*, Lycium europaeum* L. 'Boxthorn' and *Acacia tortilis* (Forssk.) Hayne 'Umbrella thorn' are the species associated with this community, in addition to herbaceous plants including *Artemisia judaica* L. 'wormwood', *Hyoscyamus muticus* L. 'Egyptian henbane' and *Zilla spinose* (L.) Prantl 'Spiny Zilla', and perennial grasses such as *Panicum turgidum* Forssk. 'Desert grass', *Stipagrostis pungens* (Desf.) De Winte 'Three-awn grass' and *S. plumosus* (L.) Munro ex T. Anderson 'Nassi' predominate.

Al-idrissi et al*.* (1996) reported that the main natural forest of Libya is in the Al Jabal Al Akhdar in the east, and in addition, some of the remnants of natural

forest in Jabal Nafusa in the west. Al-idrissi et al. (1996) noted that 35% of the total area of the forest in Al Jabal Al Akhdar had been converted to agriculture. As a consequence, the total area of forest declined from about 500,000 ha to about 320,000 ha over 20 years from 1959 to 1979. With regards plantation forest established in the western part of the coastal belt, which was planted in 1981 with various species of Eucalyptus, Acacia and Pinus on 150,000 ha, unfortunately, only 50-70,000 ha was successfully established. The Libyan Environment General Authority (2008) described the link between plant biodiversity and the pattern of the dominant ecosystems in a study highlighting that Mediterranean plants dominated Al Jabal Al Akhdar while the semi-arid region in Libya such as the Jeffara plain and the desert was dominated by desert or drought-tolerant plants with sparse shrubs. In the drylands, many plants occur surrounding the oases. These plant species do not have drought tolerant mechanisms. The humid coastal and salty desert regions of Libya are dominated by halophytes, salt-tolerant plants.

Zahran (2010) described the natural vegetation cover around Al Jabal Al Akhdar, as being predominated by forests of cypress (Cupressus spp.), ilex (Ilex spp.) and juniper (Juniperus spp); towards to the south the forests are replaced by Garrigues (i.e. Mediterranean Matorrals), and then by Steppes. These plant formations, are mentioned in OMU (2005) based on the Zunni (1977) classification into four main formations; Forest, Maquis, Batha and Steppes (Table 2.3).

Table 2.3 The plant formation of Al Jabal Al Akhdar region

Plant Formation	Description	Dominant species
Forest	Limited in the area but still existing in: - High altitude areas and some valleys toward the sea. - The northern of the area at foothills and coastal valleys.	*Cupressus sempervirens* L. *Pinus halepensis* Mill., and other species such as *Quercus coccifera* L. and *Juniperus Phoenicia* L. and *Ceratonia siliqua* L. for instance.
Maquis	A plant community does not include a layer of trees being an open community with shrubs spaced out, starting from the coastal region and extending across the Upper Plateau. It exists in all heights up to the northern border of the Steppes zone.	*Pistacia* spp.
Batha	The popular community in the coastal plain, that occurs when either there is intensive grazing associated with shallow soils (less than 15 cm) or clear cut and remove the longest plants or because of all these cases.	Thorny burnet *Sarcopoterium spinosum* L.
Steppes	Consists of plant communities of dwarf shrubs or grasses and annual herbs, representing a climatic climax particularly in the southern parts of their distribution.	

Hegazy et al. (2011) classified the vegetation of Al Jabal Al Akdar region (Figure 2.2) into three main groups based its habitat types as:

- Coastal and low-elevation vegetation dominated by shrubs and trees account for about 60% of the plant life forms;

- Mid-elevation and wadi vegetation, with the highest species diversity, dominated by shrubs and trees, representing more than 60% of the plant life forms; and

- Mountain peak vegetation dominated by herbs and few low shrubs that make up to 90% of the plant life forms.

Al-Sodany et al. (2003) studied the vegetation composition along an elevation gradient, from Alhamama at the north to Al Bayda at the south passing through Al Wasita (Al Jabal Al Akhdar district) (Figure 2.2). The results demonstrate the high number of plant species in this area, 119 species including 6 endemics, due to a variety of habitats in the study area. These habitats vary from the coastal saline sand flats, sand dunes, sand flats to hills, and inland plateau with terraces and wadis. The family with the highest number of total Flora was Asteraceae, and Poaceae (16 species for each) followed by Fabaceae (12 species). Al-Sodany et al. (2003) also grouped and described the vegetation, based on their habitats into *Juniperus phoenicea – Sarcopoterium spinosum* that occurs in a wide elevation gradient, *Crucianella maritima – Suaeda vermiculata* found in the seaward direction of the coastal hills. While *Retama raetam* occurs in the coastal sand flats and *Pancratium maritimum – Ammophila arenaria* in the coastal sand dunes. Finally, *Cichorium spinosum* and *Limoniastrum monopetalum* were found in the saline sand flats of the coastal plain. The most notable group is *Juniperus phoenicea – Sarcopoterium spinosum* where its variety and coverage increase with altitude, reaching the Mediterranean forests at the highest elevated sub-humid zones.

Several studies have investigated the flora and vegetation composition of the region (OMU, 2005; Hegazy et al., 2011; Abusaief, 2013; Abusaief and Dakhil, 2013; Abusaif, 2013; Elshatshat and Mansour, 2014; Alaib et al., 2017). In order

to estimate the status of the vegetation in the region, a survey was carried out by OMU during 2003 and 2004. The study included an inventory of plant species at 53 sites which had been chosen to represent the whole Al Jabal Al Akhdar area (Figure 2.2). Total of 500 species was collected belonging to 447 genera and 107 families. In total, 46 endemics were confirmed. The main findings revealed that the region was dominated by *Juniperus phoenicea* L. (486 tree ha^{-1}), associated with *Pistacia lentiscus* L. (685 tree ha^{-1}) together these two form the important type of species in the area (OMU, 2005). Hegazy et al*.* (2011) reported *Juniperus phoenicea* L., Family: Cupressaceae as being a keystone species found in several habitat types (coastal, the northern side and the southern side landscape) in the study within Al Jabal Al Akhdar region. However, this species does not appear on hill peaks.

In the rocky habitat of El Mansoura, in the east part of Al Jabal Al Akhdar region (Figure 2.2), a study was carried out by Abusaief and Dakhil (2013) during four seasons of autumn 2010 to summer 2011 to collect information about the flora in terms of the number of species and the family and life forms. The results indicated 175 species which belonged to 43 families were found in the area. Asteraceae was the largest family and was represented by 27 species. With regards to plant life-forms of Raunkiaer where all plants were classified based on the perennating buds' position concerning the ground surface (Figure 2.3). Abusaief and Dakhil (2013) also found that Therophytes, Chamaephytes, Hemicryptophytes, Cryptophytes 'Geophytes', and Phanerophytes were represented by 59.4, 13.1, 11.4 10.3 and 5.7%, respectively (Abusaief and Dakhil, 2013). Similar results were obtained by Elshatshat and Mansour (2014) for the coastal habitat in the western part Al Jabal Al Akhdar (out of study area Figure 2.2), the annuals were represented by 104 plant species belonging to 37 families. *Fabaceae* and *Asteraceae* as represented by 16 and 15 species, were the main families in this habitat. In terms of dividing the plant based on plant life-forms of Raunkiaer, Therophytes (buds in the seed), Chamaephytes (buds above ground but less than 25-30 cm), Cryptophytes 'Geophytes' (buds below the surface of the ground), Phanerophytes (buds more than 25-30 cm

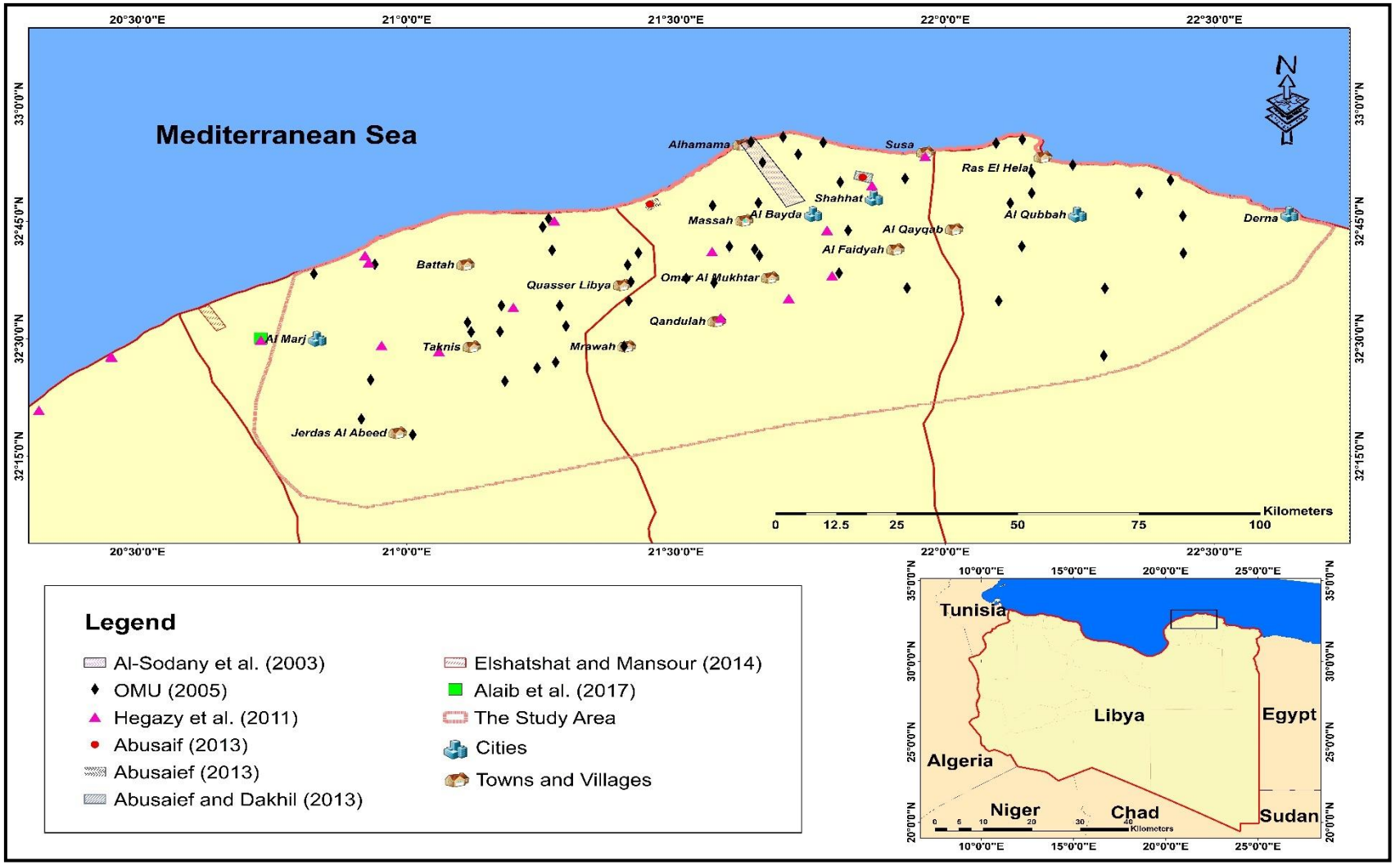

Figure 2.2 The previous studies on natural vegetation cover of the Al Jabal Al Akhdar region (source: Author)

above the ground) and Hemicryptophytes (buds at the surface of the ground) (1 species only) were represented in 64.4, 15.4, 14.4, 4.8 and 0.96% of the identified plant species, respectively (Elshatshat and Mansour, 2014).

In another study, Abusaif (2013) recorded the species in two different parts of Al Jabal Al Akhdar, namely El Mansoura and Jar' Jaramah during the autumn 2010 and winter, spring and summer of 2011 (Figure 2.2). Abusaif (2013) found that *Cistus parviflorus, Erica multiflora, Teucrium apollinis, Thymus capitatus, Micromeria Juliana, Colchium palaestinum and Arisarum vulgare* occurred in the rocky habitat associated with El Mansoura. In Jar' Jaramah, five habitats were found. The dominant species in the salt marsh, saline, rocky coastal, sandy beach and sand dune habitats were *Suaeda vera*, *Onopordum cyrenaicum*, *Rumex bucephalophorus*, *Tamarix tetragyna* and *Retama raetem*, respectively.

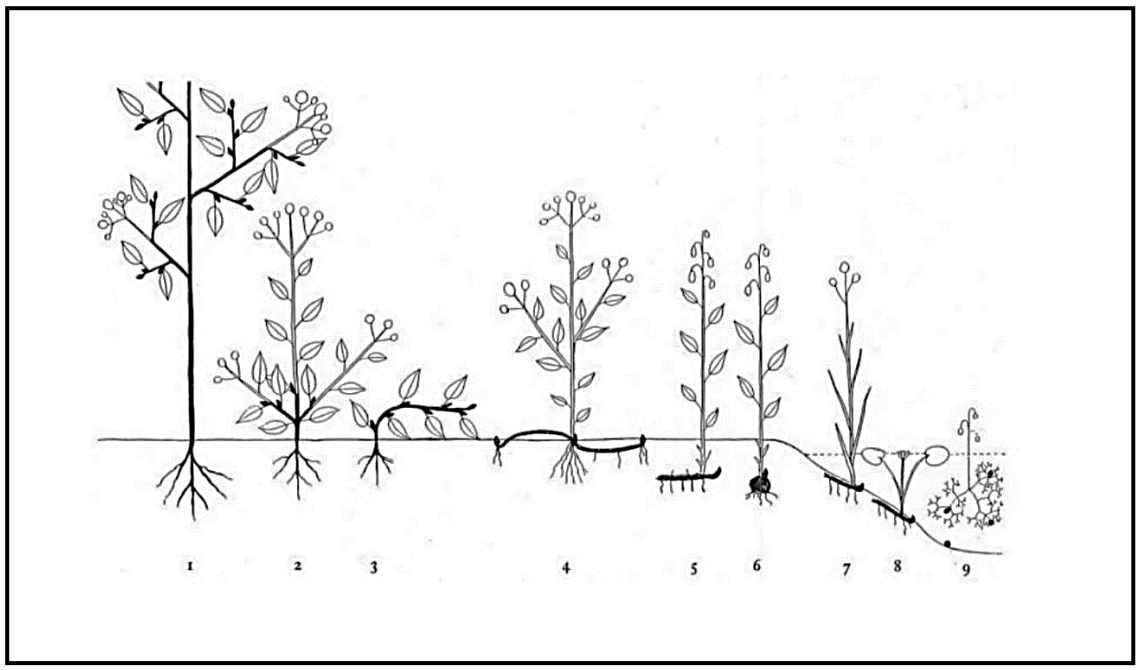

Figure 2.3 Raunkiear's plant life-forms (source: de Silva et al. (2017))

''Phanerophytes (buds >25 cm above ground [trees and shrub]) (1), Chamaephytes (buds near the ground [low shrubs]) (2-3), Hemicryptophytes (buds at the soil surface [herbaceous perennial]) (4), Cryptophytes (buds below ground [geophytes]) (5-9) (Keeley et al., 2012; da Silva et al., 2017)''

Moreover, Abusaief (2013) determined the important species of Jar' Jaramah, finding that the area characterised by *Pistacia lentiscus*, *Rhus tripartite*, *Tamarix tetragyna*, *Ceratonia siliqua* and *Nitraria retusa,* which belongs to Phanerophytes, and *Posidonia oceanica*, belongs to Hydrophytes occurred on the sand formation.

A floristic and ecological survey was carried out on Wadi Al Agar in the west part of Al Jabal Al Akhdar (Figure 2.2), 2.5 Km to the west of the study area, by Alaib et al. (2017). They stated that the vegetation community is represented by high and low Maquis; those are two of the MB vegetation types (see Table 2.2), and herbaceous plants. They collected 317 taxa of the vascular plants belonging to two families of Gymnosperms and 64 families of Angiosperms. The results indicated that Asteraceae (46 species), Poaceae (26 species), Lamiaceae (19 species), Apiaceae (13 species), Brassicaceae (13 species), Boraginaceae (11 species), Geraniaceae (11 species), Liliaceae (11 species) and Ranunculaceae (9 species) are the largest families. In total, 41 endemic taxa were confirmed in the study area, including 18 which have been collected.

2.3 **Summary of literature**

This chapter has reviewed a wide range of literature related to land degradation and has provided context for its definitions. Based on previous descriptions of land degradation (Baartman et al., 2007; Johnson and Lewis, 2007; Bai et al., 2008; FAO, 2011a, 2013; ELD Initiative and UNEP, 2015), land degradation in respect to the current study purpose can be described as "the decrease in natural vegetation cover which in turn could reflect the changes in vegetation community composition because of the deforestation in order to use the natural vegetation land for agriculture or development purposes."

Climate has been monitored in Libya in several studies over 40 years and more. The studies confirmed that significant increases in temperature and decline in the rainfall had been recorded in (Ageena et al., 2013, 2014; Zeleňáková et al., 2014). However, there are only a few studies that have addressed the relationship between climate and vegetation. OMU (2005), El-Barasi and Saaed (2013) and Elshatshat and Mansour (2014) noted the tree die-back, with dry

branches on numerous trees, they attributed the reasons for this phenomenon to climate change over the last 40 years, but none of the authors considered the impact of climate on natural vegetation cover degradation.

The fire was reported as a natural factor of losing natural vegetation cover; its effects also impacted significantly in study area; however, such fire events seem to be principally human-induced (El-Barasi and Saaed, 2013).

There are many discussion and literature on the natural factors and human activities that lead to land degradation, particularly natural vegetation cover degradation. In the study area, the key causal factor is human activities as reported in Abdalrahman et al. (2010), El-Barasi and Saaed (2013), Elshatshat and Mansour (2014), Elmahdy and Mohamed (2016). However, there is a lack literature regarding the change in natural vegetation cover specified after the 2011 Libyan uprising such as Elshatshat (2015), who observed the effect of human activities on natural vegetation cover along the roadsides of Al Jabal Al Akhdar (through Al Marg and Al Jabal districts), from 2011 to 2015. All the authors considered the change in natural vegetation cover, but none of them considered defining and mapping the transition types of land cover/land use changes; and the relationship between population growth and such changes.

The review demonstrated the type of vegetation of the MB (Archibold, 1995; Vargas, 2003; Derneği, 2010; Zahran, 2010; Radford et al., 2011), and the particular plant composition of Al Jabal Alkhdar region (Al Marg, Al Jabal Al Akhdar and Derna districts), with the dominant species provided for each form. Forest, Maquis, Batha and Steppes are the main plant formations of the area (Zunni, 1977; Al-Sodany et al., 2003; OMU, 2005; Zahran, 2010; Hegazy et al., 2011; Abusaief, 2013; Abusaif, 2013; Alaib et al., 2017). Other authors describe the plant life forms based on plant life-forms of Raunkiaer (Abusaief and Dakhil, 2013; Elshatshat and Mansour, 2014). However, again, only field surveys and plant collection are considered; and none of the authors used machine learning to predict the land use type as natural forest, planted forest or rangelands based on the relationship between the natural vegetation cover and the properties of the area under consideration.

The following chapter, Chapter 3, describes the Al Jabal Al Akhdar region, the botanical information used as a database for this research used in the classification of the study area.

3 RESEARCH CONTEXT

This chapter provides concise background information on the Al Jabal Al Akhdar area and the botanical survey undertaken by Omar Al-Mukhtar University (OMU) that is used as a baseline for the current research. Where the data is used to i) identify the boundary of the study area, ii) as a means of ground truthing data for image classification, iii) to study the impact of climate on natural vegetation cover and iv) to predict the Natural vegetation type.

This chapter presents the context of the research in three sections: A detailed background description of the physical characteristics and environmental conditions associated with the Al Jabal Al Akhdar region and a detailed review of the botanical survey of the Omar Al-Mukhtar University (OMU). The first section provides a detailed description of the study location in terms of its geographic and geological characteristics, the prevailing climatic conditions, soils, and vegetation. The second section provides detailed information of the land use in the Al Jabal AL Akhdar region. This chapter further presents the relationship between the dominant plant species with soil properties based on the OMU (2005) results.

3.1 **The Al Jabal Al Akhdar region description**

Libya is located on the south coast of the Mediterranean Basin in North Africa, between 9° 24′ E to 25° 02′ E and 19° 29′ N to 32° 55′ N. It occupies an area of 1,750,000 km^2 (175,000,000 ha) (Ben-Mahmoud, 2001), including no interior rivers or lakes (NIC, 2009; Eddenjal, 2015) and is classified as desert, hills (Jabal), mountains and valleys (Gawhari et al., 2018).

Eddenjal (2015) described the topography of Libya (Figure 3.1), as comprising the coastal plain (such as the Jeffara plain and the narrow northern coastal belt). The north low mountain areas comprise the Al Jabal Al Akhdar Highlands, located near the coastal plain of northeast Libya and the Jabal Nafousa

Mountains, which form the southern boundary of the Jeffara Plain, which rises to 960 meters above sea level (m.a.s.l.) (El-Tantawi, 2005). In the south are located, the Akakos Mountains, which rise to 1428 m.a.s.l., and the Tibesti Massif, which rises to over 2,200 m.a.s.l. In addition, The Great Sand Sea, which lies parallel to the Mediterranean coast and occupies most of the north-eastern part of the Libyan desert (Eddenjal, 2015).

The principle climatic zones of Libya, according to Dimkić et al. (2008), may be divided into four zones as follows:

1) Sub-humid Mediterranean: small areas in the Al Jabal Al Akhdar (rainfall totals 400-600 mm (Saad et al., 2011; Eddenjal, 2015), estimated at only 5000 km^2 (comprising 0.3% of the total Libyan land area) (Ben-Mahmoud, 2001; Saad et al., 2011);
2) Semi-Mediterranean (semi-arid): areas along the western and eastern coastline (rainfall totals 200-400 mm (Saad et al., 2011; Eddenjal, 2015)), at 26,000 km^2 (comprising 1.5% of the total Libyan land area) (Ben-Mahmoud, 2001; Saad et al., 2011);
3) Steppe (Dry): north slopes of Al Jabal Al Akhdar and Jabal Nafousa, and the western Jeffara Plain (100-300 mm (Zahran, 2010)), at 130,000 km^2 (comprising 7.4% of the total Libyan land area) (Ben-Mahmoud, 2001; Saad et al., 2011); and
4) Desert (Very Dry): (areas which have no rainfall or receive < 25 mm yr^{-1} (Zahran, 2010)), at 1,589,000 km^2 (comprising > 90% of the country) (Ben-Mahmoud, 2001; Saad et al., 2011). In the areas south of the zones noted above, total rainfall is ≤ 30 mm (Saad et al., 2011; Eddenjal, 2015).

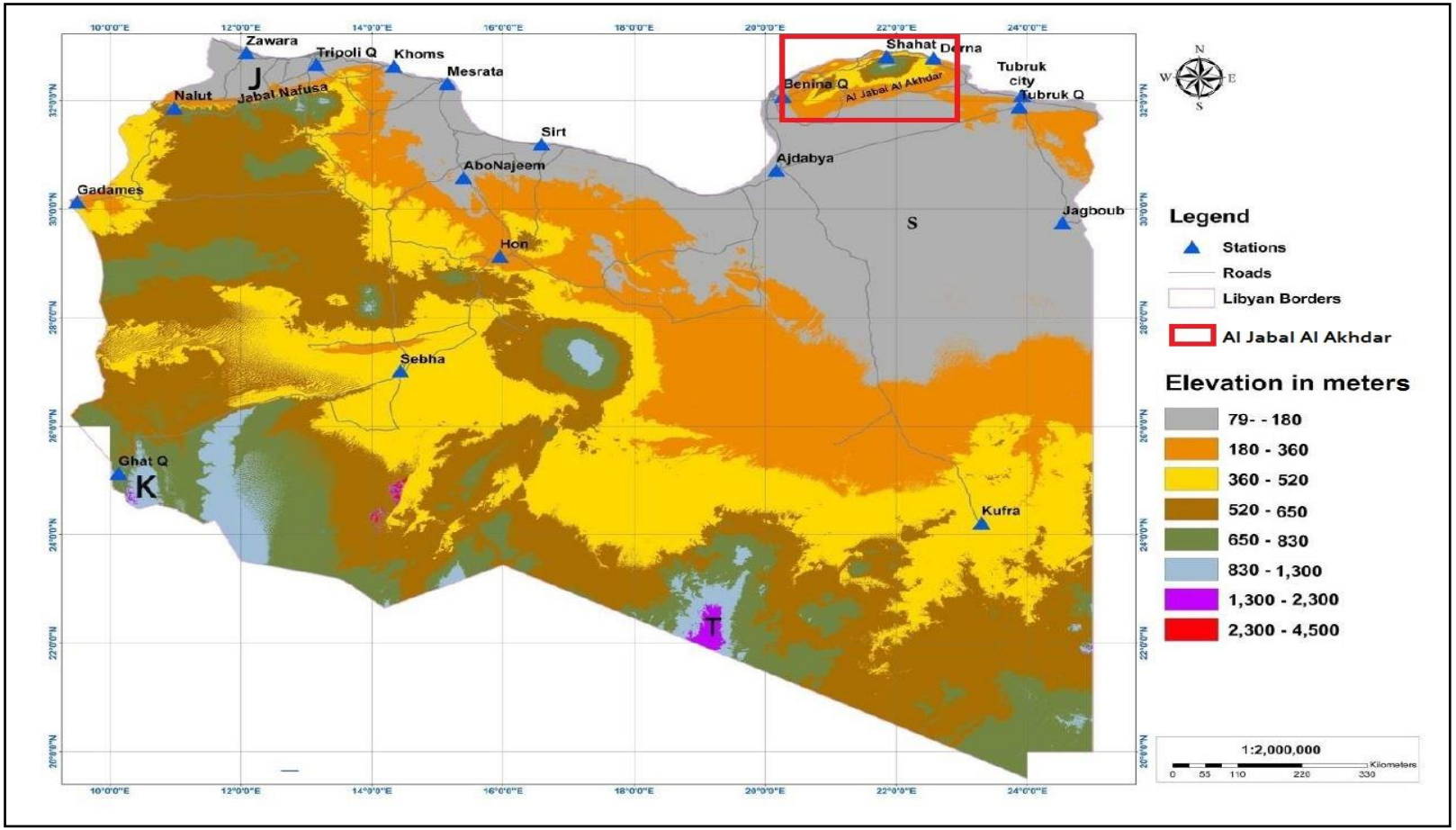

Figure 3.1 Topography of Libya (source: (Eddenjal, 2015))

The Jeffara plain (J), the Great Sand Sea (S), the Akakos Mountains (K), the Tibesti Massif (T), and Al Jabal Al Akhdar near the coastal plain of the northeast and the Jabal Nafousa, which form the southern boundary of the Jeffara plain.

3.1.1 The Al Jabal Al Akhdar Highlands

Al Jabal Al Akhdar is a high elevation plateau, rising to an altitude of >875 m.a.s.l. (El-Tantawi, 2005) in its central part. The plateau is a crescent-shaped ridge lying between 20° 35′ E to 23° 15′ E and 30° 58′ N to 32° 56′ N (OMU, 2005), covering a total area of (20,070 km^2) 2,007,000 ha. The Mediterranean Sea abuts Al Jabal Al Akhdar to the north and west, with the Marmarica Plateau to the east, and the Sahara and the Great Sand Sea to the south (Figure 3.2).

This sub-section provides the morphological description of three key districts in the study area namely Derna, Al Jabal Al Akhdar and Al Marj (see Section 3.1.9) within the Al Jabal Al Akhdar Plateau as defined by the Libyan Urban Planning Agency (LUPA) (2008), starting from the east to the west.

Firstly, Derna district lies for most of its northern part in the Al Jabal Al Akhdar Plateau, thus having its share of the Al Jabal Al Akhdar Plateau escarpments and terraces (LUPA, 2008). Where the escarpment is “a relatively continuous and steep slope or cliff breaking the general continuity of more gently sloping land surfaces and resulting from erosion or faulting” (USDA, 2015), and terrace is “a step-like surface, bordering a valley floor or shoreline, that represents the former position of a flood plain, lake, or seashore” (USDA, 2015). The first escarpment, which is the longest and steepest of the three escarpments, extends over the entire east-west length of Derna district up to Ras Et-Tin east of the city of Derna. Many short wadis (valleys) dissect the first escarpment discharging their seasonally eroded sediments into alluvial fans and eventually into the sea. The second escarpment, which rises between 80-120m above the first terrace, leads to the second terrace. The second terrace, averaging between 200-400 m.a.s.l. (OMU, 2005), is less extensive than the first terrace, having fewer wadis and characterized by moderate sloping and hilly terrain. Some wadis, which originate on the third terrace (>400 m.a.s.l. (OMU, 2005)) south of Al Faidyah (in Al Jabal Al Akhdar district), run in a west-east direction south of Al Qayqab and Al Qubbah discharging into the sea near the city of Derna. The most notable of them is Wadi Derna which ends up in the middle of the city, thus dividing it into two parts. Others (e.g., Wadi Al Ramla) run

southwards ending in the Balat area in the south of Al Mikhili and El Izziyat (LUPA, 2008).,

Secondly, Al Jabal Al Akhdar district has three main terraces which can be distinguished by escarpments that differ in elevation and slope. The first escarpment is the longest and the highest, with a height of 250-300 m.a.s.l. It rises in some areas between Susa and Ras El Helal to about 420 m.a.s.l. Many of the short wadis intersect the first escarpment, where these valleys discharge their sediments into an alluvial fan and then into the sea. The second escarpment, which ranges from 80-120 meters above the first terrace, leads to the second terrace. The second terrace, with an average altitude of 420-600 m.a.s.l is less spacious than the first terrace and has few wadis and is characterised by a moderate slope and hilltop terrain. The third escarpment leads to a limited terrace that rises to about 860 m.a.s.l in the Sidi El Homari area which is the highest point in the Al Jabal Al Akhdar Plateau, the watershed in the area is determined, and as the land begins to decline towards the south, rainwater that is not absorbed by the soil flows with the slopes as a sub-surface flow.

Thirdly, Al Marj district is characterized by three escarpments of the Al Jabal Al Akhdar Plateau, which rises from about 100 m.a.s.l. and ascends to an elevation of >600m. Behind the first escarpment overlays a plain known as the ‘First Terrace-Al Marj Plain’ which is a moderately undulating plain that stands at 200 m.a.s.l. and gradually rises to 400 m.a.s.l. to the join second escarpment of the Al Jabal Al Akhdar area (LUPA, 2008).

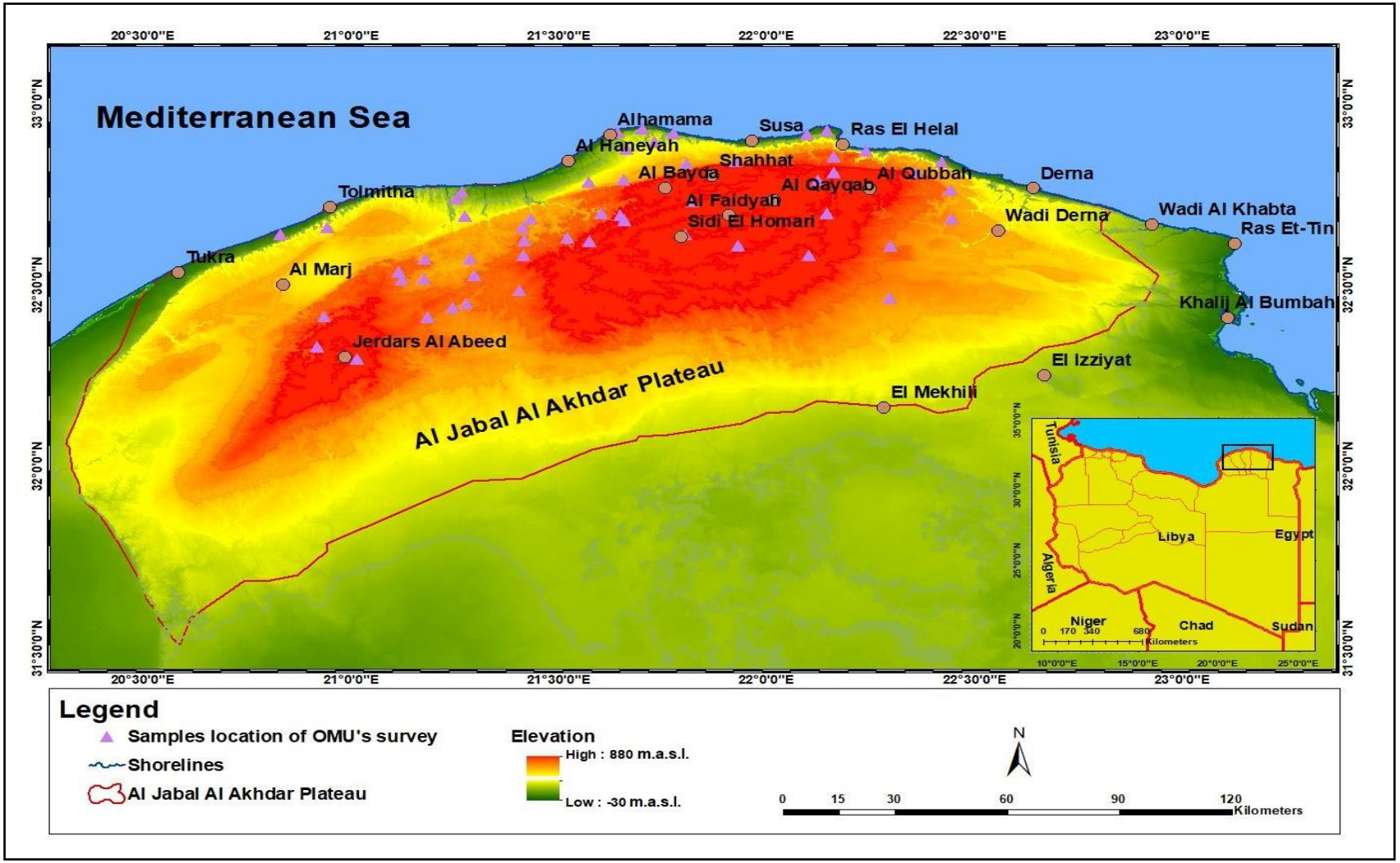

Figure 3.2 The study area location in Al Jabal Al Akhdar (Source: the author)

Terrain, geographical location and rainfall rates are directly related to the determination of the composition and status of natural vegetation cover, as well as the soil in terms of its degree of development or deterioration in a particular area. Therefore, the topographical characteristics of the Al Jabal Al Akhdar were taken into consideration in the OMU survey (OMU, 2005). The OMU survey targeted the various terraces that form the Al Jabal Al Akhdar plateau and parallel to the coast; by conducting field studies along the length of each terrace starting from the eastern borders of the area (Figure 3.2) and extending to its western borders. The study area of OMU survey was divided into three topographical units, as follows (Figure 3.3 and Appendix Table B.1.1

1st Terrace: This includes areas between the coast of the Mediterranean Sea and those in parallel with them. Average altitude is <200 m.a.s.l. The 1st terrace contains 7 sampling sites and occupies in total an area of 2,426 ha;

2nd Terrace: Average altitude is between 200-450 m.a.s.l. The 2nd Terrace contains 22 sampling sites and occupies in total an area of 6,732 ha and;

3rd Terrace: Average altitude is > 450 m.a.s.l. The 3rd Terrace contains 24 sampling sites and occupies in total an area of 16,723 ha.

In total, 53 sampling sites were selected by the OMU study including 5 sampling locations as transects passing through the terraces north to south. The OMU sampling frame is stratified random comprise six sites located within Rangelands (RL) and 43 sites within Natural Forest (NF) areas, and four sites in Planted Forest (PF) areas (Figure 3.3, Appendix Table B.1.1) and formed an area of 2.5% of the total study area

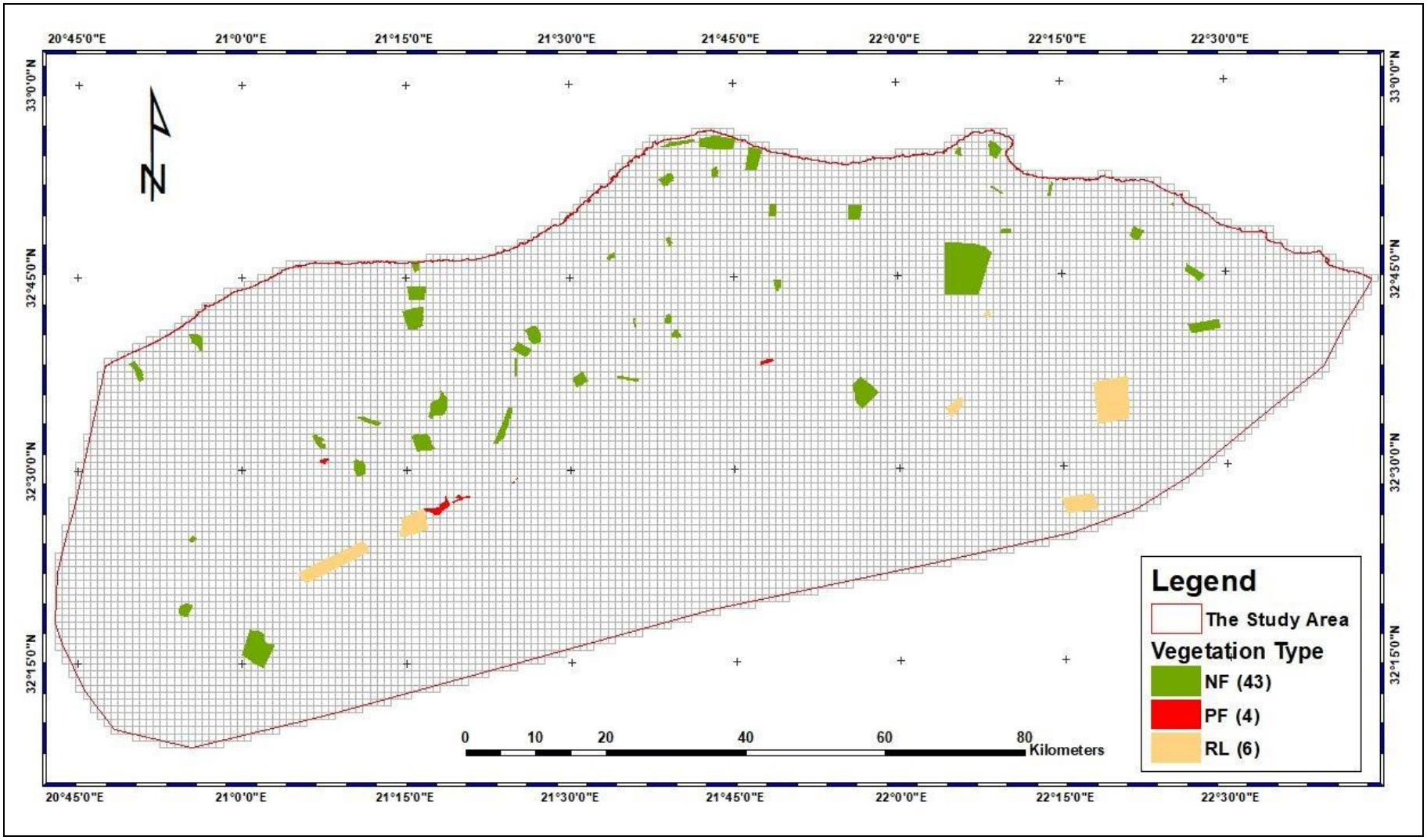

Figure 3.3 The sampling frame of the OMU suvey

3.1.2 The climate of Al Jabal Al Akhdar

The Al Jabal Al Akhdar region is the wettest region of Libya, with mean annual rainfall >500 mm in the northeast zone, with the maximum amount >600 mm falling on Massah, Al Bayda and Shahhat cities in Al Jabal Al Akhdar district. This area belongs to the Mediterranean sub-humid climatic zone (OMU, 2005; Zahran, 2010). Towards the south of Al Jabal Al Akhdar, the rainfall decreases to 270-280 mm yr^{-1} and is classified as a Mediterranean arid climatic zone (OMU, 2005; Zahran, 2010). The west and north-west of Al Jabal Al Akhdar belong to the Mediterranean semi-arid climatic zone, receiving a mean annual rainfall of between 300-400 mm yr^{-1} (OMU, 2005; Zahran, 2010). Approximately 75% of the annual rainfall occurs during the rainy period, from October to April, and the summer is a dry period with rainfall amounting to <7% of the annual total (OMU, 2005) (Figure 3.4). The daily average temperature ranges between 10-30 ºC.

The 1947-2010 data indicates that January and August are the coldest and the warmest months of the year, respectively (OMU, 2005). The Al Jabal Al Akhdar Plateau has local impacts on climate (rainfall and temperature) (El-Tantawi, 2005). The temperature of the locations at similar latitudes can differ because of the variation in elevations with a decline on average of about 0.64 °C/100 m (El-Tantawi, 2005). For example, high plateau stations (Shahhat (621 m.a.s.l), 16.6 °C) are colder than low-altitude stations (Derna (26 m.a.s.l), 20.0 °C) at nearly the same latitude.

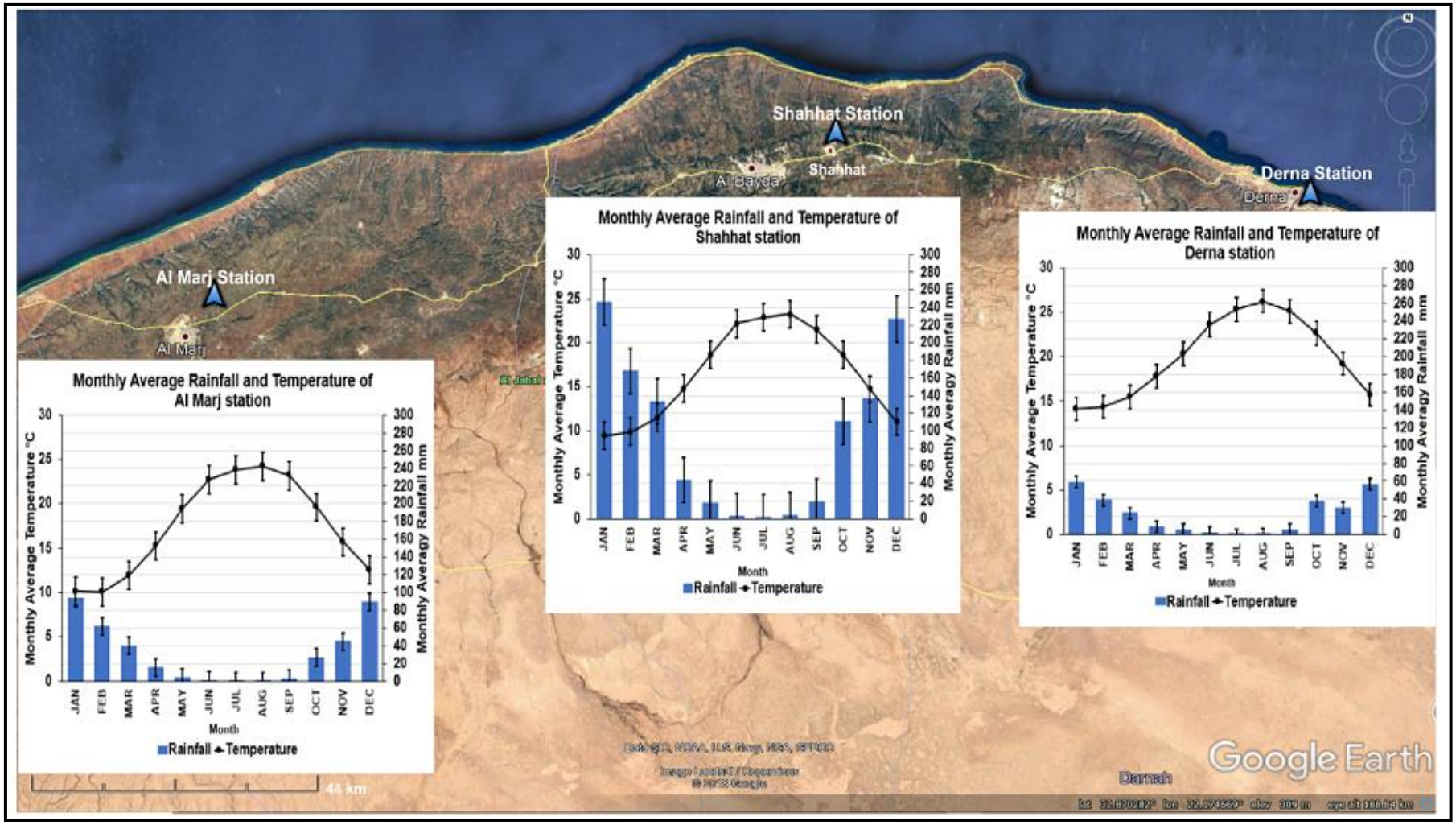

Figure 3.4 Monthly average rainfall and temperature at Shahhat, Derna and Al Marj weather stations.

In the spring and autumn, strong winds with speeds > 80 km hr^{-1} blow north from the desert toward the Mediterranean Sea (El-Tantawi, 2005; NIC, 2009). These winds are known locally as “Ghibli” (or Sirocco) (NIC, 2009; Eddenjal, 2015), filling the atmosphere with sand and dust and increasing the temperature up to 50 °C (Nwer, 2013; Eddenjal, 2015) (Figure 3.5).

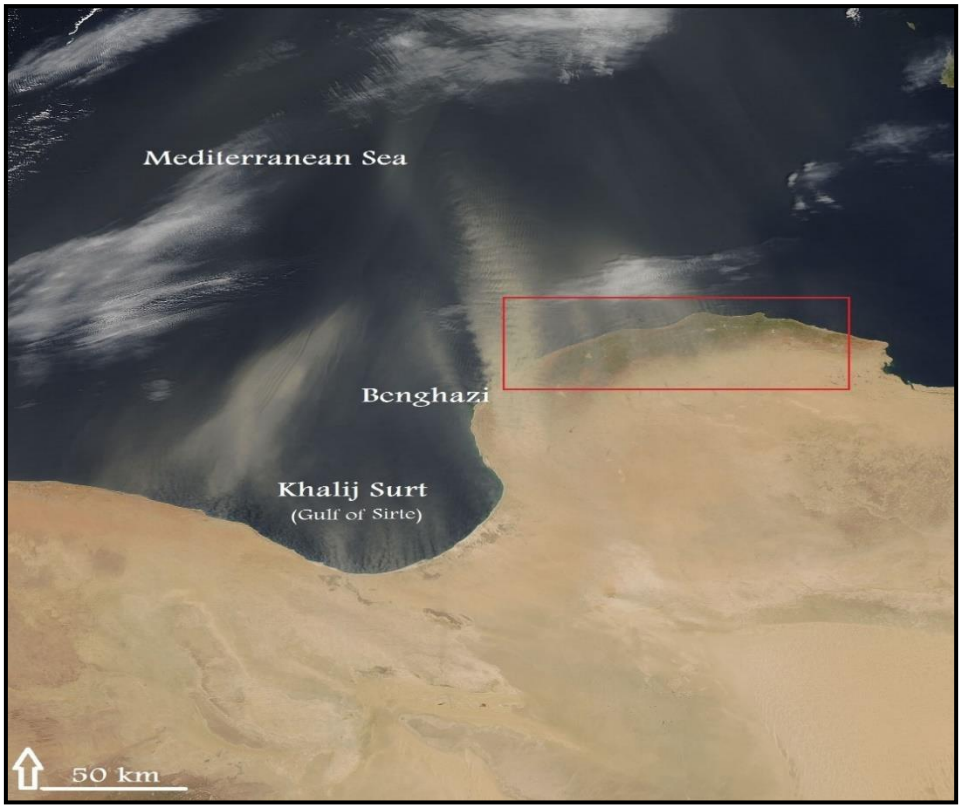

Figure 3.5 Ghibli winds (source: Google Earth- April 16, 2012)

3.1.3 Soils of Al Jabal Al Akhdar

This subsection describes the soil in Al Jabal Al Akhdar, which allocated for the OMU soil survey. The soils in the Al Jabal Al Akhdar region were studied extensively in 1980 by Selkhozpromexport (1980) and in 2005 by OMU (OMU, 2005). These studies include information on soil organic matter (SOM), $CaCO_3$ percentage, pH, cation exchange capacity (CEC), soil nutrients, electrical conductivity (EC), soil texture and soil depth In addition, in 2005 Libyan SOTER "Libyan soils and terrain digital database (SOTER)" map was generated by the Libyan Water General Authority and The Arab Centre for the Studies of Arid Zones (ACSAD) (LWGA and ACSAD, 2005) which used the USDA Soil Taxonomy (Reference) as the soil classification system.

Ben-Mahmoud (1995) reported that the soil of the Al Jabal Al Akhdar originated from limestone. It is shallow soil dominated by Terra Ross (Rhodoxeralfs) (Ben-Mahmoud, 2001), covering an area of 356,000 ha in the plain areas of the Al Marj, Al Abayar, the southern and east areas of Taksin, Daryana, Battah and Derna (LWGA and ACSAD, 2005). According to soil chemical analyses of OMU (2005) study, the calcium carbonate content ($CaCO_3$) ranges between 0.03-75; the high values of $CaCO_3$ in these soils result from a parent material that is rich in $CaCO_3$. The SOM ranges between 1-11%. The soil salinity values reveal that the mean electrical conductivity (EC_e) ranges between 0.8 and 54 dS m^{-1}, which indicates that the soil ranges between non-saline to medium or high salinity. Ben-Mahmoud (2001) classified the degree of soil salinity of Libyan soils, therefore, the soil salinity degee in Al Jabal Al Akhdar can be classified as follows:

- Strongly saline soil: Haplosalids, Aquisalids and Petrogypsids;
- Slightly to moderately saline soils: Xerofluvents, Torrifluvents, Xerorthents, Torriorthents;
- Slightly saline soils: Xerochrepts (not included in Figure 3.6) and;
- Non-saline soils: Rhodoxeralfs, Haploxeralfs and Haprendolls.

The soil sodium adsorption ratio (SAR) ranges between 0.03-1.22. The ESP (Exchangeable Sodium percentage) values range between <1 to 21, which

indicate that the soil ranges between non-sodic to strongly sodic; and the pH values range between 7.0 to 9.3 (OMU, 2005).

In the coastal area, known as the Benghazi Sabkha ‘saline flat’ (De4 in Figure 3.6), the soil is saline as well as alkaline (sodic); the soil has high total dissolved solids (TDS) values ranging between 10.7-22.6 ds m^{-1}, and pH values reaching up to 10.6 (El-Barasi and Saaed, 2013).

Based on the Libyan SOTER map, soil classes for each landform unit of the Al Jabal Al Akhdar and Benghazi are shown in Figure 3.6 and Table 3.1.

Ben-Mahmoud (2001) stated that Rhodoxeralfs, Haploxeralfs (Xeralfs) and Haprendolls (Rendolls) which are the most common soils of Al Jabal Al Akhdar region are susceptible to water erosion, where 88% of the region is subject to water erosion.

OMU survey (2005) deter determined the soil profile at each site of the 53 sampling sites. For each profile, terrain and land surface features which included: site altitude, topographic position, slope, the form and direction of the slope, vegetation cover density, the dominant plant species, rock outcrops, surface rocks, rock fragments, surface crust, surface cracks, human activity and land use are described. In addition, soil physical and chemical properties were determined.**Error! Reference source not found.** indicates those properties that are affected by degradation processes and those that have an impact on vegetation cover degradation (Table 3.3).

The study concluded that, in general, the soils of Al Jabal Al Akhdar are characterised by a high percentage of stone and rock outcrops. It was found that more than 45% of the total representative sites are very rocky and shallow soils with depths of ≤ 0.50m characterised nearly 50% of them. This is due to

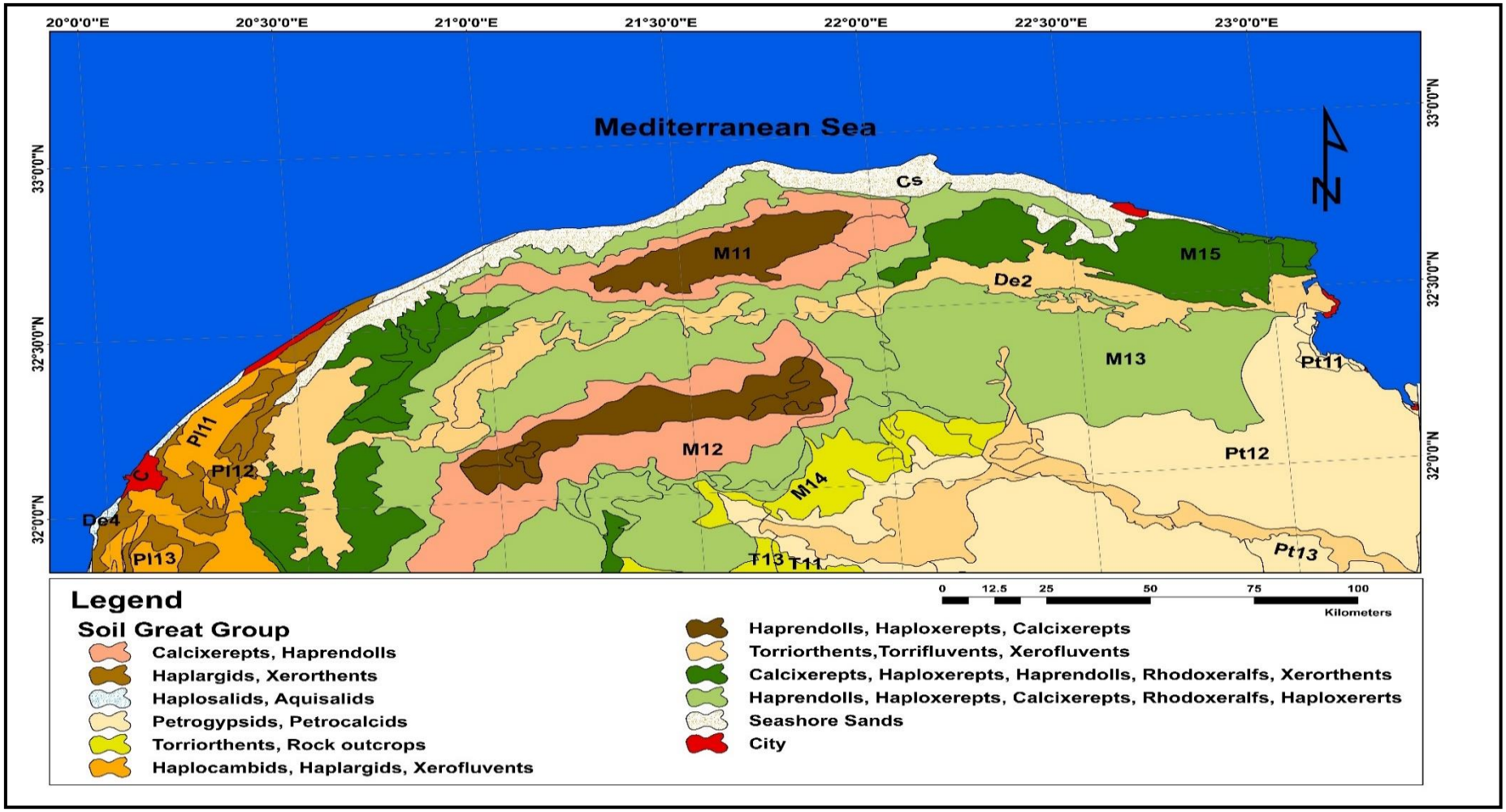

Figure 3.6 Soil Great Groups of the Al Jabal Al Akhdar and Benghazi Landforms (source: (LWGA and ACSAD, 2005)**)**

Table 3.1 Soil Classification of Al Jabal Al Akhdar and Benghazi regions

(source: (LWGA and ACSAD, 2005; OMU, 2005)**)**

Order	Suborders	Great Group	Source
Entisols	Orthents	Torriorthents	OMU/Libyan SOTER
		Xerorthents	Libyan SOTER
	Fluvents	Torrifluvents	Libyan SOTER
		Xerofluvents	Libyan SOTER
Aridisols	Salids	Haplosalids	Libyan SOTER
		Aquisalids	Libyan SOTER
	Cambids	Haplocambids	Libyan SOTER
	Argids	Haplargids	OMU /Libyan SOTER
	Gypsids	Petrogypsids	Libyan SOTER
	Calcids	Haplocalcids	OMU
		Petrocalcids	Libyan SOTER
Inceptisols	Xerepts	Calcixerepts	OMU /Libyan SOTER
		Haploxerepts	OMU /Libyan SOTER
Mollisols	Rendolls	Haprendolls	OMU /Libyan SOTER
	Xerolls	Calcixerolls	OMU
		Argixerolls	OMU
Alfisols	Xeralfs	Rhodoxeralfs	OMU /Libyan SOTER
		Haploxeralfs	OMU
		Palexeralfs	OMU
Vertisols	Xererts	Haploxererts	Libyan SOTER

Table 3.2 Code definition of Libyan SOTER map for Al Jabal Al Akhdar and Benghazi landforms

Landform code	Landform Name	within the study area
North Eastern Mountain Area (M1)		
M11	Al Jabal Al Akhdar Top	Yes
M12	Al Jabal Al Akhdar Shoulder	Yes
M13	Al Jabal Al Akhdar Backslope	Yes
M14	Al Jabal Al Akhdar Fall Face	No
M15	Al Jabal Al Akhdar Toeslope	Yes
North Eastern Plain Area (Pl1)		
Pl11	Benghazi Plain Relatively High Lands	No
Pl12	Benghazi Plain Moderately High Lands	No
Pl13	Benghazi Plain Relatively Low Lands	No
North Eastern Plateau Area (Pt1)		
Pt11	North Eastern Plateau Summit	No
Pt12	North Eastern Plateau Escarpment	No
Pt13	North Eastern Plateau Pediment	No
North Eastern Terrace Area (T1)		
T11	North Eastern Terrace 1	No
T13	North Eastern Terrace 3	No
Depression Areas (De)		
De2	**Wadies and alluvial plains**	
	Wadi Al Muallaq	Yes
	Wadi Al Qattarah	Yes
	Wadi Ar Ramlah	No
De4	Benghazi Sabkha	No
Seashore Plain		
Cs	Coastal Plain	Yes
Urban Area (C)	City	

the vulnerability of the soil to water and wind erosion, especially following the removal of natural vegetation. Generraly, the soil depth of the OMU sample sites anges from 20-110 cm. The results also showed that the soil texture in most sites was silty clay or clay (Appendix Table B.3.1). On the other hand, although the parent material was limestone, most of the soils were non-calcareous. The result also showed that the region includes a variety of soils, where the record of five orders which are Aridisols, Entisolos, Inceptisols, Alifsols and Mollisols, as well as the suborders and great groups (Table 3.1).

Table 3.3 Soil physical and chemical properties recorded in the OMU study (2005)

Soil property		Affected by degradation	Causing vegetation degradation
Physical properties	Soil Depth	✓	✓
	Soil type		✓
	Bulk density (Gm/cm^3)	✓	✓
	Soil moisture content %	✓	✓
Chemical Properties	pH		
	EC (mmhos cm^{-1})		
	$CaCO_3$		
	Soluble Cations (meq L^{-1})	✓	
	Soluble Anions (meq L^{-1})	✓	
	Available Phosphorus (ppm)		
	SOM %	✓	✓
	*ESP %	✓	✓
	*SAR	✓	✓
	*Mean EC_e (dS $m^{-1)}$	✓	✓

* Calculated by the author

The soil studies show that the rocky and shallow soil in the natural forest (NF) areas of the Al Jabal Al Akhdar confirm that the environmental conditions that help to support trees and shrubs are often confined to the area associated with

the root zone. Such conditions mean that the removal of the tree cover and subsequent soil erosion will lead to the modification of critical conditions and the creation of a new micro-ecosystem that can no longer support climax vegetation cover or is not suitable for the restoration the natural vegetation cover to its previous state or component. The changes in the micro-ecosystem may partly explain the decline in the number of Juniper trees that do not re-grow after being removed or exposed to fires. Therefore, any disturbance of the ecosystems of the Al Jabal Al Akhdar area will result in severe consequences due to the fragility of these ecosystems, which are no longer balanced but will stabilise after some time to a relatively low level than in previous periods (i.e. the plant succession is toward retrogressive changes). The OMU study (2005) also confirmed that the general landscape of large areas of the Al Jabal Al Akhdar has become barren or covered by invasive species (non-indigenous) after being occupied by evergreen natural forests because of the ecosystem disturbance.

3.1.4 Vegetation of Al Jabal Al Akhdar

The Al Jabal Al Akhdar region in Libya and the High Atlas Mountains in Morocco are the two principle centres of plant diversity of the southern Mediterranean region. Al Jabal Al Akhdar has distinct environmental characteristics associated with it, being the only evergreen forest of its kind in the area along the east and south Mediterranean Basin from the Atlas Mountains to the Levant (i.e. the easternmost part of the Mediterranean Sea) (Abusaif, 2013). Despite covering <1% of total Libyan area, it contains approximately 50 % of the total endemic plant species in Libya and is rich in medicinal and aromatic plants (Al-idrissi et al., 1996; Radford et al., 2011). The vegetation of the Al Jabal Al Akhdar has been described in Chapter 2 (See Section 2.2.1.2).

OMU (2005) selected 53 representative sampling sites of Al Jabal Al Akhdar region for detailed botanical studies. The differences in the distribution and density of plant communities and their habitats determine the location of the plot and the number and size of each sampling site to be representative of the state

of these plant communities in these sites. For each plot, plant height and its canopy diameter were measured in order to calculate vegetation cover. Tree trunk diameter was also measured. The number of seedlings of each species was counted to assess natural regeneration potential. In addition, data about cut, infected and dead trees were recorded. The percentage of coverage and composition, the density, frequency, coverage and productivity of annuals and the annual growth of the trees and shrubs were estimated. The study also included the collection and classification of plant species throughout the study period (2003-2004).

The results show that biodiversity is generally good at Al Jabal Al Akhdar, where a total of 500 species of plants belonging to 447 genera and 107 families were confirmed. A total of 46 endemic species were confirmed.The sample of Natural Forest (NF) studies included 50 species of trees and shrubs (Appendix Table B.2.1); however, not all plant species of Al Jabal Al Akhdar have covered in the OMU (2005) sampling sites. Natural Forest studies showed that the density of wood species is increased with the increase in the altitude as the number of trees and shrubs was 2517 ha in the first terrace, 3757 ha in the second terrace and 4391 ha in the third terrace, respectively. The overall average area of trees and shrubs was 3805 ha. In the Lamloda - Ras'Helal site, the number of woody plants was >11,000 per ha. On the other hand, Natural Forest studies have shown that some species have become rare, such as *Salvia fruticosa* Mill. ‘Greek sage’ and *Myrtus communis* L. ‘Common myrtle’ and some are restricted to specific places, such as *Arbutus pavarii* Pamp. the ‘Libyan Strawberry-tree’.

The OMU study showed that *Juniperus phoenicea L.* ‘Phoenicean juniper or Arâr’ is the most common tree species frequent; it is found across all the 53 studied sites. The average number of trees was 486 per ha, whereas *Pistacia lentiscus* L. the ‘lentisk or mastic tree’ was found in 93% of the sample sites with 685 shrub ha^{-1}. However, OMU (2005) confirmed that Juniper forms 80% of the plant community of studied sites. These results indicate the importance of these two species.

For planted forest (PF) sites, the results show that *Pinus halepensis* Mill. the ‘Aleppo pine’ is growing well and out-performs imported species such as *Eucalyptus camaldulensis* Dehnh. the ‘Red river gum’ and *Acacia cyanophylla* Lindl. the ‘Blue-Leafed wattle’ in wood volume, basal area and annual growth rate as well as natural regeneration capacity.

For Rangelands (RL) sites, the south natural forest area showed that the productivity of these rangelands was degraded due to overgrazing of the local plants, which increased the pressure on natural forests as sources of grazing. Grazing the trees and shrubs, in the rangelands, has led to a decline in the number of palatable species including *Artemisia herba-alba* Asso. ‘white wormwood’ and *Thymus capitatus* (L.) Hoffmanns. & Link ‘Conehead-thyme’ (Appendix Table B.2.2) and the degradation of many other species. The results also showed that the productivity of fodder crops such as *Periploca laevigata* Ait. ‘Periploca of the woods’, *Hordeum* spp ‘wild barley’ and *Rhamnus oleoides* Lam. ‘Blue-Leafed wattle’ in forest lands was good.

Appendix Table B.2.2 shows the plant species that were included in the OMU study (2005) indicating the binomial name of the species, common name, family, life span, natural vegetation cover type that species was found in, in addition to the use of the plant (Batanouny et al., 2005; OMU, 2005; El-Darier and El-Mogaspi, 2009; Louhaichi et al., 2011).

3.1.5 The Al Jabal Al Akhdar land use

Land use refers to how humans have used the land, focusing on the “functional role” of land for “economic activities” (Liping et al., 2018). The Al Jabal Al Akhdar region includes urban and as well as rural areas; therefore, the use of land differs markedly. The land use in the Al Jabal Al Akhdar is classified in the following four sections.

3.1.6 Agriculture

Over the centuries, societies residing in the Al Jabal Al Akhdar region have practised cultivation whereby the lands were converted to cultivate crops such as wheat, barley, chickpeas, lentils, and beans. Planted fruit trees including figs,

grapes, apples and olive and palm trees also are cultivated (El-Barasi and Saaed, 2013). Almost all agriculture is rainfed because of the deficiency of surface water in the region. However, there has been a shift towards the cultivation of irrigated crops such as vegetables including potatoes, cucumber, tomatoes and onions (OMU, 2005). This is due to the exploitation of underground water resources; Table 3.4 shows the number and area in ha of the rainfed and irrigated farms (LGAI, 2007). Greenhouses also are established on a total of 1287 ha to cultivate these types of horticultural crops, distributed between Drena, Al Jabal Al Akhdar and Al Marj districts (60, 243 and 984 ha, respectively) (LGAI, 2007).

Table 3.4 Number and area (ha) of agricultural fields by the source of irrigation in Al Jabal Al Akhdar region (source: (LGAI, 2007))

District	Source if irrigation								Total	
	Rainfed		Tube Well		Dam/Spring		Undefined			
	No.	Area	No.	Area	No.	Area	No.	Area	No.	Area
Derna	1,749	13,930	1,142	2,794	413	490	36	731	3,340	18,395
Al Jabal Al Akhdar	4,818	26,765	1,095	3,465	282	5,076	262	1,442	6,457	36,748
Al Marj	5,312	126,236	397	4,485	100	608	289	5,720	6,098	137,049
Total	11,879	166,931	2,634	10,744	795	6,624	587	7,893	15,895	192,192

3.1.7 Grazing

Nomadic pastoralism is considered to be a traditional activity for the people of the Al Jabal Al Akhdar region. Grazing is practited by approximately 37% of the local communities (OMU, 2005), with 916,776 head of livestock consisting of sheep, goats, cattle and camels (Table 3.5) (LGAI, 2007).

Table 3.5 Number of grazing livestock (head) in the Al Jabal Al Akhdar region of Libya (source:(LGAI, 2007))

Area	District	Sheep	Goat	Cattle	Camel	Total
Libya		3,987,651	1,080,420	/	/	5,068,071
Al Jabal Al Akhdar Region	**Derna**	147,542	52,879	6,492	3,923	210,836
	Al Jabal Al Akhdar	178,978	63,020	18,004	3,938	263,940
	Al Marj	354,538	64,817	19,023	3,622	442,000
Total of the Region		681,058	180,716	43,519	11,483	916,776

El-Barasi et al. (2013) listed the palatable plants (Table 3.6), proposing that after intensive browsing most of the palatable perennial plants that are considered as being the best for erosion control, are unable to complete their life cycle. Therefore, these species are replaced by ephemerals, which are less efficient than the perennials in terms of their production and have comparatively weak root systems. Elshatshat and Mansour (2014) explained that palatable species in the coastal habitat of the western part Al Jabal Al Akhdar (west the study area) such as *Pistacia lentiscus* 'Mastic tree', *Rhus tripartite* 'Jedari' and *Arbutus pavarii* 'Libyan Strawberry-tree' are targeted by locals when grazing their livestock.

Table 3.6 Palatable family, species and growth form in south Al Jabal Al Akhdar

Family	Species	Life span
Asteraceae	*Artemisia herba-alba*	Perennial
	Cynara cornigera	Perennial
	Echinops cyrenaicus	Perennial
	Centaurea alexandrina	Biennial
	Onopordum spinae	Biennial
	Carthamus lanatus	Annual
Fabaceae	*Retama raetam*	Perennial
	Astragalus hamosus, A. sinaicus, A. intercedens, and A. stella	Annual
	Hippocrepis bicontorta	Annual
	Lotus creticus, and L. Tetragonolobulus	Annual
	Medicago laciniata, M. minima, M. polymorpha, M. turbinata, and M. truncatula.	Annual
	Melilotus indicus, and M. sulcatus.	Annual
	Onobrychis crista-galli	Annual
	Ononis viscosa	Annual
	Trifolium campestre, T. purpureum, T. stellatum, and T. tomentosum	Annual
	Trigonella marittima	Annual
	Vicia monanza, V. pannonica	Annual
Brassicaceae	*Brassica tournefortii*	Annual
	Biscutella didyma	
	Capsella bursa-pastoris	
Rhamnaceae	*Ziziphous lotus*	Perennial
Lamiaceae	*Thymus capitatus*	Perennial
Apiaceae	*Deverra tortuosa*	Annual
Malvaceae	*Malva parviflora, and M. sylvestris.*	Annual/ Perennial
Lantaginaceae	*Plantago lagopus, p. lanceolata, and P. phaestoma.*	Annual

El-Barasi and Saaed (2013) described the movement of livestock during the year as follows; during the winter and spring, the movement is towards the south of the Al Jabal Al Akhdar region, where they graze on annual plants in the rangelands areas. In the summer and autumn, the movement is towards the Al Jabal Al Akhdar natural forest in the north, where they graze on perennial shrubs and the residues of rainfed crops (in the farms of wheat and barley) that have been left un-harvested to feed the grazing livestock. Besides, grazing in the rangelands and natural forest, they graze on fodder in cases of the dry season of the year or the dry year (El-Barasi and Saaed, 2013). Camels graze in areas close to the deserts southern Al Jabal Al Akhdar region (El-Barasi and Saaed, 2013).

3.1.8 Recreation

The Al Jabal Al Akhdar region has unique natural features; the most important of these is the El Kuf National Park, which is considered the most beautiful and diverse natural area in Libya. It is rich in a multitude of natural resources, including mountains, small rocky wadis, plains, beaches, forests, grassland, and sabkhas (saline flats) (LUPA, 2008). In addition, it contains Wadi El Khalij (Wadi Al Khabta), Ras Et-Tin Sabkha and Wetland, Khalij Al Bumbah Lagoon and Sabkhas, and Derna Waterfall (LUPA, 2008). The Al Jabal Al Akhdar region also has been the cradle of many civilisations since prehistoric times. It containing several places of ancient antiquity dating from the Greek era (631-96 BC), the Roman era (96 BC-643 AD), the Arab era (the Islamic era) during the 7^{th} and 8^{th} centuries, the Ottoman era (Turkish era) (1554-1911) and the Italian occupation period (1911-1941) (Figure 3.7). The Al Jabal Al Akhdar area is also close to the sea; therefore, there are many resorts such as Al Haneyah, Alhamama, and Susa (25, 25, and 35 km from Al Bayda city, respectively)

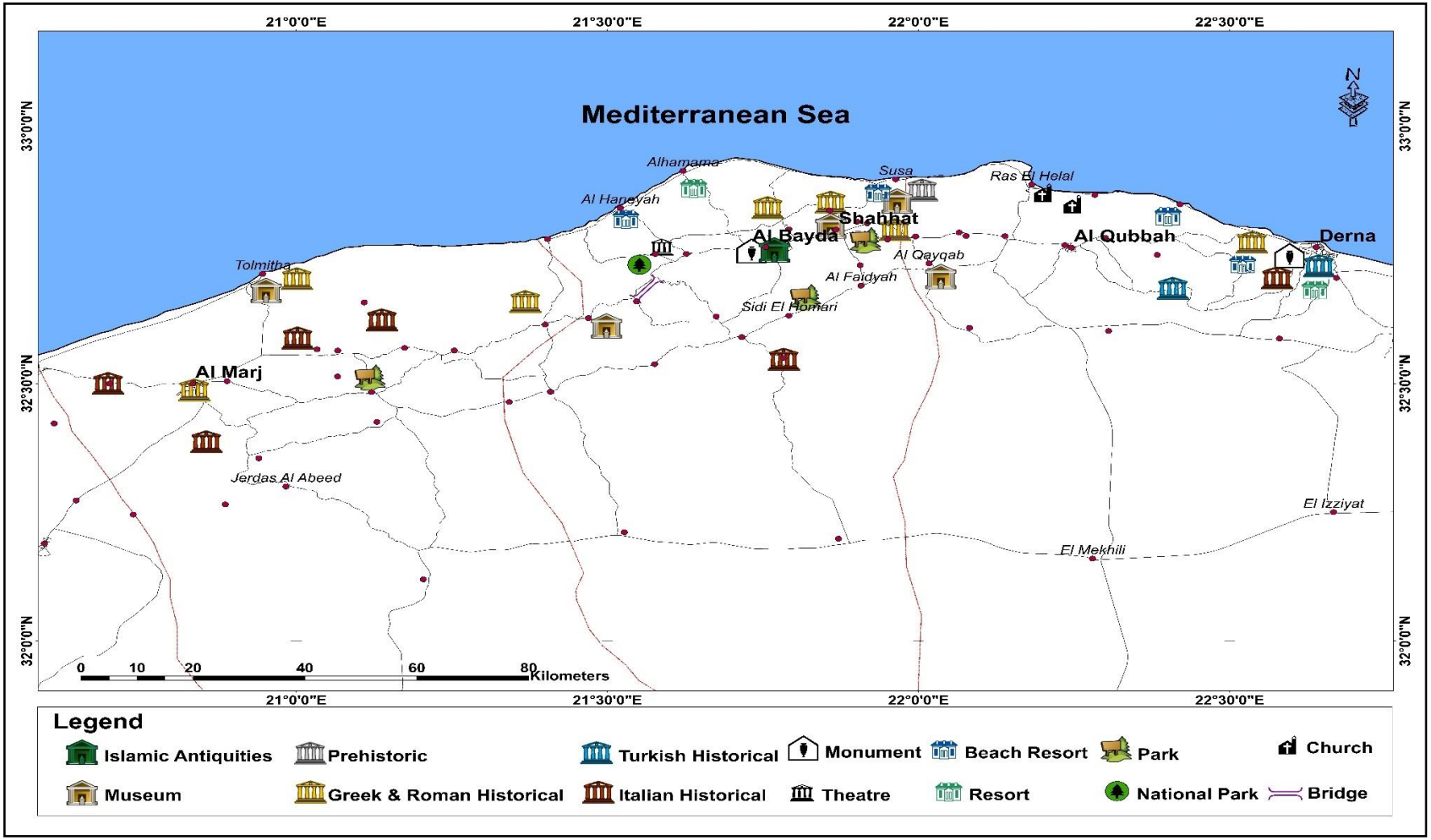

Figure 3.7 Historical and attractive area in the study area (source: (LUPA, 2008))

(LUPA, 2008). With such unique characteristics, the Al Jabal Al Akhdar region has become attractive for recreational activities by local people and people from different regions of Libya (El-Barasi and Saaed, 2013).

The most important archaeological sites are Taucheira “Arsinoe” (Tocra), Ptolemais (Tolmeitha), Barca (Al Marj), Cyrene (Shahhat), Apollonia (Marsa Susa) and Darnis (Derna) (Appendix Figure A.1.2**Error! Reference source not found.**).

3.1.9 Urbanisation

According to the Libyan bureau of statistics and census (LBC-L) (2010), the population of the Al Jabal Al Akhdar region has increased from 152,232 in 1995, to 192,689 in 2006 (+40,457). The last administrative division of Libya, in 2007, divided the country into 22 districts with the Al Jabal Al Akhdar containing three districts namely, Al Marj, Al Jabal Al Akhdar and Derna, The study area is located in the north part of these districts (Figure 3.8). There are five principle cities in the area, namely: Al Bayda, Al Marj, Al Qubbah, Darna, and Shahhat, as well as 47 smaller towns and villages.

A survey of the Al Jabal Al Akhdar Region carried out by the Libyan Urban Planning Agency (LUPA) (2008). It stated that there were spatial obstacles such as routes, high voltage lines and flight zones and natural barriers such as valleys, steep areas and agricultural areas that limit urban expansion. To name a few; the town of Al Bayda, the largest city in Al Jabal Al Akhdar district, has no suitable land for settling the population since it is surrounded by valleys, forests, agricultural land and natural barriers in all directions. As a result of these obstacles, LUPA (2008) suggested to establishing a new city to be built in Sidi El Homari which is located about 20 kilometres south of the city of Al Bayda and will have a capacity to accommodate 60,000 people. The urban growth of the town of Shahhat, the second city in Al Jabal Al Akhdar district, also is limited by the archaeological sites located in the north-west and south-east.

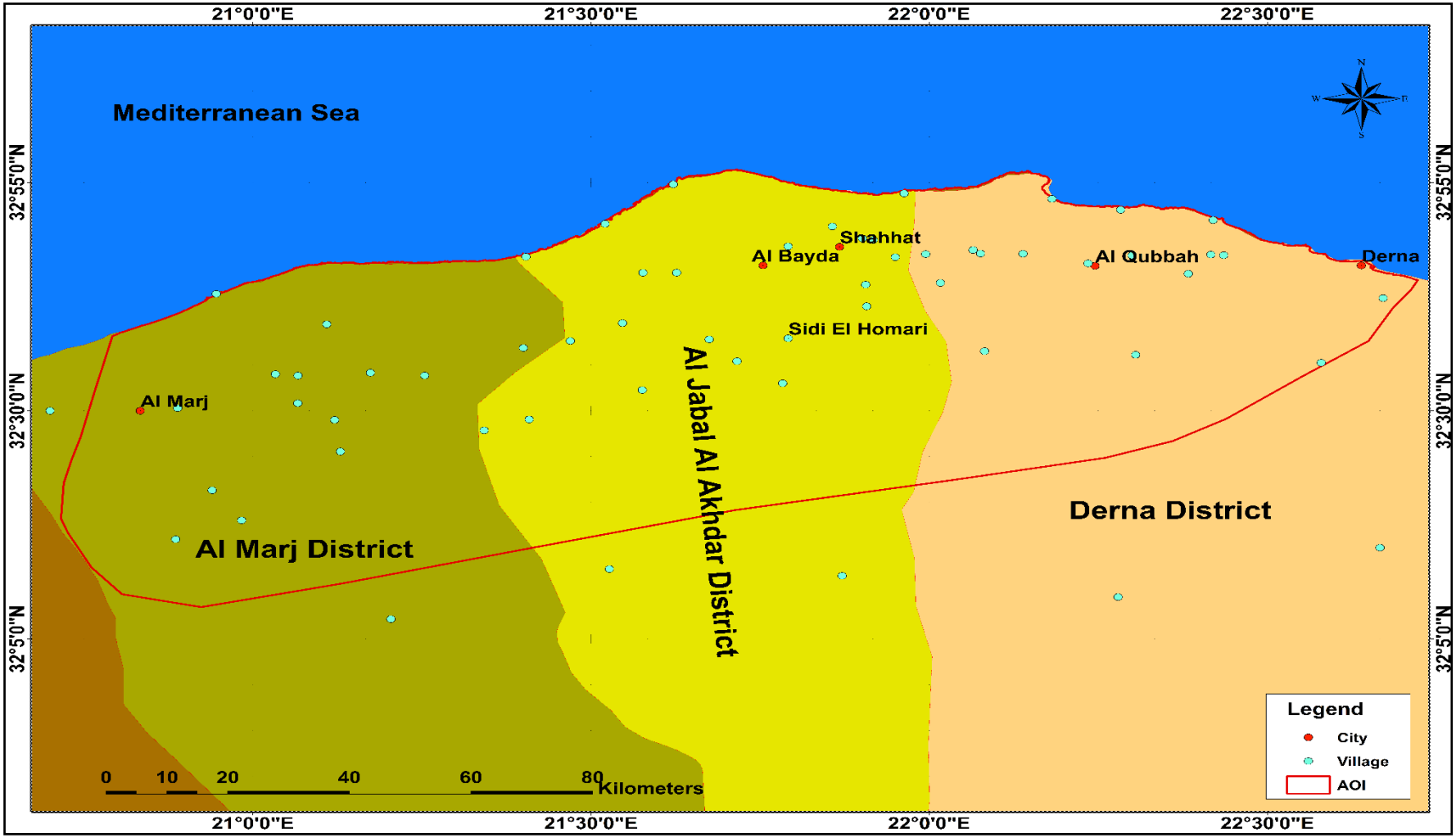

Figure 3.8 Cities and villages of the study area

On the other hand, the town is surrounded by agricultural land to the north and forest areas to the south and a series of valleys to the east and west. Therefore, LUPA (2008) suggested establishing all the new urban areas south of the existing city in order to preserve the archaeological sites and agricultural lands. This area can be called "New Shahhat" and is proposed in an area completely independent of "old Shahhat".

Moreover, both of Al Bayda and Shahhat are defined in the Cyrene Declaration in 2007 as the Al Jabal Al Akhdar protection zone, which aims to protect the cultural and natural areas. For Derna district, the district has topographical characteristics from the coastline to mountains, valleys, and desert plains. The vegetation includes forests of the Mediterranean type and desert vegetation. Derna, the largest city in the district, takes its shape, morphology, and the direction of city expansion on an east-west oriented topography. However, its future growth will be limited by restrictions imposed by the fact that it is confined between the mountain slope in the south and southwest and the edge of the plateau in the east and south-east. The Al Marj district is considered the most important agricultural production areas in the Al Jabal Al Akhdar region. The future growth of the Al Marj, the biggest city in its district, therefore, is restricted by the fact that it lies in the most valuable agricultural land in the whole country.

3.2 The relationship between the dominant plant species and physico-chemical soil properties

Based on OMU (2005) results, dominant perennial species of each site was determined. For example, Kirissah site was classified as Natural Forest which covered 17.8% of the total site area (Appendix Table B.2.1). The site is dominant by *Juniperus phoenicia* L. which forms 58.9% of the plant community.

The dominant species data were then linked with the soil properties data determined for each site (Appendix Table B.2.2 and Table B.3.1). This soils data included soil classification (order and great group), soil texture, SOM% and ESP%, as shown in Table 3.7.

As a consequence of this interpretation (Table 3.7), it can be observed that *Hammada scoparia* (Pomel) Iljin grows in non-sodic to sodic soils where ESP is 2-21% with low SOM (2-5%) as well as shallow soil (<60cm).

By reviewing the OMU (2005) botanical survey site data (Appendix Table B.1.1), it can be confirmed that *Hammada scoparia* (Pomel) Iljin is a rangeland plant found in three sites. The first site is El Nador-El Mekhili (non-sodic soils) with 49.2% of vegetation cover. *Hammada scoparia* (Pomel) Iljin alone covered only 3.64 % of total site area and formed 27.5% of the plant community. The second site is Wadi Al Mahja-Kholan (sodic soils), where the plant community covered 22.3% of the total area. *Hammada scoparia* (Pomel) Iljin alone covered 19.8 % of the total site area and formed 88.9% of the plant community. The third site is El Hesha (sodic soils) with only 20.5% of vegetation cover. *Hammada scoparia* (Pomel) Iljin alone covered 8.23% of the total site area and formed 40.2% of the plant community. Interpretation of the OMU, (2005) botanical data provides an indication of the degradation status of each of the 53 sites.

Table 3.7 Dominant Species in the study area, and properties of the associated soil

Dominant Species	Soil Order	Soil Great group	Terrace	Soil Depth (cm)	Soil texture	SOM%	%ESP
Arbutus pavarii Pamp.	Alfisols	Palexeralfs	3	20, 80	Clay, Silty Clay Loam	2-3	2-4
Cistus sps	-	-	2	20	Clay Loam	5	2
Cupressus sempervirens L.	Mollisols	Calcixerolls	1, 3	20, 40	Clay Loam Sandy Loam	2-4	1
Hammada scoparia (Pomel) Iljin	Entisols	Torriorthents	2, 3	20, 40,55	Clay, Loam	2-5	2-21
Juniperus phoenicea L.	Mollisols, Alfisols, Inceptisols	Calcixerolls, Haprendolls, Haploxeralfs, Palexeralfs, Rhodoxeralfs, Haploxerepts, Calcixerepts,	1, 2, 3	20-110	Clay, Loam, Clay Loam, Silty Clay, Silty Loam, Sandy Clay loam.	1-11	1-9
Pinus halepensis Mill.	Mollisols, Aridisols, Inceptisols	Argixerolls, Haprendolls, Haplocalcids, Haploxerepts	3	35- 45, 70	Clay Loam, Silty Clay Loam.	2-8	1-2
Pistacia lentiscus L.	Alfisols, Mollisols	Haploxeralfs, Rhodoxeralfs, Calcixerolls	1, 3	35, 40, 90	Clay, Silty Clay Loam	4-9	0-4
Quercus coccifera L.	Alfisols	Rhodoxeralfs	2	45	Clay	4	7
Stipa capensis Thunb.	Aridisols	Haplocalcids	3	40	Clay Loam	4	2
Thymus capitatus Hoff. et Link.	Inceptisols, Aridisols	Haploxerepts, Haplocalcids	3	45, 100	Clay Loam	5-9	3-4
Viburnum tinus L.	-	-	3	20	Loam	4	3

3.3 **Summary**

This chapter has provided a general background to the Al Jabal Al Akhdar region. It has also provided a summary of its climate, soil, vegetation, and human activities regarding their land use. Furthermore, this chapter provided a link between the soil results and dominant species of the botanical survey.

Due to the unstable political and security situation in Libya, the 53-sampling sites and their associated data of OMU survey (2005) have been adopted as an alternative, pragmatic approach to fieldwork (see Section 4.1.4), and used In as follows:

- To determine the area of the study area, by delineating a boundary surrounding these 53 sites (see Section 4.1.4).
- To classify Landsat satellite imagery where the 53 sites were used to ground truth the vegetation (see Section 4.2.3).
- To obtain the long-term NDVI time series from Google Earth Engine (GEE) (see Section 4.2.4).
- To obtain climate data from the Global Climate Monitor (GCMon) where the sampling sites location were used instead the ground stations (see Section 4.1.1).
- To study the impact of climate on natural vegetation cover over time (see Section 4.3.3).
- To evaluate the ability of “Machine learning” to predict the natural vegetation cover types in Al Jabal al (see Section 4.3.4).

The following chapter, Chapter Four, describes the methodology that was used to address the aim of the current study.

4 METHODOLOGY

This chapter provides the method and data sources used to accomplish the research aim of the study. It also presents the software and tools that were used for image processing, modelling, statistical analysis and prediction of the natural vegetation cover types.

This research consisted of experiments relating to the prediction of land use land cover (LULC) change and land use type (LU). Appropriate data (such as satellite imagery and climate data) for these experiments were collected, processed and stored in suitable formats. This chapter provides details regarding data sources, image processing and modelling that were used to address the aim of this research. The methodology adopted for the present work is summarised in Figure 4.1, portraying the workflows associated with assessing temporal and spatial changes in natural vegetation cover and the identification of climatic and anthropogenic disturbance factors affecting changes in natural vegetation cover. The chapter also presents a prediction model of natural vegetation cover type through the application of a novel machine learning software approach.

4.1 Data Sources

The current study examines the changes in the natural vegetation cover of a particular area (i.e. the study area") located in Al Jabal Al Akhdar north-east Libya. Chapter 3 provided a description of the study area and the OMU, (2005) survey, which was conducted in 2003-2004. Data from this survey has been used to provide primary key data for this study. The temporal period of this study spans from 2004 to 2016, and spatially some 53 sample site

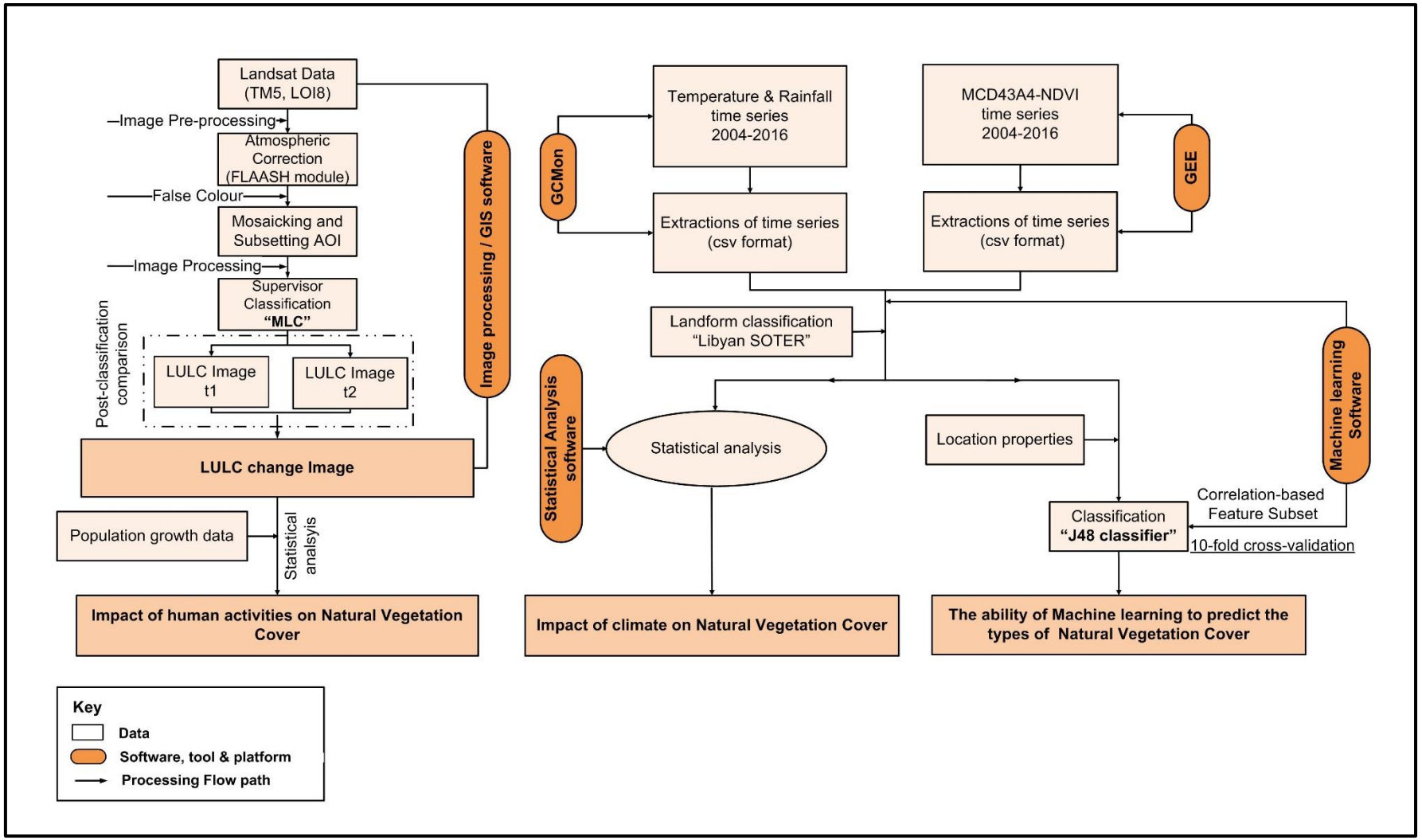

Figure 4.1 The general conceptual workflow chart of the thesis (Source: Author)

were used to provide ground-truthing and to determine the study area boundary.

To achieve the aim of the current study, a process of collection of suitable data was required, with an assessment made in terms of the availability and reliability of this data. The project benefitted from satellite data made available as a free resource; for example, cloud-free multi-temporal Landsat images were obtained for the stuady area.

The modelling approach is dependent on representative thematic data. The datasets included climate, population, infrastructure, vegetation and soil data, as well as satellite imagery, collected from several sources. The principle data forms collected were classified, as shown in Table 4.1. Each theme is detailed with its source, availability, collection processes and its use, described in the following sub-sections:

Table 4.1 Principal data classification

<table>
<tr><th>Theme</th><th>Source</th><th>Type/Format</th></tr>
<tr><td rowspan="2">LULC</td><td>Satellite imagery:
I- Landsat satellite imagery</td><td>Raster image file</td></tr>
<tr><td>II- MODIS/MCD43A4-NDVI</td><td>Spreadsheets (e.g. XLS/ XLSX) / Raster image files</td></tr>
<tr><td>Slope and Topography</td><td>DEM</td><td>Raster image file</td></tr>
<tr><td rowspan="2">Climate</td><td>GCMon.</td><td rowspan="2">Spread sheets (e.g. XLS/ XLSX)</td></tr>
<tr><td>LNMC</td></tr>
<tr><td>Population</td><td>BSC-L</td><td rowspan="4">Data associated with the OMU Report was translated and then converted to spreadsheets (e.g. XLSX)</td></tr>
<tr><td>Vegetation</td><td>OMU</td></tr>
<tr><td rowspan="2">Soil</td><td>OMU</td></tr>
<tr><td>Libyan SOTER</td><td rowspan="2">Vector GIS file (e.g. KML)</td></tr>
<tr><td>Infrastructure</td><td>LUPA</td></tr>
</table>

4.1.1 Climate data

The North-East of Libya has a number of climatic monitoring stations (Synoptic), in addition to some sub-stations which provided a single climate element, such as rainfall or temperature. The main stations that cover the study area are DarnahDerna, Benina , Al Marj and Shahhat stations (Figure 4.2). All the data from those stations up to 2010 were obtained from the Libyan National Meteorological Centre (LNMC). However, since the uprising in 2011, no climate data from the ground stations have been registered. For the sub-stations, three rainfall gauges (Figure 4.2) Altamimy, Umm Alrazam (, and Faydyia do have data, but only with varying and incomplete recorded date periods. Table 4.2 shows the attributes and available data of the main stations and rain gauges.

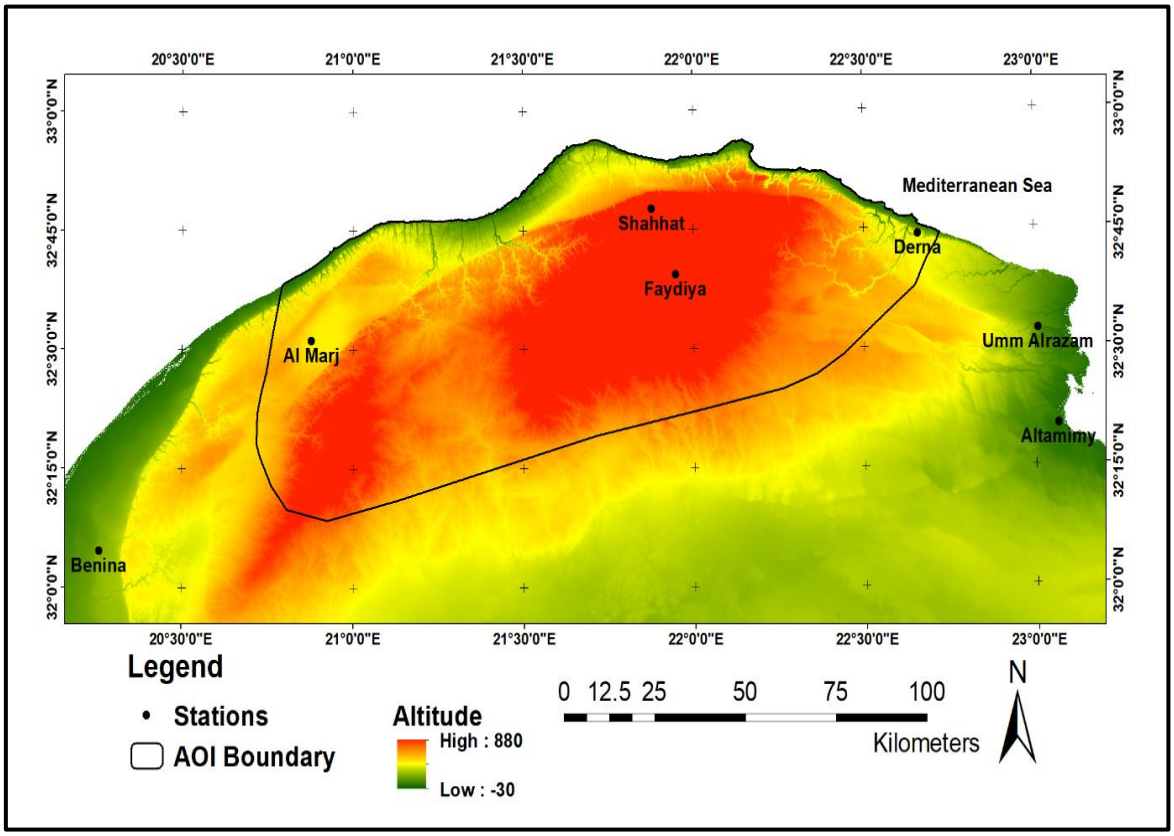

Figure 4.2 The study area with the weather stations

Figure 4.2 and Table 4.2 of the Ground station (GS) and rain gauges show the lack of empirical data, both spatially and temporally. A pragmatic approach was needed to secure suitable meteorological data for study area. The use of gridded satellite-derived climate estimates was considered as an effective means to overcome this issue. Remote satellite-derived meteorological data were available from a range of sources. These included National Oceanic and Atmospheric Administration (NOAA), NASA climate mission, and the Tropical Applications of Meteorology using SATellite data and ground-based observations (TAMSAT), established by the University of Reading at http://www.tamsat.org.uk. In addition, other sources included the Centre for Hydrometeorology and Remote Sensing University of California (CHRS RainSphere), which belongs to the University of California, Irvine (UCI) (USA) at http://rainsphere.eng.uci.edu/ (Table 4.3) (CHRS RainShere, 2016), and Global Climate Monitor (GCMon), which is generated by the University of Seville Climate Research Group at http://www.globalclimatemonitor.org/ (Table 4.3) (GCMon, 2016; Camarillo-Naranjo et al., 2018).

Table 4.2 The attributes and available climate data of the GS and rain gauges of the Al Jabal Al Akhdar

ID	Station Name	Latitude	Longitude	Altitude (m)	Rainfall	Temperature
1	Benina	32.07818	20.25912	129	1945-2010	1945-2010
2	Al Marj	32.51981	20.87869	335	1961-2005	1989-2005
3	Shehhat	32.79487	21.87764	621	1945-2010	1945-2010
4	Derna	32.73756	22.65866	26	1945-2010	1945-2010
5	Altamimy	32.33500	23.06700	10	1960-2000	-
6	Umm Alrazam	32.53500	23.00900	58	1983-2000	-
7	Faydiya	32.65700	21.94800	846	1960-1992	-

Table 4.3 Summary of the avalilabilty of the CHRS RainSphere and GCMon data and format

Websources	Perciptation		Temperature	
	Available ata	Available format	Available ata	Available format
CHRS RainSphere	1- a historical satellite observation with data from 1983 up to date	several formats based on the domain selected such as Portable Network Graphic (PNG)), and data (e.g. comma-separated values (CSV)) formats (Figure 4.3 ‘a’).	A historical data (yearly, monthly).	A graph presented in a temperature curve (Figure 4.3 ‘b’).
	2-Future IPCC projection where the data from 29 Coupled Model Intercomparison Project (CMIP5) models with data up to 2100			

Table 4.3 Summary of the avalilabilty of the CHRS RainSphere and GCMon data and format (continued)

Websources	Perciptation		Temperature	
	Available ata	Available format	Available ata	Available format
GCMon	Monthly and annual timescale with a spatial resolution of 0.5°. 1- From January 1901 to December 2012 are vailable from the Climate Research Unit (CRU TS3.21 version), at the University of East Anglia (UK)	A range of formats for data download, e.g. CSV or XLSX for downloading the data as a point (Figure 4.3‘c’), or as a CSV, XLSX, shapefile, Keyhole Markup Language (KML) placement format for the data, or as a KML, TIFF or JPG format for the image portraying the study area bounding box.	Monthly and annual timescale with a spatial resolution of 0.5°. 1. from January 1901 to December 2012 are vailable from the Climate Research Unit (CRU TS3.21 version), at the University of East Anglia (UK)	A range of formats for data download, e.g. CSV or XLSX for downloading the data as a point (Figure 4.3‘c’), or as a CSV, XLSX, shapefile, Keyhole Markup Language (KML) placement format for the data, or as a KML, TIFF or JPG format for the image portraying the study area bounding box.
	2- From January 2013 up to present are available from the Global Precipitation Climatology Centre (GPCC) First Guess precipitation dataset		2- Fom January 2013 up to present are available from Global Historical Climatology Network-Monthly (GHCN-CAMS).	

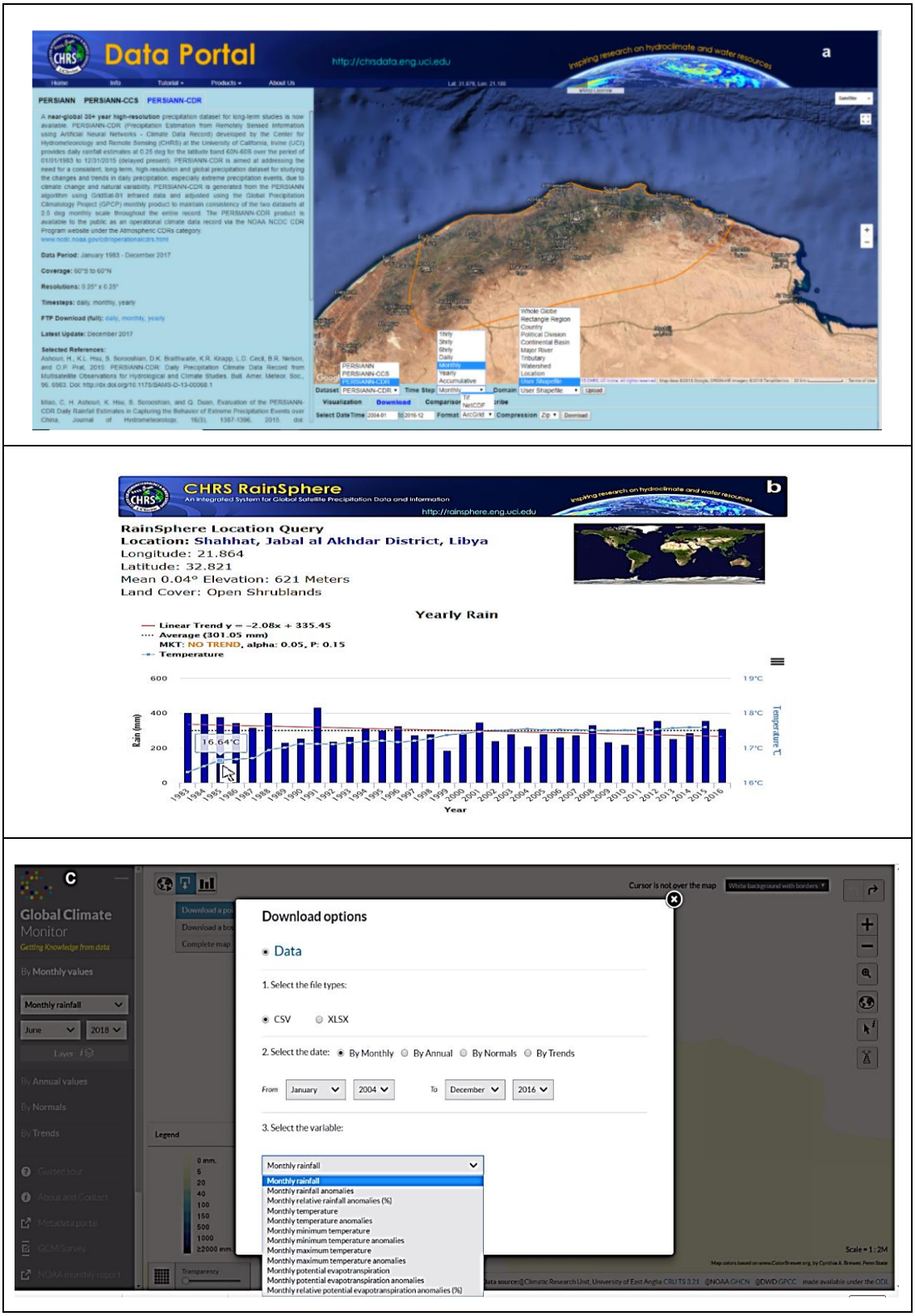

Figure 4.3 An example of climate data that can be obtained from CHRS RainSphere (a), CHRS RainSphere graph (b), and GCMon for a given point (c).

Annual rainfall and temperature of 1983 to 2016 and 1901 to 2016 were obtained from CHRS RainSphere and GCMon respectively for the stations of the Al Jabal Al Akhdar (Figure 4.2 and Table 4.2) in order to undertake statistical comparisons between both sources and GS data. These were then used to estimate rainfall and temperature data for the years (2011-2016) when, GS data for the study area was unrecorded, using the Non-Parametric Mann-Whitney tests. These were then used to investigate whether the rainfall and temperature of CHRS RainSphere and GCMon exhibited higher or lower values than the GS Values for the study area (Hadi and Tombul, 2017). For rainfall data (seven stations (Table 4.2)), the Mann-Whitney statistic results showed that the mean difference between the GS and CHRS RainSphere was significant ($P<0.05$) for all stations except Benina. Likewise, the results showed that the mean difference between the GS and GCMon is significant at the 0.05 level for all stations except Benina and Al Marj. The result of this analysis indicated that the two datasets were not intercomparable, and a future strategy would be required to form a coherent meteorological representation of the study area.

For temperature data (Four stations (Table 4.2)), a Mann-Whitney statistic test was undertaken to examine the mean difference between the GS and CHRS RainSphere. The results indicated a significant difference ($P<0.05$) for Shahhat and Al Marj stations, while the difference was insignificant between Benina and Derna. Similarly, the results showed that the mean difference between the GS and GCMon for all stations was significant ($P<0.05$)l, except Benina. A further hypothesis was tested assuming that GS data and CHRS RainSphere or GCMon data were not equal. is the hypothesis was rejected or accepted if the mean difference is significant at the 0.05 level.

Even though CHRS RainSphere and GCMon were not equivalent to GSs data (except some stations as results show); however, one of these sources have to be used as an alternative climate data source because of the lack of stations and data for the period post-2010. For the current study, therefore, GCMon was used as the rainfall and temperature data source for the period 2011-2016 (the

unrecorded years) as it provides the monthly temporal scale of both rainfall and temperature data to estimate the GS values of unregistered years. While CHRS RainSphere specialises in rainfall data only and thus as such was not used.

In order to produce a climatic map of 1986-2016, shapefiles of the 30 years of the monthly rainfall and monthly temperature for the GS were developed. This step aimed to interpolate rainfall and temperature values from each year. Practically, and based on the preliminary results, using such a technique requires a sufficiently dense network of stations. Keblouti et al. (2012) compared three methods of spatial interpolation, Inverse Distance Weighting (IDW), Splining and Ordinary Kriging, for annual rainfall values collected from 10 rain gauges located in Annaba, eastern Algeria. Keblouti et al. (2012) confirmed that using such models with a low-density measured network failed to introduce a perfect interpolation map. However, gridded satellite precipitation estimates can be used instead as a rainfall source in cases where there is a lack of available data or where there is a low-density network of rain gauges. For instance, Herrmann et al. (2005) used a combination of satellite observations from different sources and GS measurements. This was due to the sparsity and varying reliability of the Sahel (African Sahel) rain gauges and the difficulty in obtaining rainfall measurements to examine the relationship between rainfall and vegetation greenness. Eckert et al. (2015) also used the Climate Research Unit Time Series (CRU-TS) global long-term climate database to detect land degradation instead of meteorological data in Mongolia. Due to the low-density of the GS within the study area, the current study used the GCMon source to obtain the climate data (rainfall and temperature) of each of the 53 OMU sample sites (OMU, 2005) (see Figure 3.2) instead of the GSs to analyse climate variable impacts on natural vegetation change.

4.1.2 Population data

Libyan population and housing census surveys are conducted by the Bureau of Statistics and Census-Libya (BSC-L), at the Ministry of Planning. The last census was conducted in 2006 and is available online at:

http://bsc.ly/?P=5&sec_Id=18&dep_Id=6#29.

In this study, annual predictions of population growth are conducted based on the 2006 Census results. This census was the sixth population, housing and building study in Libya. BSC-L (2016) reported that the next census would be carried out before 2020 to confirm it remains within the UN 2020 round of population and housing census. Given the political uncertainties in Libya, it may not be carried out, and that the 2006 data will remain the most contemporary.

For this study, the population size of the 3 Districts (Al Marj, Al Jabal Al Akhdar and Derna, being districts of the Al Jabal Al Akhdar region) of the periods 1973, 1984, 1995 and 2006 (BSC-L, 2006; LUPA, 2008) (Figure 4.4), were analysed statistically to estimate the population size for the years investigated (2004, 2008, 2010, 2014, 2016) by using a linear regression analysis method. The population data was appended to the shapefiles of the districts to create maps of population using the ArcGIS software 10.3.1.

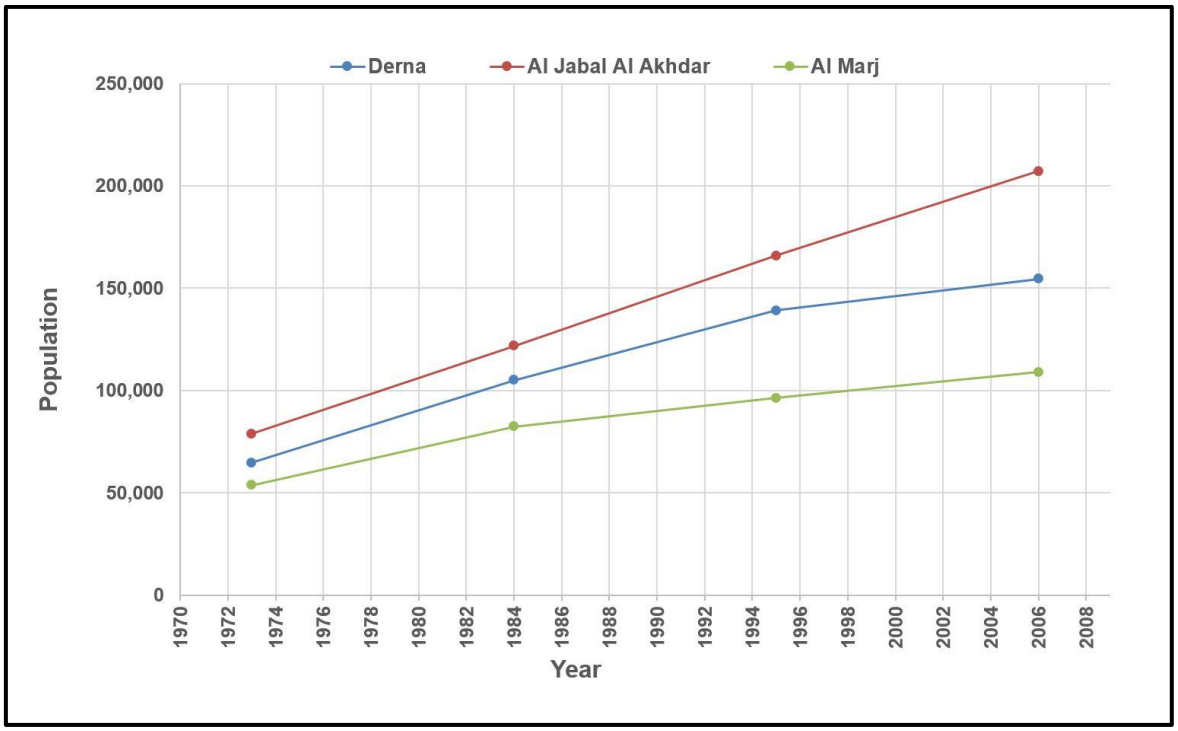

Figure 4.4 The population size of Al Marj, Al Jabal Al Akhdar and Derna districts for 1973, 1994, 1995 and 2006 (Sources: BSC-L, 2006; UPA, 2008)

4.1.3 Infrastructure data

Infrastructure data, referred to here as the transportation network, includes paved and unpaved roads, was obtained as a vector format file produced in 2008 by the Third-Generation Project of planning (3rd GPP) of the Al Jabal Al Akhdar Region. The 3rd GPP is a set of planning processes launched by Libyan Urban Planning Agency (LUPA) in participation with the United Nations Human Development Program (UN-Habitat) (LUPA, 2008), commencing in 2007 and covering the period of 2006-2030. It consisted of several studies that determine economic, social, and spatial strategies, in order to develop various policies and physical development programs for Libya, at national, sub-regional and urban levels. Based on the data from the LUPA (2008), the infrastructure which represented the expanding road network across the years of investigation was digitised from Google Earth (GE) to produce shapefiles to be used as masks, with a view to exclude the actual network from the natural vegetation cover. The infrastructure masks were then added as a layer to the classes layer of the

initial LULC classified images to develop the final classification images of LULC (see Section 4.2.3.2).

4.1.4 Vegetation and soil data

The initial methodology for this study planned to include fieldwork to serve as ground truthing for the satellite imagery interpretation and land classification model training set. However, due to the unstable political situation in Libya, it became apparent that an alternative, pragmatic approach be found. Fortunately, a detailed vegetative and soil data survey was available for the study area, based on a detailed survey conducted by OMU during the spring and summer of 2003 and 2004 (OMU, 2005). Using this data permitted the model training and ground estimation to be conducted against Landsat satellite data where images from the years 2004, 2006, 2008, 2010, 2014, and 2016 were used to classify vegetation of the study area (see Section 4.2.3.2).

For the current research, 53 representative sites from the OMU study were included within the study area, shown in Figure 3.8, with six sites located within Rangelands (RL) and 43 sites within Natural Forest (NF) areas, and four sites in Planted Forest (PF) areas. These 53 sites were georeferenced according to the Universal Transverse Mercator (UTM) projection, with reference to World Geodetic System datum (WGS84) and Zone 34N and converted to GIS format using ArcGIS. Although the spatial extent of the survey area for each site in the OMU survey is known the borders were not spatially delineated. Therefore, the locations of the 53 sites were plotted as points on GE. A boundary that surrounded these 53 sites was then delineated to create a polygon which forms the study area of the current research. By measuring the area within the polygon of the study area, it was determined that this extends across an area of 1,007,148 ha. The polygon was then converted from KML format, which was created in GE, to an ArcGIS vector (shapefile) using ArcGIS geoprocessing tools. This allows in further processing such as clipping and visualisation of the study area. The 53-sampling sites were also used to study the impact of climate on natural vegetation cover (see Section 4.3.3).

4.1.5 Landsat Data

For this study, Landsat satellite imagery with a planar spatial pixel resolution of 30 m was used. These data are available for free download. Cloud-free images can be selected to alleviate the effect of cloud cover (Fan, 2008). Where clouds and water vapour in the clouds in satellite imagery reduce their quality (van Genderen, 2011) through scattering and absorption of the solar radiation (Shen et al., 2015) and obstructs land cover (LC) classification (Sah et al., 2012). Thus, images with cloud and cloud shadow provide different reflectance properties than the actual land cover and produce inaccurate data when used in an automated mapping algorithm (Bhandari et al., 2012). Therefore, it was necessary to remove such cloud effects from the images (Shen et al., 2015) or to choose cloud-free images. Cloud-free images used for this study comprised Landsat 5 Thematic Mapper (TM5) band 2 green (0.52–0.60 µm of wavelength), band 3 red (0.63-0.69 µm of wavelength) and band Band 4 near infrared (0.77-0.90 µm of wavelength), imagery for 2004, 2006, 2008 and 2010 and Landsat 8 Operational Land Imager/Thermal Infrared Sensor (OLI8/TIRS) band 3 green (0.53–0.59 µm of wavelength), band 4 red (0.64-0.67 µm of wavelength) and band Band 5 near infrared (0.85-0.88 µm of wavelength),, imagery for 2014 and 2016 (Table 4.4). The Landsat TM5 and OLI8 imagery were downloaded from

https://landsat-ds.eo.esa.int/app/protected/collections_WRS.php

and https://earthexplorer.usgs.gov/, respectively. Both of the Landsat level -1 sets of imagery were used to classify the study area and detect the changes in LULC classes.

Table 4.4 Summary of Landsat remote sensing data properties for the study area

Landsat Scene Identifier	Sensor Identifier	Path/Row	Acquisition Date	Day of Year	Number of Bands	Radiometric Resolution
LT51830372004240ESA00	TM	183/37	27.08.2004	240	7	8 bits
LT51830382004240ESA00		183/38				
LT51830372006229ESA00	TM	183/37	17.08.2006	229	7	8 bits
LT51830382006229ESA00		183/38				
LT51830372008171ESA00	TM	183/37	19.06.2008	171	7	8 bits
LT51830382008171ESA00		183/38				
LT51830372010064ESA00	TM	183/37	05.03.2010	64	7	8 bits
LT51830382010064ESA00		183/38				
LC81830372014203LGN00	OLI/TIRS	183/37	22.07.2014	203	11	16 bits
LC81830382014203LGN00		183/38				
LC81830372016145LGN00	OLI/TIRS	183/37	24.05.2016	145	11	16 bits
LC81830382016145LGN00		183/38				

In order to derive the Normalised Difference Vegetation Index (NDVI) from the Landsat imagery shown in Table 4.4, the NDVI values were calculated as described in Section 4.2.4. Preliminary results of the NDVI values for the study area, derived from Landsat imagery for the years investigated, are shown in Figure 4.5 and Table 4.5. NDVI results showed high values for vegetation, with an average value approaching +1, meaning fully vegetated (see Table 4.10). However, the use of NDVI here was to examine the impact of climate on natural vegetation cover over the period from 2004 to 2016. Therefore, yearly images are required to generate the annual time series NDVI.

Table 4.5 NDVI values range derived from Landsat imagery from the years investigated

Image date	NDVI values Range
27.08.2004	-0.42 – 0.76
17.08.2006	-0.43 – 0.76
19.06.2008	-0.90 – 0.93
05.03.2010	-0.98 – 0.99
22.07.2014	-0.97 – 0.89
24.05.2016	-0.56 – 0.88

4.1.6 The Moderate Resolution Imaging Spectroradiometer (MODIS)

Initially, Landsat imagery was selected from every other year over the period 2004-2016, where for each of these biannual images, an NDVI assessment was to be undertaken. However, it was ascertained that in 2012, there was no imagery available at all, and in the other years, it not possible to source cloud-free imagery from the same date, so preventing the creation of intercomparisons of NDVI. It was, therefore, necessary to seek another source of satellite imagery, such as MODIS to calculate monthly NDVI from 2004 to 2016. Consequently, a decision was made to use Google Earth Engine (GEE) as a resource to access satellite imagery and to provide robust online geoprocessing of these data. Google Earth Engine is an online, cloud-based platform that facilitates access to high-performance computing resources for processing geospatial big data. It is designed to assist researchers to publish their results efficiently for use by other researchers, policymakers, NGOs, field workers, and even the public (Gorelick et al., 2017). It is also designed to be used by remote sensing experts (Schmid, 2017).

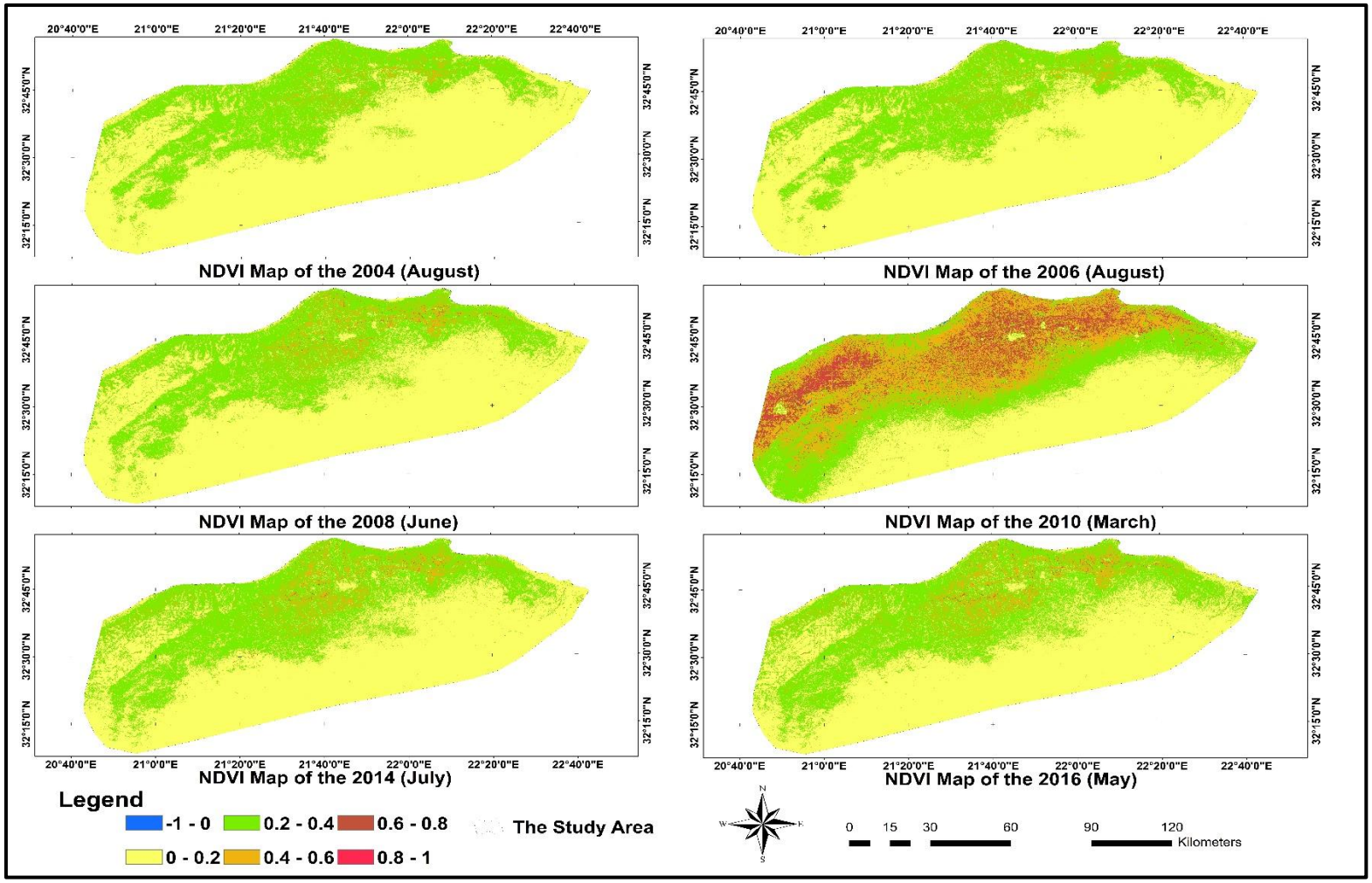

Figure 4.5 Spatio-temporal NDVI of the study area, derived from Landsat imagery

The data catalogue of GEE is built from Earth-observing remote sensing imagery, including the whole Landsat archive as well as complete archives of data from Sentinel 1-2, MODIS and ASTER (Gorelick et al., 2017; Schmid, 2017). The data catalogue also contains data relating to climate, land cover and topography. In GEE, users can also upload their private data via the **Re**presentational **S**tate **T**ransfer (REST) interface, using either a browser-based approach or via direct command-line tools, sharing the results with other users or groups as applicable (Gorelick et al., 2017). The resultant data can be then represented or plotted in time series graphs using GEE (Schmid, 2017), and the data and images are then downloadable for offline use (Gorelick et al., 2017; Schmid, 2017). In GEE, all the datasets can be obtained and processed in a JavaScript and Python application programming interface (API) (Schmid, 2017). The code editor, which is a web-based Integrated Development Environment (IDE) using the JavaScript API (GEE, 2018). In the GEE code editor, the complex spatial analysis can be modelled and visualised rapidly (GEE, 2018). The analysis undertaken in GEE is described in full in Section 4.2.4.

In this study, the MODIS combined 16-day NDVI product that is generated from the MODIS/MCD43A4 (500 m spatial resolution) reflectance composites were used; it is available every eight days from 18.02.2000 to 14.03.2017 in the GEE (GEE, 2017). The monthly MCD43A4-NDVI time series data for the 53 OMU sample sites within the study area over the time period 2004-2016 was developed in GEE and downloaded; see Section 4.2.4. The monthly MCD43A4-NDVI data was used to examine the impact of climate on natural vegetation cover.

4.1.7 The Digital Elevation Model (DEM)

A one arc-second for global coverage (30 meters) resolution Digital Elevation Model (DEM) was downloaded from https://earthexplorer.usgs.gov/. In order to derive elevation, slope and aspect from the DEM, the spatial analyst tool in ArcGIS was used. The DEM was used to visualise the elevations of the study area.

4.1.8 Soils terrain digital databases (SOTER)

The SOTER project aimed to utilise information technologies to generate a World Soil and Terrain Database, comprising digitised map units and their attribute data, SOTER also provides the required data for improved mapping and monitoring changes to world soils and terrain (UNEP et al., 1995). SOTER was described by van Engelen and Dijkshoorn (2013) as “a land resource database with a focus on soil and terrain conditions”. Where the landscape can be stratified by dividing it into landform classes based on its homogeneity (Mulder et al., 2011; Pourabdollah et al., 2012).

The SOTER database/vector format for the study area was clipped from Libyan SOTER that was generated by Libyan Water General Authority “LWGA” and The Arab Centre for the Studies of Arid Zones “ACSAD” (2005) and used to examine the impacts of topography and climate factors on the natural vegetation cover for each landform class (see Section 4.3.34.3.3). Detail of the landscape that included landform classes/relief and dominant soils of the Al Jabal Al Akhdar and Benghazi regions are shown in Appendix Table C.1.1. Figure 4.6 shows seven classes of Landform within the study area based on the Libyan SOTER database and the 53 sites of the OMU’s survey presented as their LULC.

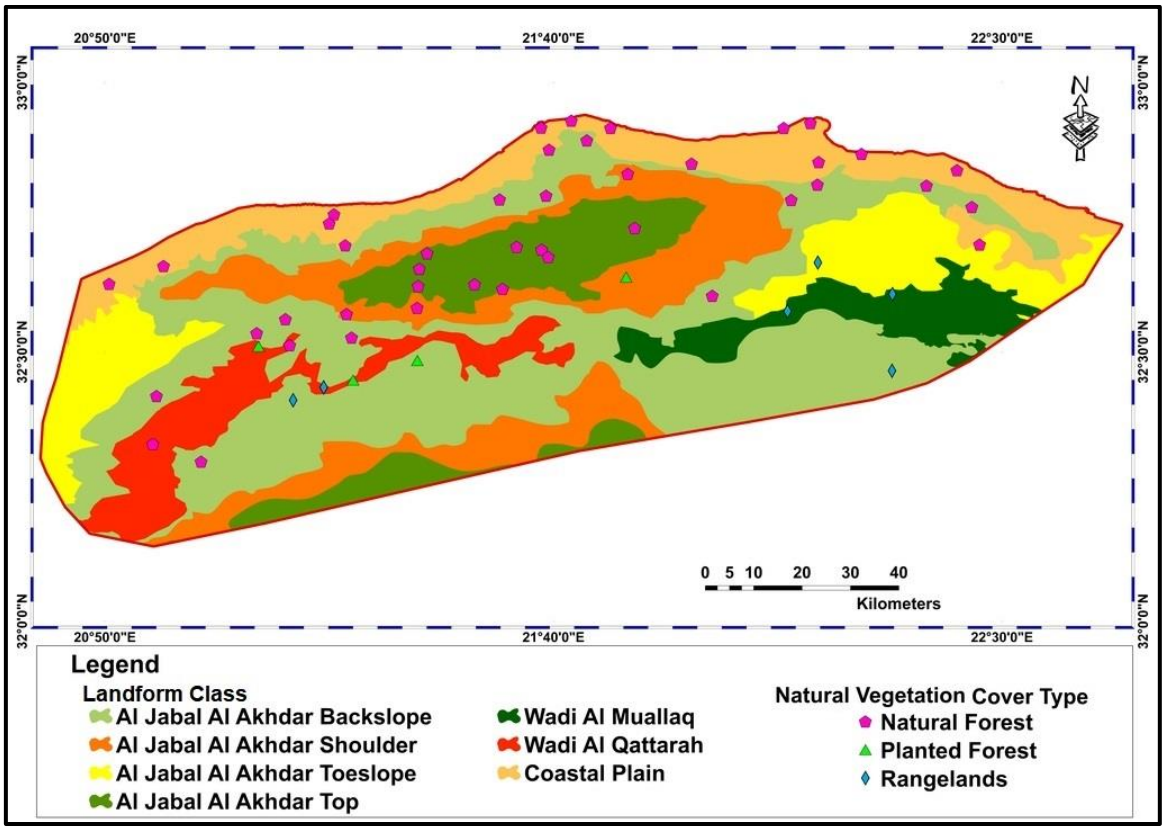

Figure 4.6 Landform classes of the study area based on Libyan SOTER map (Source: LWGA and ACSAD (2005))

4.2 **Image Processing**

Pre-processing of satellite images is required before vegetation attributes data can be extracted from remotely sensed imagery, whereby vegetation extraction refers to the process of obtaining the information of vegetation by interpreting satellite images (Xie et al., 2008). The aim of image pre-processing is to remove image 'noise' and to increase the interpretability of image data, especially when using time series imagery and several scenes to encompass an study area - as in the current study where two Landsat scenes each year were used over the period 2004-2016 (Table 4.4). Data pre-processing is essential to harmonise these images spatially and spectrally (Xie et al., 2008). Radiometric correction is also further necessary for some applications such as image mosaicking (Yang and Lo, 2000; Al-fares, 2013). All the image processing, classification and production of final images and mapping were conducted using two software suites: first was an image processing software (Environment for Visualizing

Images ENVI, Version 5.4) and secondly GIS software (ArcGIS, Version 10.3.1).

The Landsat satellite constellation provides high resolution images of the entire Earth every 16 days. All the images used were already geometrically corrected to level one terrain correction (L1T) (USGS, 2017), where L1T offer the highest levels of spatial accuracy. Therefore, no geo-rectification or image-to-image registration was required (Wingate et al., 2016), and the Landsat scenes were resampled to the WGS 84 Zone 34N geographic coordinate system. Atmospheric correction, mosaicking the tiles for each year and clipping the data to the selected study area were conducted using image processing software.

4.2.1 Atmospheric correction

Satellite images contain radiometric errors which can result from the effect of the atmosphere (Richards, 2013), where the atmosphere absorbs and scatters light as a function of wavelength (Shaw and Burke, 2003). Removing atmospheric errors in an essential step for studies encompassing multiple dates and sensors (Schowengerdt, 2007); it is considered a crucial pre-processing step (ENVI version 4.7, 2009; Hadjimitsis et al., 2010). Since the Landsat images (Table 4.4) are taken from six years (2004, 2006, 2008, 2010, 2014, and 2016), and by different sensors (Landsat TM and OLI8/TIRS) those used for monitoring LULC changes of the study area, it was necessary to remove the atmosphere impact from Landsat data. ENVI ver.5.4 offers Fast Line-of-sight Atmospheric Analysis of Spectral Hypercubes (FLAASH) as an atmospheric correction module (Figure 4.7). Wavelengths were corrected in the visible through near-infrared and shortwave infrared regions, up to 3 µm (Milas et al., 2015). FLAASH requires some information related to scene and sensor including the scene centre location (Lat/Lon), the average ground elevation of the scene, the sensor type, the sensor altitude, and the flight date and time. Such data allows FLAASH to determine the suns position and the pathway of its light through the atmosphere to the ground surface and back to the sensor (ENVI version 4.7, 2009). For the FLAASH atmospheric model used in this study, because the data of the Landsat are from the spring and summer months

(Table 4.4), Mid-Latitude Summer (MLS) was used to run the correction (Milas et al., 2015).

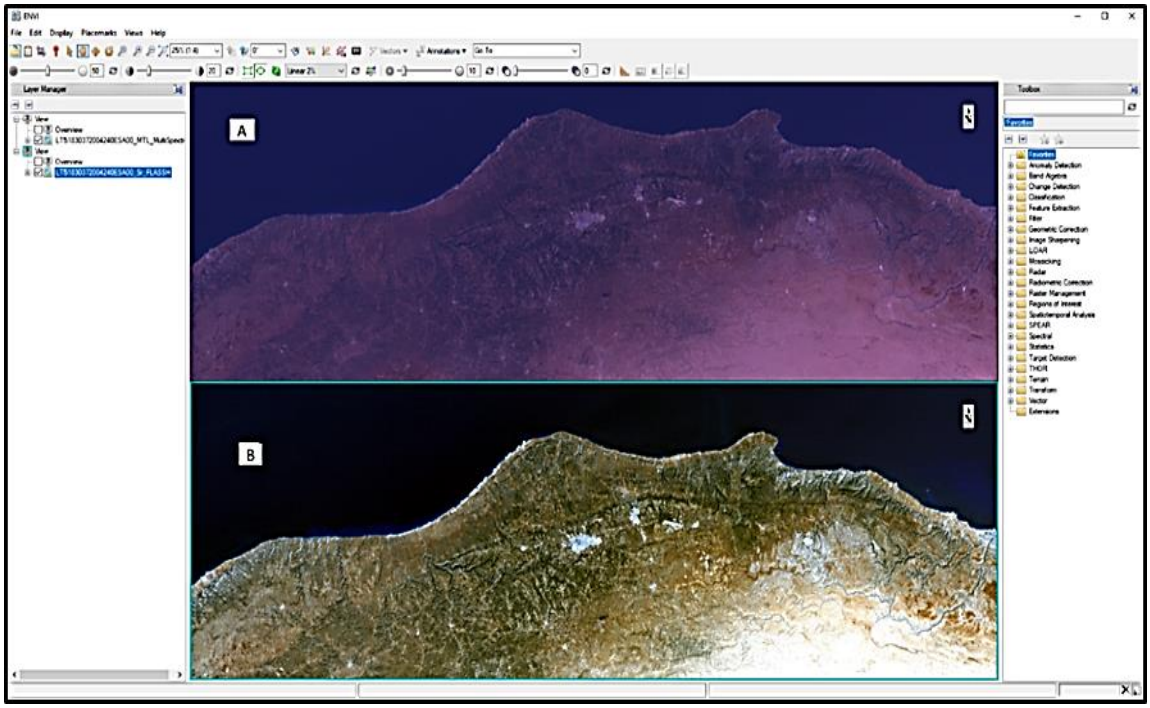

Figure 4.7 Image processing in the ENVI software for 2004, (A) without and (B) with atmospheric correction (FLAASH) (Source: Author)

4.2.2 Mosaicking and Clipping the study area

To encompass the study area, 2-Landsat scenes for each year were required. In order to mosaic the 2-Landsat scenes' images (path/row: 183/37, and 183/38) of each year of the years investigated, seamless mosaics were generated using image processing software. Seamless mosaics allow finer image control and better fusion of the image edges (Jiang et al., 2017). The respective scenes were mosaicked only after the corrections described in the previous sections had been applied. Then, the study area was clipped from the whole data set of the mosaicked scenes by a process known as subsetting (Figure 4.8). The objective of performing the subsetting procedure was to reduce subsequent processing time; and to decrease the local geographical extent that increased the spectral variations of the actual ground surface features (Al-fares, 2013).

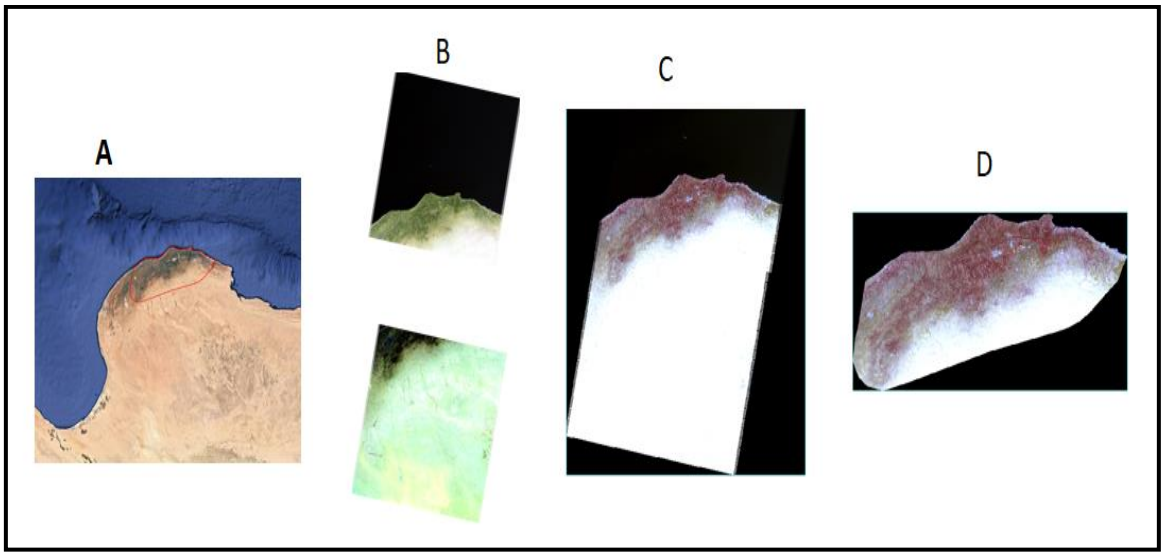

Figure 4.8 The study area (A) Landsat 5 images for the study area acquired in August 2014 (path/row 183/37 and 183/38) (B) Mosaicking the 2 tiles (C) and Clipping the study area (D) (Source: Author)

4.2.3 Classification

Classification of remotely sensed digital data necessitates extracting the differentiated classes or theme categories from the raw image (Ismail and Jusoff, 2008). Based on the 2003-2004 OMU botanical and soil dataset (see Section 0), the LULC classification comprises three classes which are an NF, PF, RL on which the OMU's survey was focused (see Appendix Table B.1.1). Firstly, each of the 53 OMU sampling locations was classified on the basis of the dominant species of the perennial plant (Step I on Figure 4.9) in an attempt to classify the study area into plant communities/species. Then the study area was classified based on the LULCs (Step II on Figure 4.9) that are utilised in this study.

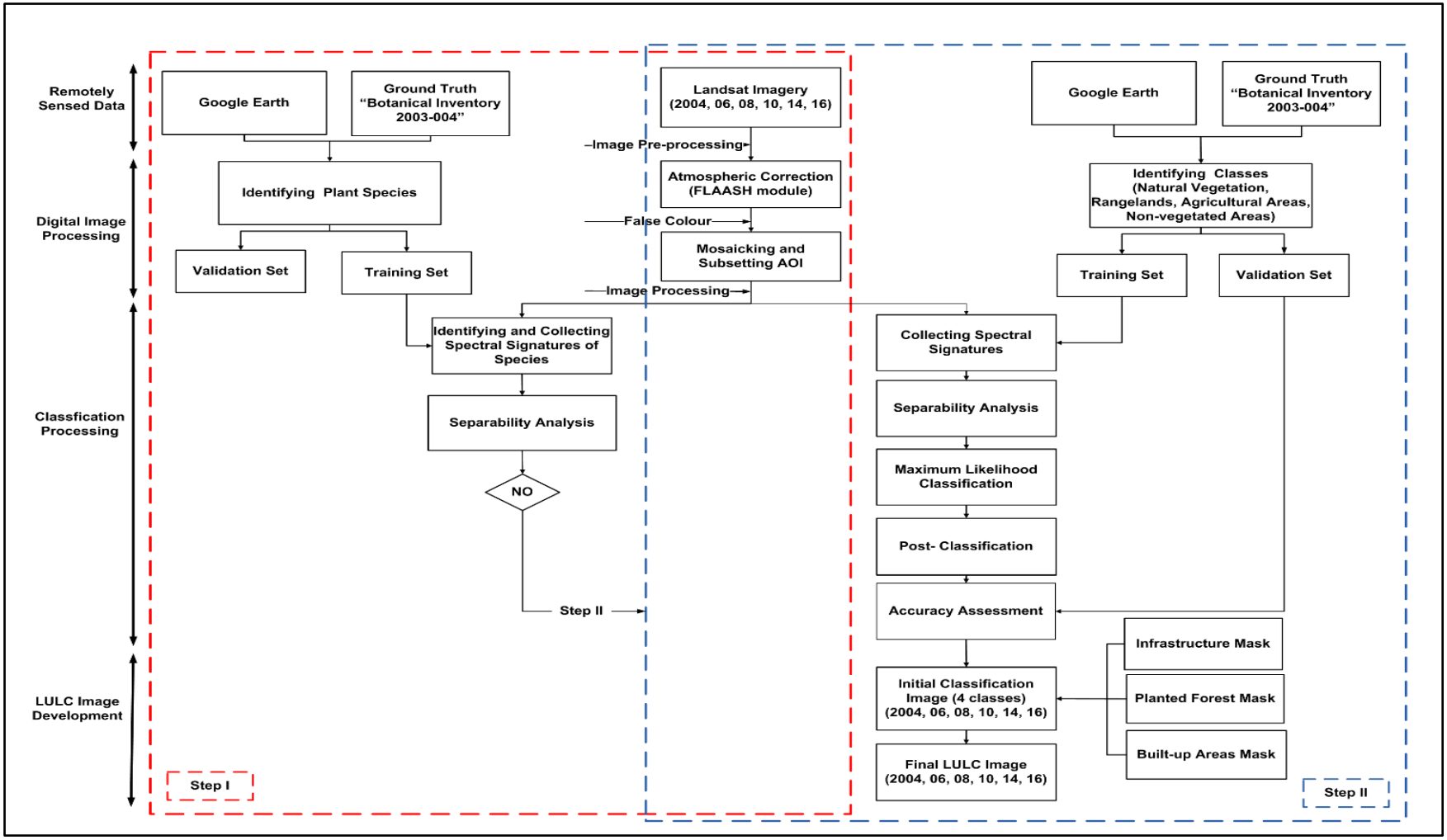

Figure 4.9 Image processing and LULC image production scheme used in the study area

4.2.3.1 Step I of the LULC classification

This approach was undertaken to assess the feasibility of using Landsat imagery to distinguish between plant communities/species. Preliminary work was undertaken to discriminate Juniper trees (*Juniperus phoenicea* L.), which is a climax species and accounts for 70% of natural vegetation cover of the vegetated areas of the study area (OMU, 2005; Suleiman et al., 2014), from other species and other land use types (bare soil, buildings, infrastructure and farms) by extracting the sites that were dominated by Juniper based on the OMU survey (2005).

Five sites were selected, based on % bare soil then increasing % Juniper cover within the plant community (Table 4.6). Subsequently, for each site, a boundary was digitised from GE assuming a representative site area; a shapefile was then created for each site. The shapefiles were used for clipping the selected sites from the 2004 Landsat image data using Image processing software. Juniper trees and all other cover types were identified from ground truthing data (gathered through GE, 2004 date). Spectral coincident plots (SCP's) and the Jeffries-Matusita (JM) distance statistical measure were used for investigating the spectral separability between training classes' signatures.

Table 4.6 Summary of the five selected sites' properties across study area based on the OMU (2005) data

Site Name	Area (ha)	% Bare soil	%Vegetation Cover	%Juniper Cover
Shnaishnn Forest	950	78.3	21.7	98.3
Azzrada	4225	49.5	50.5	21.0
Sidi Al Qarib	190	65.3	34.7	74.3
Arqoob Sidi Hamad	245	70.6	29.4	47.3
Argoob Al Abiad	80	50.3	49.7	31.6

4.2.3.1.1 Graphical representations of separability

SCP as a graphical representation of separability was used mainly to determine the best band combinations for discrimination and to illustrate the range of spectral responses for each class and the amount of overlap between categories. It can also be used to visualise separability between classes.

4.2.3.1.2 tatistical analysis

SCP can be used for rapid data examination if the training classes are separable and non-overlapping; however, it cannot be used to quantify the degree of separation or overlap between classes (Bennington, 2008). JM distance, therefore, was used where the separability values range from 0 to 1414 (see Section 4.2.3.1.2 and Table 4.9).

4.2.3.2 Step II of the LULC classification

In Step II (Figure 4.9), it has been noted that there was an increase in the road network through the natural vegetation areas over the duration of the study (GE visualising). Therefore, to exclude the actual area of the natural vegetation cover, two classes of artificial features were made, infrastructure (IN), and built-up areas (BA). Consequently, seven distinguishable classes of LULC were identified in this study: NF, PF, RL, agricultural areas (AA), non-vegetated areas (NV), IN, and BA (Table 4.7). An initial visual assessment of the results of the Landsat image classification revealed misclassifications that were found between the BA, NV, and IN (road network) due to spectral mixing. A similar misclassification was found between the PF and NF, as species with a similar spectral signature occur in the NF and are used as windbreaks and in reforestation. Therefore, the three classes, BA, IN, and PF, were excluded from the initial classification. For BA (i.e. cities and big villages), IN (i.e. roads network) and PF of the investigated years, shapefiles were produced by digitising each of these LULC from GE. The shapefiles were then utilised as masks, adding the class layers of the initial LULC classification in order to develop the final LULC classification images. Image processing steps and LULC image production of the study area is shown in Figure 4.9.

Table 4.7 Characteristics of Land Use/Land Cover Classes in study area

LULC types	Description
Natural Forest (NF)	Mixed forest land, Maquis formation and scrubs (coniferous and Broadleaf evergreen trees).
Planted Forest (PF)	Forest stands planted mainly by *Pinus halepensis*, in addition to *Eucalyptus camaldulensis* and *Acacia cyanophylla*.
Rangelands (RL)	Herbaceous and shrubs rangeland.
Agricultural Areas (AA)	Field crop , vegetable, fruit trees, and other agriculture crops.
Built-up Areas (BA)	Cities and big villages.
Infrastructure (IN)	Road network, primary, secondary, residential and non-paved roads.
Non-Vegetated areas (NV)	Exposed soil, bare exposed rock, sandy areas, beaches, quarries.

4.2.3.2.1 Ground data (Training and Evaluating sample)

For supervised classification, the primary factor in choosing training sample sites is that all the variability within classes is representative (Al-fares, 2013). Statistically, the number of pixels in each class must be at least 10 times greater than the number of bands. Schowengerdt (2007) and Zhu (2016) noted that in the case of training sites with >10 pixels, the ideal number of sites is 6 out of 10 pixels in each class. Al-fares (2013) mentioned a range of additional sources which can be used to collect training samples such as fieldwork/in situ, fine spatial resolution aerial photographs and satellite images/in-image, and recently, Google Earth (GE). In this study, the ground truth data were collected from GE, based on the OMU soil and botanical survey (OMU, 2005), where polygons of the sites' plots for the NF, RL, AA and NV classes were digitised

and converted to shapefiles using GIS software then exported to an excel spreadsheet. Ground truthing data were divided randomly into training and validation samples using a random number function in excel and sorted into two levels, the first level represented land cover, and the second was randomised in order to create the training (60%) and validation (40%) datasets (Table 4.8) (Al-fares, 2013; Zhao et al., 2016). The Ground truthing data (training and validation datasets) were then converted to shapefile format. The training shapefiles were used to classify the Landsat imagery of the study area by applying the classification workflow tool, and the validation shapefiles were used to evaluate the accuracy of classified images by comparing classified data with reference data in the a tabular form (confusion matrix).

Table 4.8 The number of ground truth samples within the study area

LULC	Total	Training (60 %)	Validation (40 %)
Natural Forest (NF)	227	136	91
Rangelands (RL)	31	19	12
Agricultural Areas (AA)	75	45	30
Non-Vegetated (NV)	94	56	38
Total	**427**	**256**	**171**

4.2.3.2.2 Separability analysis

Spectral classes should always be examined to avoid any significant overlapping of spectral classes in order to find separate spectral signatures (Richards, 2013). Therefore, the spectral classes were evaluated to examine how each selected class remained independent of the others. The importance of the separability is that a perfect (e.g. no or little overlap (Apan et al., 2002)) separability value between classes will improve the accuracy of the classification (Al-fares, 2013). The spectral separability between classes can be computed statistically using several criteria such as the divergence (D), the

transformed divergence (TD), the Bhattacharyya distance (B-distance) and the Jeffreys-Matusita (JM) distance (Mausel et al., 1990; Al-fares, 2013). Murakami et al. (2001), Niel et al. (2005), Yeom et al. (2013), and Hao et al. (2014) reported that the JM distance could offer a more accurate classification than the other three distance criteria. Further, the preliminary results of Step 1 to discriminate Juniper trees from other species and other LULC types by the applying JM distance indicates a perfect separability between natural vegetation cover (represented by Juniper trees) and other LULC types including BA, IN and NV areas. For this purpose, therefore, the JM distance, which is a statistical measure of the distance between pairs of spectral class signatures (i.e. two features), was used. The spectral signatures of training samples were collected for each LULC class, referred to as the ROI in ENVI, and JM distance is computed.

A measurement distance value < 1,000 indicates a poor spectral separability, 1,000-1,900 = limited, and >1,900 is defined as a very good separability (Al-fares, 2013). In ENVI, the values range from 0 to 2.0 where values greater than 1.9 indicate that the class pairs have good separability, and values lower than 1 have poor separability. Lillesand et al. (1989) defined the maximum value of JM distance as 1414, which can be calculated according to Bennington (2008) using the square root of the ENVI output multiplied by 1000 (Table 4.9).

Table 4.9 Range indicators of separability (Bennington, 2008)

Measure of Separability between 2 classes	Equation	Distance Values
Very poor separation (Minimum to Maximum)		0-1000
Poor separation (Minimum to Maximum)	$\sqrt{1.9} * 1000$	1000-1378
Good separation (Minimum to Maximum)	$\sqrt{2.0} * 1000$	1378-1414

4.2.3.2.3 Image classification and accuracy

The Maximum Likelihood Classifier (MLC) and the Minimum Distance Classifier (MDC) are the most general and employed widely supervised classification techniques (Xie et al., 2008; Al-fares, 2013). The MLC is a conventional statistical technique for evaluating the standard LULC (Al-fares, 2013; Zaidi et al., 2017). It is a robust algorithm for remote sensing image classification and offers an accurate classification of results as long as the data have normal distribution (Lu and Weng, 2007; Ismail and Jusoff, 2008; Xie et al., 2008; Fichera et al., 2012; Li et al., 2012; Al-fares, 2013; Corner et al., 2014; Huang et al., 2015). Almost all remote sensing and image processing software packages offer the MLC (Al-fares, 2013), for example, ERDAS Imagine and ENVI software. Therefore, the supervised MLC was utilised in the current study.

For the study area, the MLC was conducted on Landsat 5 (TM5) images of 2004, 2006, 2008 and 2010 and Landsat 8 (OLI8) images of 2014 and 2016. After spectral training samples were selected and evaluated using JM distance, the MLC was run using ENVI software ver.5.4 through using classification workflow. MLC for each pixel in the image is calculated as follows(Richards, 2013; HARRIS Geospatial Solution, 2017a):

$$g_i(x) = 1np(\omega_i) - {}^{1}/_{2}\, 1n|\sum_i| - {}^{1}/_{2}\,(x-\mu_i)^T \sum_i^{-1}(x-\mu_i) \qquad \textbf{4.1}$$

Where:

i = *the* i^{th} *class*

x = *n-dimensional data (where n is number of bands)*

$p(\omega_i)$ = *probability that a class occurs in the image and is assumed the same for all classes*

$|\sum_i|$ = *determinant of the covariance matrix of the data in a class.*

$\sum_i^{-1}$=*the inverse of the covariance matrix of a class*

μ_i=*mean ROI of a class*

A post-classification smoothing algorithm that aims to reduce the ‘salt-and-pepper’ effect, namely where bit errors occur with pixels classified incorrectly appearing in classified classes (Lillesand et al., 1989); thus, a 3-by-3 majority

filter was applied to the classified LULC data (Lillesand et al., 1989; Fichera et al., 2012; Corner et al., 2014). The next step was to evaluate the accuracy of the classification through an accurate assessment and to produce the initial LULC classification images.

The accuracy assessment was applied to all initial LULC maps produced from Landsat 2004, 2006, 2008, 2010, 2014 and 2016 imagery of the study area and through Kappa coefficient calculation applying 'the confusion matrix using the ground truth ROIs' tool in ENVI software ver. 5.4.

4.2.4 Normalised Difference Vegetation Index (NDVI)

NDVI is an indication of greenness (FAO, 2011b), it is one of the most commonly used Vegetation Indices (VIs) adapted to detect the changes in natural vegetation cover (Bannari et al., 1995). Consequently, NDVI shows the quantity of green vegetation that exists in a pixel (Chen et al., 2014); it is also considered as a robust index over a broad range of situations regarding the combination of its formulation and using the highest absorption and reflectance regions of chlorophyll (Chen et al., 2014). NDVI is also proposed as a measure of land cover status as it is included in the UNCCD Minimum set of Impact Indicators (Yengoh et al., 2014). The FAO (2011b) reported that NDVI value decreases according to the decline in vegetation greenness of a given area; therefore NDVI can be considered as an indicator of vegetation health and can be used for monitoring the degradation of vegetation. For example, a dense healthy forest is greener than a degraded forest within the same forest type.

The NDVI is calculated from reflectance measurements in the red and near-infrared (NIR) portion of the spectrum as follows:

$$\mathrm{NDVI} = \frac{\mathrm{R_{NIR}} - \mathrm{R_{Red}}}{\mathrm{R_{NIR}} + \mathrm{R_{Red}}} \qquad \textbf{4.2}$$

Where R_{NIR} is the reflectance of NIR radiation, and R_{Red} is the reflectance of visible red radiation (Franklin, 2001; Govaerts and Verhulst, 2010; Richards, 2013).

NDVI values range from -1 to +1 (Table 4.10) with maximum greenness at NDVI= 1 and less or non-vegetated coverage at zero. NDVI values that are less than 0.1 correspond to buildings and infrastructure, while higher values refer to high photosynthetic activity linked to scrubland, forest, and agricultural (FAO, 2011b).

Table 4.10 Classification ranges of NDVI (Alex et al., 2017)

NDVI	Feature
-1 – 0	Water, snow, cloud
0 – 0.2	Barren land, built up, rock
0.2 – 1	Vegetation

GEE is used to access satellite imagery resources for free by using the MCD43A4-NDVI product as inputs. GEE also provides long-term (>16-year period) and short-term (≤1-year period) NDVI time series for the study area. The GEE Code Editor scripts that were used to extract the NDVI data developed in this study built upon the approach of Ceccato et al. (2016) and GEE (2018).

The first stage was to extract a long-term NDVI time series (13 years for the period 2004 and 2016) for the 53-OMU sites ; The tool was not able to generate the chart of NDVI for all the sites over the13-year period, because of the large number of features and image collections associated with the 53-OMU sites (53 sites and 598 images which formed together over 5,000 elements (Figure 4.10 (a)). The chart of NDVI data can also be extracted for the whole study area that gives the average NDVI of the entire area over the same time period (Figure 4.10 (b)), which are visualised in Figure 4.10 (c). A short-term NDVI time series of (1-year period) for the 53-OMU sample sites was used to generate the NDVI data for each study year in order to prevent this issue (Figure 4.11).

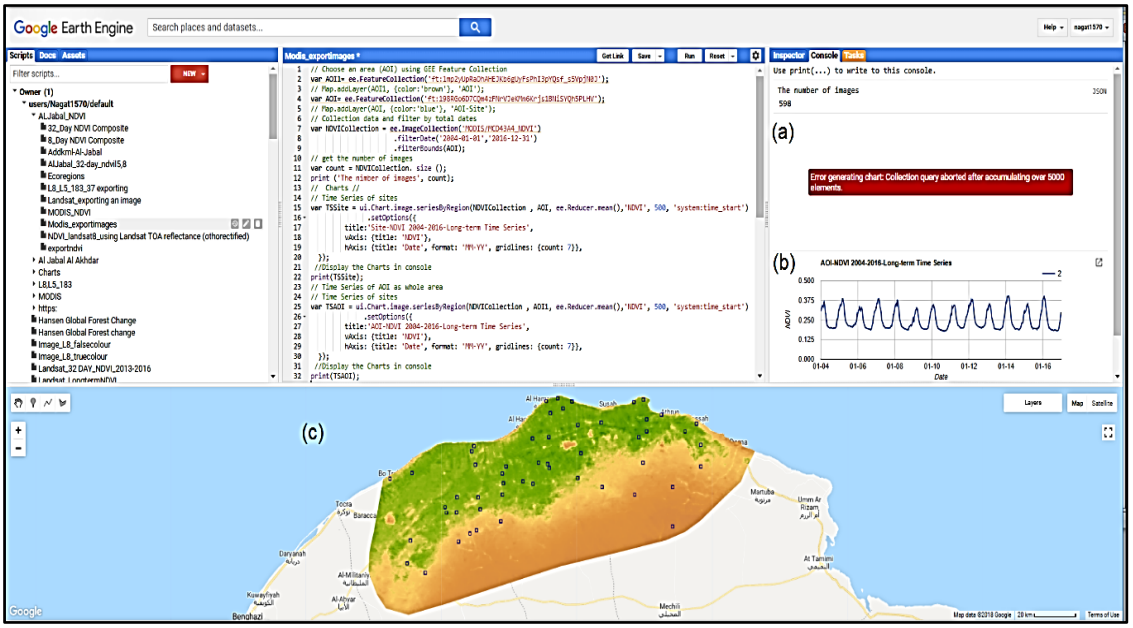

Figure 4.10 The GEE interactive development environment with the NDVI long-term time series

Chart in the GEE Console (a) failed to display the chart of 53-MOU site, (b) the chart of whole study area and (C) NDVI images of the whole study area and 53 OMU sites (shown as squares) as Map layers

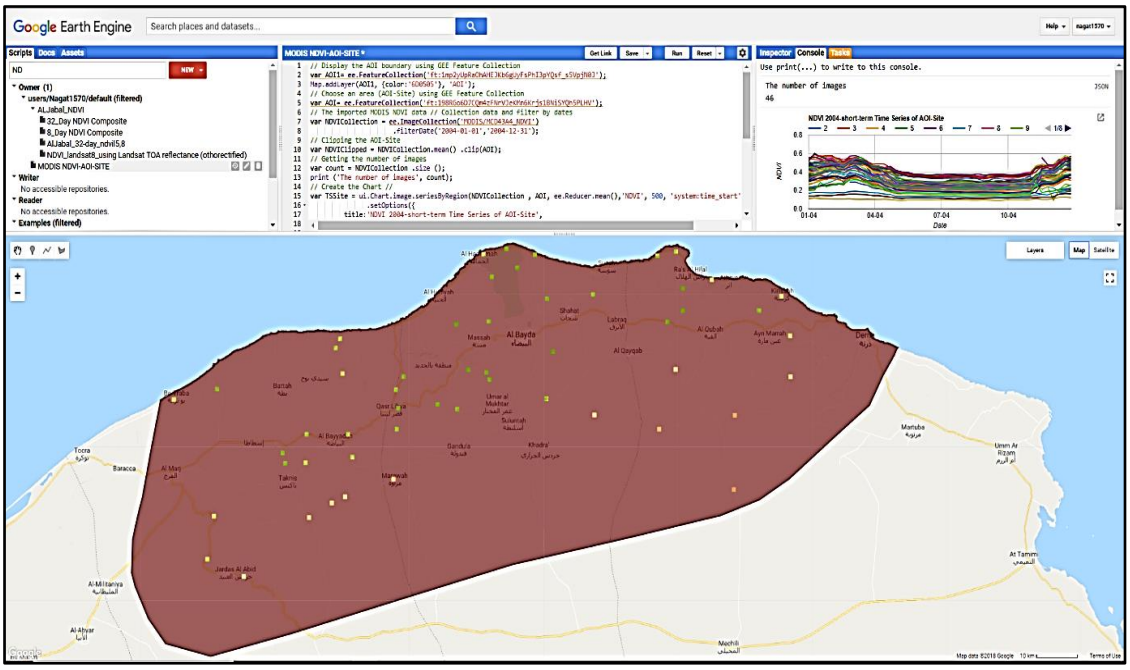

Figure 4.11 GEE Code Editor with an executed script (an example of 2004)

All data then was downloaded from each year of interest (2004–2016) as a CSV-file which was used outside GEE for correlation and regression analyses with rainfall and temperature data to study the impact of climate on the natural vegetation cover of the study area(see Section 4.3.3).

4.3 Modelling

This section is divided into four subsections, each subsection describes the way that the data sources and techniques were employed to address the research questions and accomplish the study objectives.

4.3.1 Change detection

To detect the changes, the changes between two maps with different dates was carried out using cross tabulation.

Post-classification comparison (PCC) is a technique for change detection used to determine the changes in LULC between different years (Corner et al., 2014). PCC requires independently produced classified images (Singh, 1989; Mundia and Aniya, 2005; Mahmoodzadeh, 2007) to compare the two classification outputs using analyst-specified class pairs and to generate a map showing the areas of change (Mahmoodzadeh, 2007). The PCC technique also provides a complete conversion matrix between two classes on both dates (Singh, 1989; Megahed et al., 2015). PCC is the most common approach used when comparing data from different dates, as it can avoid the difficulties associated with the analysis of images obtained at different times of the year and, or by different sensor platforms (Corner et al., 2014). Therefore, PCC is the appropriate method to use in this study to detect the changes of LULC that have taken place within the study area between prescribed time intervals T1, T2…. etc. PCC was performed using the thematic change workflow tool in ENVI software version 5.4 and the classified images for 2004, 2006, 2008, 2010, 2014, and 2016, see Section 4.2.3.2. The flowchart of LULC change detection is demonstrated in Figure 4.12.

The thematic change workflow tool in ENVI ver. 5.4 is a convenient method to estimate the post-classification change dynamics based on change statistics (Haque and Basak, 2017). The tool takes two classification images of the same scene obtained at different times and identifies differences between them. The outcome classification image shows class transitions, for example, from class 1 (i.e. a class at T1) to class 2 at T2 (HARRIS Geospatial Solution, 2017b).

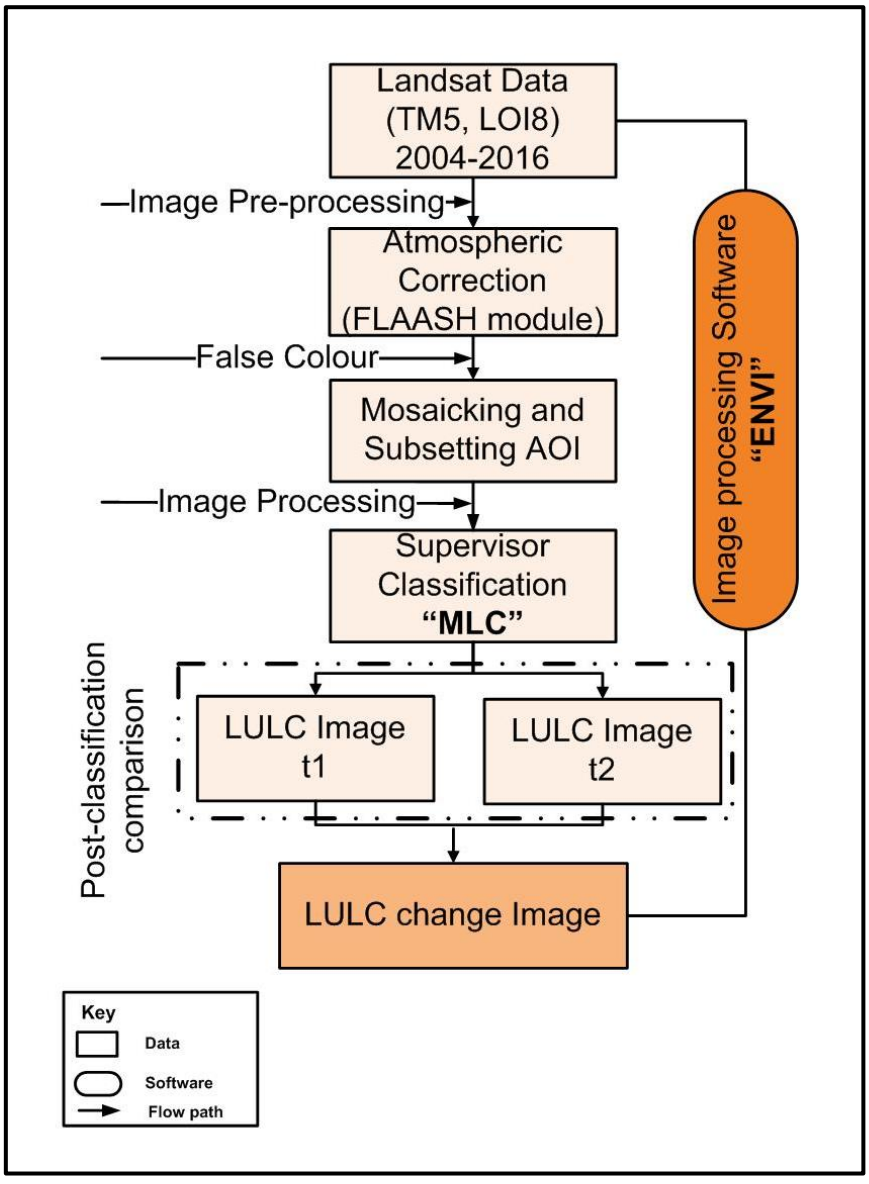

Figure 4.12 LULC change detection flowchart (Source: Author)

The output of ENVI's thematic change workflow tool has 42 unique classes which were introduced as change factors between the two time periods investigated, in addition to the seven original LULC classes (which were kept

without any changes). A majority filter was applied to smooth the output map. At the final stage of the PCC, three resultant files of thematic change were created. The first resultant file is a raster file, the second a vector file with area units in m^2; and the third is a statistical report. The statistical report shows "from-to" changes, area in m^2, and % of the change. The cross-tabulation matrices, were generated using statistical report data for the years investigated. Furthermore, to give an improved visualisation of the transition map, the LULC classes that changed to the same 'new class' were grouped under transition groups (Table 4.11). A Python script was created to group transition types (see Appendix Figure E.1.1 for the full code) by the application of the field calculation tool in GIS software; Figure 4.13 shows an example of the Python script that was written to group the land use class in considering reforestation.

Table 4.11 Transition type of the LULC classes as shown in the statistical report (In general*) classified by group

Transition Group	Reforesta-tion	Rangelands Expansion	Agricultural Recession	Agricultural Expansion	Urbanis-ation	Disturbed Lands
Transition Type	PF →NF	NF→RL	AA→NF	NF→AA	NF→BA	NF→NV
	RL→NF	PF→RL	AA→PF	PF→AA	PF→BA	PF→NV
	BA→NF	BA→RL	AA→RL	RL→AA	RL→BA	RL→NV
	IN→NF	IN→RL	AA→BA	BA→AA	IN→BA	AA→NV
	NV→NF	NV→RL	AA→IN	IN→AA	NV→BA	BA→NV
	NF→PF			NV→AA	NF→IN	IN→NV
	RL→PF				PF→IN	
	BA→PF				RL→IN	
	IN→PF				NV→IN	
	NV→PF				BA→IN	

* Note: In ENVI, all the potential "from- to" changes are provided in the statistical report of the PCC.

```
def Recode (class_t1, class_t2):
  if (class_t2=="Planted Forest"):
     if (class_t1=="Natural Forest" or class_t1==" Non-Vegetated areas" or class_t1=="Rangelands" or class_t1=="Built-up Areas" or class_t1=="Infrastructure"):
        return "Reforestation"
  if (class_t2=="Natural Forest"):
     if (class_t1==" Non-Vegetated areas" or class_t1=="Planted Forest" or class_t1=="Rangelands" or class_t1=="Built-up Areas" or class_t1=="Infrastructure"):
        return "Reforestation"
```

Figure 4.13 An extract example of the transition group processing Python script

4.3.2 Population growth impacts on natural vegetation cover

Population growth or “population changes” is a term used to cover changes in numbers of the population, inhabitants of an area during a particular period of time (Ashraf, 2016). Population growth has been considered as the most crucial factor for most land use changes in developing countries (Li et al., 2015). The relationships and interaction between human and natural phenomena can be well understood through timely and accurate change detection (Lu et al., 2004; Showqi et al., 2014). These relationships aid decision makers to manage and use land resources (Showqi et al., 2014).

In order to study the population changes within the study area, population data were analysed at the district level (Al Marj, Al Jabal Al Akhdar and Derna which are the districts of the Al Jabal Al Akhdar region) using census data of 1973, 1984, 1995 and 2006. Although the study area received numbers of immigrants from the Ajdabiya district and from west and south of Libya during the Libyan revolution (2011), as well as during the war of Benghazi and Derna districts (2014 to the present), immigrants’ data were ignored because they were not available. Therefore, a linear regression analysis method was used to generate

the population of 2004, 2008, 2010, 2014 and 2016 from the data of 1973, 1984, 1995 and 2006.

In the study area, there are five principal cities and 47 small towns and villages based on the 2007 administrative divisions of Libya (see Section 3.1.9). Only 30 urban areas have available data which were used in this study. A population size map was created to visualise the habitation patterns of each city and village within the study area districts .

Population data were analysed in order to examine the changes in the population density and its impact on the natural vegetation cover (Gallego, 2005; Showqi et al., 2014). Population density for each district was determined for investigated years by dividing the total population of the district by its area, which was estimated from its shapefile. The relationship between population density and land use changes was analysed using Spreadsheet.

4.3.3 Climate impact on natural vegetation cover

Climate and topography are important environmental factors affecting vegetation cover (Xiao et al., 2018; Zhou et al., 2019). Accordingly, temperature and rainfall data and topographic data such as elevation, slope and aspect can be utilised to study the driving forces of NDVI changes (Liu et al., 2018). In the Mediterranean region, the formation of vegetation patterns is related to topography (Carmel and Kadmon, 1999). Therefore, in this study, terrain characteristics are considered by using Libyan SOTER (see Section 4.1.8). There are seven landforms within the study area, where landform of the 53 OMU samples was defined (Figure 4.14), and the climate (rainfall and temperature) impact on natural vegetation cover (representing in NDVI) was studied in each landform class.

Monthly rainfall and temperature data for the period 2004-2016 for the 53 OMU sample sites were obtained from the GCMon (see Section 4.1.1). The sample sites were allocated to the climate grids of GCMon, and each grid that included one or more sites was assigned a number starting from the north-west and

progressing to the south-east of the study area (Figure 4.14 and Appendix Table D.1.1).

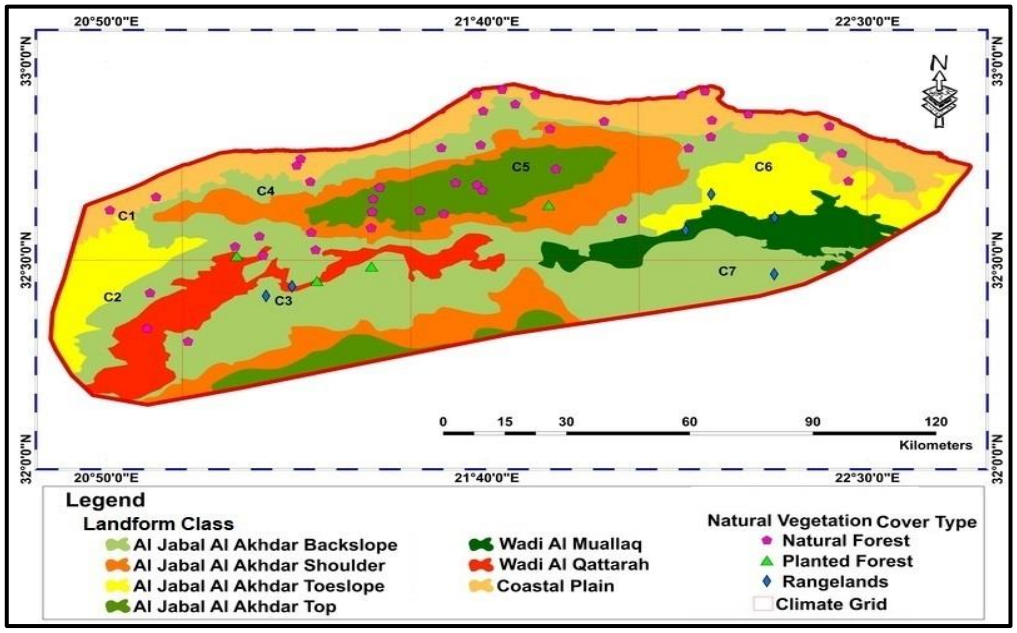

Figure 4.14 Landform classes, natural vegetation cover types and the Climate Grids of the study area samples sites (Source: Author)

The NDVI dataset derived from the MCD43A4-NDVI product was obtained from the GEE platform. A short-term NDVI time series of (1-year period) for the study area of the 53 OMU sites was then used to generate the NDVI data for each year from 2004 to 2016 (see Section 4.2.4). The NDVI data were then organised monthly and gathered together for the whole period (13 years) in an Excel spreadsheet.

In order to examine the impact of rainfall and temperature on the natural vegetation cover, the monthly average NDVI (ANDVI), temperature and rainfall time series trends were analysed for each landform in each grid of climate using Excel 2016. Pearson's rank correlations between ANDVI–rainfall, ANDVI–Rainfall minus 1-month, ANDVI–temperature and ANDVI–temperature minus 1-month for each landform were also analysed using IBM SPSS statistical package ver.25, and two-tailed P-values were used to determine significant relationships. Figure 4.15 illustrates the steps used to assess climate impact on the natural vegetation cover scheme.

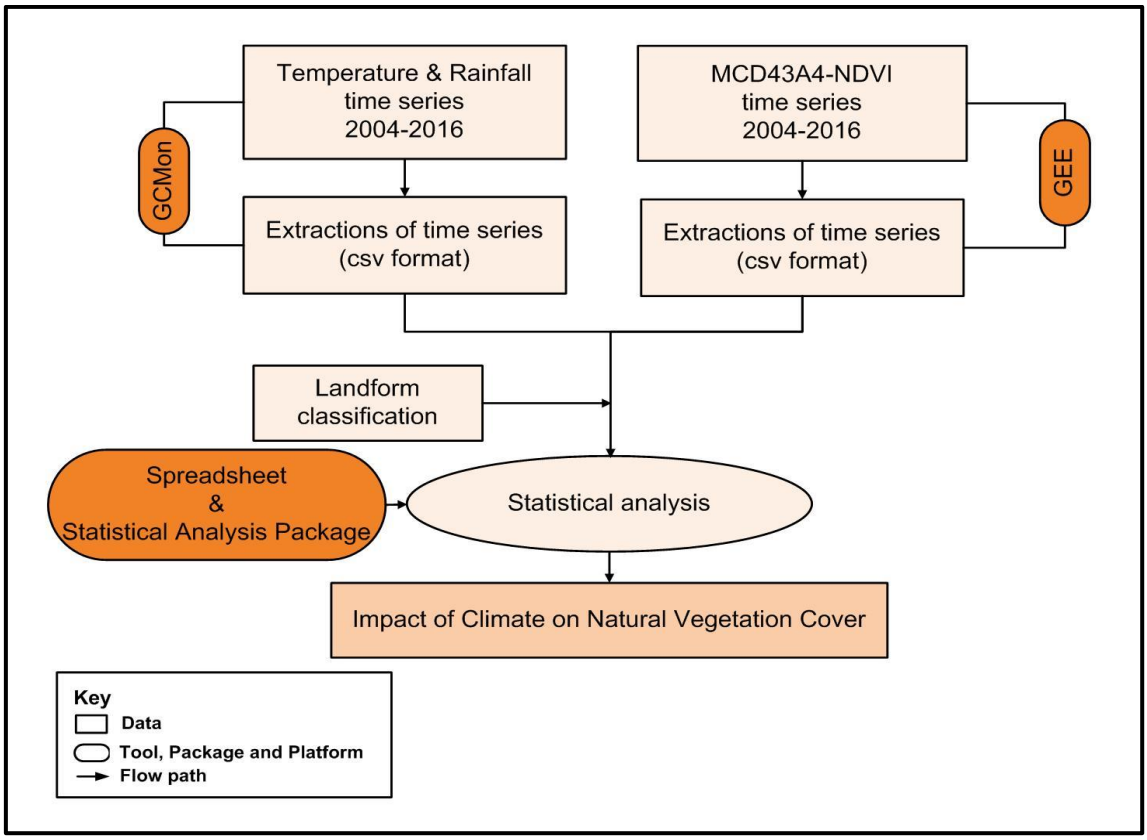

Figure 4.15 Flowchart of steps used to assess climate impact on natural vegetation cover

4.3.4 Prediction of the natural vegetation cover type using Machine-learning

This section explores the potential of Machine-learning algorithms for modelling a prediction of the natural vegetation cover type for the study area based on remote sensing and site characteristic datasets. Such techniques could prove of interest in future land management strategies in the fragile rangeland and forested areas. In general, Machine-learning algorithms are nonparametric methods, able to model multiplex class signatures, and are designed to accept a different set of input predictor data (Maxwell et al., 2018). Biswal et al. (2013) for example used the decision tree classifier ('J48' algorithm) amongst other approaches to extract LULC data from Landsat images, comparing the result with MLC supervised (MLC) and unsupervised (iterative self-organising data analysis technique - ISODATA clustering) classification techniques. Of these approaches, the J48 algorithm produced the most accurate LULC map (with an

overall accuracy of 92% and kappa =0.90). Adesuyi and Munch (2015) also used time-series NDVI to model land cover change by the application of the decision tree classifier (J48) algorithm.

The current study used the available dataset of the 53 OMU sample sites to model the natural vegetation cover type using a decision tree algorithm (Figure 4.16). The dataset contains monthly rainfall and temperature data for the period 2004-2016 obtained from the GCMon (see Section 4.1.1), a monthly time-series of MODIS NDVI (2004-2016) obtained from the GEE platform (see Section 4.2.4) and landform classes of the study area obtained from Libyan SOTER (see Section 4.1.8). The OMU (2005) study data of 53 sample sites included the altitude, terrace, some soil properties such as soil depth, soil texture, available water%, sand%, silt% and clay% and the type of natural vegetation cover. All the data was a spreadsheet.

The J48 algorithm was developed initially as a Java implementation of the C4.5 decision tree classifier. The C4.5 algorithm had initially been developed by Quinlan (1993). J48 is a flexible algorithm in that can process both continuous and discrete attributes (Chauhan and Vania, 2013; Sathyaraj and Prabu, 2015). The algorithm builds a tree-based data output for a set of input values (Sathyaraj and Prabu, 2015).

In order to undertake this analysis, the 'Waikato Environment for Knowledge Analysis' (WEKA) ver.3.8.3, open source software was used (https://www.cs.waikato.ac.nz/ml/weka). WEKA contains a wide selection of machine learning algorithms, (including J48) for data mining tasks, and also contains tools for data pre-processing, classification, regression, clustering, association rules, and visualisation (Vitti and Bezzi, 2004; Biswal et al., 2013; Samardžić-Petrović et al., 2017).

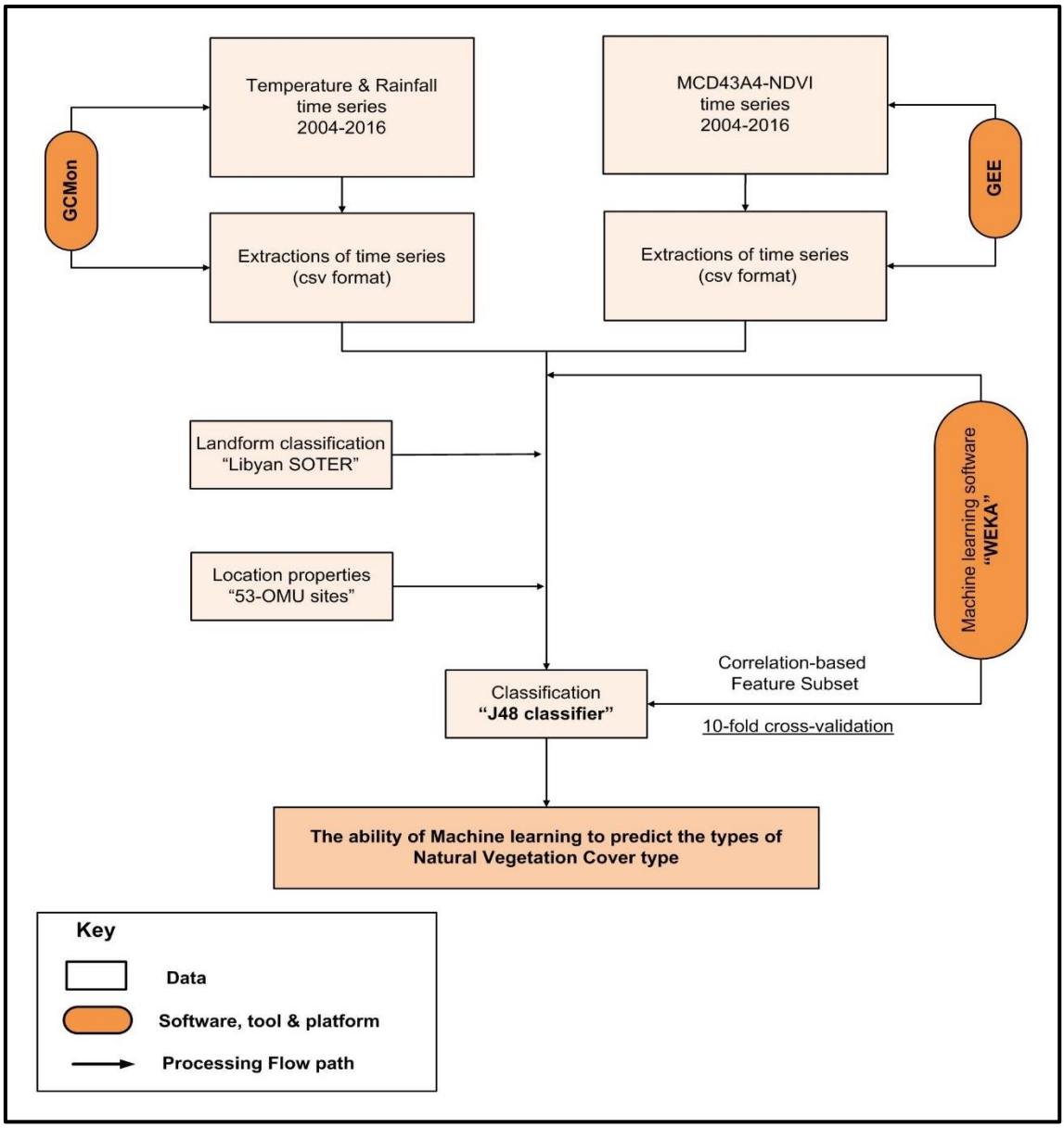

Figure 4.16 Flowchart of steps used to predict the natural vegetation type using Mavhine learning

To perform the classifier (J48), the database file (held in CSV format) was first converted to the 'Attribute-Relation File Format' (ARFF) used for processing in WEKA. The ARFF file format was developed by the University of Waikato for use with the WEKA machine learning software (Jagtap and Kodge, 2013), and comprises in effect a CSV file with a data dictionary header section. Figure 4.17 shows the processed ARFF file, describing 8,268 data instances (sites) sharing a common set of attributes properties (19), including Month, ANDVI (Average

NDVI), MNDVI (Minimum NDVI), XNDVI (Maximum NDVI), ΔNDVI, Terrace, and Altitude (Figure 4.18).

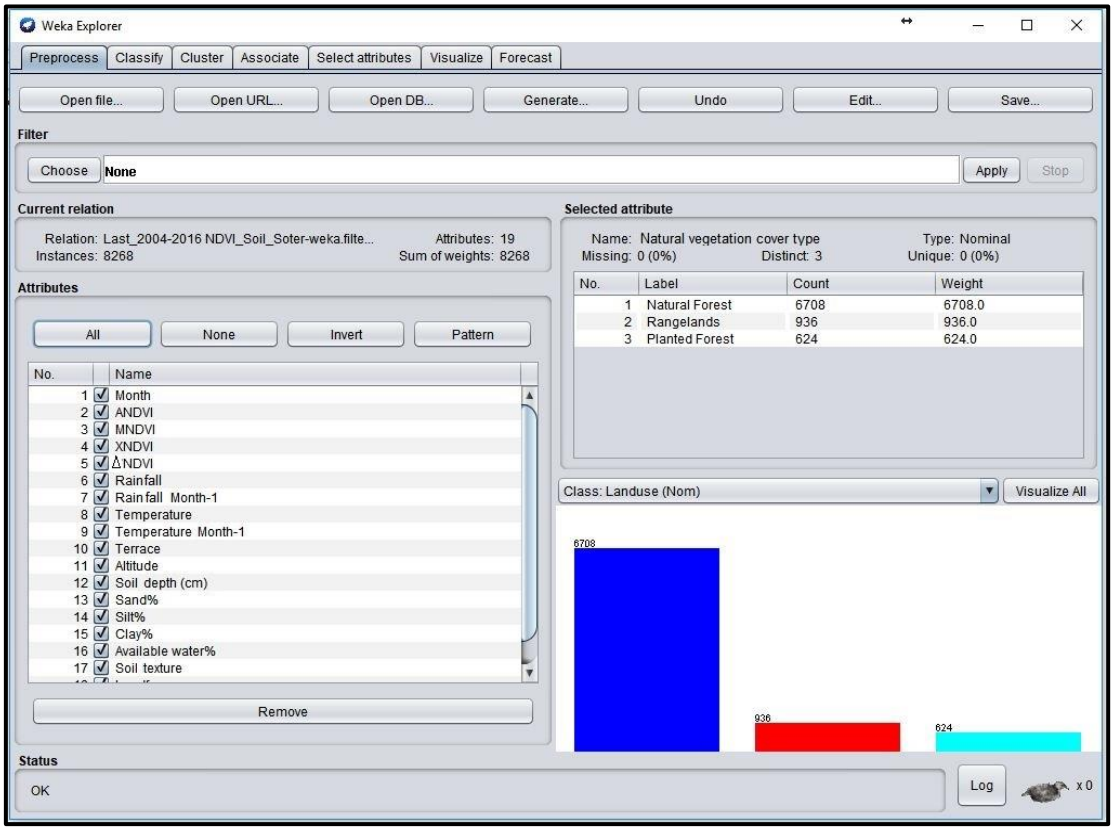

Figure 4.17 WEKA explorer user interface shows the processed ARFF file

The processed attributes can be visualised in WEKA in a graphical representation, Figure 4.18. The second step was to select a subset of attributes these have high impacts or predictive information on the overall modelling process and to eliminate those with insignificant or absent relevant information (Samardžić-Petrović et al., 2016). In this step, the Correlation-based Feature Subset (CFS) method was chosen which has the ability to extract a subset of relevant attributes by evaluating each attribute according to its respective correlation with the land cover (natural vegetation cover type) classes. This method was applied in WEKA by using “CfsSubsetEva” algorithm as an attributes evaluator (Hall, 1999) and “BestFirst” algorithm also used as a search method.

Figure 4.18 Graphical visualisation of processed attributes

The third step was to run the selected J48 classifier model. Different parameters set for J48 algorithm were as follows: binarySplits = false; collapseTree = True; confidenceFactor = 0.25; debug = false; doNotMakeSplitPointActualValue = False; minNumObj = 2; numFolds = 3; reducedErrorPruning = False; saveInstanceData = False; subtreeRaising = True; unpruned = False; useLaplace = False; and useMDLcorrection = True. The subtree raising was implemented with pruning, used to reduce the tree complexity without a decline in the classification accuracy (Mohamed et al., 2012). This step the J48 algorithm was run with 10-fold cross-validation to examine the producer accuracy (Kohavi, 1995; James et al., 2013). After running the classifier model, the outcome model could be saved for use in making new predictions with new data.

Comparing between the two supervised classifiers maximum likelihood classifier (MLC) that was used to classify the LULC images (see Section

4.2.3.2.1) and J48 that used here to predict the natural vegetation types. MCL algorithm is available in remote-sensing image-processing software package.

In the MLC, data of 60% of the ground was used as training data and data of 40% was used to evaluate the classifier. While J48 is a supervised learning used data to train and evaluate the mode using k-fold cross-validation (10-fold); the model is available in WEKA data mining tool.

The accuracy of the classifier model present as a confusion matrix (same to MLC), with overall classification accuracy and kappa. In addition, performance parameters include regression measures and correlation coefficient. J48 as a machine learning algorithm produce higher accuracy compared to traditional parametric classifiers such as MLC, particularly for complex data with a high-dimensional feature space (Maxwell et al., 2018). WEKA results present the accuracy of the classifier model as a confusion matrix (Figure 4.19), with overall classification accuracy and kappa, and accuracy by class. The accuracy acquired by the true positive rate (TP Rate), false positive rate (FP Rate), precision, recall and F-measures and calculated as follows (Sathyaraj and Prabu, 2015; Gandhi et al., 2016):

TP Rate = True Positive / (True Positive + False Negative) **4.3**

FP Rate = False Positive / (False Positive + True Negative) **4.4**

Precision = True Positive / (True Positive + False Positive) **4.5**

Recall = True Positive / (True Positive + False Negative) **4.6**

F-Measure = 2 × Precision × Recall / (Precision + Recall) **4.7**

Accuracy = (True Positive + True Negative) / total actual of all classes **4.8**

Where:

True Positive (TP) = the number of correctly classified as calss x;

False Positive (FP) = Total Classified as class x, except class x (i.e. proportion incorrectly classified as class x);

True Negative (TN)= Total Correct, except class x; and

False Negative (FN)= Total actual class x, except x.

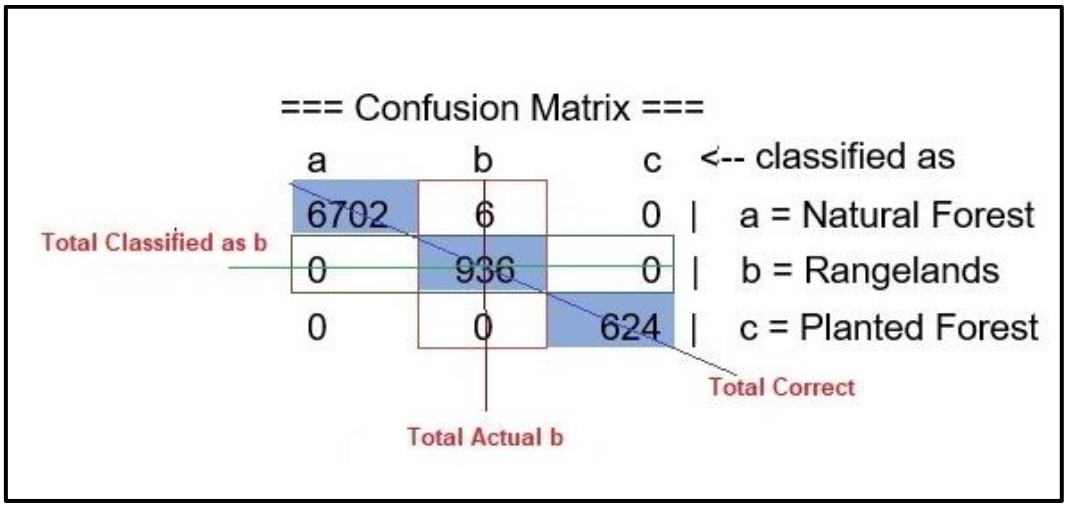

Figure 4.19 An example of the confusion matrix (3 classes) produced in WEKA

In addition, Mathews Correlation Coefficient (MCC) which a measure used to quantify the quality of classification; and returns a value between −1 and +1 which is a correlation coefficient between the observed and predicted binary classifications (Gandhi et al., 2016). The MCC calculated as follows:

$$\mathrm{MCC} = \frac{(\mathrm{TP} \times \mathrm{TN}) - (\mathrm{FP} \times \mathrm{FN})}{\sqrt{(\mathrm{TP} + \mathrm{FP})(\mathrm{TP} + \mathrm{FN})(\mathrm{TN} + \mathrm{FP})(\mathrm{TN} + \mathrm{FN})}} \qquad \textbf{4.9}$$

The accuracy also includes measurs of regression as follows (Galdi and Tagliaferri, 2019):

Mean absolute error (MAE) = $\frac{1}{N}\sum_{i=1}^{N}|\hat{y}_i - y_i|$ **44-10**

Root mean squared error (RMSE) = $\sqrt{\frac{1}{N}\sum_{i=1}^{N}(\hat{y}_i - y_i)}$ **4-11**

Relative absolute error (RAE) = $\frac{\sum_{i=1}^{N}|\hat{y}_i - y_i|}{\sum_{i=1}^{N}|\bar{y} - y_i|}$ **4-12**

Root relative squared error (RRSE) = $\sqrt{\frac{\sum_{i=1}^{N}(\hat{y}_i - y_i)^2}{\sum_{i=1}^{N}(\bar{y} - y_i)^2}}$ **4-13**

Where:

$\hat{y} = a\ vector\ of\ N\ predictions\ target\ values$

$y = a\ vector\ of\ N\ actual\ observed\ target\ values$

$\bar{y}$ = the mean of vector y

In addition, the Receiver Operating Characteristic (ROC) area and Precision-Recall (PRC) area of each class

4.4 **Summary**

This Methodology chapter provides a detailed overview of the image processing and data modelling approaches used in this study and the data sources that were collected to address the aim of this research.

Besides the data sources, the methodology was classified into two parts, Image processing and Modelling. The image processing provides the schemes that were used in pre-image processing, including atmospheric correction, scene image mosaicking, and extracting the study area from the mosaicked scene. The second scheme in image processing is image classification and producing LULC maps of the study area.

Modelling, part 2 of the methodology, describes the methodologies that were used to detect the changes in LULC of the study area through use of a post-classification comparison approach, to analyse the impact of population and climate on natural vegetation cover. The last method describes the machine

learning algorithm that was used to classify and predict the natural vegetation type based on site properties and remote sensing data.

The following chapter, Chapter Five, presents the results that were obtained from applying the methodological approaches adopted in this study.

5 RESULTS

This chapter presents the findings of this research, obtained from the application of the methodological approaches adopted in this study, in order to examine the three objectives set further to the overarching research aim.

This chapter presents the results and findings obtained by applying the methodological approaches adopted in this study (discussed in Chapter 4). The results are organised in five sections, each linked to the principle themes of this research. The first section shows the results of the classification of the series of Landsat satellite images representing a span across biannual intervals from 2004 to 2016; it includes the outcomes of data pre-processing and the accuracy assessment of the produced Land Use and Land Cover (LULC) maps. The second section describes the changes that have been observed and quantified across the years investigated (2004, 2006, 2008, 2010, 2014, 2016). The third section presents the statistical analysis of the population and demographic data and the correlation between population density and LULC changes. The fourth section presents the results for the analysis of climatic and satellite-derived vegetation indices based on the Normalised Difference Vegetation Index (NDVI). Finally, the fifth section represents the results of the natural vegetation type prediction using machine learning approaches.

5.1 Image Classification Processing and LULC thematic map production

The results presented here are of the LULC classification maps assessed across biannual images from 2004 to 2016 (excepting 2012 due to the localised unavailability of satellite imagery that year). The results are given in three sections. The first presents the results of class separability, LULC mapping and the presented classification, the second represents the accuracy assessments

for the classified images of the years investigated, and finally, the third section presents the temporal and spatial dynamics (i.e. changes) of the LULC.

5.1.1 Separability Analysis

5.1.1.1 The preliminary results of Step I

The resukt of discrimination Juniper trees from other species and other LULC types is presented as follows:

5.1.1.1.1 Graphical representations of separability results

Figure 5.1 (a, b, c) shows the SCPs created from the training signatures collected using Landsat imagery acquired on 27.08.2004 for five selected sites (Table 4.6). The mean value for Juniper training signatures (blue triangle) is shown in Landsat bands 1-5 and 7, together with the means of other species (orange circle), bare soil (grey square) and other land use types (yellow diamond) in the sites of Azzrada and Sidi Al Qarib.

For each band (1-5 and 7), the mean spectral response for each category and the variance of the distribution can be used to show the range of spectral responses for each category. The length of the upper and lower limits of each category range denotes the degree of variability within each category.

Figure 5.1 (a), Shnaishnn Forest for example, shows that Juniper class means were different from all other class means in all bands. This was also the case in the other four sites. Considering the separability between Juniper and other species, in Figure 5.1, Arqoob Al Abiad site shows the class ranges overlapped in all bands. The same was found in all bands in Azzrada, and in some bands in Sidi Al Qarib and Arqoob Sidi Hamad sites. The overlapping class ranges also show large in-class variability. On the contrary, non-overlap between the two class was shown in Shnishin Forest in all bands excepting band 1 (Blue) indicated separability between the two classes existed.

The figures also show the good separability between Juniper class ranges and bare soil and other LU types in both bands 5 and 7 (SWIR1 and SWIR2, respectively) in all sites. The poor separability was anticipated between Juniper

and ‘other species class’ because of the overlap, that will likely cause errors in the subsequent classifications affecting the classification accuracies for all sites except Shnaishnn Forest.

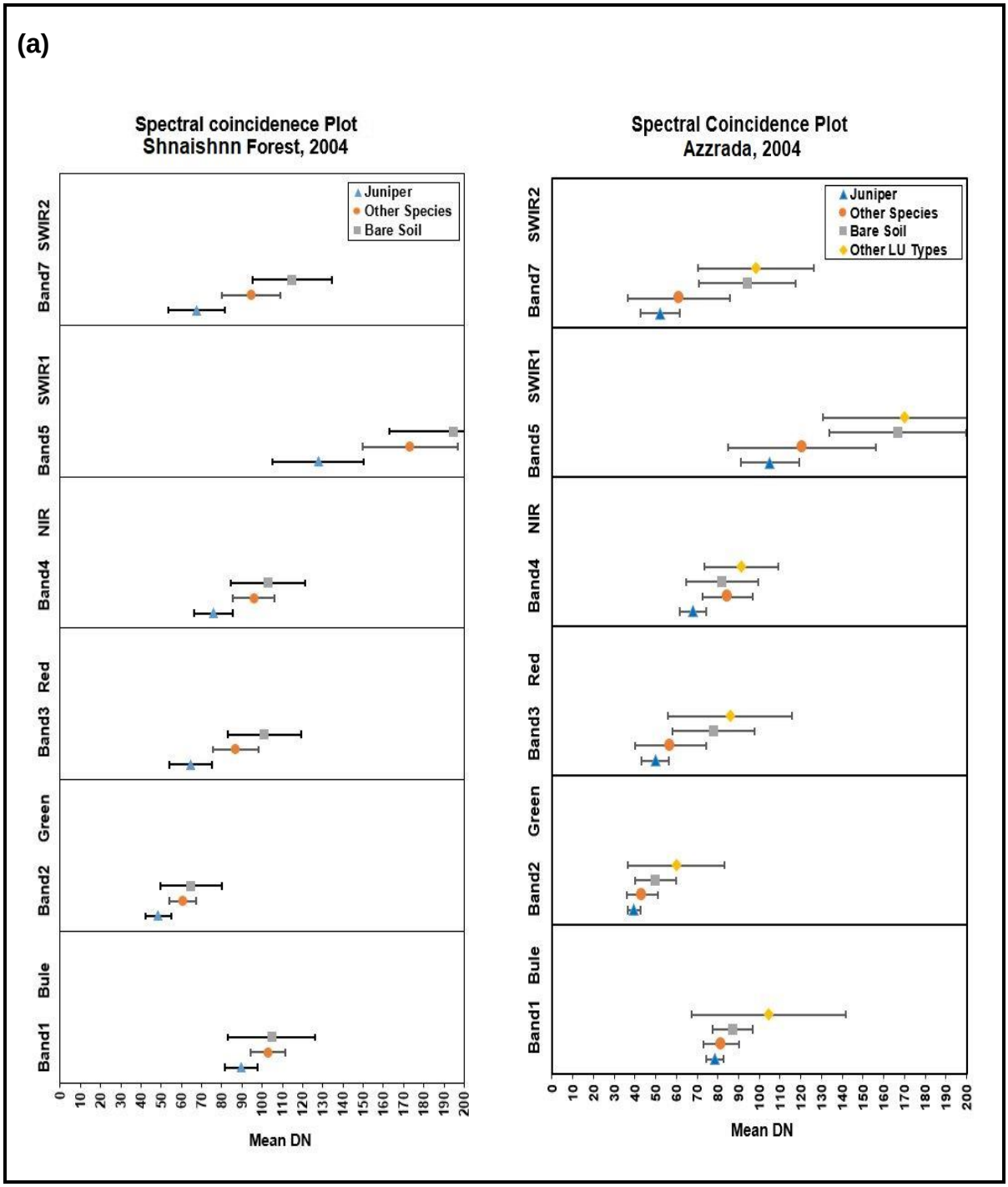

Figure 5.1 a-c Spectral coincidence Plot from Landsat imagery in 2004

The bands 1-5 and 7 displayed using ± 2 Standard Deviations. Class ranges are indicated by ⟷.

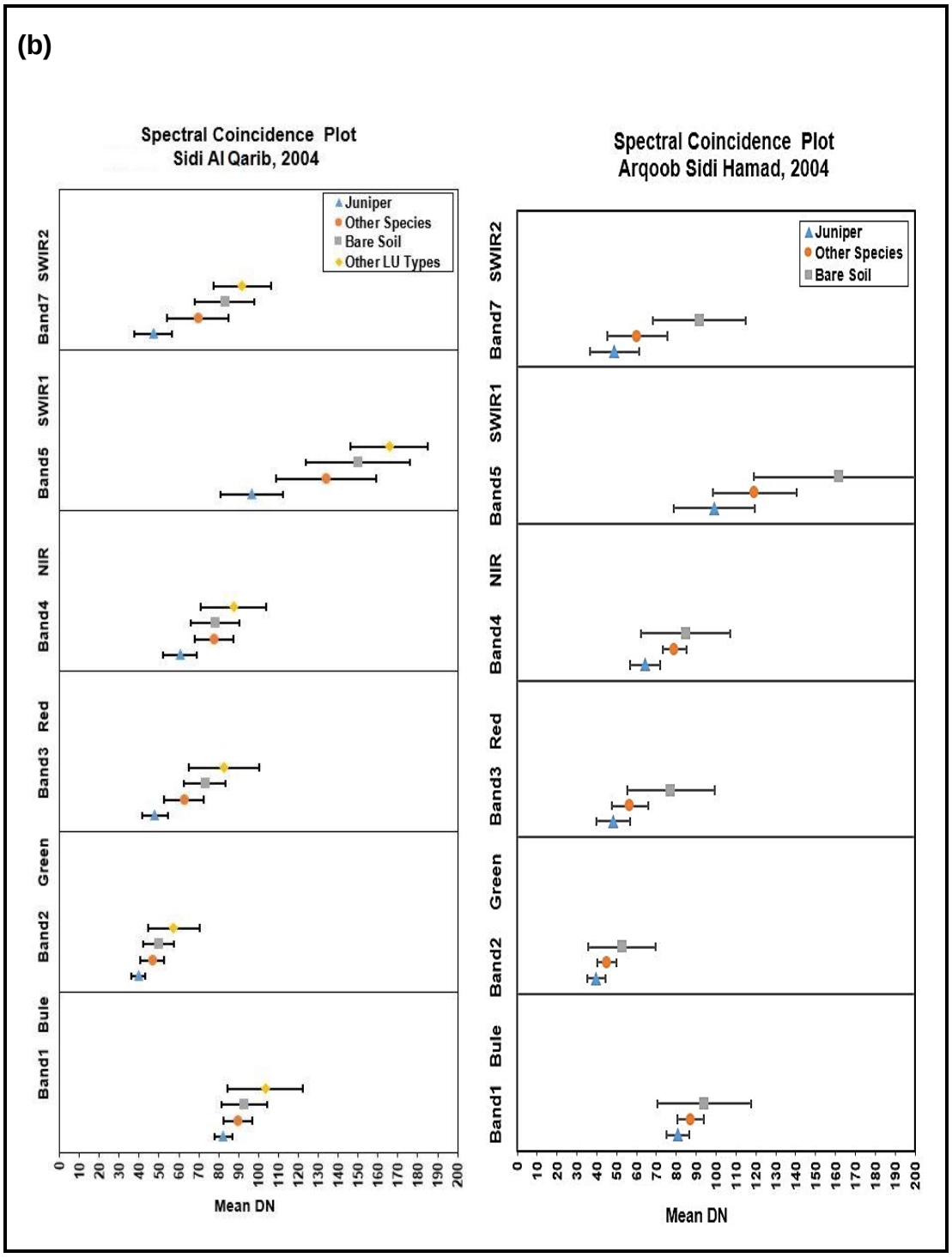

Figure 5.1 a-c Spectral Coincidence Plot from Landsat imagery in 2004

The bands1-5 and 7 displayed using ± 2 Standard Deviations. Class ranges are indicated by ⟼.

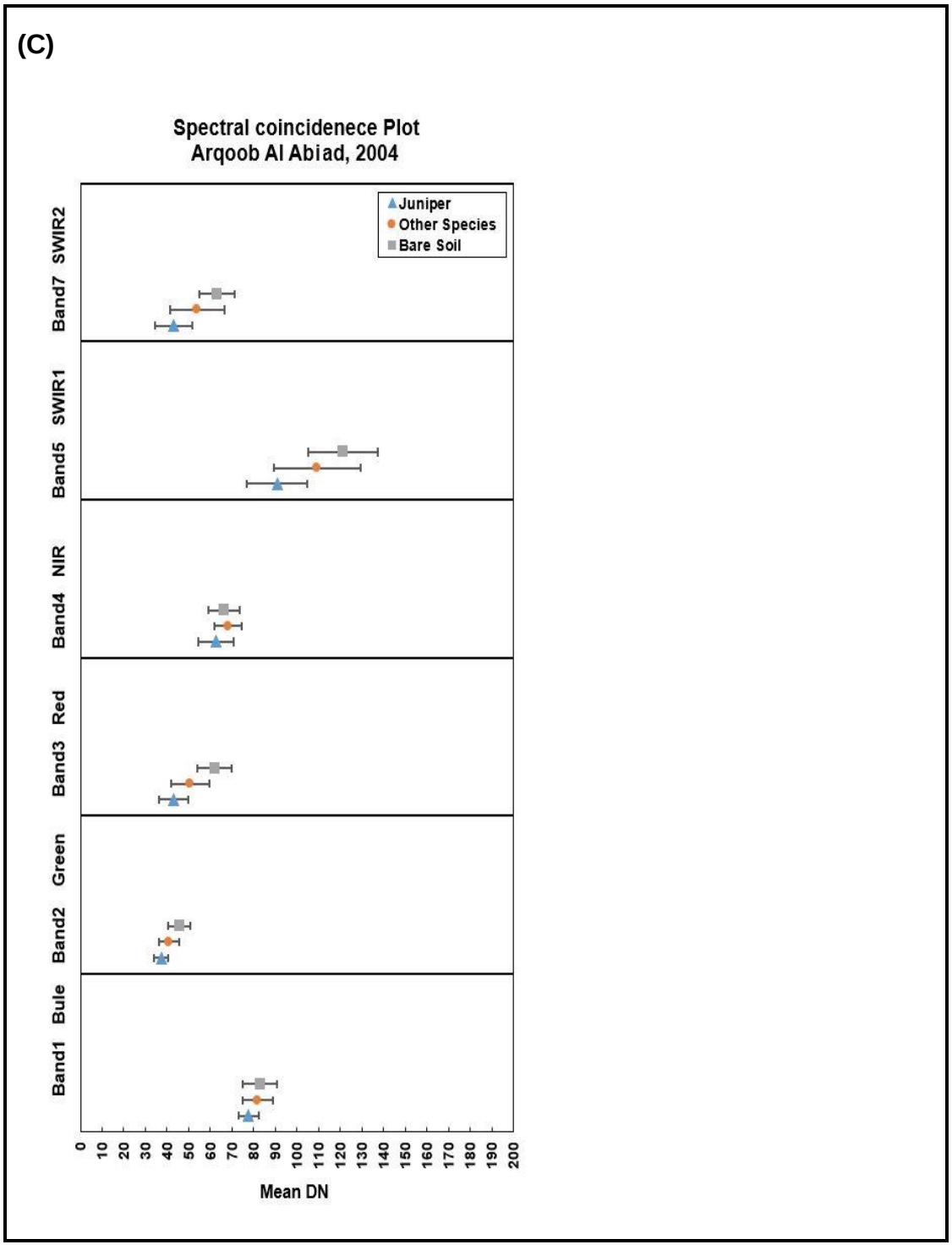

Figure 5.1 a-c Spectral Coincidence Plot from Landsat imagery in 2004

The bands 1-5 and 7 displayed using ± 2 Standard Deviations. Class ranges are indicated by ⊢⊣.

5.1.1.1.2 Statistical analysis results

Table 5.1 shows the JM distance between the Juniper and other LULC classes based on the indicators of separability for the five selected sites. Results highlight the potential for discrimination of Juniper from other land use types and bare soil (100%, 80% of sites) with less opportunity from other plant species (20% of sites). Very poor separability was found between the Juniper class and other plant species class in all sites except Shnainshnn Forest which

	Site	Other plant species	Bare soil	Other LU types
Juniper	Shnainshnn Forest	1385	1414	
	Azzrada	1346	1414	1414
	Sidi Al Qarib	1266	1414	1414
	Arqoob Sidi Hamad	1255	1367	
	Arqoob Alabiad	1113	1410	
% of the signature separability		20	80	100
		80	20	0
		0	0	0
Key to Separability		**Very Poor**	**Poor**	**Good**
Distance Value		0-1000	1000-1378	1378-1414

shows a separability value of 1385. The results also showed good separability between the Juniper and Bare soil class with high JM values (> 1410) except for the Arqoob Sidi Hamad site which shows a poor separability value of 1376, and reasonable separability between Juniper class and other LU types class in Azzrda and Sidi Al Qarib sites with 1414 of separability value.

The result confirms the ability of JM distance method to distinguish between the Juniper tree class and the bare and other land uses LULC classes and the inability to distinguish between the Juniper and other species classes consistently.

Table 5.1 Separability of Juniper and other classes based on JM distance

5.1.1.2 Classes separability of Step II

Table 5.2 lists the results of JM distance between the LULC classes from the least separability, i.e. there is overlap between the spectra of the two classes, to the greatest separability which has a perfect separation between pairs of classes. The table also shows the number of training pixels of each LULC class for the years 2004 to 2010, and 2014 and 2016.

The results reveal a poor separation between AA and NF, with a JM distance value computed of 1,292 for the years 2004 to 2010, and 1,298 for the years 2014 and 2016. The poor separation was also indicated between the spectral of training sets of AA and NV areas with a JM distance value of 1,333 for the year 2004 to 2010, and 1,337 for the years 2014 and 2016. The spectral separability between NV and RL also shows a poor separation with JM distance values of 1,366 for the years 2004 to 2010, and 1,376 for the years 2014.

Table 5.2 JM distance between the Land Cover / Land Use Classes (LULC) and the number of training pixels of each class

***for 2004, 2006, 2008, and 2010 (A), and 2014 and 2016 (B).**

(A) 2004 to 2010					
Pair separation (least to most)	AA	NV	RL	NF	Number of training pixels
AA		1,333	1,392	1,293	640
NV	1,333		1,366	1,397	181
RL	1,392	1,366		1,413	244
NF	1,293	1,397	1,413		3,064
(B) 2014 and 2016					
Pair separation (least to most)	AA	NV	RL	NF	Number of training pixels
AA		1,337	1,389	1,298	653
NV	1,337		1,376	1,394	175
RL	1,389	1,376		1,413	249
NF	1,298	1,394	1,413		3,097

Key to Separability	Very Poor	Poor	Excellent
Distance Value	0-1,000	1,000-1,378	1,378-1,414

Very strong and/or perfect separations were, however, shown between AA and RL, NV and NF, and RL and NF. The JM distance between the spectra of AA and RL was 1,392 for the years 2004 to 2010, and 1,389 for the years 2014 and 2016. The JM spectral separability between NV and NF was 1,392 for the years 2004 to 2010, and 1394 for the years 2014 and 2016 while the highest JM

distance separability value was shown between RL and NF class of 1413 for the years investigated.

5.1.2 Classification and thematic accuracy assessment

The resultant maps show that RL areas are a significant land cover type in the southern part of the study area, with NF, along with the major AA areas, in the northern part of the study area for the study period 2004 - 2016.

Table 5.3 shows the confusion matrices for the initial LULC maps of the study area over the years of investigation. Overall, the accuracy assessment revealed an overall classification ranging from 94.6 – 97.9%, with a Kappa coefficient ranging from 0.86-0.94 for the initial classified images, Table 5.3, which indicates a high level of accuracy. From the user and producer accuracies perspective, the results show that there are pixels which were misclassified between classes. Where the results of separability analysis (pre-classification processing) showed the poor separabilties were between AA and NV, AA and NF classes and between RL and NV classes, and good separbilities between other classes. The results also showed there is no very poor sperability and AA class has the lowest sperability values that leads increase the proparity of the misclassification between the those classes. However, the use of a majority filter (post-classification processing) and suitable classfier (MLC) can be attributed to enhancing and improving the quality of the classified image. The misclassified pixels of classes were shown to differ in accordance with the date of the image. The final thematic classified images that were produced by adding the masks of the PF, BA, and IN areas to the initial LULC maps (Figure 5.2 to Figure 5.7), showing the distribution of the LULC classes areas of study area for the years investigated.

For the initial 2004 classified image, the accuracy assessment was generated from 4,004 reference pixels (i.e. the evaluation pixels). The report of land cover classification map is shown in Table 5.3, having an overall classification accuracy of 97.1%, and a Kappa coefficient of 0.92, with individual classes being mapped at accuracies of >88% and >79% for user and producer, respectively. Table 5.3 also shows the user’s and producer’s accuracies of the

NF and RL classes, representing the classes of most interest to this study, provide accuracies of 99% (for NF) and 95.9% (for RL) (user), and 98.1% (for NF) and 98.2% (for RL) (producer). Thus, some 98.1% of the total classified NF pixels have been correctly identified as NF, and 99 % of total actual NF pixels were NF pixels. Similarly, 98.2% of the total classified RL pixels (214/218) have been correctly identified as RL, and 95.9% of the total actual RL pixels were RL pixels. From the commission and omission accuracies perspective, the majority of pixels were misclassified between NF, NV and AA, where 12.3% of total actual AA pixels have been incorrectly classified to NV and NF. Generally, 21% of the total classified NV pixels were AA, NF and RL pixels those have been classified incorrectly to NV class. Some 5.2% of the total classified AA pixels were NF and RL have been incorrectly classified to AA. In addition, 1.9% and 1.8% of the total classified NF, and RL pixels respectively have also been classified incorrectly.

Table 5.3 Confusion matrices for the initial LULC maps of study area derived by MLC using RS data of the years 2004, 2006 and 2008

2004								
	Class names	Reference pixels				Total of the classified pixels	Producer's Accuracy (%)	User's Accuracy (%)
		AA	NV	RL	NF			
Classified Data	AA	515	17	0	55	587	94.8	87.7
	NV	0	104	4	3	111	78.8	93.7
	RL	7	2	214	0	223	98.2	95.9
	NF	21	9	0	3,053	3,083	98.1	99
Total of the reference pixels		543	132	218	3,111	4,004		
Overall Accuracy		97.1				Kappa Coefficient (k_c)		0.92

2006								
	Class names	Reference pixels				Total of the classified pixels	Producer's Accuracy (%)	User's Accuracy (%)
		AA	NV	RL	NF			
Classified Data	AA	537	22	0	42	601	98.4	89.4
	NV	4	100	3	0	107	79.4	93.5
	RL	0	1	207	3	211	98.6	98.1
	NF	5	3	0	3,084	3,092	98.6	99.7
Total of the reference pixels		546	126	210	3,129	4,011		
Overall Accuracy		97.9				Kappa Coefficient (k_c)		0.94

2008								
	Class names	Reference pixels				Total of the classified pixels	Producer's Accuracy (%)	User's Accuracy (%)
		AA	NV	RL	NF			
Classified Data	AA	519	27	7	16	569	95.8	91.2
	NV	9	101	0	0	110	71.1	91.8
	RL	2	6	209	2	219	96.8	95.4
	NF	12	8	0	3,102	3,122	99.42	99.4
Total of the reference pixels		542	142	216	3,120	4,020		
Overall Accuracy		97.8				Kappa Coefficient (K_c)		0.94

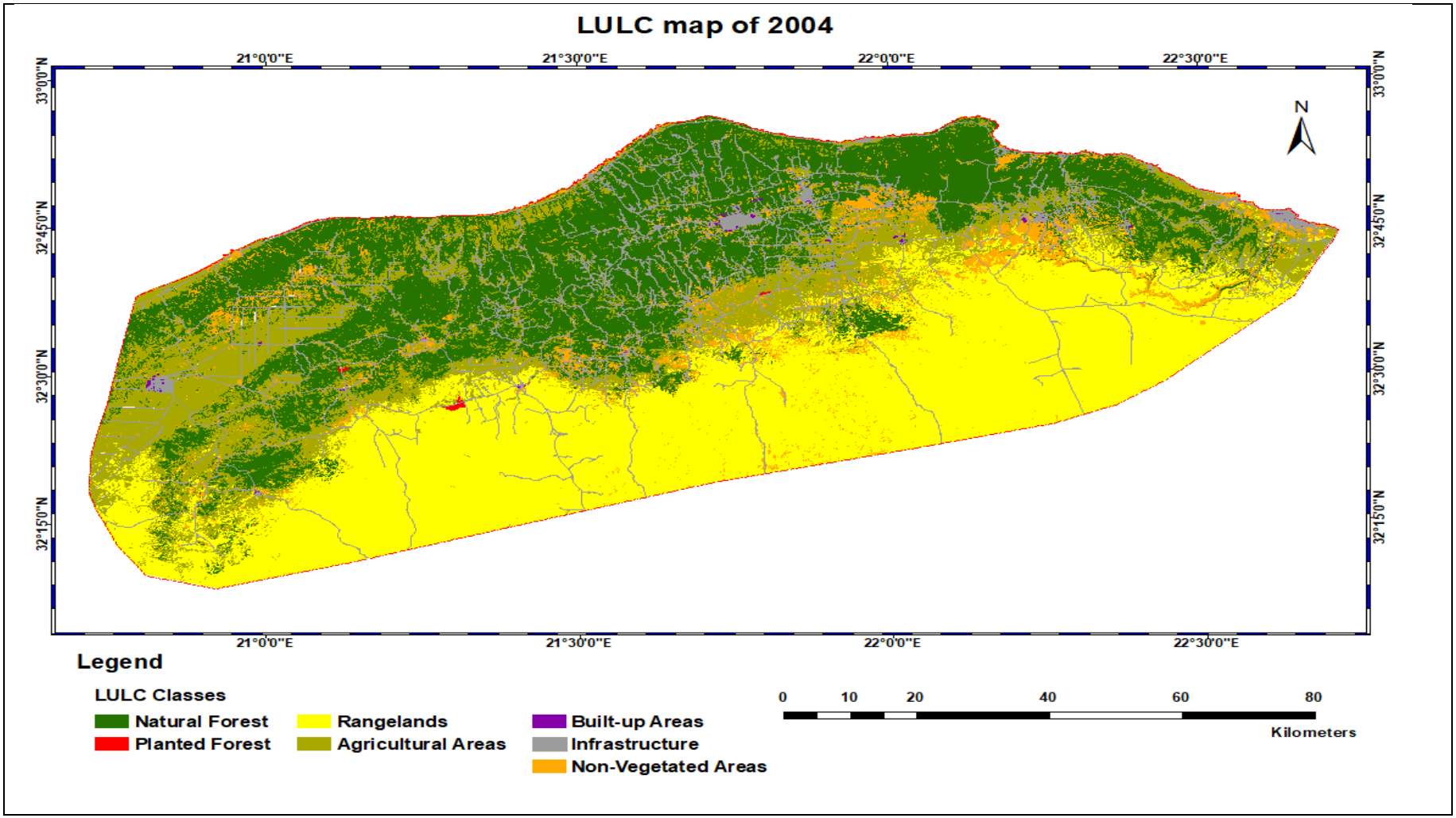

Figure 5.2 The land use land cover classification of the study area for 2004

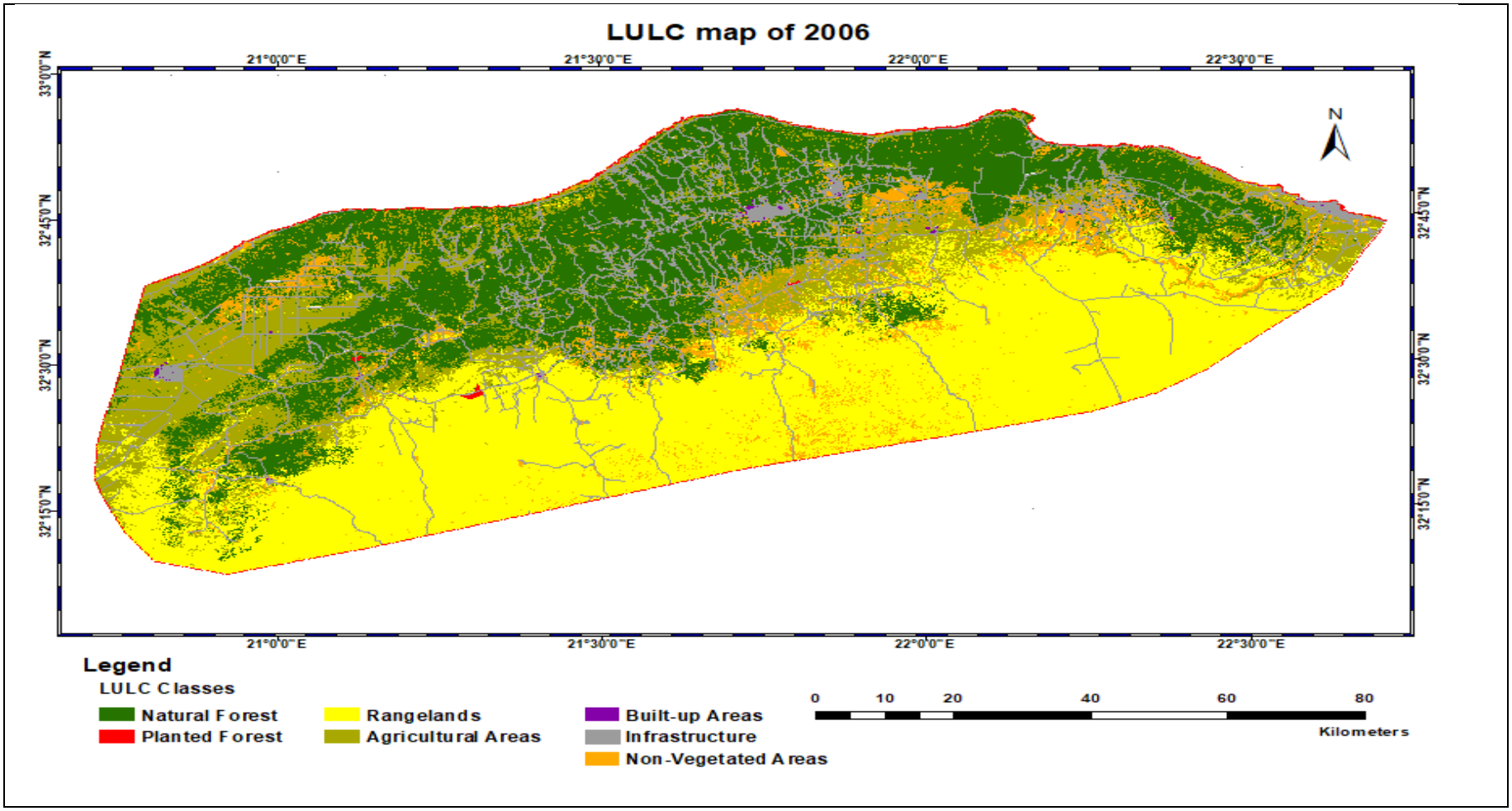

Figure 5.3 The land use land cover classification of the study area for 2006

Likewise, an overall high classification accuracy of 97.9% was observed with an overall Kappa statistic of 0.94 (almost perfect) achieved for the 2006 initial classified image (Table 5.3). The accuracies of user and producer of each class of LULC classes were >89% and >79%, respectively. The accuracy assessment was generated from 4,011 reference data pixels (i.e. ground truth data see Section 4.2.3.2.1. The user's and producer's accuracies of the NF and RL classes provided accuracies of 99.7% (for NF) and 98.1% (for RL - user), and 98.6% (for NF and RL - producer) respectively. From the perspective of the commission and omission accuracies, the majority of pixels were seen to be misclassified between NF, NV and AA, where 10.7% of total actual AA pixels were incorrectly classified to NV and NF. Generally, 20.6% of the total classified NV pixels were AA, NF and RL pixels those have been classified incorrectly to NV class. 1.65% of the total classified AA pixels and 1.4% of the total classified NF and RL (pixels; have been classified incorrectly too.

Similarly, the accuracy assessment of the 2008 initial classified image was generated from 4,020 reference data pixels (Table 5.3) The overall classification accuracy was 97.8%, and the Kappa coefficient 0.94, with individual classes being mapped at accuracies of >91% and >71% for user and producer, respectively. The confusion matrix also identifies the user's and producer's accuracies of the NF and RL classes, providing accuracies of 99.4% and 95.4% (user), and 99.4 and 96.8% (producer), respectively. It also highlights that when miscalculations occurred, that this 28.9 % of the total classified NV pixels were AA, RL and NF have been incorrectly classified to NV. Approximately 4.24% of the total classified AA pixels were NV, NF and RL, and 3.24% of classified RL pixels were AA.

For the 2010 initial classified image, the accuracy assessment was generated from 3,965 reference data pixels (Table 5.4). The overall classification accuracy was 94.6%, and the Kappa coefficient was 0.86, with individual classes being mapped at accuracies of >78% and >84% for user and producer, respectively.

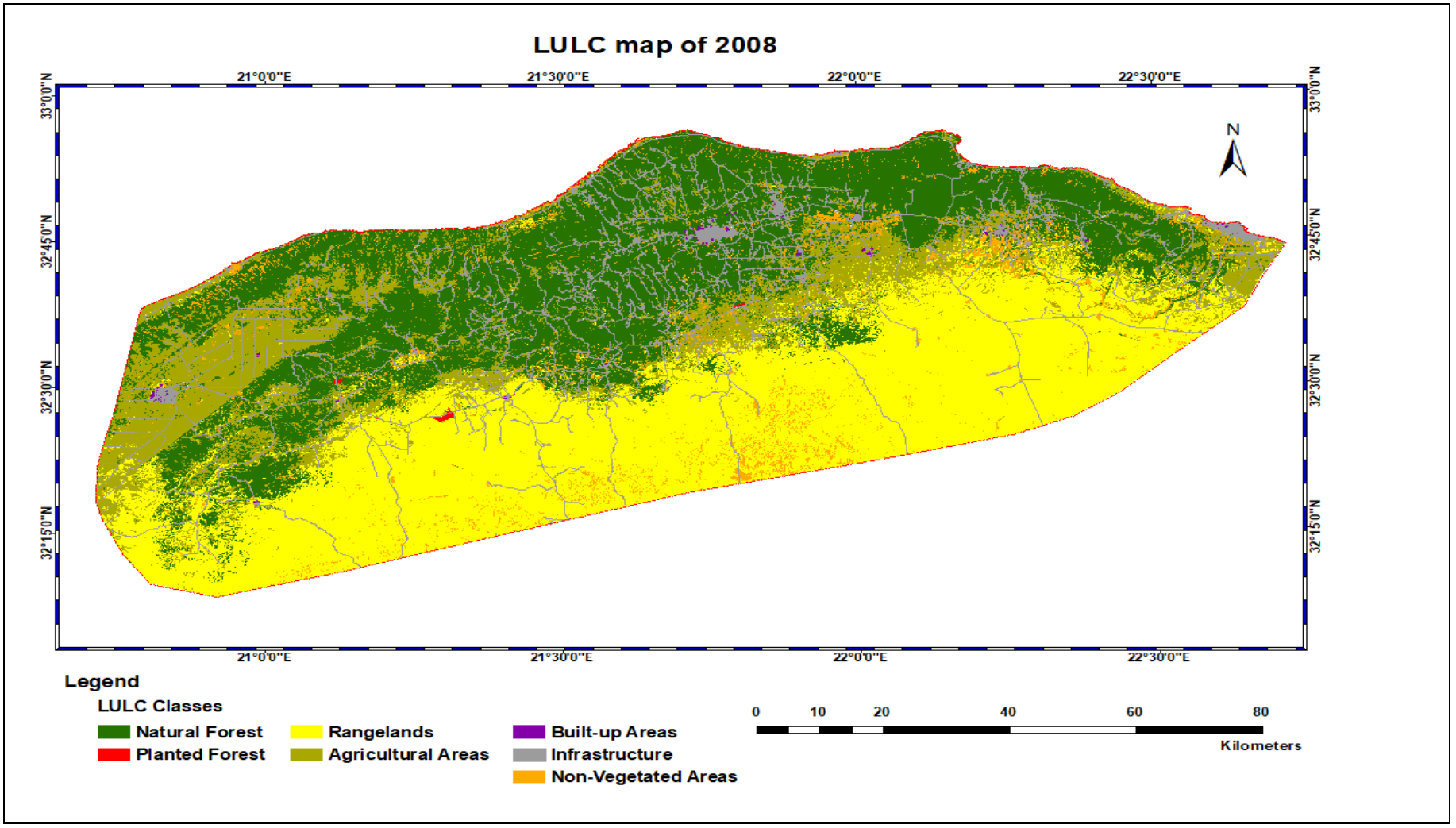

Figure 5.4 The land use land cover classification of the study area for 2008

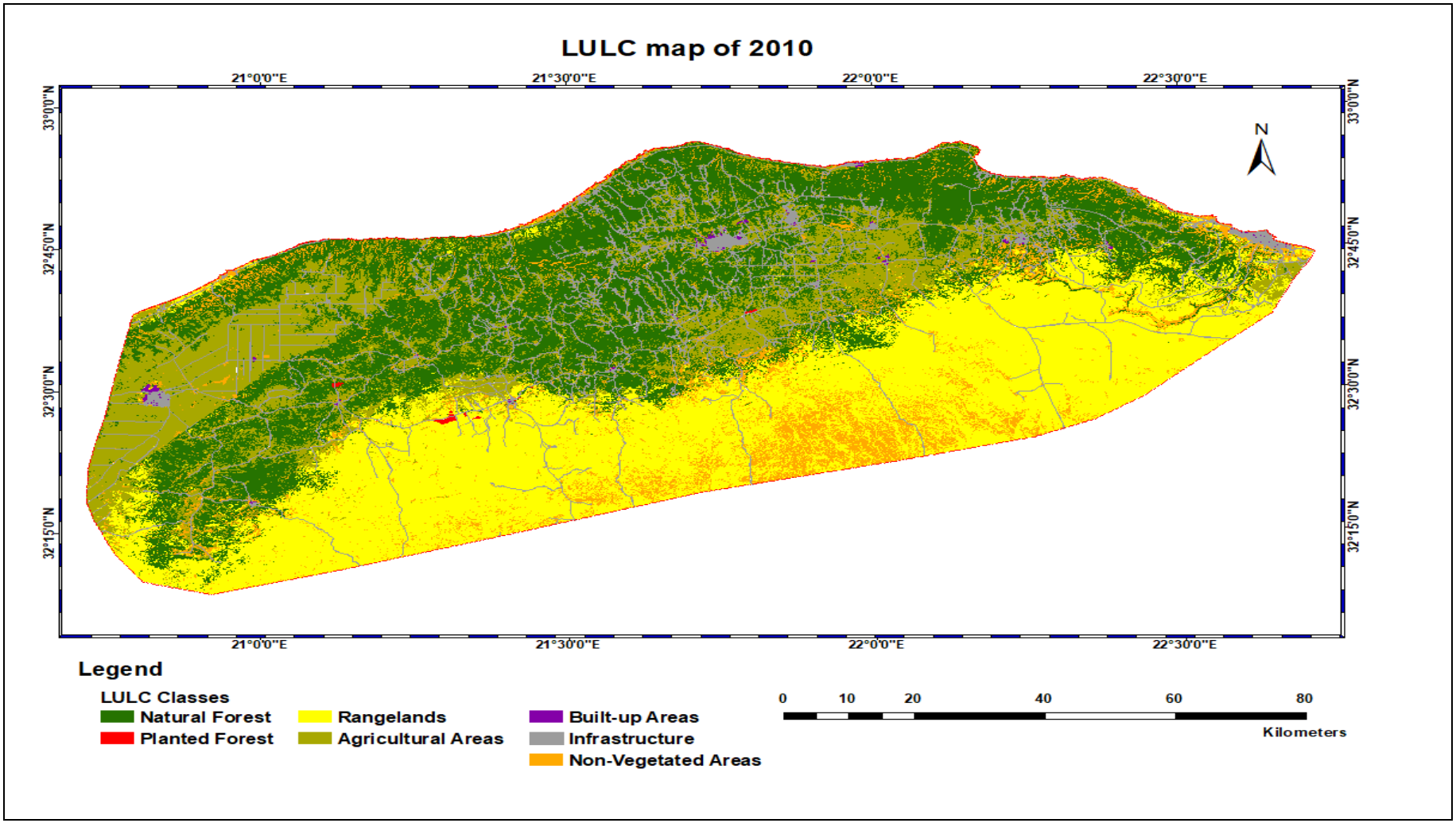

Figure 5.5 The land use land cover classification of the study area for 2010

Table 5.4 Confusion matrices for the initial LULC maps of the study area derived by MLC using RS data of the years 2010, 2014 and 2016

2010								
	Class names	Reference pixels				Total of the classified pixels	Producer's Accuracy (%)	User's Accuracy (%)
		AA	NV	RL	NF			
Classified Data	AA	551	12	0	106	669	98.2	82.4
	NV	3	107	13	13	136	84.3	78.7
	RL	3	2	189	41	235	89.2	80.4
	NF	4	6	10	2,905	2,925	94.78	99.3
Total of the reference pixels		561	127	212	3,065	3,965		
Overall Accuracy		94.6				Kappa Coefficient (k_c)		0.86
2014								
	Class names	Reference pixels				Total of the classified pixels	Producer's Accuracy (%)	User's Accuracy (%)
		AA	NV	RL	NF			
Classified Data	AA	559	15	8	50	632	97.6	88.5
	NV	0	86	20	8	114	80.4	75.4
	RL	7	2	187	60	256	84.2	73.1
	NF	7	4	7	3,048	3,066	96.3	99.4
Total of the reference pixels		573	107	222	3,166	4,068		
Overall Accuracy		95.4				Kappa Coefficient (k_c)		0.88
2016								
	Class names	Reference pixels				Total of the classified pixels	Producer's Accuracy (%)	User's Accuracy (%)
		AA	NV	RL	NF			
Classified Data	AA	558	12	3	39	612	97.4	91.2
	NV	8	82	6	3	99	76.6	82.8
	RL	3	1	199	95	298	89.6	66.8
	NF	4	12	14	3,029	3,059	95.7	99
Total of the reference pixels		573	107	222	3,166	4,068		
Overall Accuracy		95.1				Kappa Coefficient (K_c)		0.87

The user's and producer's accuracies of the NF and RL classes, providing accuracies of 99.3% and 80.4% (user), and 94.8% and 89.2% (producer)

respectively. From the commission and omission accuracies perspective, the majority of pixels were misclassified between NF, NV and AA, where 17.6% of total actual AA pixels have been incorrectly classified to NV and NF. Generally, 15.8% of the total classified NV pixels were AA, NF and RL those have been classified incorrectly to NV class. By comparison, 10.9% of the total classified RL pixels were NF and NV pixels, 5.2% of the total classified NF pixels were AA, NV and RL, and 1.8% of the total classified AA pixels were NF, NV and RL.

The accuracy assessment for the 2014 initial classified image was generated from 4,068 reference data pixels (Table 5.4). The overall classification accuracy was 95.4%, with a Kappa coefficient of 0.88, and individual classes being mapped at accuracies of >73% and >80% for user and producer, respectively. The user's and producer's accuracies of the NF and RL classes were 99.4% and 73% (user), and 96.3 and 84.2% (producer), respectively. From commission and omission perspective, the majority of pixels were misclassified between NF, NV and AA. Where 26.6% of total actual RL pixels have been incorrectly classified to NF, NV and AA. 24.6% of total actual NV pixels have been incorrectly classified to NF and RL, and 11.6% of total actual AA pixels have been incorrectly classified to NF, NV and RL.

For the 2016 initial classified image, the accuracy assessment was generated from 4,068 reference data pixels, showing overall very high classification accuracies of 95.1% with an overall Kappa statistic of 0.87 (Table 5.4). The individual LULC classes were mapped at accuracies of ≥66.8% and ≥76.6% for user and producer, respectively. The user's and producer's accuracies of the NF and RL classes, provide accuracies of 99% and 66.8% (user), and 95.7% and 89.6% (producer), respectively. From the commission and omission accuracies perspective, the majority of pixels were misclassified between NF, NV and AA, where 33.2% of total actual RL pixels have been incorrectly classified to NF, AA and NV; 17.2% of total actual NV pixels have been incorrectly classified to AA RL and NF. Also, 8.82% of total actual AA pixels have been incorrectly classified to NF, NV and RL.

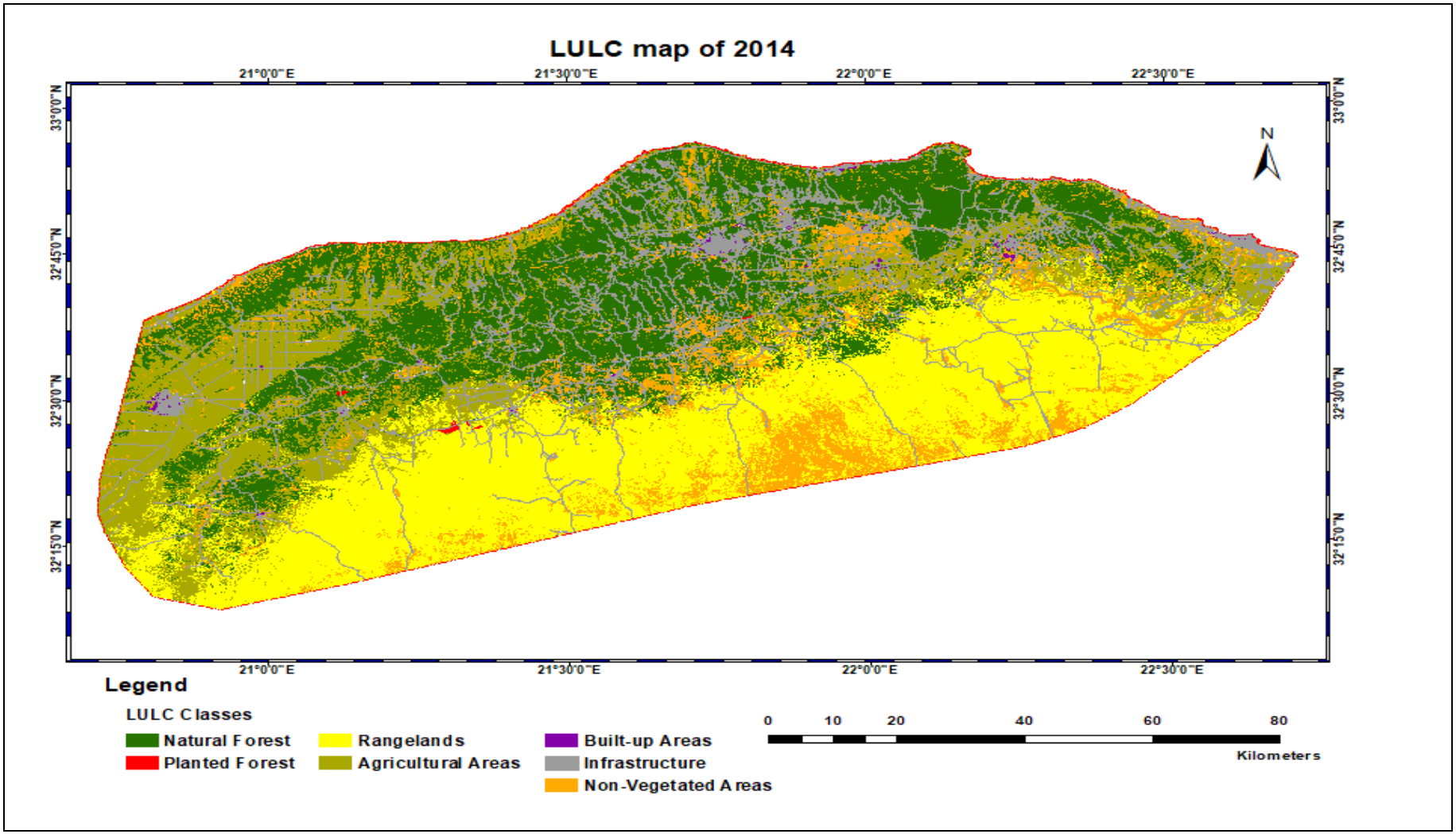

Figure 5.6 The land use land cover classification of the study area for 2014

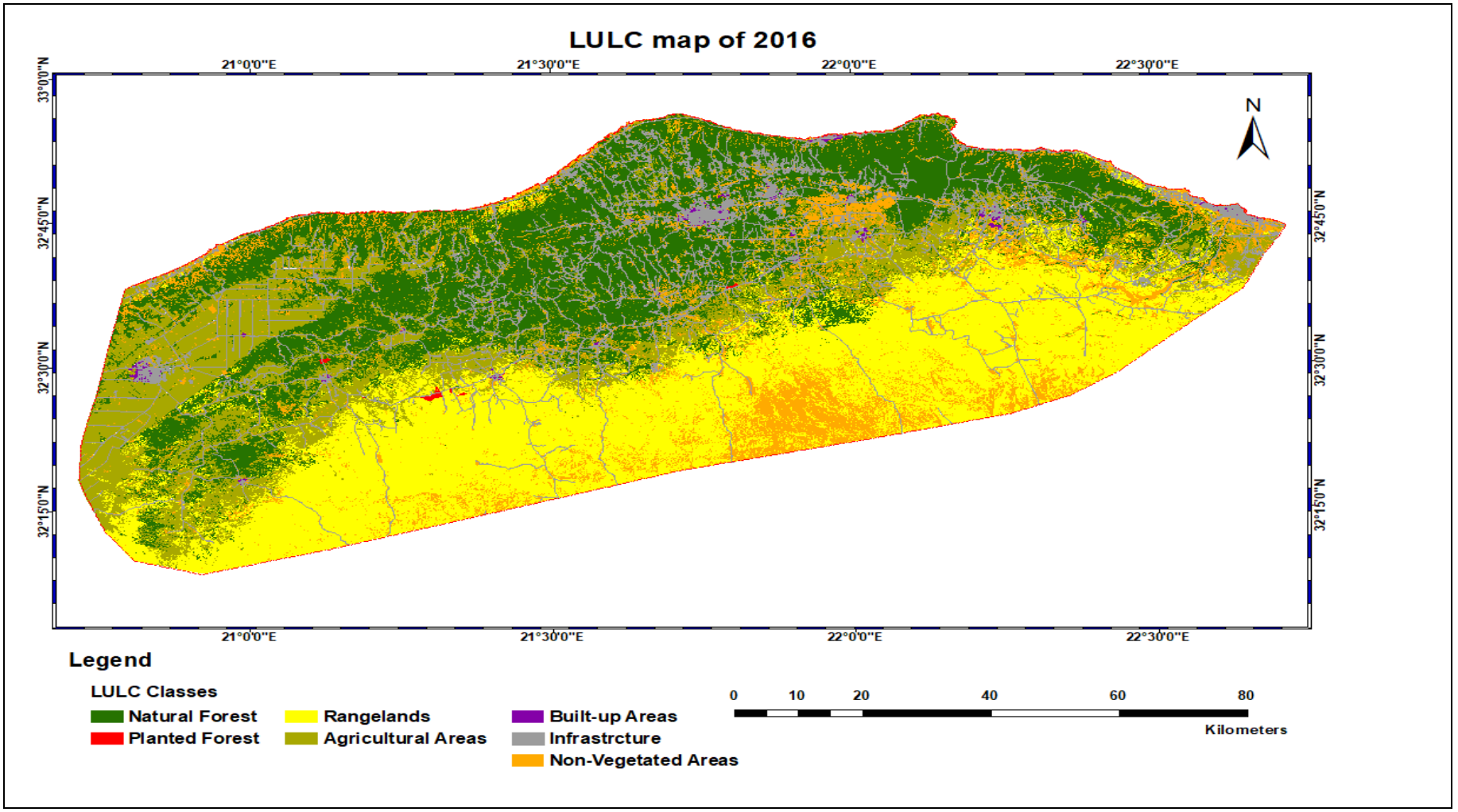

Figure 5.7 The land use land cover classification of the study area for 2016

5.1.3 Land Use and Land Cover Dynamics

The results presented here obtained from the final classified images data. Those images have been produced by adding the three masked classes (PF, IN and BA) to the initial images.

The LULC for the period 2004-2016 shows an overall fluctuation in the NF, RL and AA classes and a concurrent increase in the NV class until 2014, except in 2008 which showed a decline in the NV class to 3.55% of the total area (35,719 ha) associated with an increase in NF for that year. This was followed by a decrease in the NV class in 2016 to 11.1% (112,092 ha) from 12.1% of the total area (121,516 ha) in 2014. The fluctuation observed in changes in LULC classes may in large part be due to the acquisition date of the images which were from different months of the year, reflecting the seasonal variation between the years investigated. A steady increase was found in the BA class from 0.26% of the total area (2,636 ha) in 2004 up to 0.52% (5,291 ha) in 2016. The IN class showed the same pattern as BA except in 2008 where there was a negligible decline from 0.61% of the total area in 2006 to 0.54% of the total area (5,447 ha) in 2008, then an increase up to 1.22% of the total area (12,239 ha) in 2016. The decrease in IN observed in 2008 could be attributed to Temporary tracks used during crop harvest, pastoral activities and camping seasons. Therefore, these IN (temporary track) did not appear during the digitising process of road network from GE.

The AA class showed a decrease from 21% of the total area (211,141 ha) in 2004 to 18.7% of the total area (188,690 ha) in 2008, followed by an increase up to 21.7% of the total area (218,500 ha) in 2016. The decrease in AA in 2008 classified image caused by pixels of 8.79% of the total actual AA pixels were classified to the other classes.

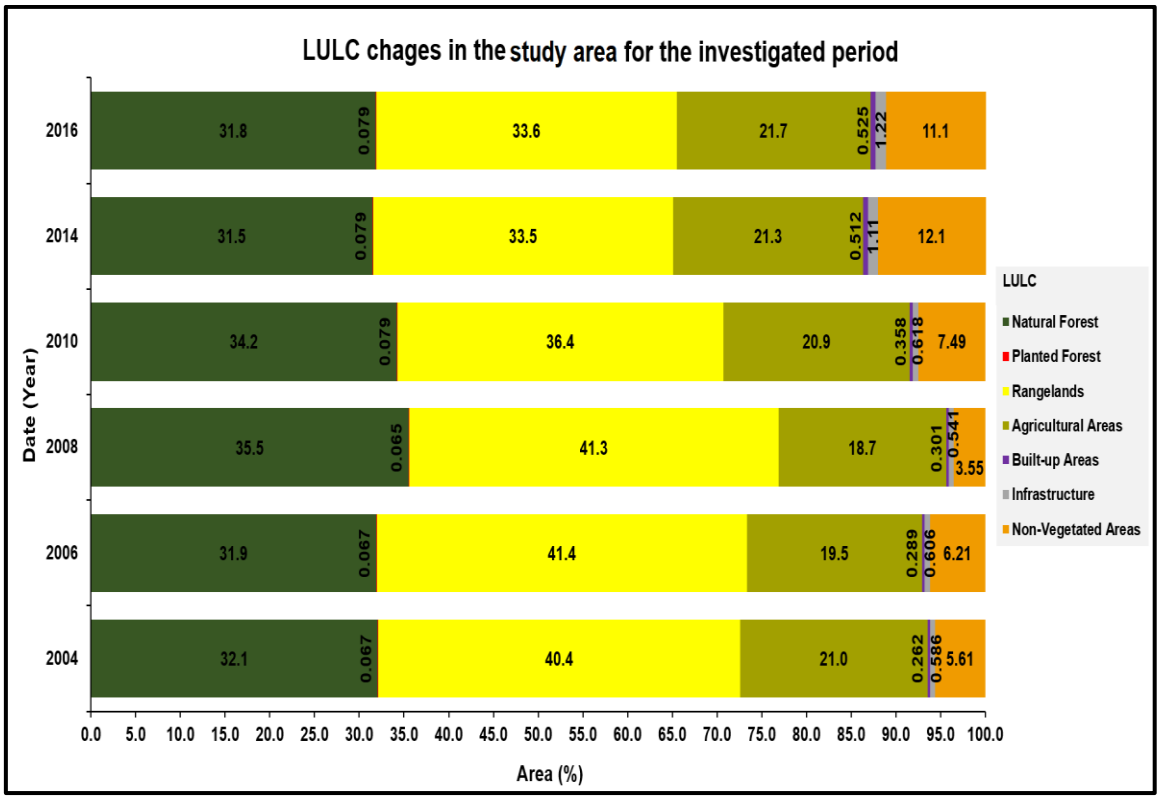

Figure 5.8 The land use land cover changes in the study area for the period 2004-2016

For natural vegetation cover classes, in general, RL showed an increase to 41.4% of the total area (417,038 ha) in 2006 followed by a decrease to 33.5 and 33.6% of the total area (337,525 and 338,125 ha) in 2014 and 2016, respectively. By comparison, the PF shows a slight increase up from 0.07% of the total area for the years 2004 – 2008 (679, 679 and 658 ha for the years 2004, 2006 and 2008 respectively) to 0.08% for the period 2010-2016 (795, 796 and 792 ha for the years 2010, 2014 and 2016 respectively). The tiny decrease in the PF area in 2008 and 2016 could be due to the cutting down the trees, while the increase of the area is a result of the reforestation that has occurred in the study area.

In contrast, the NF class showed an evident fluctuation between an increase and a decline throughout the study period with a maximum increase in 2008 to 34.6%, of the study area dropping to 30.2% in 2014 then increasing again to 30.9% of the study area in 2016. This condition of fluctuation in NF area can result from the 2013 fire that led to the NF land being unvegetated in 2014 (El

Shatshat, 2015; Alsoul, 2016) then after two years, some burn areas of the NF was recovered. Differences in the month when the Landsat image was captured has an effect on the total area of NF in the study area reflecting the variation in vegetation growth with an increase in NF area following the wet season and decrease in the dry, hot months during the summer. The growth of seasonal plants (grasses) in Winter and early Spring season (2010 image) and early Summer season (2008 image) can be taken into account also in explaining such changes, where the annual plants increase the vegetated area of NF especially in Spring season.

5.2 Land Use Land Cover Change Detection

This section describes the quantifiable results of LULC change assessment that was undertaken in the study area, following the application of a Post-Classification Comparison (PCC) technique. The change detection results are represented as tabulated data, maps and charts. The research outcomes here are organised in two sections, the first presenting the changes in LULC between the periods from the year 2004 to 2016, and the second specifying the gain, loss, and the percentage of net changes in LULC classes.

5.2.1 Past land use and land cover changes

The change detection was undertaken for five periods (from 2004 to 2006, from 2006 to 2008, from 2008 to 2010, from 2010 to 2014, and from 2014 to 2016). Where the results are divided into two subsections; the first shows the results of the period before the 2011 Libyan uprising (2004-2010), and the second the results of the period after the 2011 Libyan uprising (2010-2016).

5.2.1.1 Land use land cover change before the 2011 Libyan uprising

The results for the detection of changes in LULC for the three periods, from 2004 to 2006, from 2006 to 2008 and from 2008-2010 is presented here. Where the cross-tabulation matrix (Apppendix Table G.1.1) represents the transition in LULC classes from 2004 to 2010, while the distribution of the existing LULC classes and the transition groups in the LULC for the 2004-2010 periods is

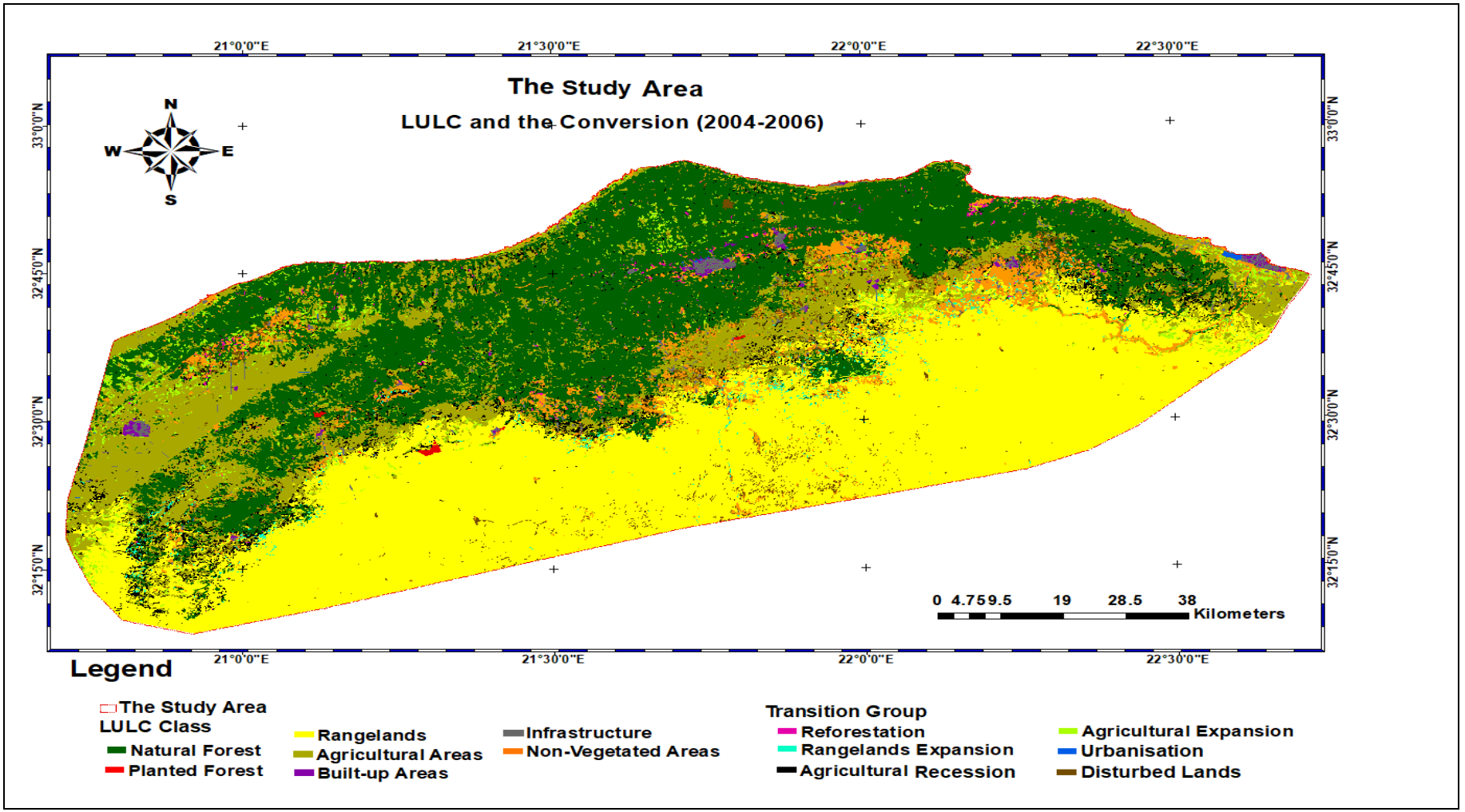

Figure 5.9 Resultant thematic change analysis of the study area of the 2004-2006 period

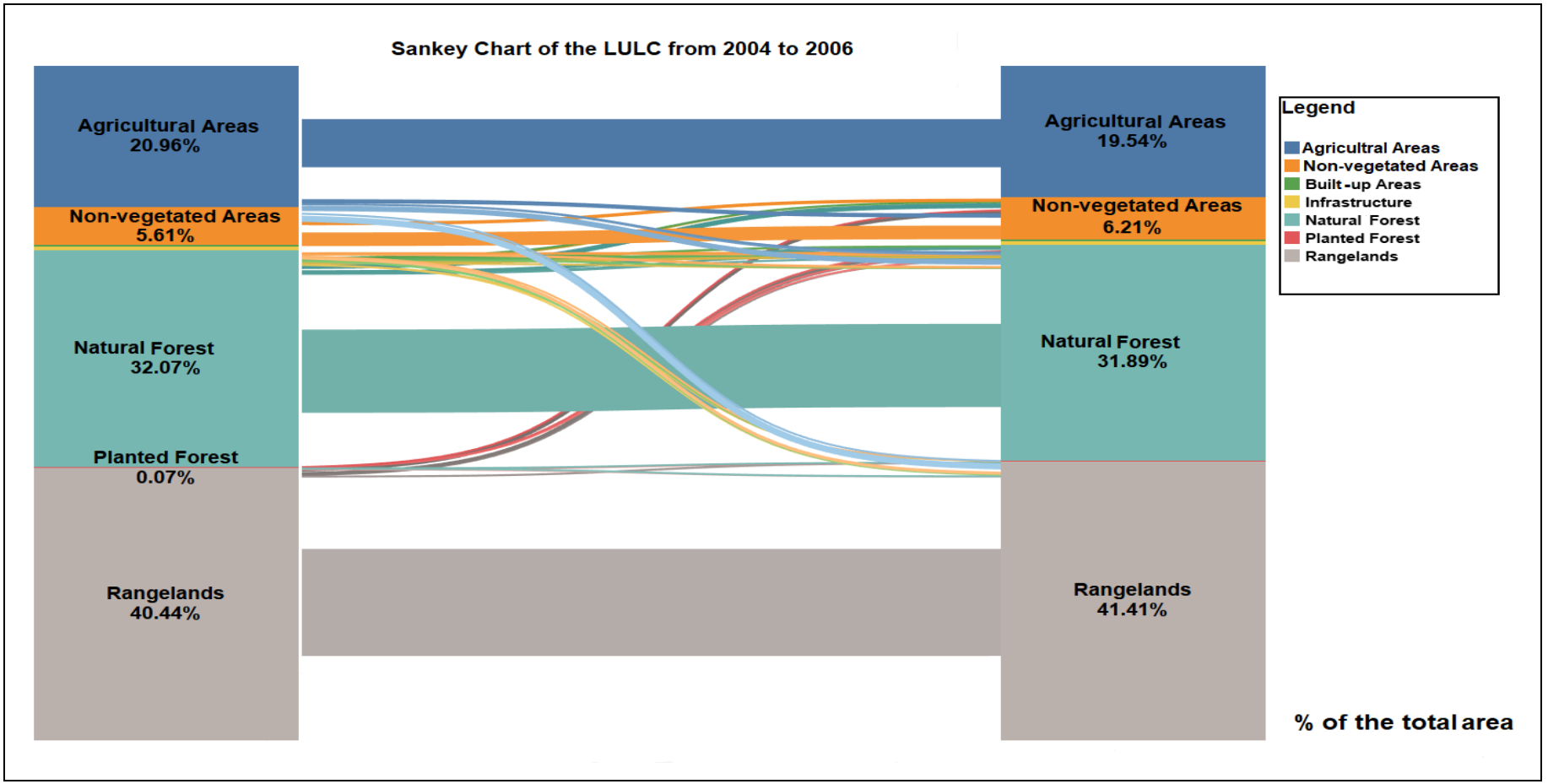

Figure 5.10 Sankey chart showing the "from-to" change trajectory of the LULC classes of the 2004-2006 period

illustrated in Figure 5.9, Figure 5.11 and Figure 5.13, and the path of the transition is illustrated in Figure 5.10, Figure 5.12 and Figure 5.14. The critical changes in the study area were associated with AA, RL and NV for the 2004-2006, and NF, NV, and AA for 2006-2008, and RL, NV, AA, and NF for the 2008-2010 period. In general, BA and IN are shown to have experienced a steady increase over the years investigated (Apppendix Table G.1.1).

The results indicated that:

-The NV coverage increased from 56,547 ha in 2004 to 62,521 ha in 2006, which accounts for only 0.59% of the total area . A decline in NV to 35,198 ha was observed in 2008, accounting for 2.63% of the total area. In 2010 the NV coverage increased to 75,609 ha, accounting for 3.96% of the total area. In contrast,

-Fluctuation of AA area which has declined from 211,141 ha in 2004 to 196,765 ha in 2006 accounts for 1.43% of total area, and to 190,442 ha in 2008, raising then to 209,320 ha in 2010 that accounts for net increases of 2.05 % (20,609 ha) of the total area. This fluctuation related to the types of cultivated crops such as the rainfed crops (wheat and barley) which are the dominant crops in the study area.

-The BA and IN classes, have slightly increased in 2006, the net increase observed being 0.03% (296 ha) and 0.02% (205 ha) followed by a slight decline in IN where the net decrease was 0.02% (177 ha), and no changes from BA were detected in 2008. The decrease in IN in 2008 (221km) can be referred to the temporary tracks used by locals during crop harvest, pastoral activities or camping seasons. These tracks sometimes disappear because they are occasionally used. In 2010 the net increase in the BA and IN classes were 442 and 279 ha (0.04% and 0.03% of the total area of the study area, respectively).

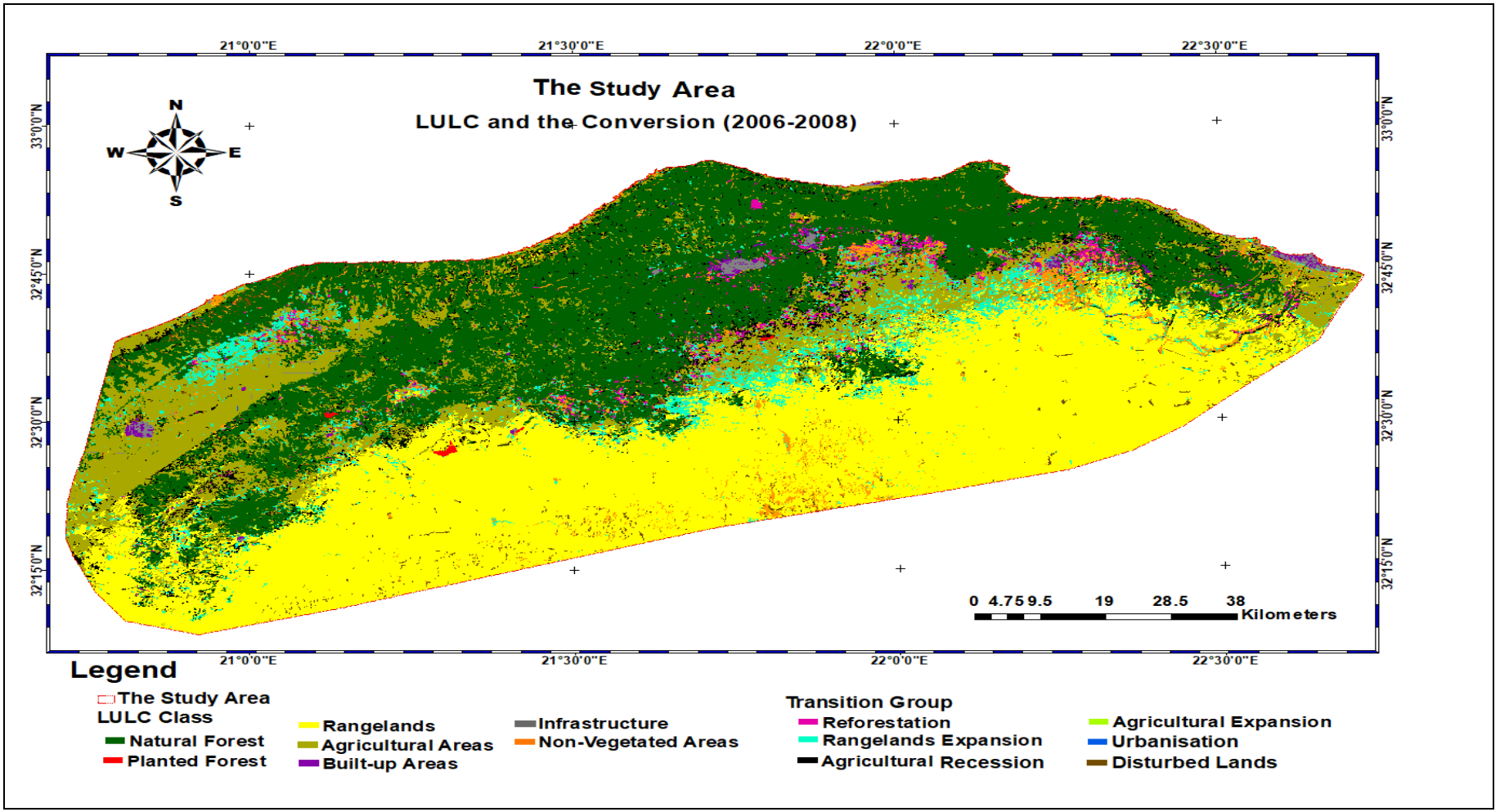

Figure 5.11 Resultant thematic change analysis of the study area of the 2006-2008 period

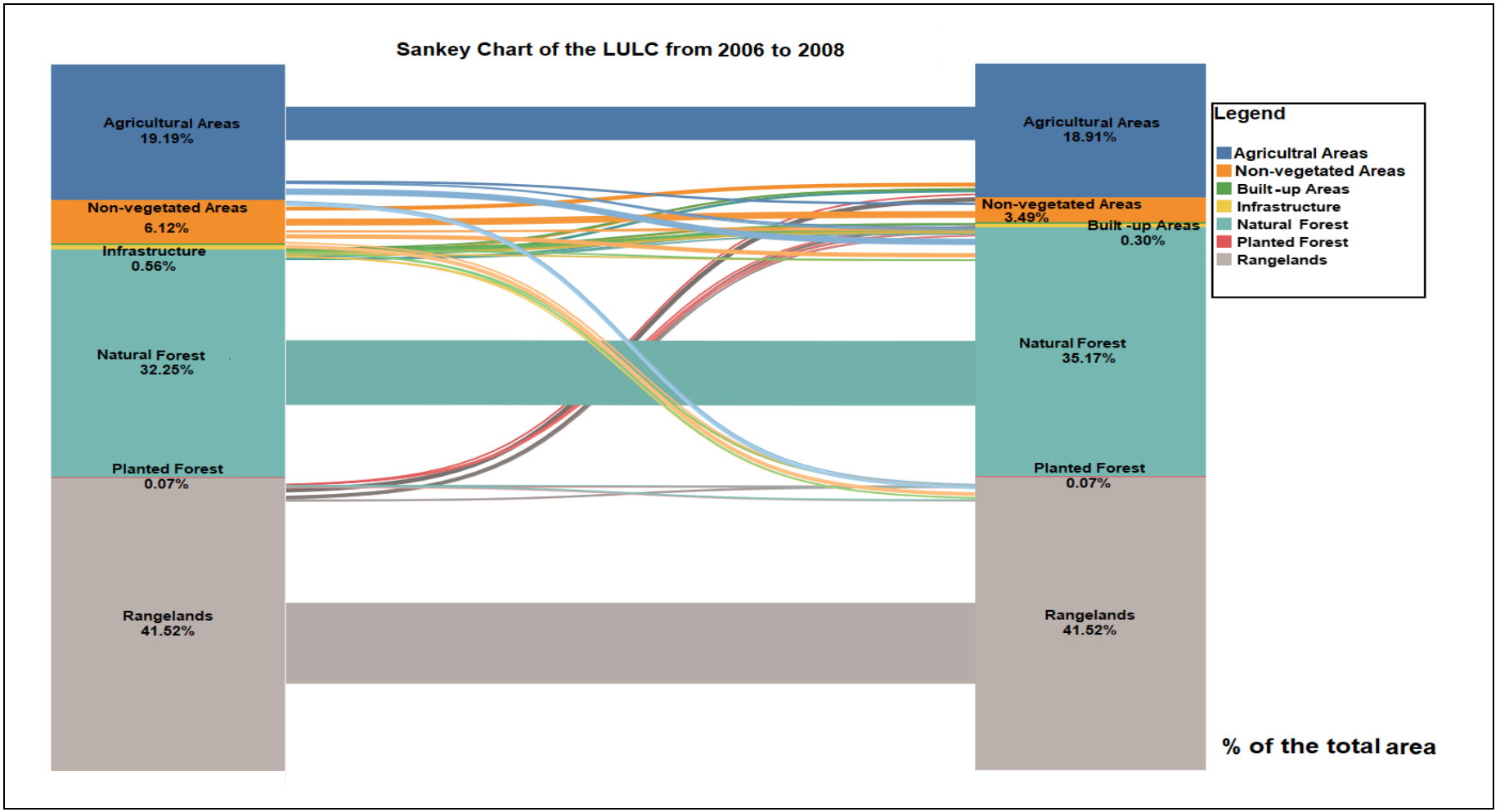

Figure 5.12 Sankey chart showing the "from-to" change trajectory of the LULC classes of the 2006-2008 period

-The natural vegetation cover:

No conversions from PF were detected in the first two time periods (2004-2006 and 2006-2008), in 2010 there was a slight increase shown account for a net increase of 0.01% of the total area (105 ha) due to the reforestation (the new PFs detected and digitized from GE).
In contrast, NF and RL revealed some changes throughout the entire study period. An increase of *circa* 10,000 ha was observed from 407,256 ha in 2004 to 418,164 ha in 2006 for the RL area, then decreasing to 416,314 ha in 2008 (a net decrease of an area of 66 ha '0.01% of the total area') and to 366,933 ha in 2010 that accounts for a net decrease of 4.90% of the total area (49,381 ha). For NF, a net decrease of 1854 ha (0.18% of the total area) was detected from 323,001 ha in 2004 to 321,146 ha in 2006, a net increase of an area of 29,463 ha (2.93% of the total area) then was detected in 2008, followed by a decline to 345,495 ha in 2010 that accounts for a net decrease of 1.19 % of the total area (11,963 ha).

Regarding the transition groups (Table 5.5) (see Section 4.3.1), the important transition groups for 2004-2006 were observed to be associated with agricultural recession, agricultural expansion, and distyrbed lands accounting for 2.85% (28,725 ha), 2.27% (22,839 ha) and 1.86% (18,726 ha) of the total area, respectively. In contrast, rangelands (RL) expansion, reforestation and urbanisation accounted for 0.54% (5,425 ha), 0.27% (2,687 ha) and 0.04% (416 ha) of the total area, respectively. Agricultural expansion, agricultural recession, reforestation, and RL expansion were the important transition groups for the 2006-2008 period accounting for 3.10% (31,259 ha), 3.02% (30,433 ha), 1.39% (14,036 ha) and 1.22% (12,260 ha) of the total area, respectively. Disturbed lads and urbanisation were 0.92% (9,267 ha), and 0.01% (125 ha) of the total area, respectively, for the 2006-2008 period. During the 2008-2010 period, the important transition groups were agricultural expansion, disturbed lands of NF, RL and AA, agricultural recession, and reforestation which were associated with 6.26% (63,083 ha), 5.29% (53,309 ha), 3.64% (36,670 ha) and 1.90% (19,137 ha) of the total area, respectively. Rangelands expansion and urbanisation

represented 0.45% (4,566 ha), and 0.08% (760 ha) of the total area, respectively.

Table 5.5 Transition Group of the study area between years from 2004 to 2016 (ha)

Transition Group	2004-2006	2006-2008	2008-2010	2010-2014	2014-2016
Agricultural Recession	28,726	30,433	36,670	38,038	31,511
Agricultural Expansion	22,839	31,259	63,083	73,103	46,526
Urbanisation	416	124	760	2,646	901
Rangelands Expansion	5,435	12,259	4,565	19,487	13,352
Reforestation	2,687	14,036	19,137	5,226	7,550
Disturbed lands	18,726	9,266	53,309	63,881	27,150

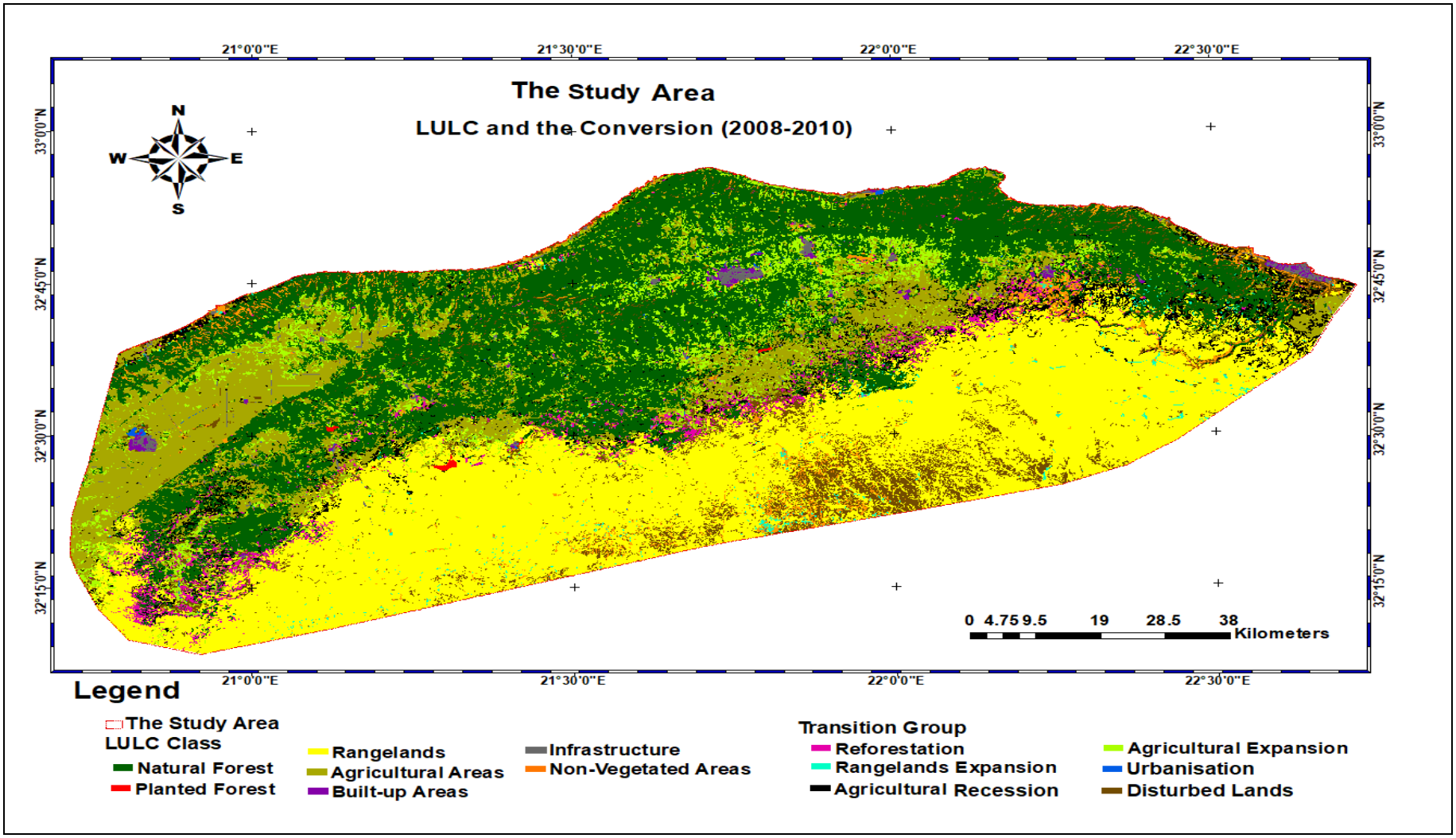

Figure 5.13 Resultant thematic change analysis of the study area of the 2008-2010 period

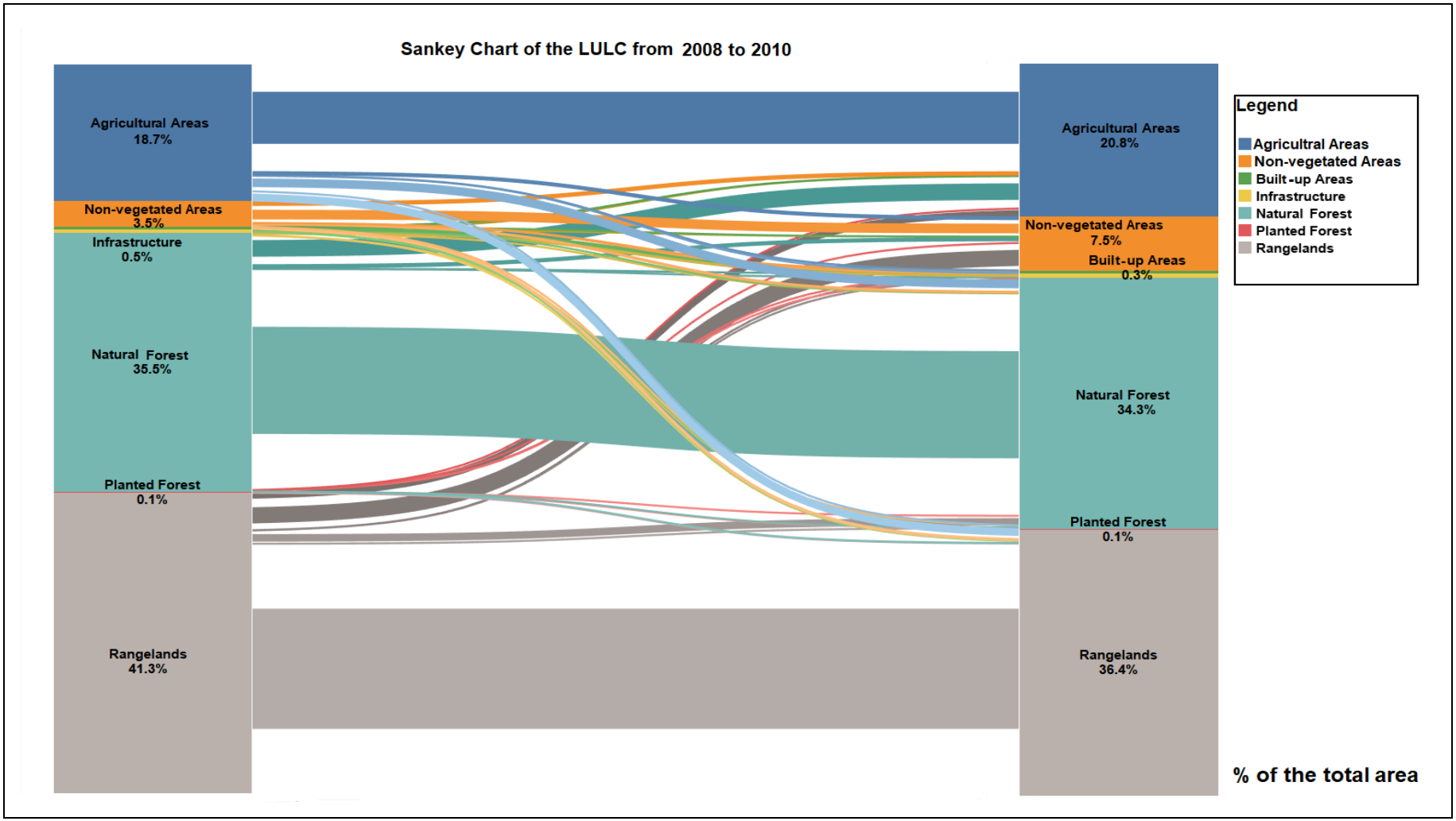

Figure 5.14 Sankey chart showing the "from-to" change trajectory of the LULC classes of the 2008-2010 period

5.2.1.2 Land use land cover change after the 2011 Libyan uprising

The outcomes of two time periods, from 2010 to 2014, and from 2014 to 2016 (noting the satellite imagery of 2012 was unavailable), are presented. A cross-tabulation matrix (Appendix Table G.1.2) represents the magnitude of conversions for the 2010-2016 period: while the distribution of the existing LULC and the transition groups in the LULC in the study area for the entire study period is demonstrated in Figure 5.15 and Figure 5.17, and the path of the transitions are illustrated in Figure 5.16 and Figure 5.18. The important changes in the study area for the 2010-2014 period were in NV, RL, and NF, while there were only slight conversions between these classes in the period 2014-2016 (Appendix Table G.1.2).

The NV coverage has increased from 75,460 ha in 2010 to 120,716 ha in 2014, which accounts for 4.49% of the total area (the net increase from 2010-2014). The reason of the increase in NV area in 2014 was due to the date of image capture where the 2014 image was in July 2014 and the 2010 image in March when the land is more likely to be covered with herbaceous plants and annuals. This was followed by a decrease to 112,093 ha in 2016, accounting for 0.94% of the total area. In other words, in 2014 NV decreased by 36,573 ha, and in 2016 the NV gained an area of 27,150 ha; therefore, the NV has a net decrease from of 9,423 ha (0.94% of the total area). The AA area also increased from 210,033 ha in 2010 to 217,734 ha in 2014 that accounts for a net increase of 0.76% of the total area (7,700 ha), and to 218,501 ha in 2016 that accounts for a net increase of 0.40% of the total area (4,009 ha).

For the 2010-2014 period, an increase in IN was detected from 6,225 ha in 2010 to 8,867 ha in 2014, which accounts for a net increase of 2,643 ha or 0.26% of the total area. Similarly, for BA, an increase from 3,601 ha in 2010 to 4,855 ha in 2014 was detected that accounts for a net increase of 1,253 ha or 0.12% of the total area. Both the IN and BA areas also showed a slight increase from 2014 to 2016 of 1,050 ha and 132 ha, respectively.

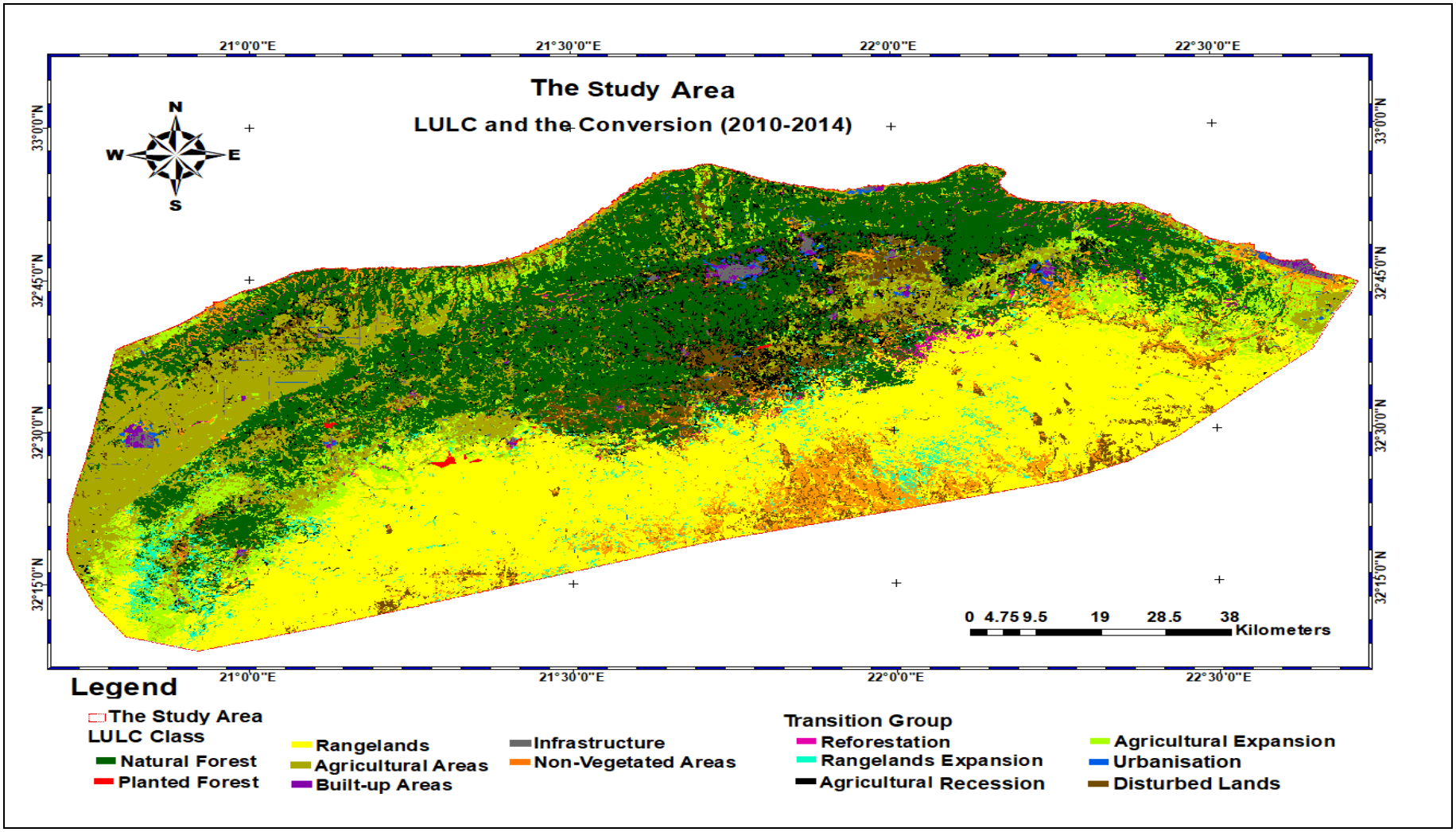

Figure 5.15 Resultant thematic change analysis of the study area of the 2010-2014 period

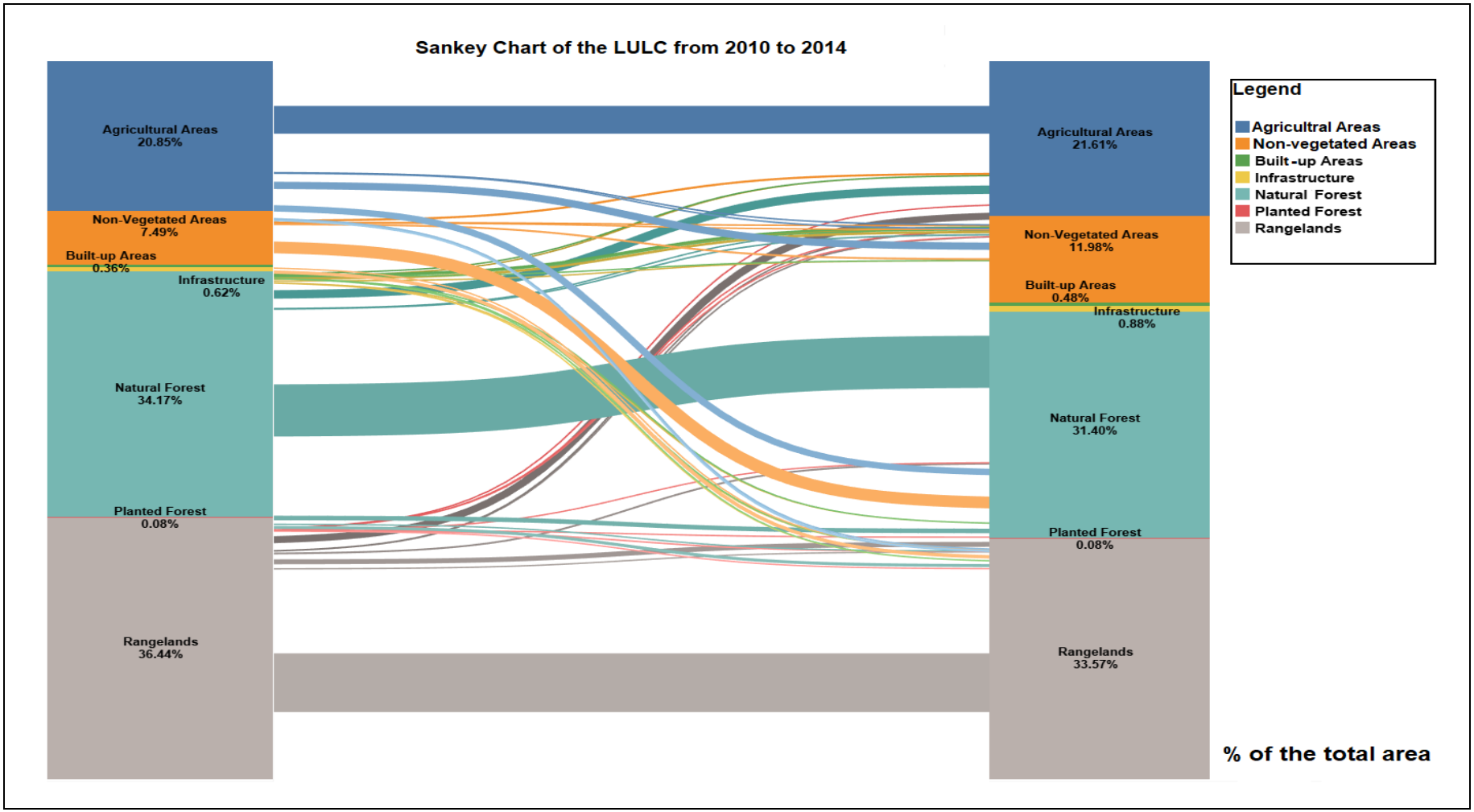

Figure 5.16 Sankey chart showing the "from-to" change trajectory of the LULC classes of the 2010-2014 period

For the natural vegetation cover in the study area, no changes in PF were detected in the 2010-2014 period where only a negligible decline from 796 ha in 2014 to 762 ha in 2016 was observed. In contrast, changes in NF and RL were observed. A decrease of *circa* 30,000 ha was observed from 367,073ha in 2010 to 337,526 ha in 2014 for the RL area, followed by an increase to 338,125 ha in 2016 for RL, accounts for a net increase of 0.06% of the total area (599 ha). For NF, a decrease from 344,201 ha in 2010 to 316,290 ha in 2014 was observed. This accounts for a net decrease of 27,910 ha or 2.77% of the total area. NF subsequently, increased by 3,636 ha to 320,589 ha in 2016, accounting for an additional 0.36% of the total area.

Regarding the transition groups (Table 5.5), the important groups organised based on their % of the total area, for the 2010-2014 periodwere agricultural expansion, disturbed lands, agricultural recession, and rangeland expansion with values of 7.26%, 6.34%, 3.78% and 1.93%, respectively. While reforestation and urbanisation were associated with values of 0.52%, and 0.26%; respectively. For the 2014-2016 period, the important transition groups were agricultural expansion, agricultural recession, disturbed lands, and rangelands expansion with values of 4.62%, 3.13%, 2.69% and 1.33%, respectively, while reforestation and urbanisation were associated with a change of 0.75%, and 0.09%, respectively.

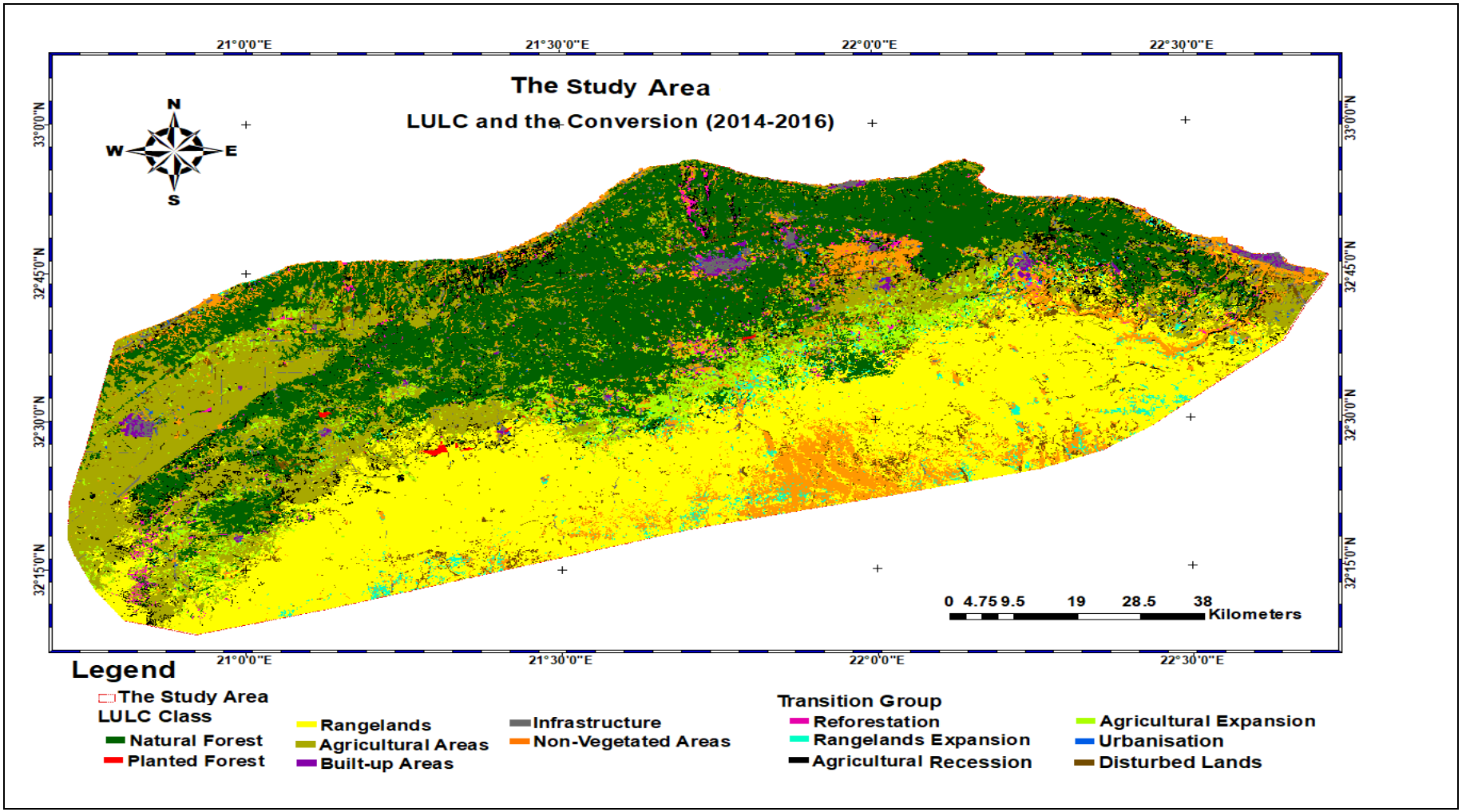

Figure 5.17 Resultant thematic change analysis of the study area of the 2014-2016 period

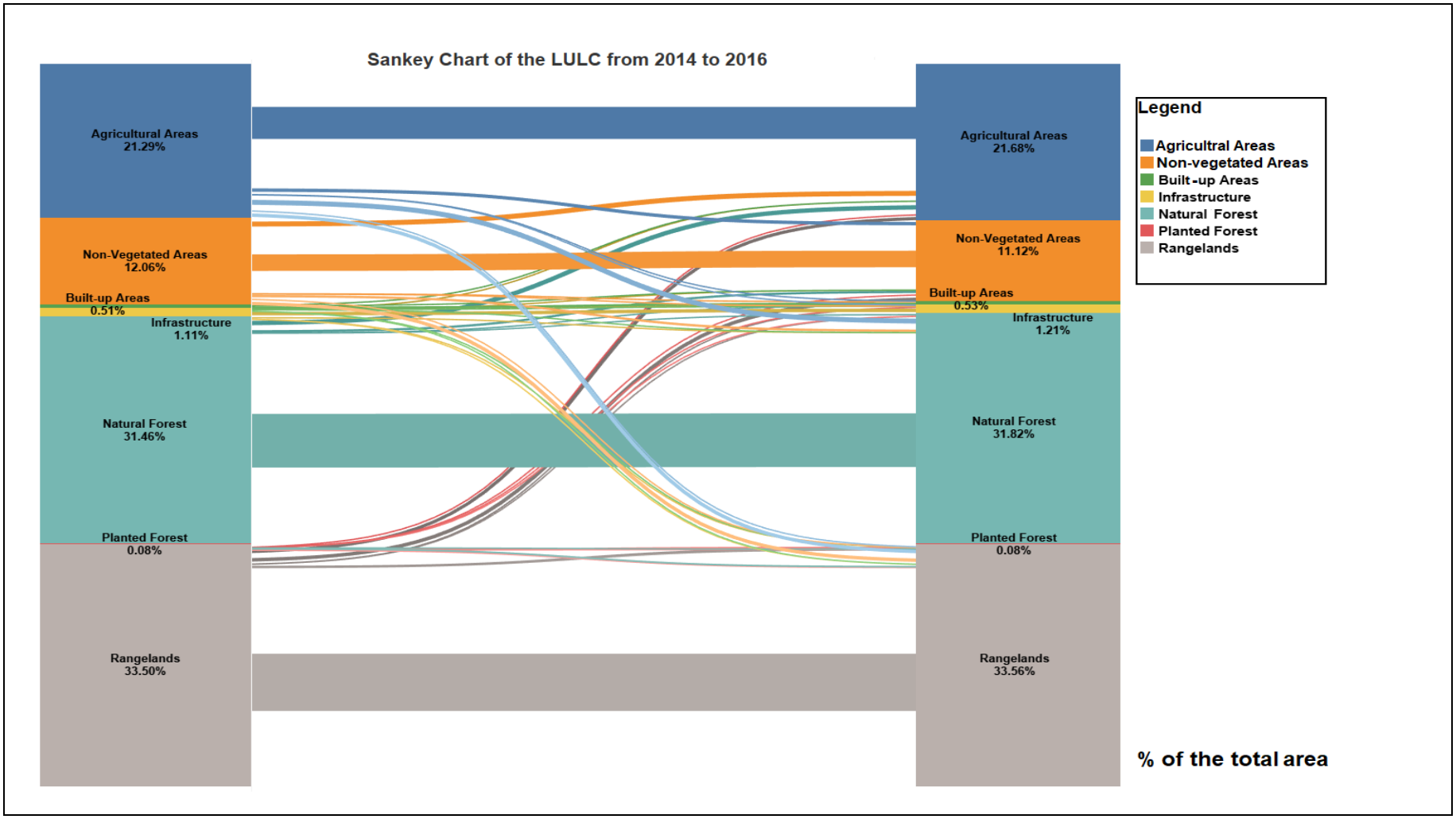

Figure 5.18 Sankey chart showing the "from-to" change trajectory of the LULC classes of the 2014-2016 period

5.2.2 Gains, Losses and Net changes in LULC

This section focuses on the dynamics measured across the natural vegetation categories (NF, PF, RL) that were under investigation in this study. Figure 5.19 shows the gain, loss, and net change (ha) of each LULC category for the five time periods (from 2004 to 2006, from 2006 to 2008, from 2008 to 2010, from 2010 to 2014, and from 2014 to 2016).

Looking at the five time periods, regarding natural vegetation, RL and NF have experienced the most noteworthy change as shown by their gain from and loss as compared with PF. With regards NF and RL, the results show that NF gained greater areas than RL except in the 2004-2006 period; and vice versa when considering the loss of natural vegetation areas. NF lost smaller areas than RL except in 2004-2006 and 2010-2014 (Figure 5.19 (a, b and c)).

PF shows an increase in the 2008-2010 period as a result of the reforestation that was carried out by the Development Project of Vegetation Cover in Al Jabal Al Akhdar (Zatout, 2011). Referring to Appendix Table G.1.1, the reforestation work was done in some areas located in RL and NV LULC classes. These results also showed that 108 ha of AA was converted to PF. Having such AA within the results may be due to the misclassification of the NF class as AA in the 2010 classified image (Table 5.3). In the 2014-2016 period, the results show a net decline of 4.14 ha in the PF area, which was converted to AA (Appendix Table G.1.2**Error! Reference source not found.** (B)).

The net change shows whether a LULC class has increased or decreased across transition periods (Figure 5.19 (a)). The net changes in the LULC of the study area for the five transition periods. NF was observed to has a net decrease in the 2004-2006 period due to the transition of 1855 ha of NF to IN (75 ha), BA (26 ha), RL (634 ha) and NV (2942 ha) and 1823 ha was converted from NF to AA (Appendix Table G.1.1 and Table G.1.2). A net increase in RL of 9782 ha was observed due to areas of NV (68 ha), AA (9111 ha), and NF (634 ha) BA (9.7 ha) and IN (22 ha) being converted to RL (Appendix Table G.1.1 (A)).

The 2006-2008 period shows a different dynamic to the previous period (Figure 5.19 (a)), where NF increased, and RL decreased (based on their net change). The net increase in NF (29,463 ha) was due to the transition of areas of IN (94 ha, temporary tracks), AA (18,396 ha) and NV (11,875 ha) to NF, and 902 ha of NF being converted to RL. While the net decrease of RL (66 ha) resulting from loss of 7,556 ha that transitioned to AA, and from the gain of 902 ha, 6,549 and 39 ha of NF, NV and IN; respectively, which converted RL (Appendix Table G.1.1 (B)).

In the 2008-2010 period (Figure 5.19 (b)) the net decline of NF (11,963 ha) resulting from the transition of 23,296 ha to AA,186 ha to IN (186 ha), 54 ha to BA 3,523 to NV areas; also there is an area of 15,095 ha being converted to NF from RL. (Appendix Table G.1.1 (C)). Beside of the 15.095 ha of RL converted to NF, the RL also has lost 85 ha to PF, 26 to BA, 104 ha to IN and 37,724 to NV areas, also, the RL has gained an area of 3,652 from AA. All these transition types formed the net decrease in RL (49,382 ha) in this period.

For the 2010-2014 period, the net decline of NF was due to the transition an area of 27,910 ha to RL (6,385 ha), AA (6,276 ha), IN (840 ha), BA (145 ha) (Appendix Table G.1.2(A)). Appendix Table G.1.1 (C) and Table G.1.2 (A) show that a larger area of NF was lost in the 2010-2014 period than the 2008-2010 period can be accounted for from a forest fire that occurred in 2013 (El Shatshat, 2015; Alsoul, 2016).(Figure 5.24). Regarding RL, the net decline of RL results from the conversion of a total of 49,381 ha as follows to NF (15095 ha); PF (85 ha); BA (26 ha); IN (103 ha) and NV (37,724 ha). In addition, 3,652 ha was converted from AA to RL from 2008-2010 (Appendix Table G.1.1 (C)). For the 2010-2014 period, a net decrease area of 28,942 ha was due to the transition from RL to AA (26,357 ha), BA (84 ha), IN (412 ha), and NV (8,473 ha), and to an area of 6,385 was transitioned from NF to RL. (Appendix Table G.1.2 (A)).

A slight increase was shown in the net change of NF and RL during the 2014-2016 period (Figure 5.19 (c)). The net increase of in NF of 3,926 ha was due to the transition of 105, 3,182 and 506 ha of RL, AA and NV to NF respectively,

and to 3.0 and 154 ha being converted from NF to BA and IN, respectively. The observed net 599 ha increase of the RL was due to the transition of 1,328 ha from AA to RL, and 105, 14.0, 2.0 and 608 ha being converted from NF to BA, IN and NV, respectively (Appendix Table G.1.2 (B)).

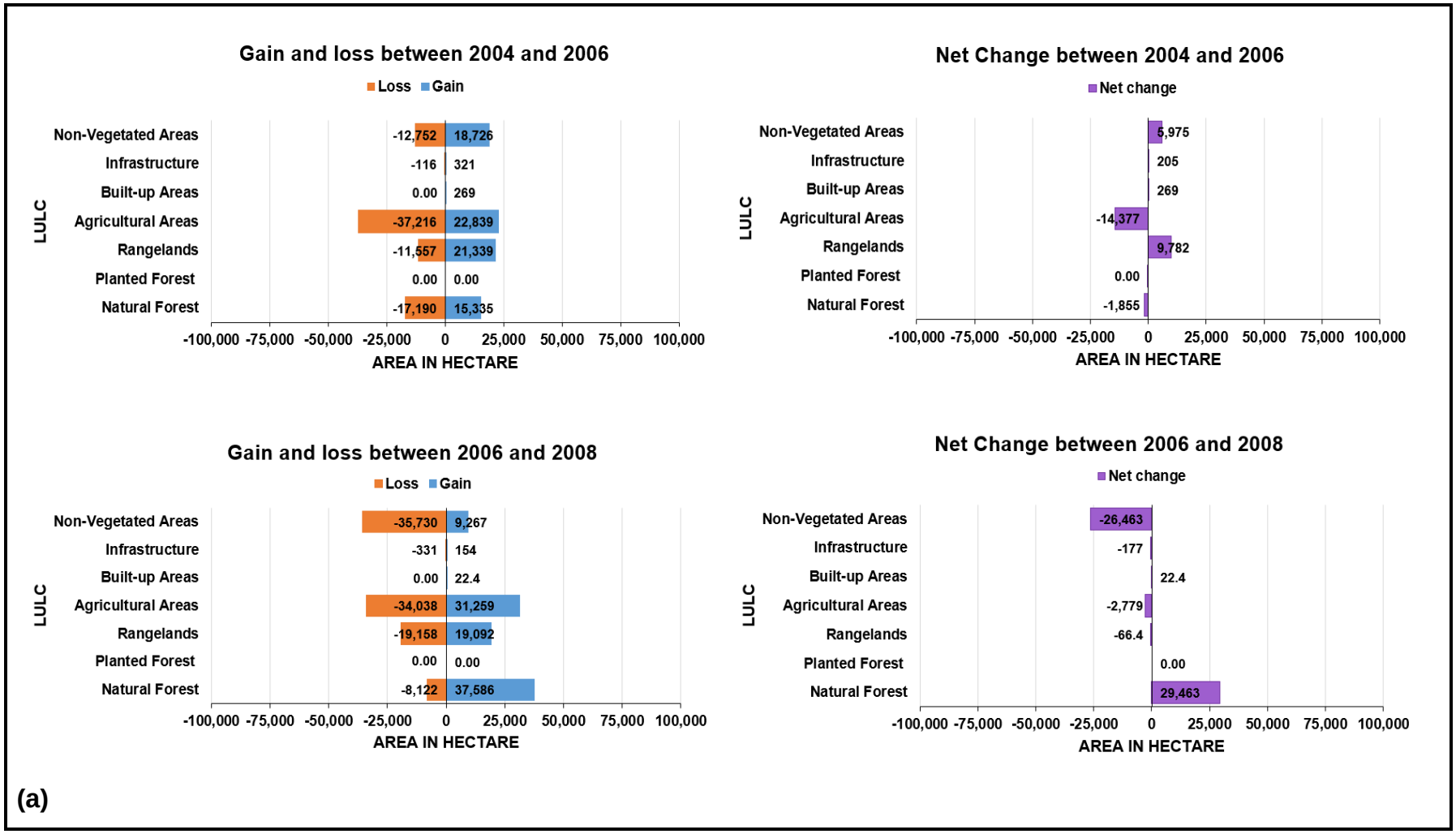

Figure 5.19a-c Gains and losses, and net changes (ha) between 2004-2006 and 2006-2008

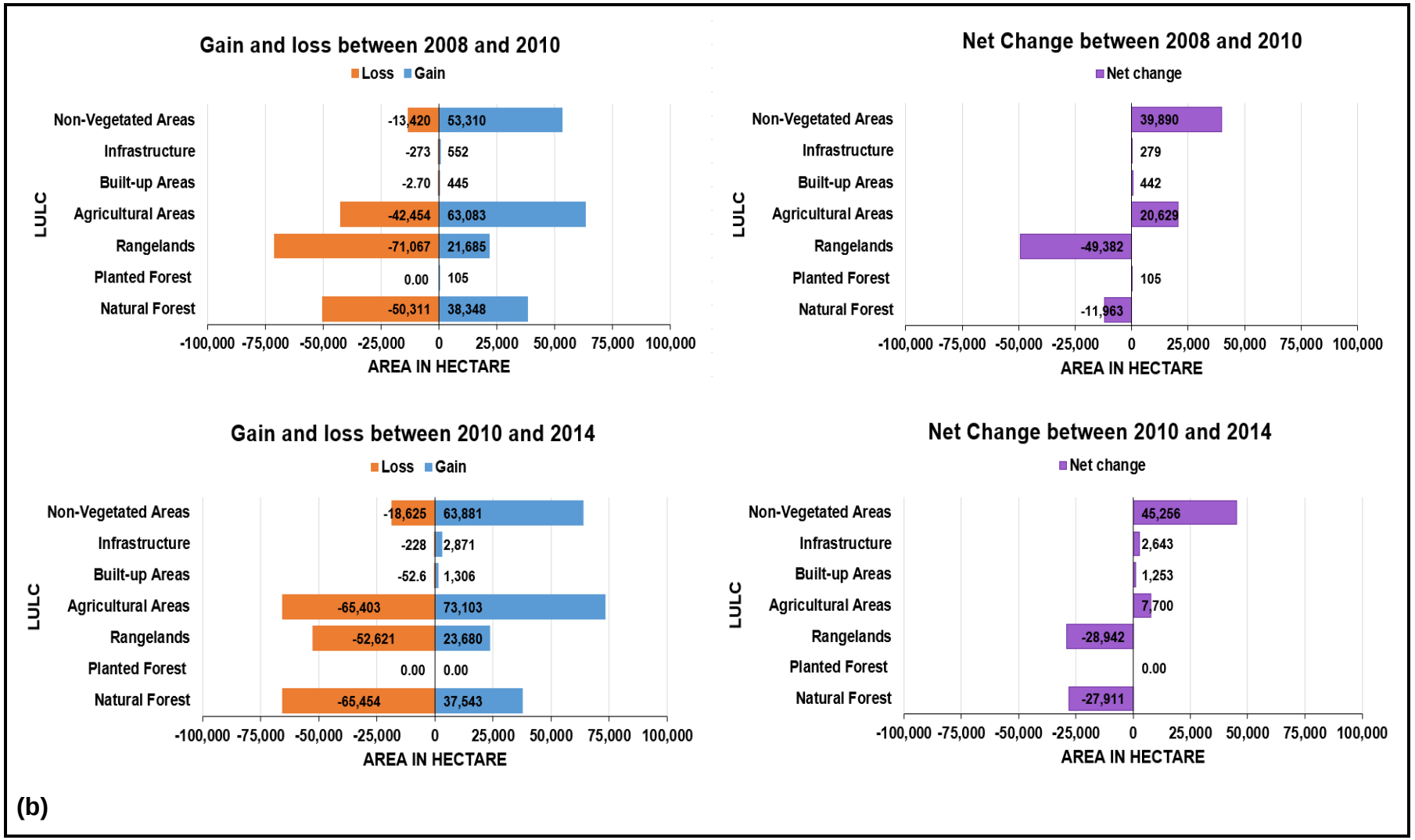

Figure 5.19a-c Gains and losses, and net changes (ha) between 2008-2010 and 2010-2014

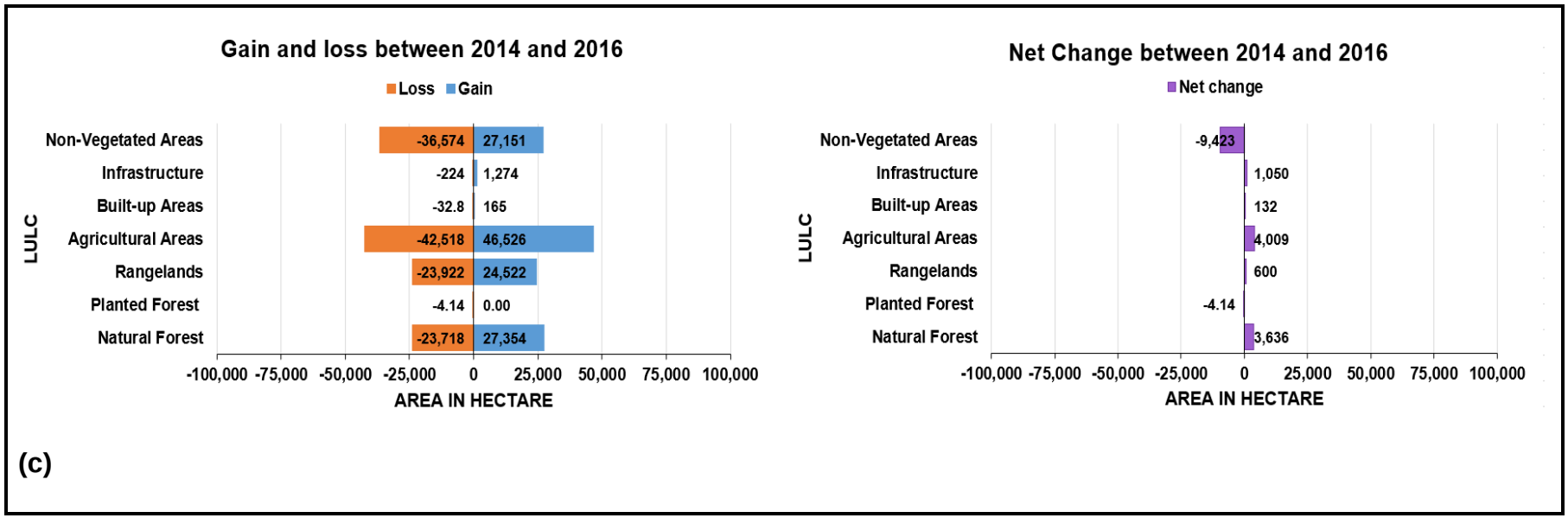

Figure 5.19a-c Gains and losses, and net changes (ha) between 2008-2010 and 2010-2014

5.3 **Population Dynamics**

This section presents the results of population analysis within the study area. The statistical analyses undertaken included comparisons performed between population density and population growth rate, all within the study area districts for the years investigated (namely 2004, 2006, 2008. 2010, 2014 and 2016). The results are estimated from data derived from the 30 cities, towns and villages which had available census data for the years investigated. However, the region also received large numbers of immigrants from the Ajdabiya district (located to the west of Benghazi district), and from west and south of Libya during the Libyan revolution (2011), as well as during the war in the Benghazi and Derna districts (2014 to the present. Therefore, these developments are not included in the assessment as the corroborating data is not available. This section is divided into two subsections, the first subsection is providing population statistical analysis, and the second subsection is presenting the relationship between population change and the observed changes in natural vegetation cover.

5.3.1 Population growth

The census surveys of 1973, 1984, 1995 and 2006 were conducted by the Bureau of Statistics and Census-Libya (BSC-L) and the LUPA. These were used to obtain the population data for the cities, towns, and villages within the study area. Fifty-two urban areas occur within the study areadistributed in three districts, Al Marj, Al Jabal Al Akhdar and Derna (see Figure 3.8) based on the 2007 administrative divisions of Libya. The population of the years investigated were estimated statistically, based on the census data (see Section 4.1.2) for 30 urban areas which have available data.

Figure 5.20 presents the population for the years investigated (2004, 2006, 2008, 2010, 2014, 2016) and 1973, 1984 and 1995, for each city and village located within the study area. Half of the 30 urban areas located within the study area are located within the Al Jabal Al Akhdar district.

Comparing the three individual districts within the study area, Al Jabal Al Akhdar district has higher populations than those in the Derna and Almarj districts (Table 5.6). The high population of Al Jabal Al Akhdar district is because there is a relatively higher number of the cities, towns, and villages of the study area found within this area. Similarly Al Jabal Al Akhdar district has higher densities, whilst the Al Marj district has the lowest densities over all the years investigated.

Table 5.6 presents the population statistics of the study area and the Al Marj, Al Jabal Al Akhdar and Derna districts. The statistical analyses include population density and population growth rate of the study area districts for the years investigated. The population within the study area was only 410,614 in 2004 and increased to 499,851 in 2016.

The average population density in study area was 41 capita per km^2 in 2004, increasing to 50 capita per km^2 in 2016 (Table 5.6). Al Jabal Al Akhdar district had the highest population density (50 capita per km^2) in 2004, which increased to 61 capita per km^2 in 2016, followed by Derna district with 43 capita per km^2 in 2004 and 52 capita per km^2 in 2016. Al Marj district had a low population density, with only 30 capita per km^2) in 2004, which increased to 36 capita per km^2 in 2016.

Based on Table 5.6, the average annual population growth rate was 1.84 % for the population of the study area in 2004 and decreased to 1.77 % between 2004 and 2006, and dropped to 1.5 % between 2014-2016. Generally, the growth rate of the study area area tends to decrease during the period between 2004 and 2016.

5.3.2 The impact of human activities on the natural vegetation cover

For the five transition periods from 2004 to 2006, from 2006 to 2008, from 2008 to 2010, from 2010 to 2014, and from 2014 to 2016) LULC analysis showed that the most significant changes in natural vegetation cover were observed between NF and RL and AA, BA, IN and NV.

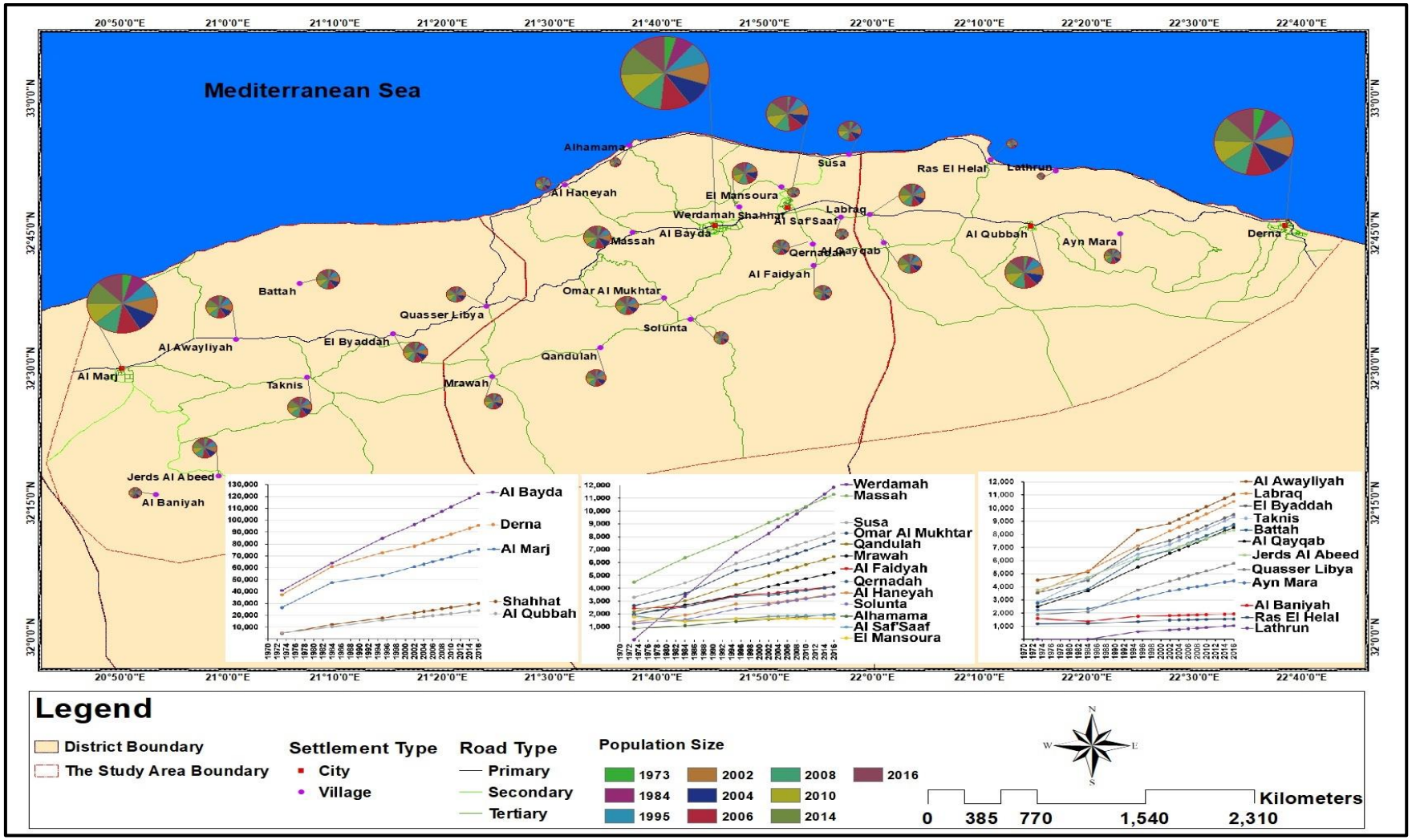

Figure 5.20 Population size within the study area, displayed as cities, towns and villages

Table 5.6 Population statistics of the study area divided into the Al Marj, Al Jabal Al Akhdar and Derna districts

Characteristics / District	Al Marj	Al Jabal Al Akhdar	Derna	study area
2004				
Population (Capita)	107,919	181,868	120,827	410,614
Density (Capita per km^2)	30	50	43	41
Growth rate (%)	1.76	1.99	1.76	1.84
2006				
Population (Capita)	111,627	188,890	124,969	425,486
Density (Capita per km^2)	31	51	45	42
Growth rate (%)	1.70	1.91	1.70	1.77
2008				
Population (Capita)	115,337	195,914	129,108	440,359
Density (Capita per km^2)	32	53	46	44
Growth rate (%)	1.65	1.84	1.64	1.71
2010				
Population (Capita)	119,047	202,936	133,247	455,230
Density (Capita per km^2)	33	55	48	45
Growth rate (%)	1.60	1.78	1.59	1.65
2014				
Population (Capita)	126,467	216,987	141,525	484,979
Density (Capita per km^2)	35	59	50	48
Growth rate (%)	1.52	1.69	1.52	1.58
2016				
Population (Capita)	130,176	224,008	145,667	499,851
Density (Capita per km^2)	36	61	52	50
Growth rate (%)	1.46	1.60	1.45	1.50

The transition type from one class to another was grouped under the transition group (Table 5.5). Agricultural Expansion refers to converting NF, PF and RL to AA; and urbanisation represents the transition from NF, PF and RL to either BA or IN. Disturbed lands can be referred to the non-vegetated areas where their natural vegetation cover was removed whether by cutting down the trees and shrubs,

overgrazing, or experiencing fire (El-Barasi and Saaed, 2013; Zatout, 2014). Figure 5.9, Figure 5.11, Figure 5.13, Figure 5.15Figure 5.17 show the distribution of the LULC and displays the spatial distribution of the transition groups. The most critical transition groups that represent the impact of human activities on the natural vegetation cover are agricultural expansion, urbanisation and disturbed lands. Therefore, AA, BA, IN, and NV categories were chosen to analyse their relationship with population change within the study area during the study period (see Section 5.1.2 and Table 5.7).

Table 5.7 Area under different LULC classes in the study area from 2004-2016

Class name	Area (km^2)						Change (km^2) 2004-2016
	2004	2006	2008	2010	2014	2016	
NF	3,230	3,212	3,575	3,442	3,170	3,206	-24
PF	6.79	6.79	6.58	7.95	7.96	7.92	1.13
RL	4,073	4,170	4,163	3,671	3,375	3,381	-692
AA	2,111	1,968	1,887	2,100	2,145	2,185	74
BA	26.4	29.1	30.3	36	51.6	52.9	26.5
IN	59	61	54.5	62.3	112	122	63
NV	566	625	357	755	1,215	1,121	555

Figure 5.21 (a) shows the increasing trend in AA was associated with the increasing trend in population density in the study area (R^2=0.271, 0.976 and for AA). Similarly, the increasing trend in BA, IN and NV were associated with the increase in population density within the study area (Figure 5.21 (b, c, and d)) (R^2=0.885, 0.713 and 0.630 for BA, IN and NV, respectively).

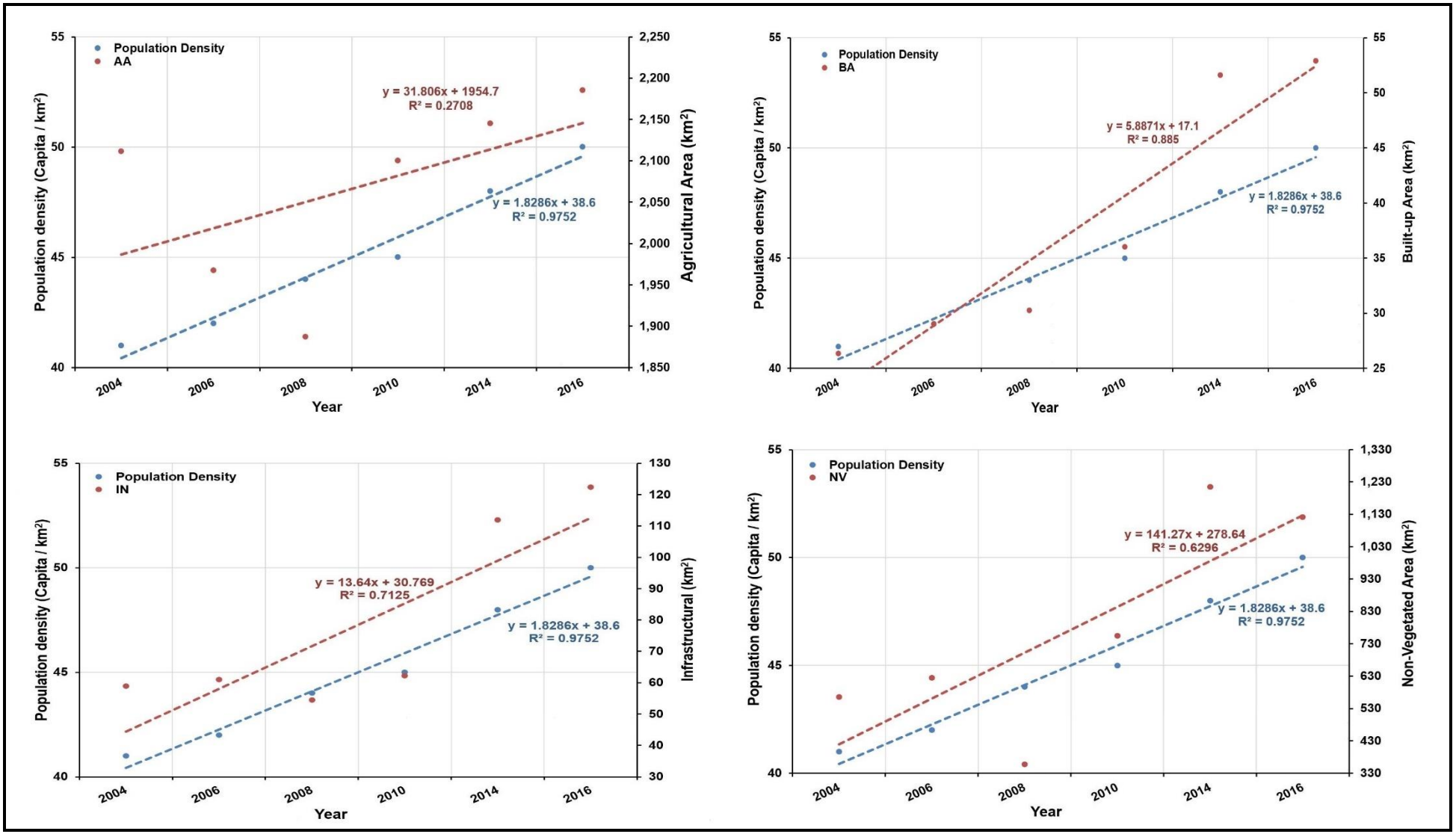

Figure 5.21 Changes in population density, (a) AA, (b) BA, (c) IN and (d) NV from 2004 to 2016

5.4 Climate impacts on natural vegetation cover changes

This section presents the results of the relationships between vegetation represented by NDVI, and climate factors represented by rainfall and temperature over the study period from 2004 to 2016. This section is divided into two, the first part showing the changes in ANDVI results for each landform which were performed by using speardsheet , and the second showing the statistical analysis results of the correlation between ANDVI and climate variables which was undertaken using IBM SPSS statistics software ver.25.

In General, the vegetation (ANDVI) responded positively to rainfall, and inversely to temperature, where the vegetation (ANDVI) increased as expected during the rainy months of the year and decreased in the hot, dry months. This reflects the importance of rainfall in arid and semi-arid areas of the Mediterranean region where soil moisture is considered the limiting factor of vegetation growth (Al-Bakri and Suleiman, 2004; Ibrahim and Assayah, 2014).

From the changes in ANDVI, rainfall, and temperature figures (Figure 5.22, Figure 5.23, Figure 5.25, Figure 5.26, Figure 5.28 to Figure 5.33 and Figure 5.35), it was clear that there was a high monthly variation in ANDVI associated with the rainfall and temperature variability in all study area landforms. This response of ANDVI to rainfall and temperature could be related to the vegetation dynamic where the study area area is dominant by natural vegetation, which is a rainall dependent. In the winter season, the perennial vegetation is in the dormancy phase as a response to the low temperature in January the coldest month of the year in the study area. With the presence of soil moisture and start rising in temperature, the vegetation grows to peak and the the highest ANDVI will be obtained in March and April, in early Spring, where the temperature is suitable for plants growth. Vegetation growth then starts to recess, due to the decrease in soil moisture and the increase in temperature, which reaches the highest degree in August, the hottest month of the year. Therefore, the low values of ANDVI observed during the Summer season with hot months without rainfall. This behaviour of ANDVI particularly agreed with the findings of Ibrahim (2008) who found the highest NDVI values occur in the rainy season from October to May, whereas the lowest values occur in the dry season in rainfed agricultural lands and rangelands in Tarhuna, Libya over a period from 1981-2006. Ibrahim and

Assayah (2014) observed the rapid increase in the vegetation of the Al Jabal AL Akhdar Libya, to reach the highest amount during the Spring (March-May), and decline during June to September.

5.4.1 The changes in temperature, rainfall and ANDVI from 2004-2016

This section shows the results of the changes in temperature and rainfall for seven climate grids and the results of ANDVI changes of the 53 OMU sites of the study area according to their landforms associated with the climate grid for each site over the period from 2004-2016. The results are presented the following subsections.

5.4.1.1 The Coastal Plain landform

Coastal Plain landform includes 14 sites within four climatic grids (1, 4, 5, 6); all the sites are natural forest as listed in Table 5.8.

Table 5.8 Properties of the Coastal Plain landform sites

Site name	Abbreviation	Climate Grid	Type of vegetation	Altidtude (m.a.s.l.)
Bo Traba	BTB	C 1	NF	52
Tolmitha-Sidi Erhoma	T-Roh	C 1	NF	294
Mirad Massoad (the Coast)	MMC	C 4	NF	198
Mirad Massoad	MM	C 4	NF	221
Mirad Massoad (Roman's dams)	MMD	C 4	NF	75
Wadi Bo annidi	WBA	C 5	NF	34
RasAmer	RMR	C 5	NF	44
Alhamama-RasAmer	HRMR	C 5	NF	38
Sattia	Sati	C 5	NF	403
Karsa	Krs	C 6	NF	90
Alaslab	Aslb	C 6	NF	63
Wadi El Mahbool	WMah	C 6	NF	30
Wadi Margos	Wmarg	C 6	NF	378
Arqoob Al Abiad	AqAb	C 6	NF	540

Figure 5.22 and Figure 5.23 illustrate the trend in monthly temperature, rainfall and ANDVI during 2004-2016 in the Coastal Plain landform. The results of the changes of rainfall, temperature and vegetation on each sites are summarised in Table 5.9.

For climate grid 1 (C1) (Table 5.9 and Figure 5.22), There are three sites in this grid Bo Traba and Tolmitha-Sidi Erhoma showed a small decrease in the natural vegetation cover. For climate grid 4 (C4) (Table 5.9 and Figure 5.22), There are three sites in this grid, Mirad Massoad (Romans dams) (MMD), Mirad Massoad (the Coast) (MMC) and Mirad Massoad (MM). The natural vegetation cover (ANDVI trend) for the three sites showed an insignificant decrease. The highest decreased in ANDVI linear trend was shown in MM.

Table 5.9 Summary of monthly rainfall, temperature and ANDVI during 2004-2016 in the Coastal Plain landform

Site name	Rainfall		Temperature		Vegetation	
	Trend	R^2	Trend	R^2	Trend	R^2
Bo Traba	$+3.11\times10^{-2}$	0.002	$+2.13\times10^{-2}$	0.037	-2×10^{-5}	0.00005
Tolmitha-Sidi Erhoma					-2×10^{-4}	0.006
Mirad Massoad (Coast)	+0.122	0.021	$+7.8\times10^{-3}$	0.005	-7×10^{-5}	0.0008
Mirad Massoad					-2×10^{-4}	0.009
Mirad Massoad (Roman's dams)					-9×10^{-5}	0.0015
Wadi Bo annidi	$+8.61\times10^{-2}$	0.009	$+7.4\times10^{-3}$	0.004	$+2\times10^{-5}$	0.0002
RasAmer					-6×10^{-4}	0.099
Alhamama-RasAmer					-6×10^{-5}	0.0013
Sattia					-3×10^{-4}	0.019
Karsa	$+1.05\times10^{-2}$	0.0002	$+1.25\times10^{-2}$	0.012	-6×10^{-5}	0.003
Alaslab					-2×10^{-4}	0.015
Wadi El Mahbool					-7×10^{-5}	0.005
Wadi Margos					-3×10^{-5}	0.0004
Arqoob Al Abiad					-1×10^{-5}	0.00007

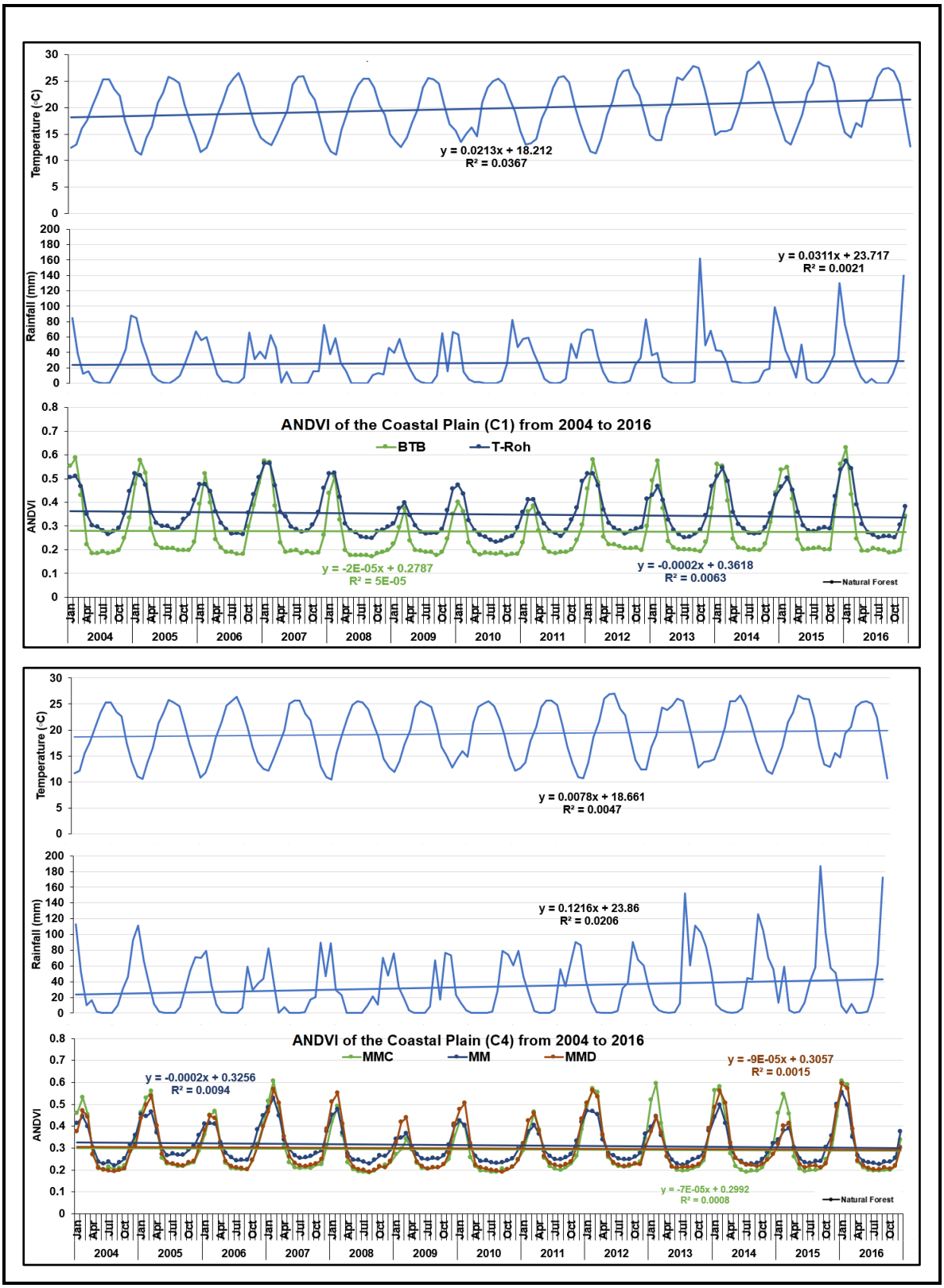

Figure 5.22 Time series of the monthly temperature, rainfall and ANDVI from 2004 to 2016 for the Coastal Plain C1 and C4-grid

For climate grid 5 (C5) (Table 5.9 and Figure 5.23), there are four sites in this grid, Wadi Bo annidi (WBA), RasAmer (RMR), Al Hmama-RasAmer (HRMR) and Sattia (Sati). Moreover. it could be noticed from Figure 5.23, among the four sites the natural vegetation cover trend of RasAmer site has dropped more rapidly than other sites, which may in large part be due to the 2013-fires which occurred in Ras'Helal region (Elshatshat, 2015), the fires occurred in May, with an area of 3,308 ha being damaged (Alsoul, 2016). The RasAmer site was included in the areas affected by those fires (Figure 5.24).

The last climate grid within the Coastal Plain landform is C6 (Table 5.9 and Figure 5.23), the Five sites in this grid, Karsa (Krs), Asslab (Aslb), Wadi El Mahbwol (WMah), Wadi Wadi Margos (Wmarq) and Arqoob Al Abiad (AqAb); have a negligible decrease in the vegetation cover trend. The highest decreases in ANDVI changes was shown to be in the Asslab comparing with the other sites.

Overall, the results of all climate grids (C1, C4, C5 and C6) in the Coastal Plain landform showed a slight increase in both temperature and rainfall during 2004-2016. In contrast, a decrease in vegetation cover was shown in all Coastal Plain landform sites except Wadi Bo lanidi site. The average of ANDVI values of the Coastal Plain landform ranged from 0.313 2004 to 0.308 in 2016, indicating the general slight decrease in the natural vegetation cover in this landform.

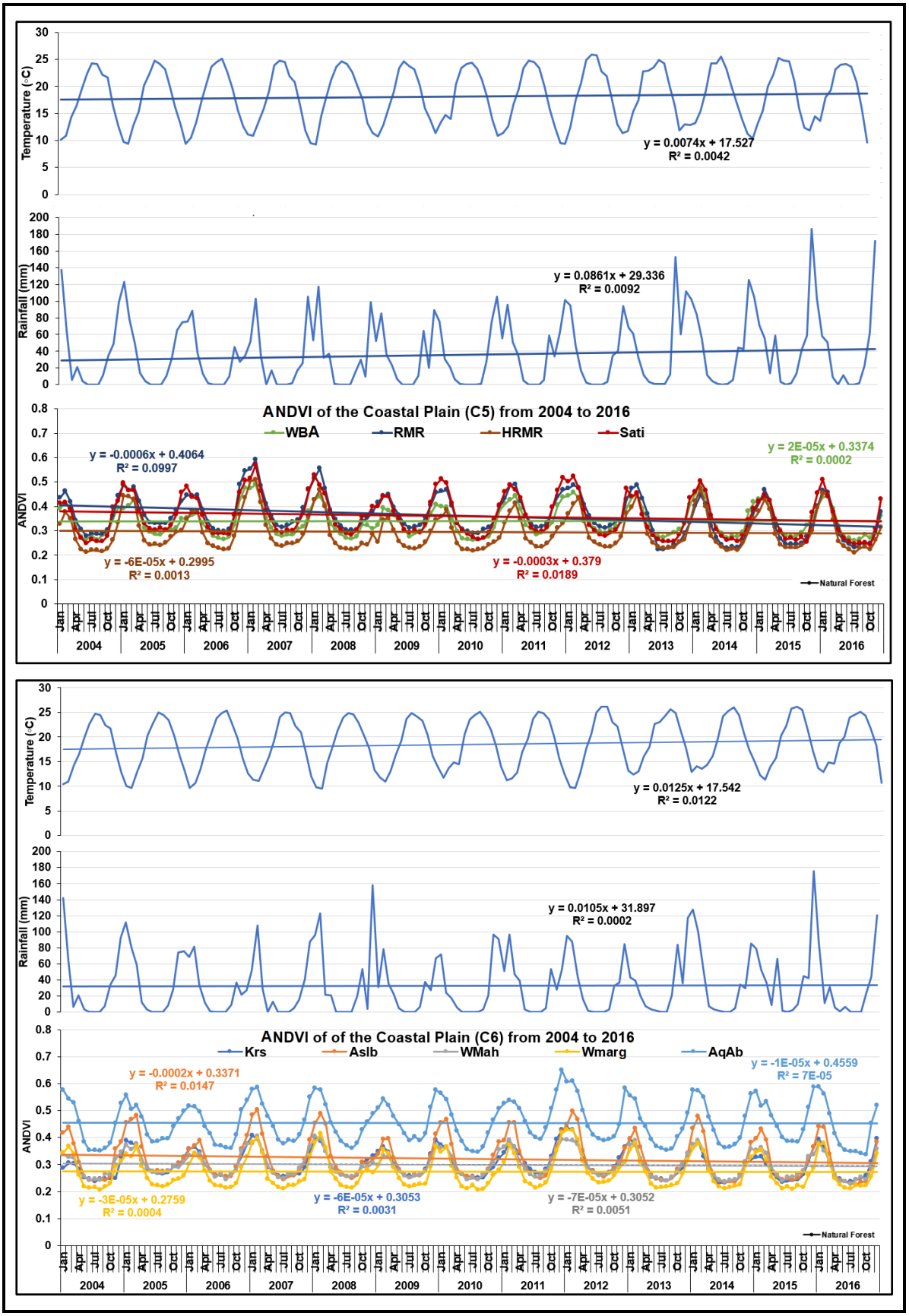

Figure 5.23 Time series of the monthly temperature, rainfall and ANDVI from 2004 to 2016 for the Coastal Plain C5 and C6-grid

Figure 5.24 Landsat 8 images showing a part of the May 2013-fires (in red) north the study area

5.4.1.2 The Al Jabal Al Akhdar Backslope landform

Al Jabal Al Akhdar Backslope landform includes 17 sites from the OMU study within six climatic grids (2, 3, 4, 5, 6, 7); the three types of the natural vegetation cover are included in this landform as listed in Table 5.10.

Figure 5.25, Figure 5.26 and Figure 5.28 illustrate the trends in monthly temperature, rainfall and ANDVI during 2004-2016 in the Al Jabal Al Akhdar Backslope landform. The results of the changes of rainfall, temperature and vegetation on each sites are summarised in Table 5.11. For climate grid 2 (C2) (Table 5.11 and Figure 5.25), the NF cover of Jardas Al Abeed (Jrd) site showed an insignificant decrease, while the NF cover of Jardas-Jabanet Sidi Saad, and RL cover of Taknis-El Caroba, in climate grid 3 (C3) showed a slight increase. The PF cover of Marawah Forest is also in climate grid 3 (C3) showed an insignificant decrease (Table 5.11 and Figure 5.25).

Table 5.10 Properties of the Al Jabal Al Akhdar Backslope landform sites

Site name	Abbreviation	Climate Grid	Type of vegetation	Altidtude (m.a.s.l.)
Jerdas Al Abeed	Jrd	C 2	NF	464
Marawah Forest	MarF	C 3	PF	490
Jerdas-Jabanet Sidi Saad	Jrd-JSS	C 3	NF	600
Taknis-El Caroba	Tak-Crob	C 3	RL	460
Sidi Al Qarib	SQrib	C 4	NF	355
Quassser Libya-El Bayada (Qud Khalil)	QL-Bd	C 4	NF	465
Bo Querawa	BoQrw	C 4	NF	458
Ghot Maibara	GMb	C 5	NF	226
Qandafora	Qand	C 5	NF	280
Eqfanta	Eqf	C 5	NF	282
Al Wasita-Salion	Wast	C 5	NF	360
Shnaishnn Forest	ShnF	C 5	NF	780
Arqoob Sidi Hamad	AqSH	C 6	NF	420
Sidi Khaled	SKh	C 6	NF	385
Lamloda-Ras El Helal	Lam-Hel	C 6	NF	684
Azzrada	Zrda	C 6	NF	680
El Nador-El Mekhili	Nd-Mekh	C 7	RL	414

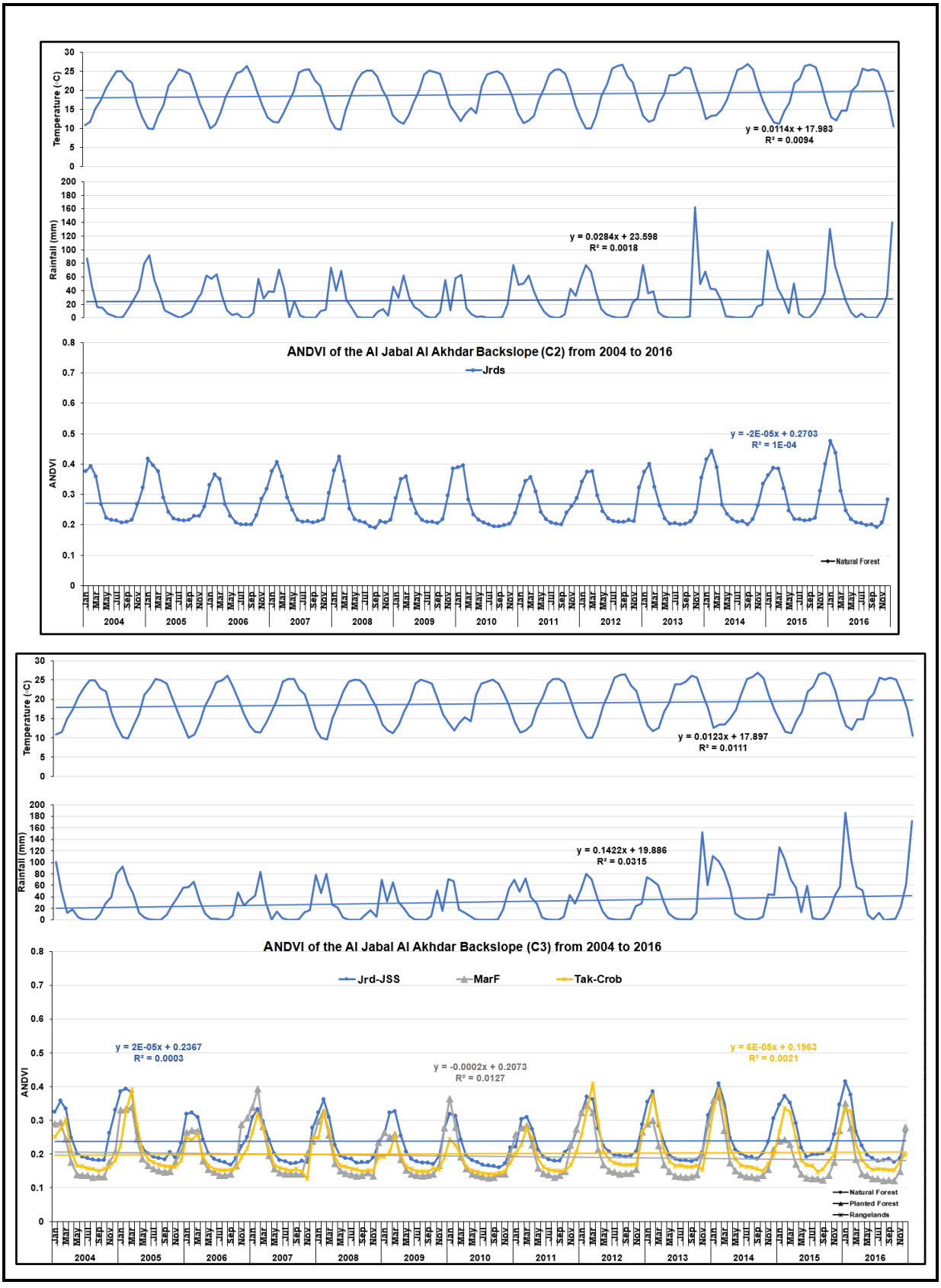

Figure 5.25 Time series of the average monthly temperature, rainfall and ANDVI from 2004 to 2016 for the Al Jabal Al Akhdar Backslope C2 and C3- grid

Table 5.11 Summary of monthly rainfall, temperature and ANDVI during 2004-2016 in the Al Jabal Al Akhdar Backslope landform

Site name	Rainfall		Temperature		Vegetation	
	Trend	R^2	Trend	R^2	Trend	R^2
Jerdas Al Abeed	$+2.84\times10^{-2}$	0.002	$+1.14\times10^{-2}$	0.009	-2×10-4	0.0001
Marawah Forest	$+1.42\times10^{-2}$	0.032	$+1.23\times10^{-2}$	0.011	-2×10^{-4}	0.013
Jerdas-Jabanet Sidi Saad					$+2\times10^{-5}$	0.0003
Taknis-El Caroba					$+6\times10^{-5}$	0.002
Sidi Al Qarib	+0.122	0.021	$+7.8\times10^{-3}$	0.005	-1×10^{-5}	0.00002
Quasser Libya-El Bayada (Qud Khalil)					-5×10^{-5}	0.001
Bo Querawa					-2×10^{-4}	0.006
Ghot Maibara	$+8.61\times10^{-2}$	0.009	$+7.4\times10^{-3}$	0.004	-9×10^{-5}	0.002
Qandafora					-8×10^{-4}	0.158
Eqfanta					-1×10^{-4}	0.004
Al Wasita-Salion					-8×10^{-6}	0.00005
Shniashnn Forest					-9×10^{-5}	0.006
Arqoob Sidi Hamad	$+1.05\times10^{-2}$	0.0002	$+1.25\times10^{-2}$	0.012	-2×10^{-6}	0.0000009
Sidi Khaled					-2×10^{-4}	0.011
Lamloda-Ras El Helal					-2×10^{-4}	0.008
Azzrada					-1×10^{-4}	0.004
El Nador-El Mekhili	$+6.5\times10^{-2}$	0.008	$+1.46\times10^{-2}$	0.015	-5×10^{-5}	0.066

For climate grid 4 (C4) (Figure 5.26), there are three NF sites, which have a negligible decrease in ANDVI trends over the entire time period. The highest decreased in ANDVI linear trend was shown in Bo Qerawa (BoQrw) compared with Sidi Al Qarib (SQrib) and Quasser Libya-El Bayada (QL-Bd) sites (Table 5.11).

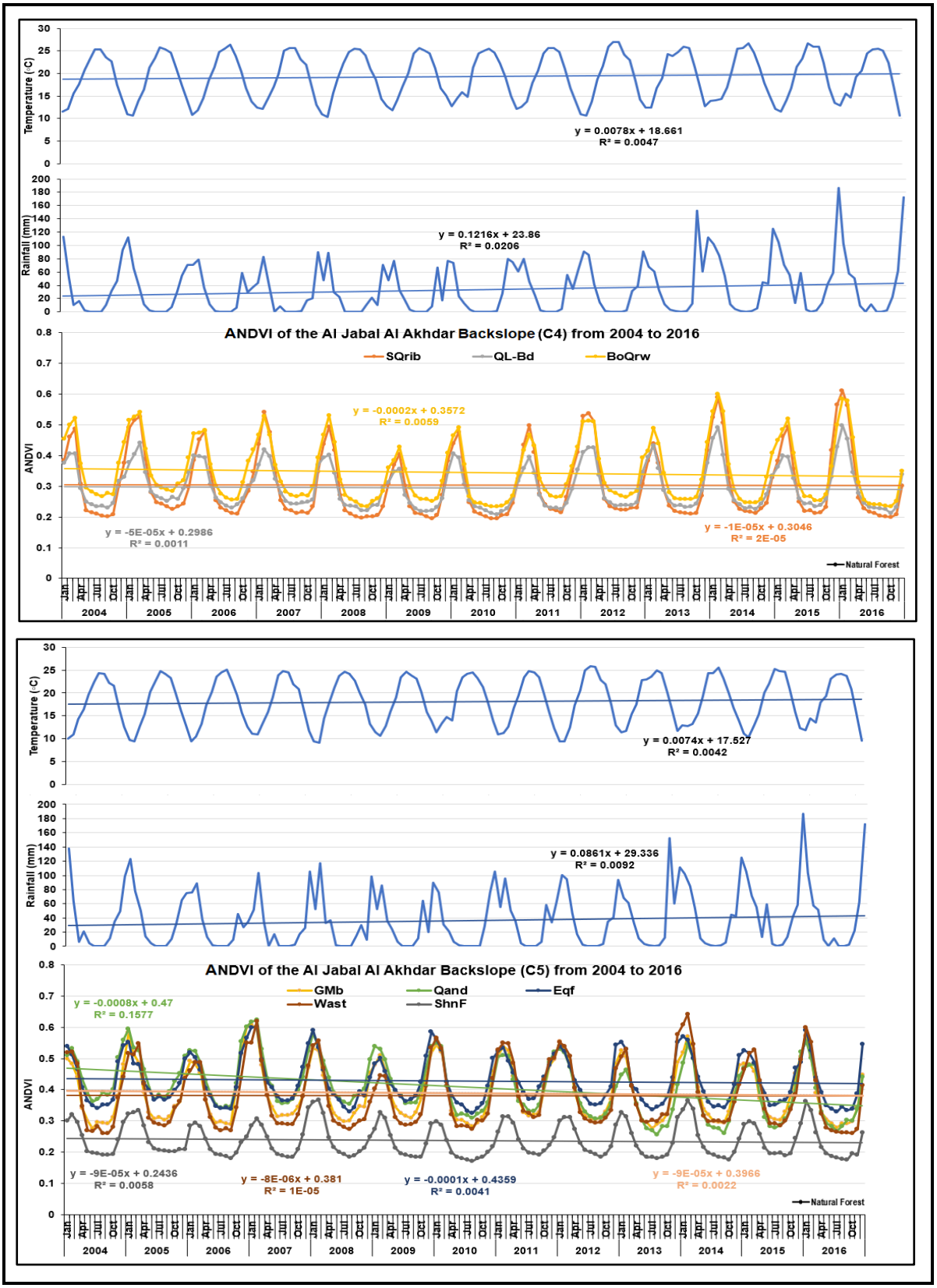

Figure 5.26 Time series of the average monthly temperature, rainfall and ANDVI from 2004 to 2016 for the Al Jabal Al Akhdar Backslope C4 and C5- grid

For the natural vegetation cover in C5 (Figure 5.26), there are five NF sites, which have an insignificant decrease in ANDVI trends (Table 5.11). Moreover, it can be noticed from Figure 5.26, among the five NF sites the natural vegetation cover trend of Qandafora (Qand) site has a greater decrease than other sites which could be caused in part due to the changes in the landcover from NF to AA and NV areas, established from LULC changes map of 2014 (Figure 5.27).

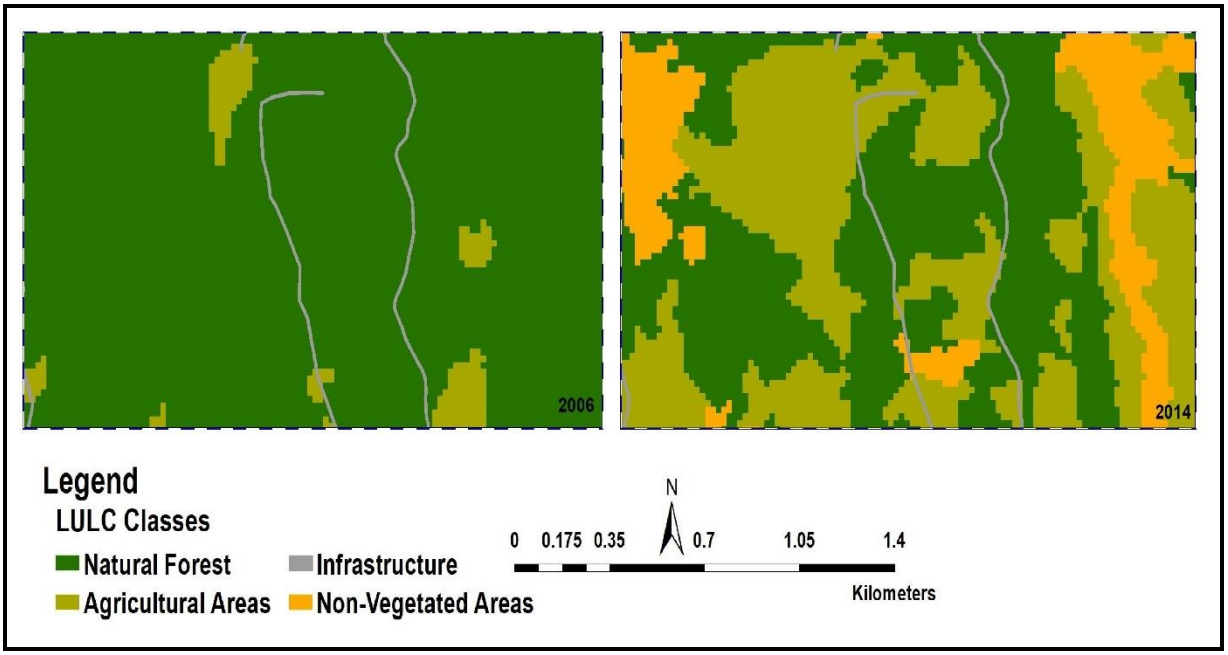

Figure 5.27 Changes in LULC in Qandafora (LULC changes map result)

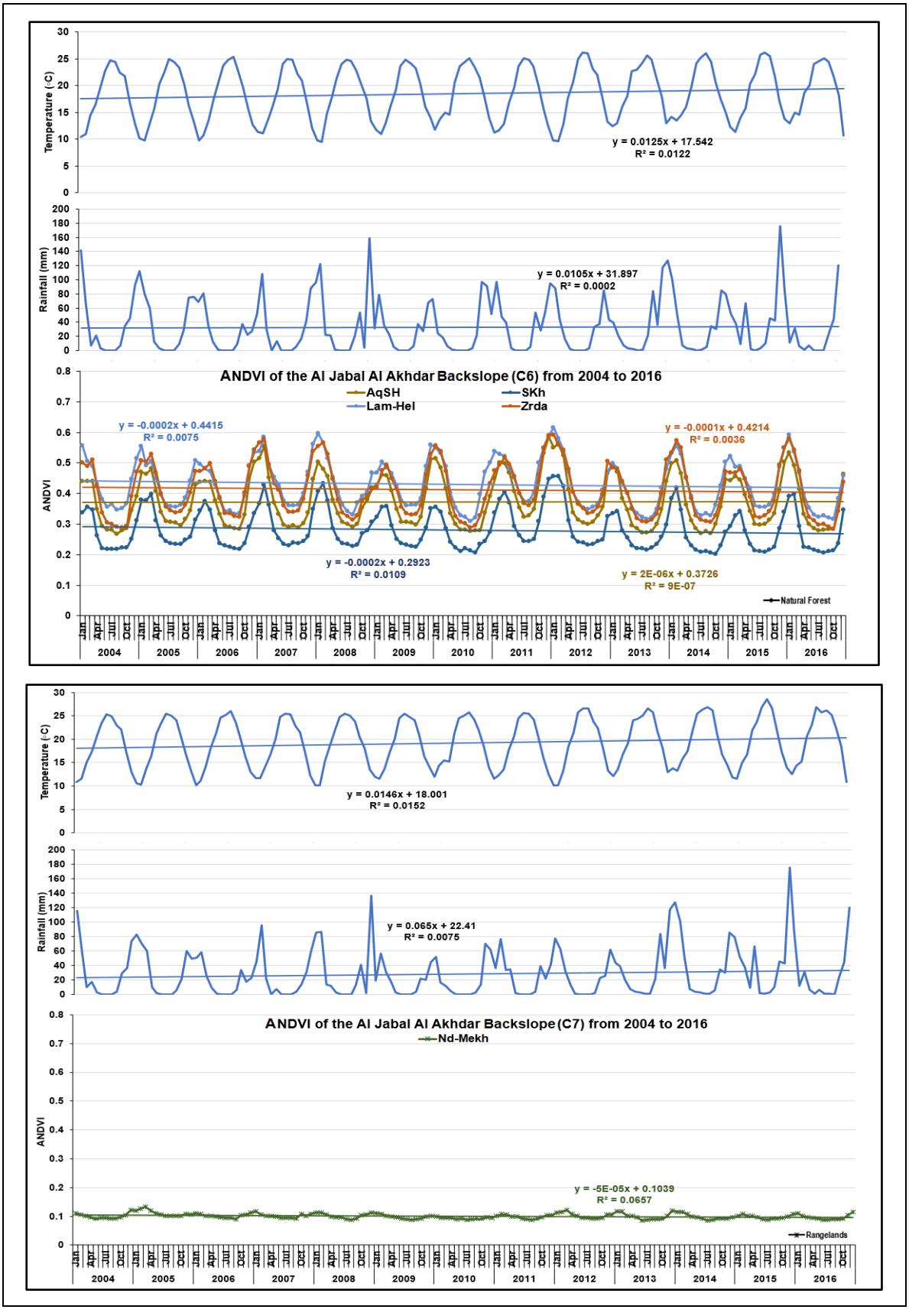

Figure 5.28 Time series of the average monthly temperature, rainfall and ANDVI from 2004 to 2016 for the Al Jabal Al Akhdar Backslope C6 and C7- grid

An insignificant decrease in vegetation cover was observed in the four NF sites located in climate grid 6 (C6) and 7 (C7) (Table 5.11 and Figure 5.29).

. Furthermore, the degraded condition of the EL-Nador-El Mekhili site (in C7) can be noticed in Figure 5.28, reflected by the low values of ANDVI. The ANDVI ranges from to 0.086 recorded in June 2013 and in July 2014 to 0.133 in March 2005. The El Nador-El Mekhili site classified by OMU (2005) as RL where % of vegetation cover was 49.2% of the total area of the site, dominated by *Hammada scoparia* (Pomel) Iljin formed only 3.64% of the total area (Appendix Table B.2.1).

Overall, the Al Jabal Al Akhdar Backslope landform encompass the three types of natural vegetation (NF, RL and PF). The results of all climate grids (C2, C3, C4, C5, C6 and C7) in the landform showed a slight increase in both temperature and rainfall during 2004-2016. In contrast, a decrease in natural vegetation cover was shown in most of the landform sites except Jardas-Jabanet Sidi Saad, Taknis-El Caroba and Arqoob Sidi Hamad sites. The average of ANDVI values of Al Jabal Al Akhdar Backslope landform ranged from 0.306 2004 to 0.295 in 2016, indicating the general slight decrease in the natural vegetation cover in this landform.

5.4.1.3 The Al Jabal Al Akhdar Shoulder landform

Al Jabal Al Akhdar Shoulder landform includes four sites within two climatic grids (4, 5); the sites of this landform are listed in Table 5.12.

Table 5.12 Properties of the Al Jabal Al Akhdar Shoulder landform sites

Site name	Abbreviation	Climate Grid	Type of vegetation	Altidtude (m.a.s.l.)
Mirad Massoad (Terraces)	MMT	C 4	NF	416
Marawah-Quasser Libya	Mar-QL	C 4	NF	558
El Mansoura-El Dabadeb	Mans	C 5	NF	336
Sidi El Homari Forest	SHF	C 5	PF	830

Figure 5.29 illustrates the trend of monthly temperature, rainfall and ANDVI during 2004-2016 in the Al Jabal Al Akhdar Shoulder landform. The results of the changes of rainfall, temperature and vegetation on each sites are summarised in Table 5.13.

Table 5.13 Summary of monthly rainfall, temperature and ANDVI during 2004-2016 in the Al Jabal Al Akhdar Shoulder landform

Site name	Rainfall		Temperature		Vegetation	
	Trend	R^2	Trend	R^2	Trend	R^2
Mirad Massoad (Terraces)	+0.122	0.021	$+7.8\times10^{-3}$	0.005	-7×10^{-5}	0.0013
Marawah-Quasser Libya					-1×10^{-4}	0.004
El Mansoura-El Dabadeb	$+8.61\times10^{-2}$	0.009	$+7.4\times10^{-3}$	0.004	-3×10^{-4}	0.021
Sidi El Homari Forest					-2×10^{-4}	0.013

Overall, the Al Jabal Al Akhdar Shoulder landform encompass two climate grids (C4 and C5) and two types of natural vegetation (NF and PF). The results of the climate grids show a slight increase in both temperature and rainfall during 2004-2016. In contrast, a decrease in natural vegetation cover is shown in the landform sites. The average of ANDVI values of the AlJabal Al Akhdar Shoulder landform ranged from 0.358 2004 to 0.317 in 2016, indicating the general decrease in the natural vegetation cover in this landform

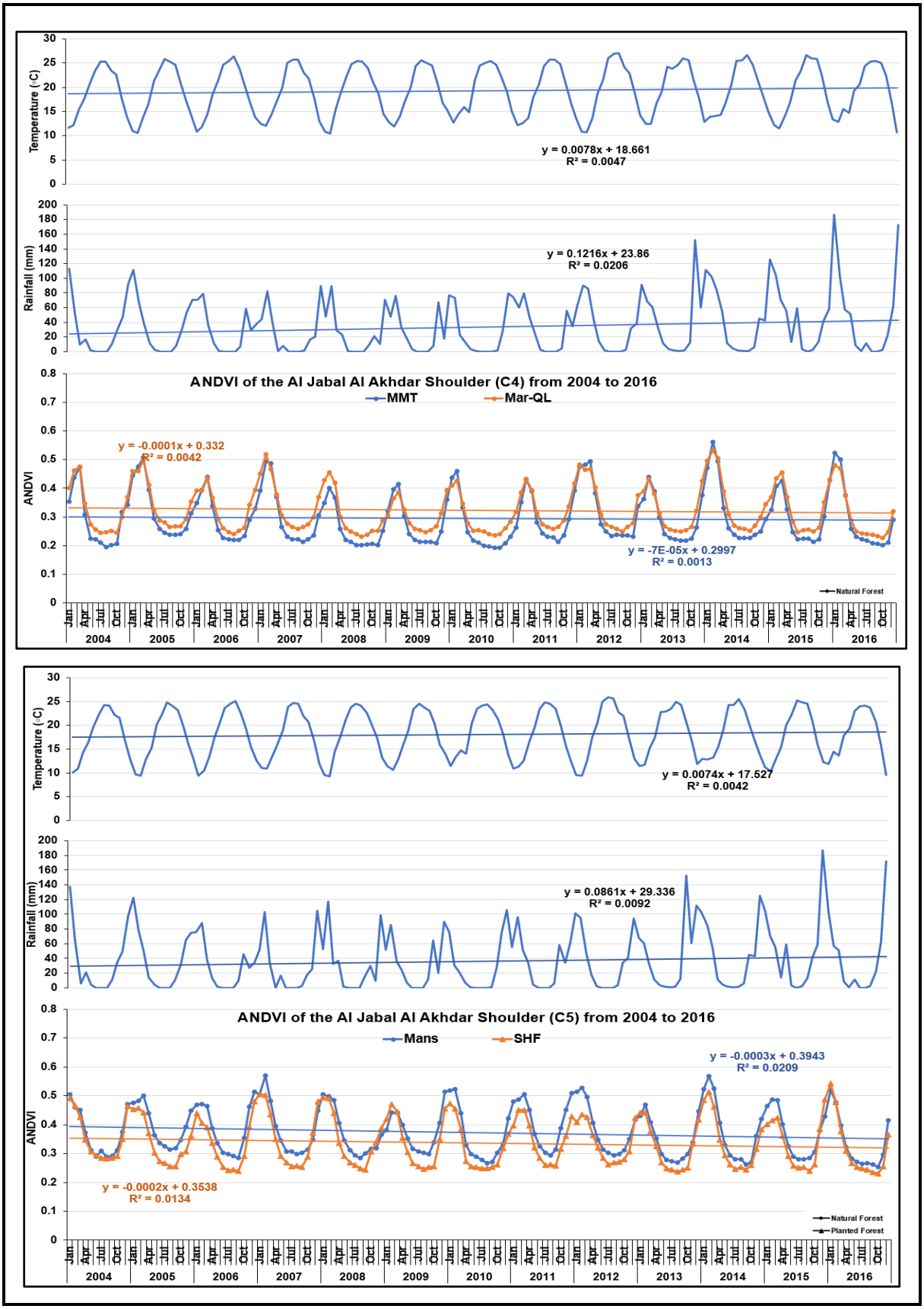

Figure 5.29 Time series of the average monthly temperature, rainfall and ANDVI from 2004 to 2016 for the Al Jabal Al Akhdar Shoulder C4 and C5- grid

5.4.1.4 The Al Jabal Al Akhdar Toeslope landform

Al Jabal Al Akhdar Toeslope landform includes two sites within climatic grid 6; the sites of this landform are listed in Table 5.14.

Table 5.14 Properties of the Al Jabal Al Akhdar Toeslope landform sites

Site name	Abbreviation	Climate Grid	Type of vegetation	Altidtude (m.a.s.l.)
El Daher El Hammer	DaHa	C 6	NF	450
Bo Draa	BoDr	C 6	RL	660

Figure 5.30 and Table 5.15 show an increase in the vegetation cover in the RL site, Bo Draa (BoDr), and the NF site, El Daher El Hammer (DaHa).Generally, The average of ANDVI values of the Al Jabal Al Akhdar Toeslope landform ranged from 0.211 2014 to 0.225 in 2016, indicating the general slight increase in the natural vegetation cover in this landform.

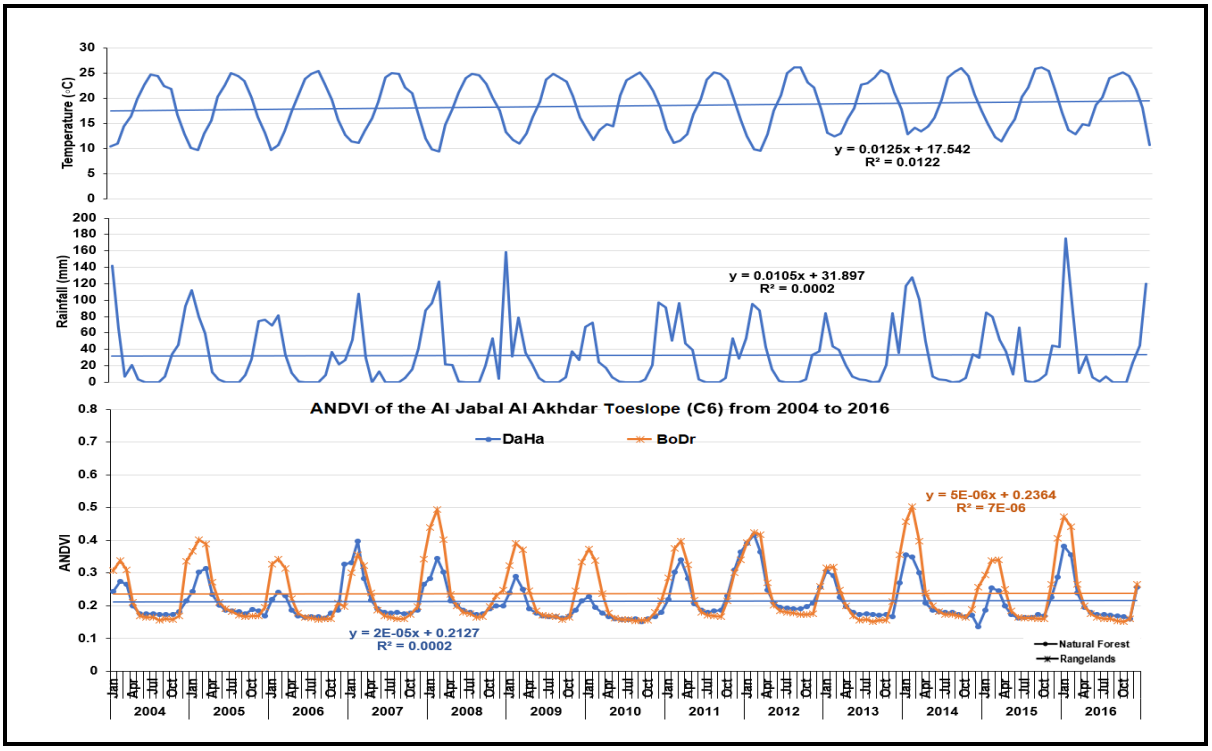

Figure 5.30 Time series of the average monthly temperature, rainfall and ANDVI from 2004 to 2016 for the Al Jabal AL Akhdar Toeslope

Table 5.15 Summary of monthly rainfall, temperature and ANDVI during 2004-2016 in the Al Jabal Al Akhdar Toeslope landform

Site name	Rainfall		Temperature		Vegetation	
	Trend	R^2	Trend	R^2	Trend	R^2
El Daher El Hammer	$+1.05\times10^{-2}$	0.0002	$+1.25\times10^{-2}$	0.012	$+5\times10^{-6}$	0.0002
Bo Draa					$+2\times10^{-5}$	0.000007

5.4.1.5 The Al Jabal Al Akhdar Top landform

Al Jabal Al Akhdar Top landform includes nine sites within two climatic grids (C4, C5); all the sites are natural forest as listed in Table 5.16.

Table 5.16 Properties of the Al Jabal Al Akhdar Top landform sites

Site name	Abbreviation	Climate Grid	Type of vegetation	Altidtude (m.a.s.l.)
Wadi El Mogawah	WMog	C 4	NF	420
Wadi Al Sudan	Wsu	C 4	NF	415
Wadi Al Zawia	WZw	C 4	NF	451
Al Hejab	Hjb	C 5	NF	430
Wadi El Kuf stream	WkufS	C 5	NF	360
Al Ghriqa-Ras Atrab	Gh-Trb	C 5	NF	669
Alquasser Alromani	Qrom	C 5	NF	659
Wadi El Kuf	WKuf	C 5	NF	600
Wadi El kuf (Cyperss Forest)	WkufCF	C 5	NF	660

Figure 5.31 illustrates the trend of monthly temperature, rainfall and ANDVI during 2004-2016 in the Al Jabal Al Akhdar Shoulder landform. The results of the changes of rainfall, temperature and vegetation on each sites are summarised in Table 5.13.

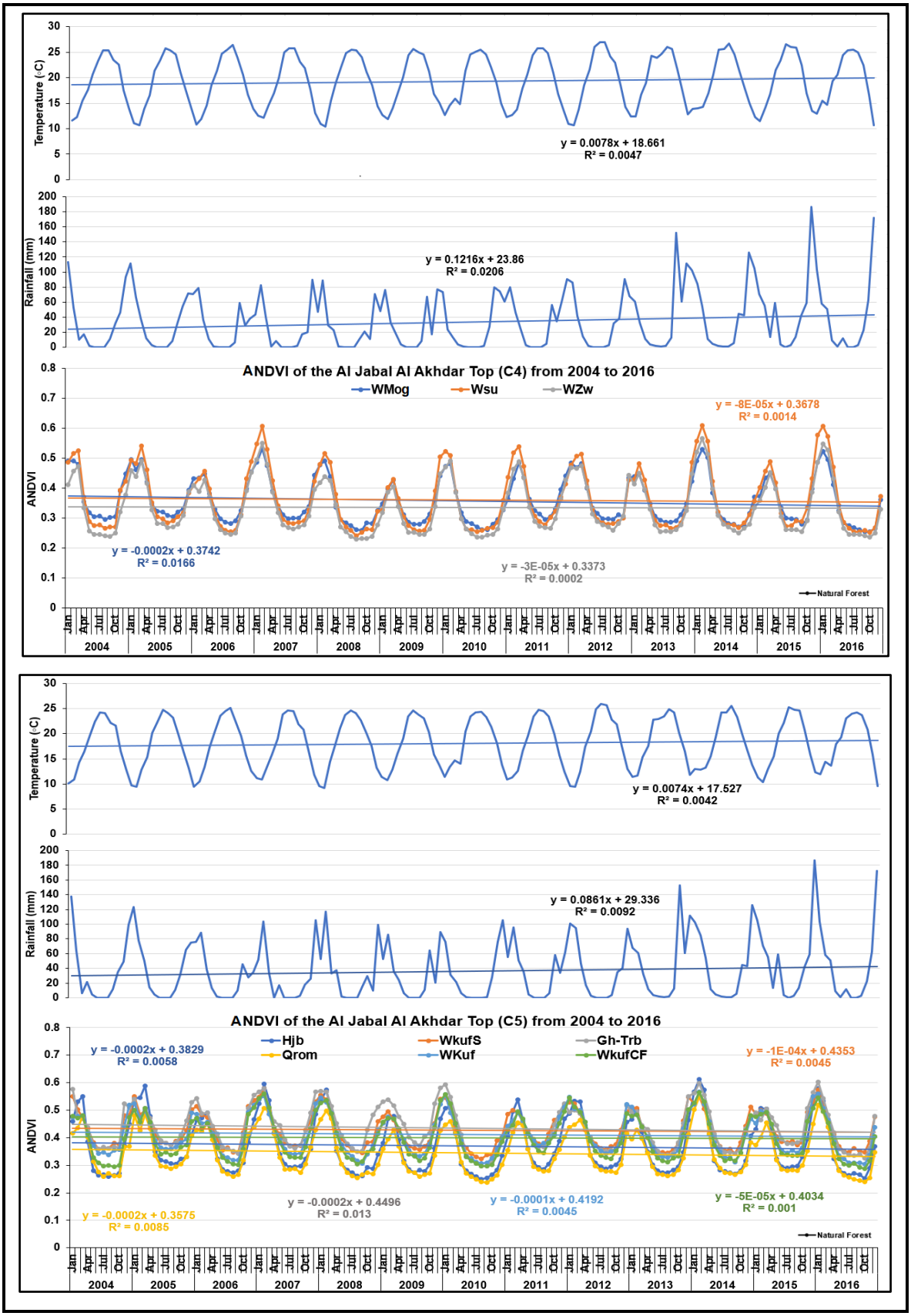

Figure 5.31 Time series of the average monthly temperature, rainfall and ANDVI from 2004 to 2016 for the Al Jabal Al Akhdar Top C4 and C5- grid

Table 5.17 Summary of monthly rainfall, temperature and ANDVI during 2004-2016 in the Al Jabal Al Akhdar Top landform

Site name	Rainfall		Temperature		Vegetation	
	Trend	R^2	Trend	R^2	Trend	R^2
Wadi El Mogawah	+0.122	0.021	$+7.8\times10^{-3}$	0.005	-2×10^{-4}	0.017
Wadi Al Sudan					-8×10^{-5}	0.001
Wadi Al Zawia					-3×10^{-5}	0.0002
Al Hejab	$+8.61\times10^{-2}$	0.009	$+7.4\times10^{-3}$	0.004	-2×10^{-4}	0.006
Wadi El Kuf stream					-1×10^{-4}	0.005
Al Ghriqa-Ras Atrab					-2×10^{-4}	0.013
Alquasser Alromani					-2×10^{-4}	0.009
0Wa9di El Kuf					-1×10^{-4}	0.005
Wadi El kuf (Cyperss Forest)					-5×10^{-5}	0.001

Overall, two climate grids (C4 and C5) are included in the Al Jabal Al Akhdar Top landform. The results of both temperature and rainfall showed a slight increase during 2004-2016. In contrast, a decrease in natural vegetation cover (NF) was shown in all landform sites. The average of ANDVI values of Al Jabal Al Akhdar Top landform ranged from 0.379 2004 to 0.361 in 2016, indicating the general slight decrease in the natural vegetation cover in this landform.

5.4.1.6 Wadi Al Muallaq landform

Wadi Al Muallaq landform includes two rangelands sites within climatic grid 6 as listed in Table 5.18.

Table 5.18 Properties of Wadi Al Muallaq landform sites

Site name	Abbreviation	Climate Grid	Type of vegetation	Altidtude (m.a.s.l.)
Wadi Al Mahja-Kholan	WMhj-Kh	C 6	Rangelands	640
El Hesha	Hesh	C 6	Rangelands	470

Figure 5.32 illustrates the trend of temperature, rainfall and ANDVI during 2004-2016 in climate grid 6 (C6) in Wadi Al Muallaq landform. The results of the changes of rainfall, temperature and vegetation on each sites are summarised in Table 5.19 A decrease in vegetation cover was in the two sites. Generally, The average of ANDVI values of Wadi Al Muallaq landform ranged from 0.139 2004 to 0.137 in 2016, indicating the general decrease in the natural vegetation cover in this landform. Also, the low values of ANDVI reflected the situation of the sites in this landform; where it was used for grazing and cultivation of cereal crops (OMU, 2005).

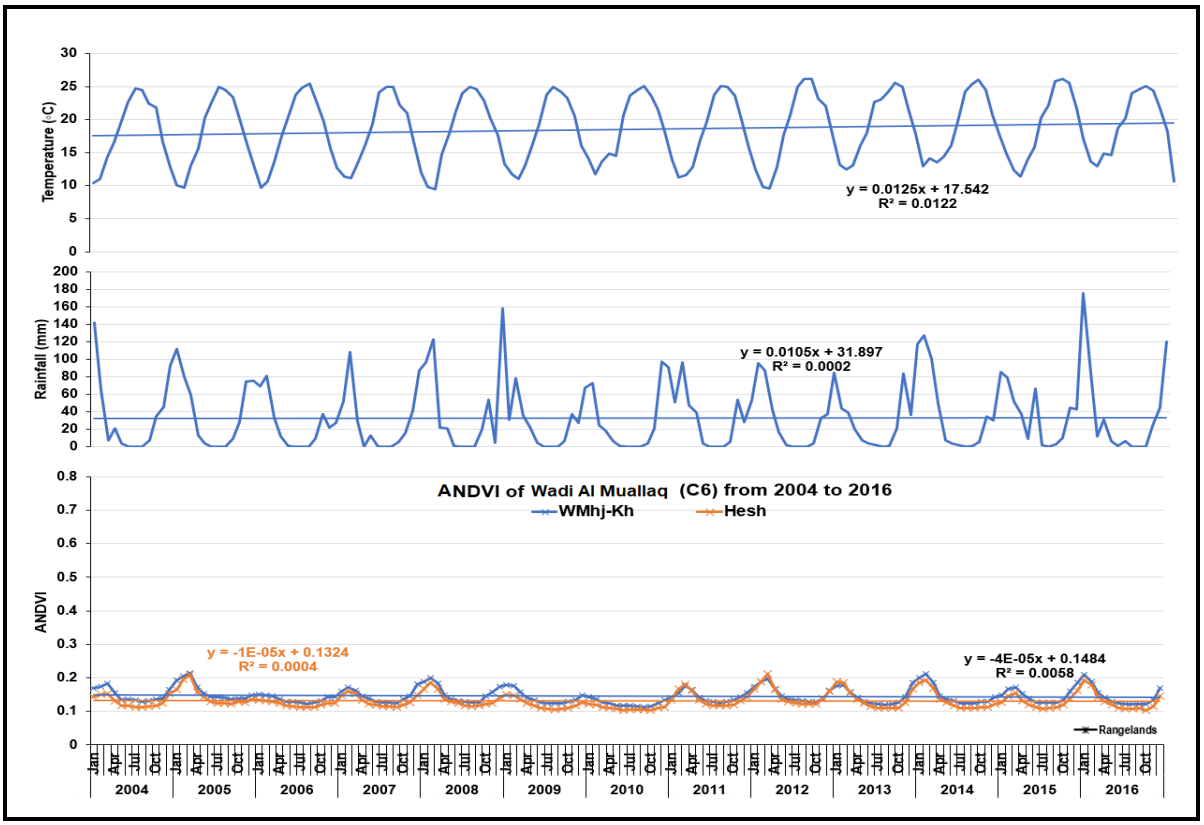

Figure 5.32 Time series of the average monthly temperature, rainfall and ANDVI from 2004 to 2016 for Wadi Al Muallaq

Table 5.19 Summary of monthly rainfall, temperature and ANDVI during 2004-2016 in the Wadi Al Muallaq landform

Site name	Rainfall		Temperature		Vegetation	
	Trend	R^2	Trend	R^2	Trend	R^2
Wadi Al Mahja-Kholan	$+1.05\times10^{-2}$	0.0002	$+1.25\times10^{-2}$	0.012	$+5\times10^{-6}$	0.0002
El Hesha					$+2\times10^{-5}$	0.000007

5.4.1.7 Wadi Al Qattarah landform

Wadi Al Qattarh landform includes five sites within three climatic grids (2, 3, 4); the three types of natural vegetation are included in his landform as listed in Table 5.20.

Table 5.20 Properties of Wadi Al Qattarah landform sites

Site name	Abbreviation	Climate Grid	Type of vegetation	Altidtude (m.a.s.l.)
Zawat Alqsoor-Jardas	ZQ-Jrd	C 2	Natural Forest	550
Madwer El Zaitoon (Plantation)	MadZF	C 3	Planted Forest	440
Madwer El Zaitoon (Rangelands)	MadzR	C 3	Rangelands	520
Wadi Alakki	Waki	C 4	Natural Forest	420
Kashaf Forest	Kash	C 4	Planted Forest	465

Figure 5.33 and Figure 5.35 illustrate the trend of monthly temperature, rainfall and ANDVI during 2004-2016 in Wadi Al Qattarh landform. The results of the changes of rainfall, temperature and vegetation on each sites are summarised in Table 5.21.

The natural vegetation cover (NDVI trend) in Zawit El Qusor-Jardas (ZQ-Jrd) in C2 showed a tiny increase (Figure 5.33).For C3 (Figure 5.33), The two types of natural vegetation (PF and RL) in Madwer El Zaitoon site showed different trends of changes. The natural vegetation cover (ANDVI trend) for the PF site, Madwer El Zaitoon plantation (MadZF), showed a tiny decreased; while the RL site, Madwer El

Zaitoon (MadzR), showed a slight increase in its vegetation cover. The PF in Madwer El Zaitoon experienced cutting trees of *Pinus halepensis* Mill. down in 2016 (Figure 5.34).

Table 5.21 Summary of monthly rainfall, temperature and ANDVI during 2004-2016 in the Wadi Al Qattarah landform

Site name	Rainfall		Temperature		Vegetation	
	Trend	R^2	Trend	R^2	Trend	R^2
Zawat Alqsoor-Jardas	$+2.84\times10^{-2}$	0.002	$+1.14\times10^{-2}$	0.009	$+4\times10^{-5}$	0.001
Madwer El Zaitoon (Plantation)	$+1.42\times10^{-2}$	0.032	$+1.23\times10^{-2}$	0.011	-7×10^{-5}	0.002
Madwer El Zaitoon (Rangelands)					$+1\times10^{-4}$	0.011
Wadi Alakki	+0.122	0.021	$+7.8\times10^{-3}$	0.005	$+1\times10^{-4}$	0.004
Kashaf Forest					-1×10^{-4}	0.003

For the natural vegetation cover trend, in C4, there are two different kind of natural vegetation (NF and PF), were also showed different trends. The vegetation cover of the NF site, Wadi Alakki (Waki), has increased while the PF site, Kashaf Forest (Kash) has decreased.

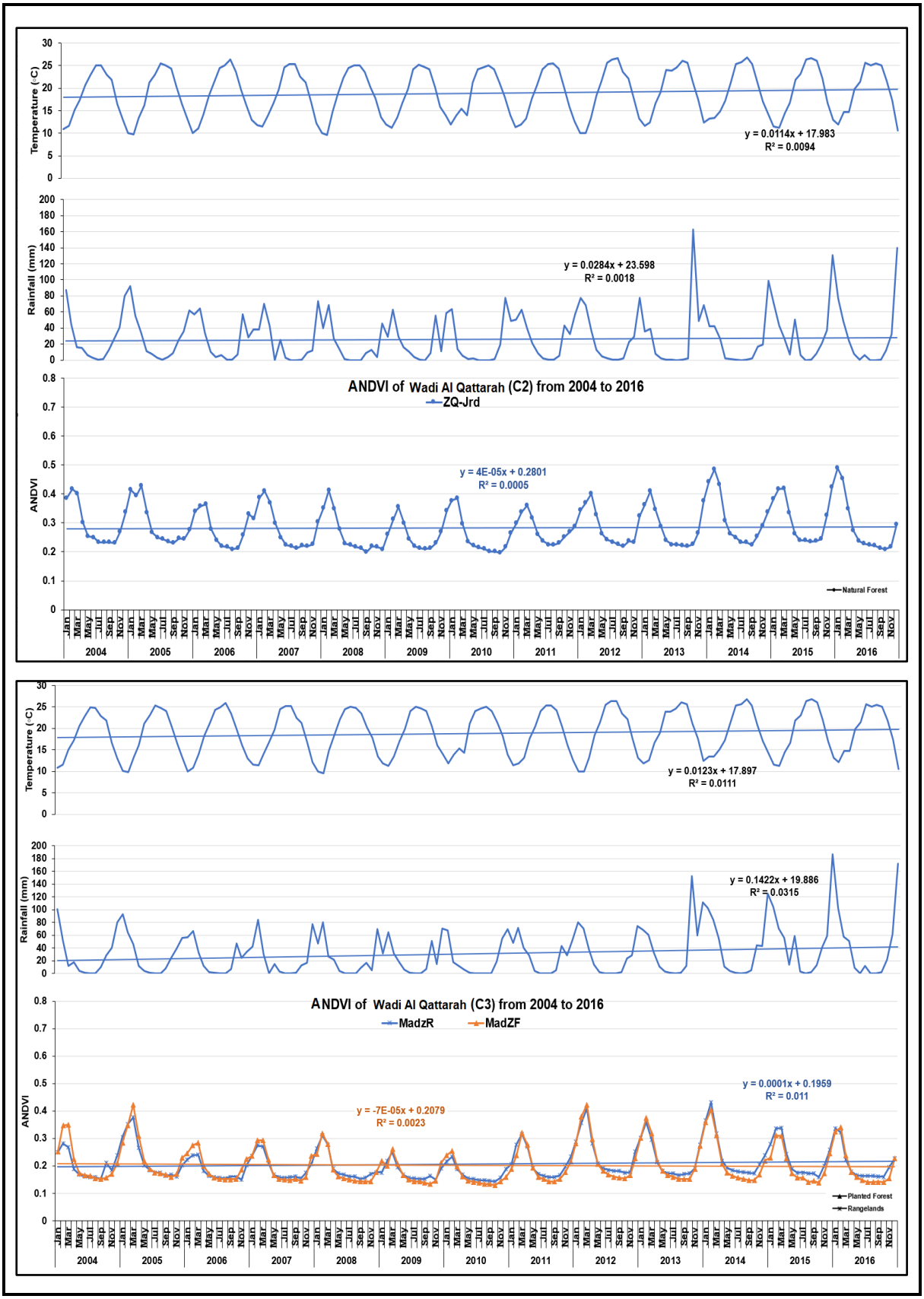

Figure 5.33 Time series of the average monthly temperature, rainfall and ANDVI from 2004 to 2016 for Wadi Al Qattarah C2 and C3- grid

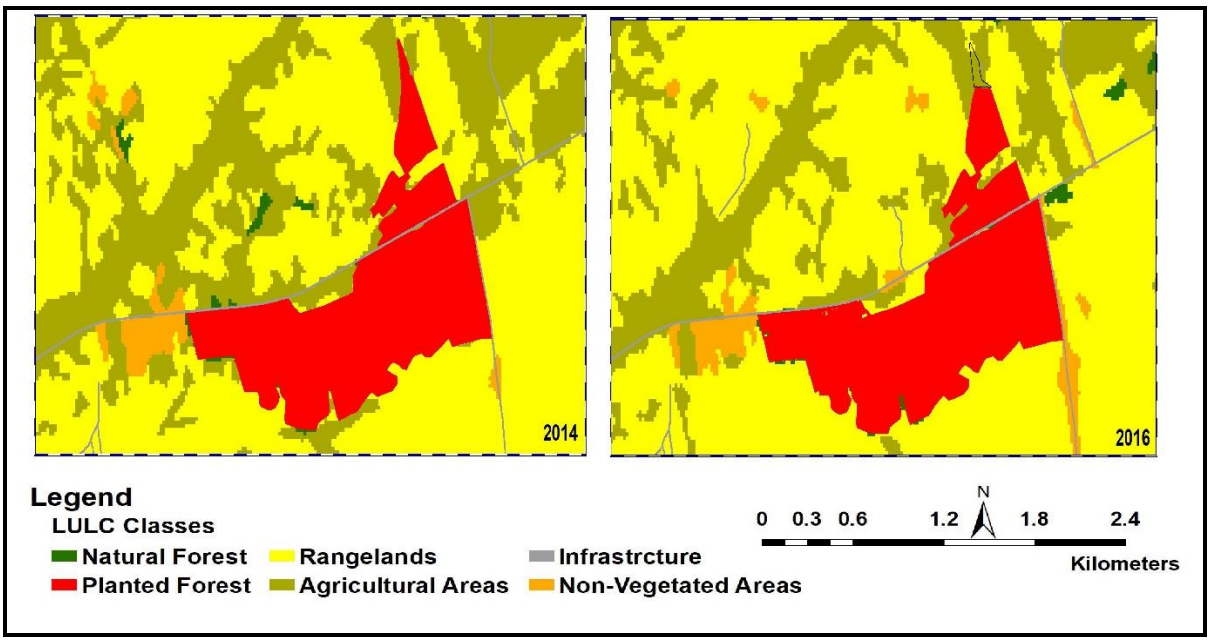

Figure 5.34 Cutting pine trees down and changes in the LULC in Madwer El Zaitoon plantaion

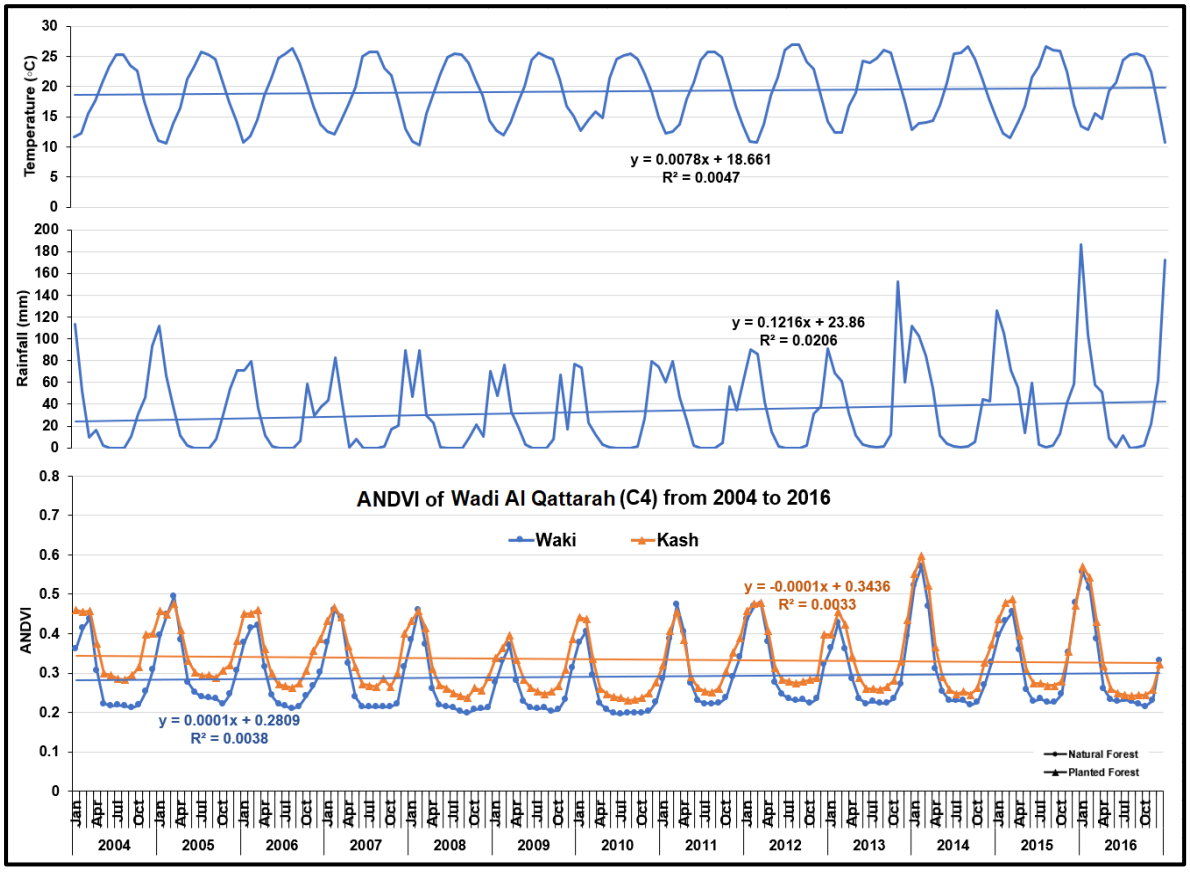

Figure 5.35 Time series of the average monthly temperature, rainfall and ANDVI from 2004 to 2016 for Wadi Al Qattarah C4- grid

Overall, Wadi Al Qattarh landform encompasses three climate grids (C2, C3 and C4) with the three types of natural vegetation (NF, RL and PF). The results of the climate grids showed a slight increase in both temperature and rainfall during 2004-2016 in all climate grids. The natural vegetation cover showed different trends in this class of landform. The NF and RL sites showed an increase in ANDVI trend, while the PF sites showed a decrease trend. The average of ANDVI values of Wadi Al Qattarah landform ranged from 0.270 2004 to 0.263 in 2016, indicating a general decrease in the natural vegetation cover in this landform.

5.4.2 Statistical analysis of the ANDVI climate variables

In this section, the results of the statistical analysis between ANDVI and climate variables in the study area landforms are presented, in order to investigate the impact of climate on the natural vegetation cover changes in the study area over the period from 2004-2016. Monthly Average of ANDVI and two climate variables were used to achieve the aim of this investigation. Monthly rainfall was represented as rainfall and rainfall minus 1-month (rainfall that had fallen in the previous month) and monthly temperature which also was represented in temperature and temperature minus 1-month (temperature associated with the previous month). The results are presented in the following four subsections.

5.4.2.1 The Correlation between ANDVI and Rainfall

Figure 5.36 (a and b) and Table 5.26 show the correlation analyses between monthly ANDVI and monthly rainfall in different landforms of the study areaduring 2004-2016. The results showed that the correlation between ANDVI in study area landforms and rainfall was a moderate positive correlation and statistically significant (P-value <0.000). However, the regression analysis showed that rainfall can explain ≤36% of the changes in the natural vegetation cover in the different study area landforms. Table 5.22 represents the summary of the regression analysis between ANDVI and rainfall results for each landform within the study area. While the pearason correlation coefficient between ANDVI and rainfall (P-value <0.000) is shown in Table 5.26.

Table 5.22 Statical analysis between ANDVI and Rainfall in the study area

Landform	Population (capita)	No. of Sites	Type of Vegetation	Alitude (m.a.s.l.)	Annual Rainfall (mm)	R^2	Std. Error of the Estimate
Coastal Plain	102,656	14	NF	30 -540	338	0.288**	0.081
Al Jabal Al Akhdar Backslope	26,775	17	NF-RL-PF	226 -780	374	0.179**	0.109
Al Jabal Al Akhdar Shoulder	82,383	4	NF-PF	336 -830	401	0.349**	0.073
Al Jabal Al Akhdar Toeslope	104,246	2	NF-RL	450, 660	419	0.358**	0.062
Al Jabal Al Akhdar Top	126,446	9	NF	360 -669	401	0.344**	0.072
Wadi Al Muallaq		2	RL	470, 620	419	0.333**	0.020
Wadi Al Qattarah	10,245	5	NF-RL-PF	420-550	351	0.255**	0.081

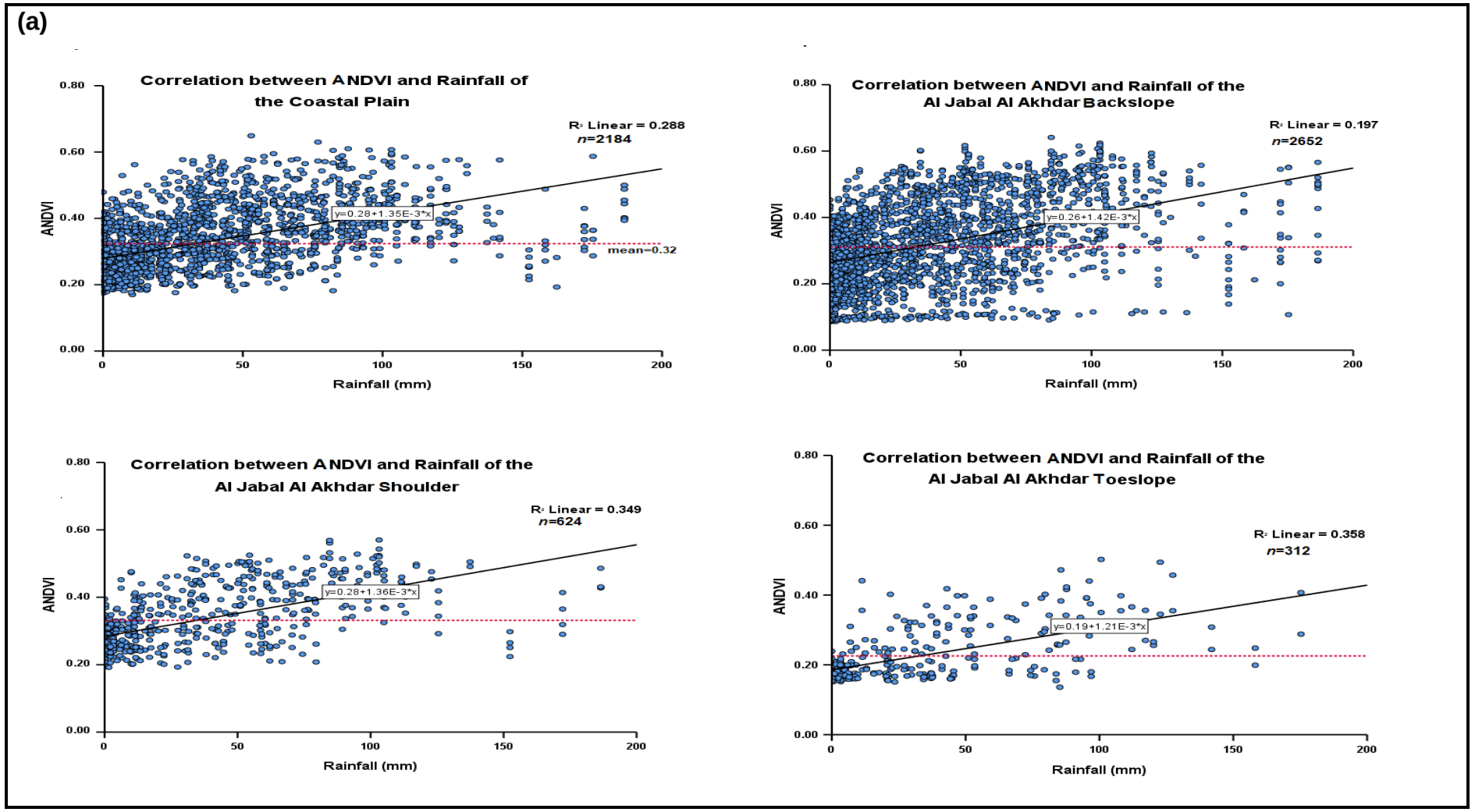

Figure 5.36 The correlation between ANDVI and rainfall in study area landforms

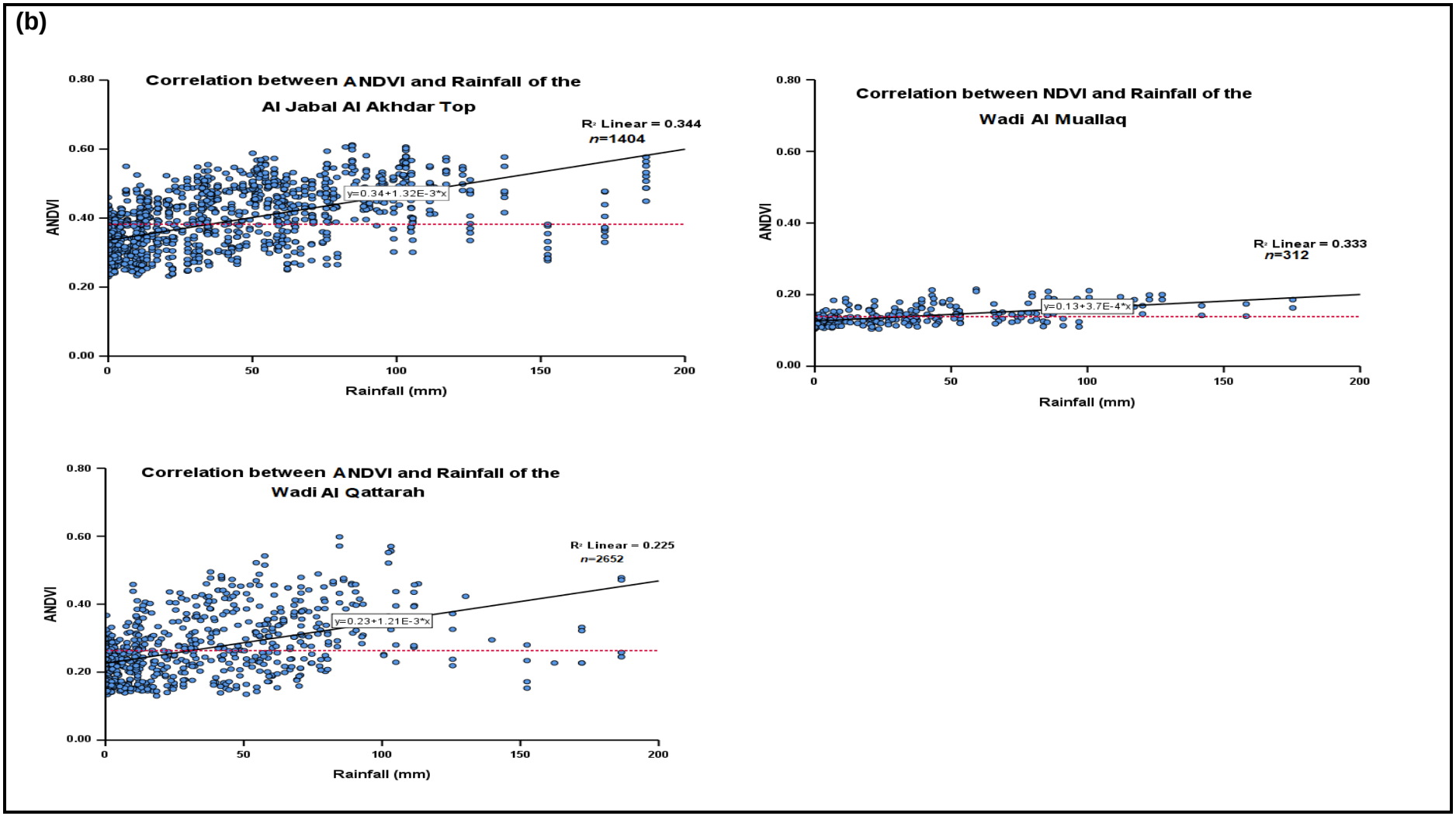

Figure 5.36 The correlation between ANDVI and rainfall in study area landforms

5.4.2.2 The Correlation between ANDVI and Rainfall minus 1-month

Figure 5.37 (a and b) and Table 5.26 show the correlation analyses between monthly ANDVI and monthly rainfall minus 1-month, in different landforms of the study areaduring 2004-2016. The results showed that the correlation between ANDVI in study area landforms and rainfall minus 1-month was a moderate to strong positive correlation and statistically significant (P-value <0.000). However, the regression analysis showed that rainfall minus 1-month can explain ≤58% of the changes in the natural vegetation cover in the different study area landforms.

Table 5.23 represents the summary of the regression analysis between ANDVI and rainfall minus 1-month results for each landform within the study area. While the pearason correlation coefficient between ANDVI and rainfall minus 1-month (P-value <0.000) is shown in Table 5.26.These low values of the coefficient of determination (R^2) explained that the rainfall less influenced the natural vegetation cover in the study area landforms. Where the natural vegetation cover has a slight decrease in all landforms except Al Al Jabal Al Akhdar Shoulder landform, despite the increase in rainfall.

Table 5.23 Statical analysis between ANDVI and Rainfall minus 1-month in the study area

Landform	Population (capita)	No. of Sites	Type of Vegetation	Alitude (m.a.s.l.)	Annual Rainfall Minus 1-Month (mm)	R^2	Std. Error of the Estimate
Coastal Plain	102,656	14	NF	30 -540	295	0.404**	0.074
Al Jabal Al Akhdar Backslope	26,775	17	NF-RL-PF	226 -780	297	0.271**	0.104
Al Jabal Al Akhdar Shoulder	82,383	4	NF-PF	336 -830	305	0.581**	0.058
Al Jabal Al Akhdar Toeslope	104,246	2	NF-RL	450, 660	326	0.556**	0.052
Al Jabal Al Akhdar Top	126,446	9	NF	360 -669	305	0.515**	0.062
Wadi Al Muallaq		2	RL	470, 620	326	0.529**	0.017
Wadi Al Qattarah	10,245	5	NF-RL-PF	420-550	267	0.437**	0.069

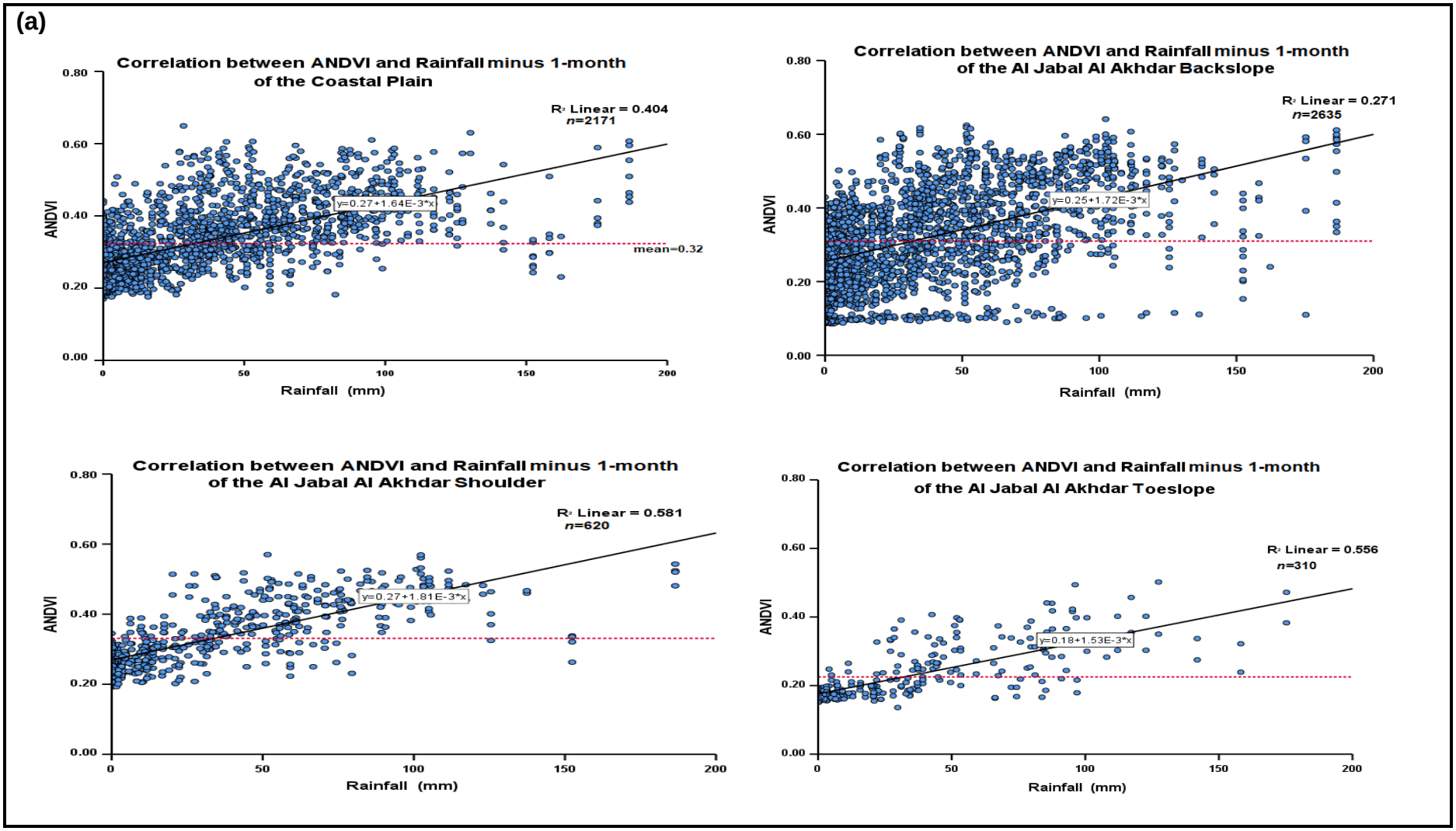

Figure 5.37 The correlation between ANDVI and rainfall minus 1-month in study area landforms

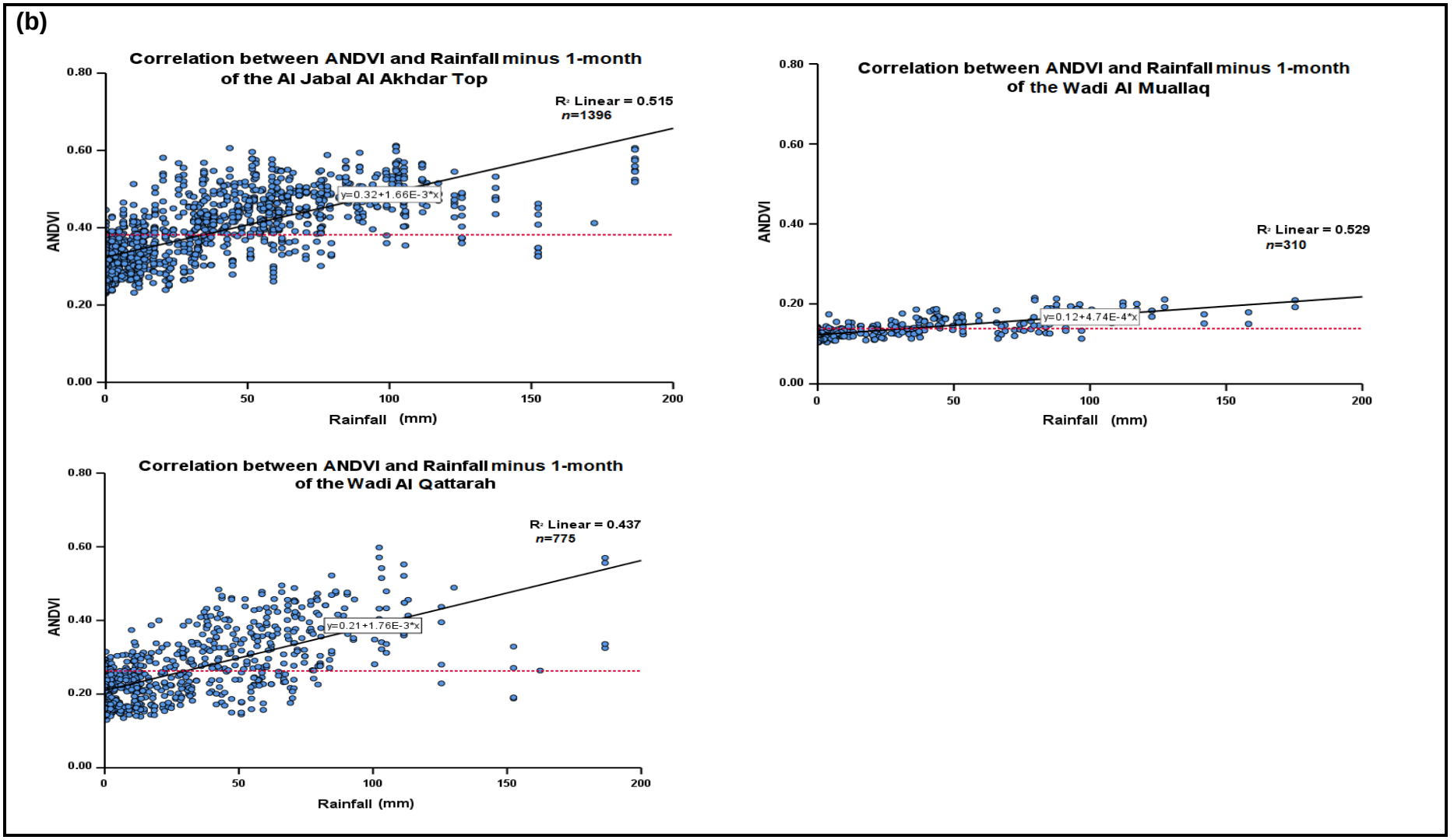

Figure 5.37 The correlation between ANDV6I and rainfall minus 1-month in study area landforms

5.4.2.3 The Correlation between ANDVI and Temperature

Figure 5.38 (a and b) and Table 5.26 show the correlation analyses between monthly ANDVI and monthly temperature in different landforms of the study area during 2004-2016. The results showed that the correlation between ANDVI in study area landforms and temperature was moderate to strong negative correlation and statistically significant (P-value <0.000). However, the regression analysis showed that temperature can explain ≤70% of the changes in the natural vegetation cover in the different study area landforms.

Table 5.24 represents the summary of the regression analysis between ANDVI and temperature results for each landform within the study area. While the pearason correlation coefficient between ANDVI and temperature (P-value <0.000) is shown in Table 5.26.

Table 5.24 Statical analysis between ANDVI and temperature in the study area

Landform	Population (capita)	No. of Sites	Type of Vegetation	Alitude (m.a.s.l.)	Mean annual Temperature (°C)	R^2	Std. Error of the Estimate
Coastal Plain	102,656	14	NF	30 -540	18.6	0.528**	0.066
Al Jabal Al Akhdar Backslope	26,775	17	NF-RL-PF	226 -780	18.5	0.317**	0.101
Al Jabal Al Akhdar Shoulder	82,383	4	NF-PF	336 -830	18.5	0.702**	0.049
Al Jabal Al Akhdar Toeslope	104,246	2	NF-RL	450, 660	18.1	0.574**	0.051
Al Jabal Al Akhdar Top	126,446	9	NF	360 -669	18.5	0.662**	0.052
Wadi Al Muallaq		2	RL	470, 620	18.1	0.512**	0.172
Wadi Al Qattarah	10,245	5	NF-RL-PF	420-550	18.7	0.382**	0.723

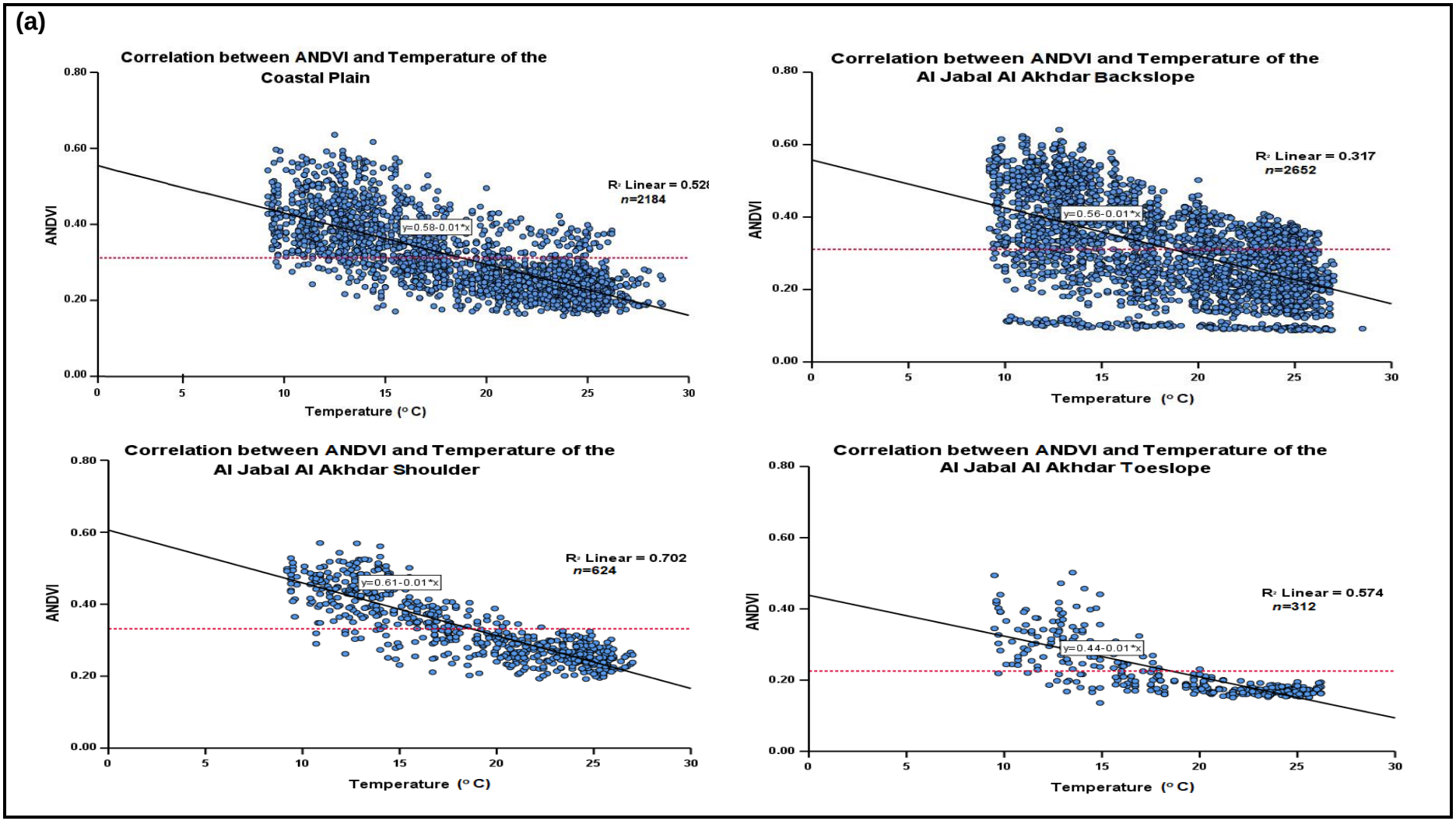

Figure 5.38 The correlation between ANDVI and Temperature in study area landforms

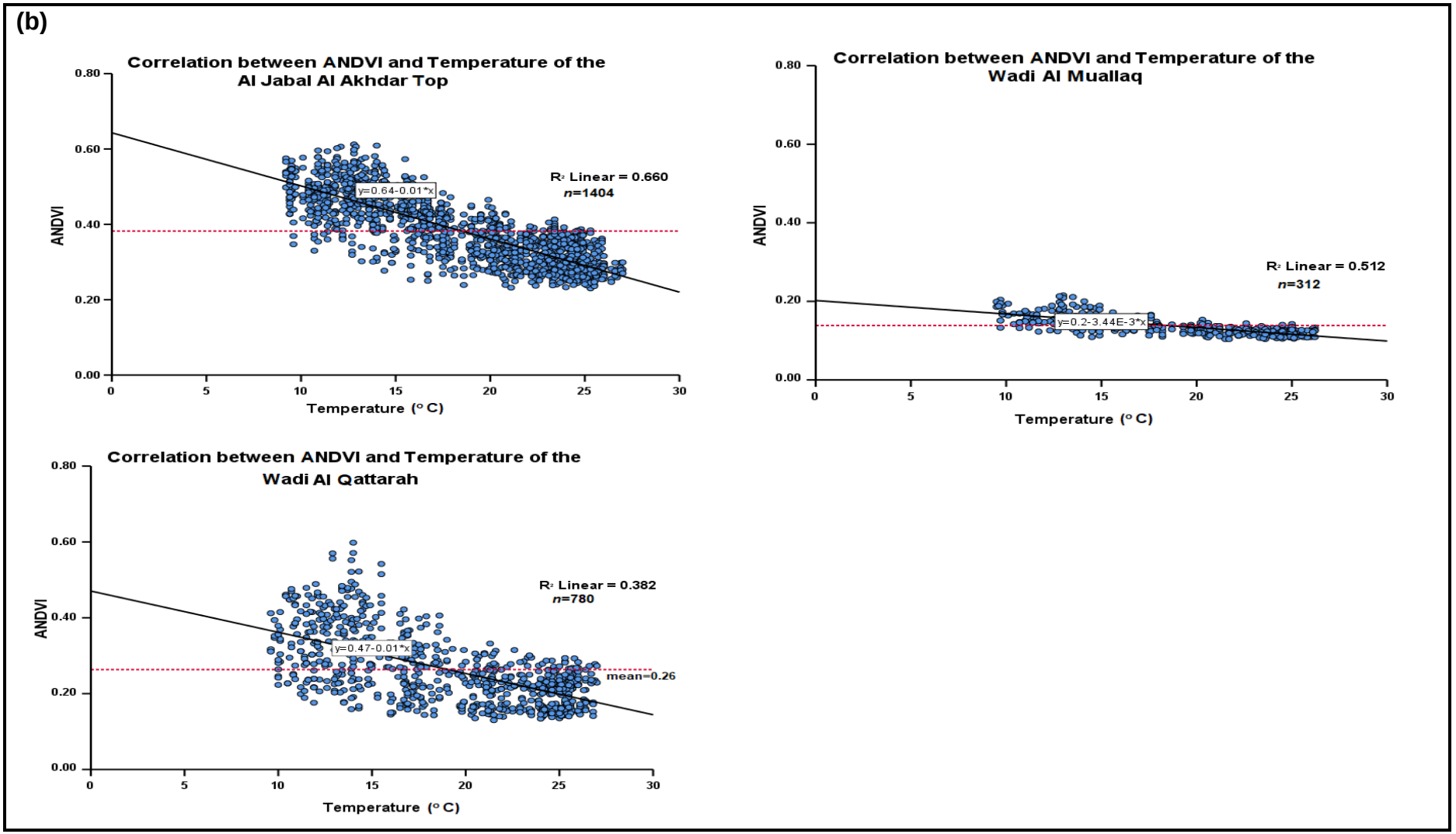

Figure 5.38 The correlation between ANDVI and Temperature in study area landforms

5.4.2.4 The Correlation between NDVI and Temperature minus 1-month

Figure 5.39 (a and b) and Table 5.26 show the correlation analyses between monthly ANDVI and monthly temperature minus 1-month in different landforms of the study area during 2004-2016. The results showed that the correlation between ANDVI in study area landforms and temperature minus 1-month was moderate to strong negative correlation and statistically significant (P-value <0.000). However, the regression analysis showed that temperature minus 1-month can explain ≤67% of the changes in the natural vegetation cover in the different study area landforms.

Table 5.25 represents the summary of the regression analysis between ANDVI and temperature minus 1-month results for each landform within the study area. While the pearason correlation coefficient between ANDVI and temperature minus 1-month (P-value <0.000) is shown in Table 5.26.

Table 5.25 Statical analysis between ANDVI and temperature minus 1-month in the study area

Landform	Population (capita)	No. of Sites	Type of Vegetation	Alitude (m.a.s.l.)	Mean Temperature Minus 1-Month (°C)	R^2	Std. Error of the Estimate
Coastal Plain	102,656	14	NF	30 -540	17.5	0.435**	0.072
Al Jabal Al Akhdar Backslope	26,775	17	NF-RL-PF	226 -780	17.4	0.273**	0.103
Al Jabal Al Akhdar Shoulder	82,383	4	NF-PF	336 -830	17.4	0.667**	0.052
Al Jabal Al Akhdar Toeslope	104,246	2	NF-RL	450, 660	17.1	0.534**	0.053
Al Jabal Al Akhdar Top	126,446	9	NF	360 -669	17.4	0.590**	0.057
Wadi Al Muallaq		2	RL	470, 620	17.1	0.502**	0.174
Wadi Al Qattarah	10,245	5	NF-RL-PF	420-550	17.6	0.419**	0.069

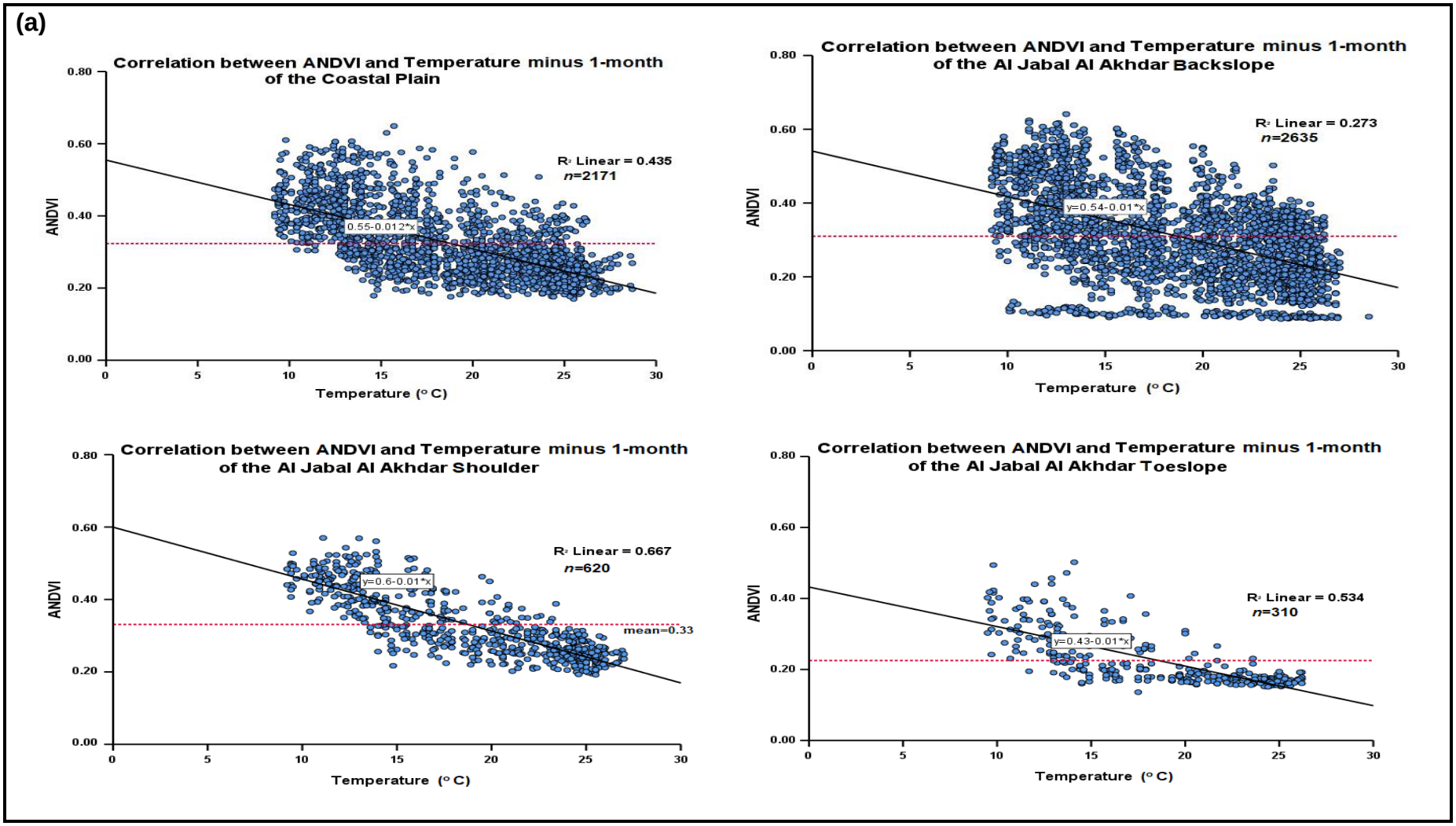

Figure 5.39 The correlation between ANDVI and Temperature minus 1-month in study area landforms

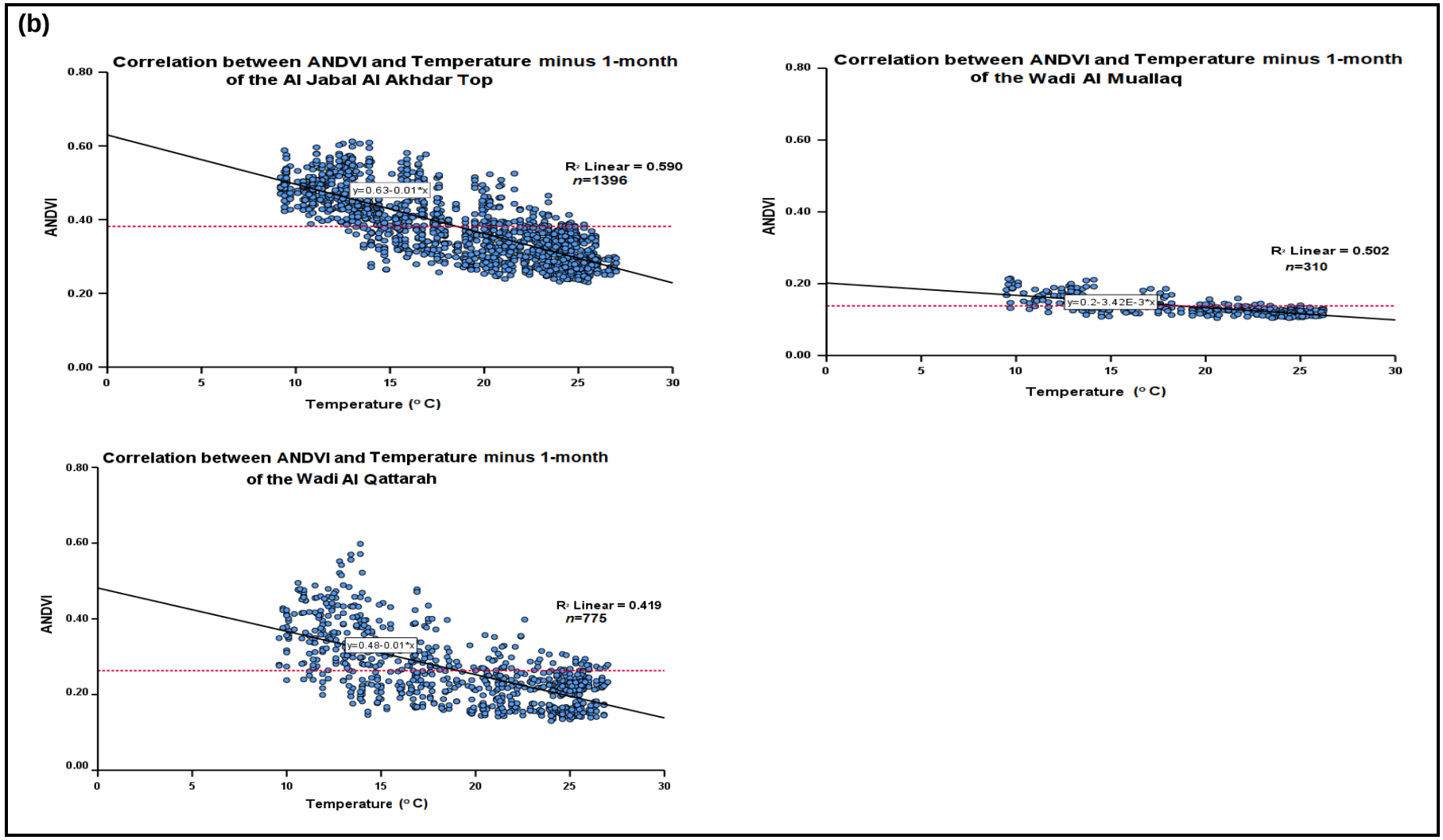

Figure 5.39 The correlation between ANDVI and Temperature minus 1-month in study area landforms

Table 5.26 Pearson correlation coefficients (r) and two-tailed significance test values (P) for ANDVI, rainfall, rainfall minus 1-month, temperature, and temperature minus 1-month, for different landforms of the study area over the period 2004-2016

ID	Landform	ANDVI-rainfall		ANDVI-Rainfall minus 1-month		ANDVI-Temperature		ANDVI-Temperature minus 1-month	
		r	P-value	r	P-value	r	P-value	r	P-value
1	Coastal Plain	0.536**	<0.000	0.636**	<0.000	-0.726**	<0.000	0.659**	<0.000
2	Al Jabal Al Akhdar Backslope	0.443**	<0.000	0.521**	<0.000	-0.563**	<0.000	-0.523**	<0.000
3	Al Jabal Al Akhdar Shoulder	0.591**	<0.000	0.762**	<0.000	-0.838**	<0.000	-0.817**	<0.000
4	Al Jabal Al Akhdar Toeslope	0.599**	<0.000	0.746**	<0.000	-0.758**	<0.000	-0.731**	<0.000
5	Al Jabal Al Akhdar Top	0.586**	<0.000	0.717**	<0.000	-0.813**	<0.000	-0.768**	<0.000
6	Wadi Al Muallaq	0.577**	<0.000	0.728**	<0.000	-0.716**	<0.000	-0.709**	<0.000
7	Wadi Al Qattarah	0.474**	<0.000	0.661**	<0.000	-0.618**	<0.000	-0.648**	<0.000

** Correlation is significant at the 0.01 level (2-trailed)

5.5 Natural vegetation cover type prediction

This section presents the results of the prediction of land cover (natural vegetation cover type) in the study area using data mining techniques and using ancillary information. ANDVI, meteorological data and the topography (landform classes) as well as some location properties such as the altitude, terrace, and soil properties were used as the ancillary data to separate the natural vegetation classes. The results of the prediction of natural vegetation cover type classes provided here were obtained by applying the decision tree ('J48' algorithm (Quinlan, 1993)). The section is divided into three subsections; the first subsection shows the result of attributes selection, the second sub-section presents the result of the prediction model, and the last sub-section shows the accuracy results of the predictive model.

5.5.1 Attributes Selection results

Figure 5.40 shows part of the resulting ARFF file which contains 8,268 instances/tuples and 19 attributes/columns, which are the values of the training and testing. The ARFF format contains the data in the form of the CSV file, but in addition, the net contains a head data dictionary section listing all the variables and the data type and categories for each.

```
@relation 'Last_2004-2016 NDVI_Soil_Soter-weka'

@attribute Month {Jan,Feb,Mar,Apr,May,Jun,Jul,Aug,Sep,Oct,Nov,Dec}
@attribute ANDVI numeric
@attribute MNDVI numeric
@attribute XNDVI numeric
@attribute ΔNDVI numeric
@attribute Rainfall  numeric
@attribute Rainfall Month-1 numeric
@attribute Temperature numeric
@attribute Temperature Month-1 numeric
@attribute Terrace numeric
@attribute Altitude numeric
@attribute 'Soil depth (cm)' numeric
@attribute 'Sand\%' numeric
@attribute 'Silt\%' numeric
@attribute 'Clay\%' numeric
@attribute 'Available water\%' numeric
@attribute Soil texture {'Clay Loam', 'Sandy Loam', 'Silty Clay Loam', 'Loam', ’Clay’, 'Silty Clay', 'Silty Loam', 'Sandy Clay Loam'}
@attribute Landform {'Coastal Plain', 'Al Jabal Al Akhdar Top', 'Wadi Al Qattarah', 'Al Jabal Al Akhdar Backslope', 'Al Jabal Al Akhdar Shoulder', 'Al Jabal Al Akhdar Toeslope','Wadi Al Muallaq'}
@attribute Natural vegetation cover type {'Natural Forest', 'Rangelands', 'Planted Forest'}

@data
Jan,0.287,0.254,0.316,0.062,141.9,?,10.4,?,1,90,20,23.39,40.59,36.02,15.64,'Clay Loam', 'Coastal Plain', 'Natural Forest'
Feb,0.306,0.268,0.331,0.063,65.7,141.9,11,10.4,1,90,20,23.39,40.59,36.02,15.64,'Clay Loam', 'Coastal Plain', 'Natural Forest'
Mar,0.304,0.281,0.329,0.048,6.9,65.7,14.4,11,1,90,20,23.39,40.59,36.02,15.64,'Clay Loam', 'Coastal Plain', 'Natural Forest'
Apr,0.281,0.264,0.305,0.041,20.7,6.9,16.5,14.4,1,90,20,23.39,40.59,36.02,15.64,'Clay Loam', 'Coastal Plain', 'Natural Forest'
```

(where symbol ‘?’ = null value)

Figure 5.40 Header part of the ARFF file and first four instances

The results of the Correlation-based Feature Subset (CFS) method showed the most relevant attributes among those listed in Figure 5.40. The CFS result showed that altitude, followed by soil properties (silt%, clay% and available water%) were the more predictor attributes than landform and ANDVI has the most significant discriminator.

```
=== Attribute Selection on all input data ===

Search Method:
    Best first.
    Start set: no attributes
    Search direction: forward
    Stale search after 5 node expansions
    Total number of subsets evaluated: 145
    Merit of best subset found:    0.475
Attribute Subset Evaluator (supervised, Class (nominal): 19 Natural vegetation cover type):
    CFS Subset Evaluator
    Including locally predictive attributes
Selected attributes: 2,11,14,15,16 : 5
                ANDVI
                Altitude
                Silt%
                Clay%
                Available water%
```

Figure 5.41 The selection of the important predictive attributes of natural vegetation cover type

5.5.2 Prediction model

The J48 algorithm, generated in 0.23 second, provides a simple pruned classification tree with a size of 29, and 15 leaves. It is generated with a high accuracy (99.9 %, see Section 5.5.3) as shown in Figure 5.42 and Figure 5.43.

```
=== Classifier model (full training set) ===
J48 pruned tree
------------------
ANDVI <= 0.176
|   Silt% <= 44.76
|   |   Clay% <= 31.37: Rangelands (582.0/1.0)
|   |   Clay% > 31.37
|   |   |   Sand% <= 23.39: Rangelands (72.0)
|   |   |   Sand% > 23.39: Natural Forest (73.0)
|   Silt% > 44.76: Planted Forest (177.0)
ANDVI > 0.176
|   Terrace <= 2: Natural Forest (4364.0)
|   Terrace > 2
|   |   Altitude <= 780
|   |   |   Silt% <= 40.59
|   |   |   |   Altitude <= 490
|   |   |   |   |   Altitude <= 460: Natural Forest (105.0)
|   |   |   |   |   Altitude > 460: Rangelands (12.0)
|   |   |   |   Altitude > 490: Natural Forest (1385.0)
|   |   |   Silt% > 40.59
|   |   |   |   Sand% <= 30.19
|   |   |   |   |   Altitude <= 460
|   |   |   |   |   |   Soil depth (cm) <= 40: Natural Forest (156.0)
|   |   |   |   |   |   Soil depth (cm) > 40: Rangelands (159.0)
|   |   |   |   |   Altitude > 460
|   |   |   |   |   |   Available water% <= 8.08: Natural Forest (468.0)
|   |   |   |   |   |   Available water% > 8.08
|   |   |   |   |   |   |   Altitude <= 464: Natural Forest (156.0)
|   |   |   |   |   |   |   Altitude > 464: Planted Forest (291.0)
|   |   |   |   Sand% > 30.19: Rangelands (112.0)
|   |   Altitude > 780: Planted Forest (156.0)

Number of Leaves  :   15
Size of the tree :        29
Time taken to build model: 0.32 seconds
```

Figure 5.42 Pruned Tree using the J48 algorithm

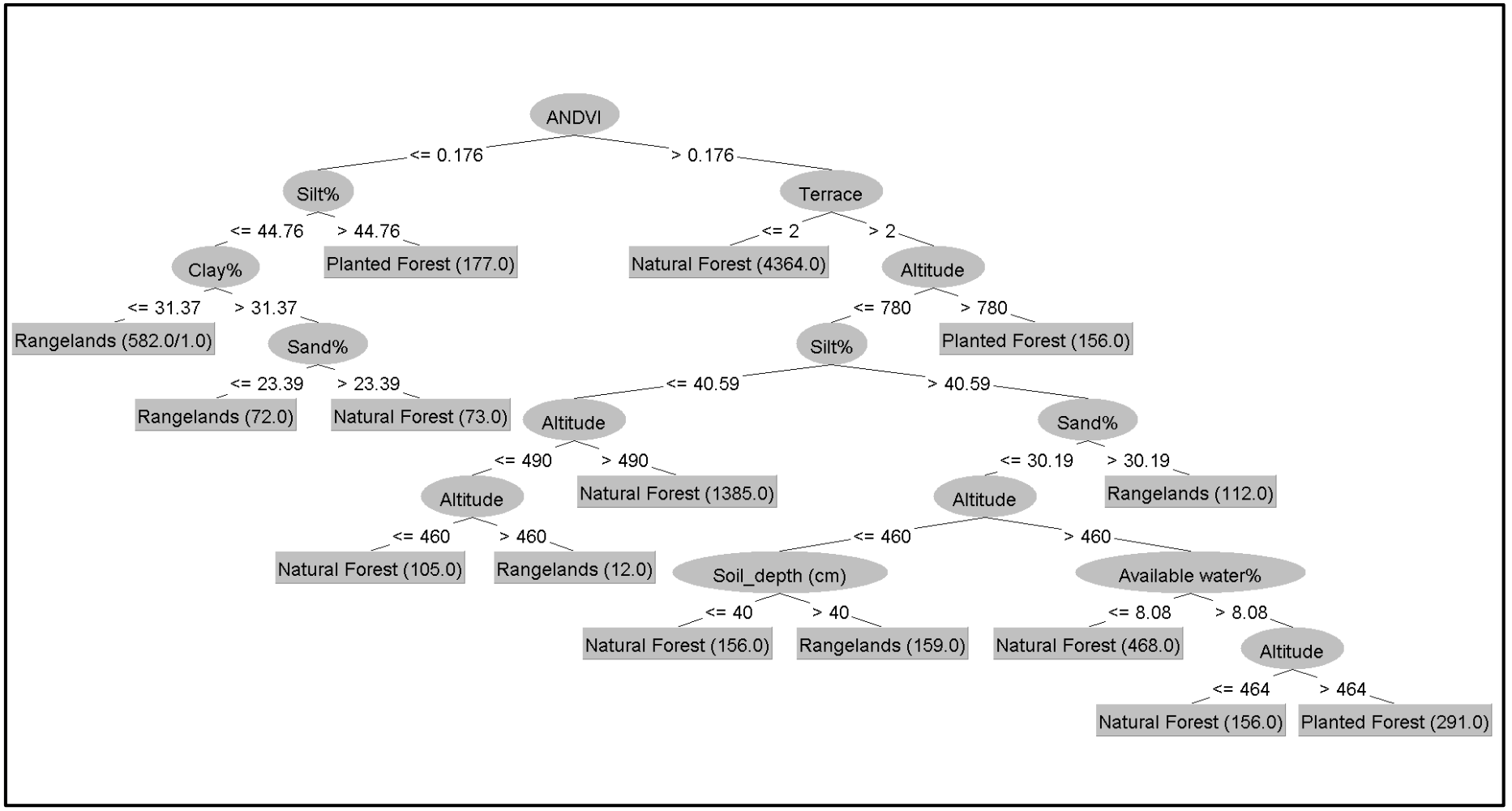

Figure 5.43 Hierarchical structure of J48 tree, in graphical form, where branches correspond to the values of attributes; leaves indicate the classes

5.5.3 The evaluating of the prediction model

The performance results of the predicted model are presented in this section in three tables. The analysis results of the J48 approach are presented in Table 5.27, while the detailed accuracy by class is presented in Table 5.28.Table 5.29 shows the confusion matrix of the J48 classifier. A 10-fold cross-validation method was used to evaluate the classifier (Kohavi, 1995; James et al., 2013).

The stratified cross-validation approach results (Table 5.27) showed the accuracy of the natural vegetation type prediction model using J48. The results showed that the predictive model has a 99.9 % accuracy rating and a Kappa of 0.99 (i.e. it has a near perfect agreement). The model also has false positives (0.073%). The accuracy measurements' results of the J48 algorithm listed in Table 5.27 show small error estimates. The error results obtained had a mean absolute error of 0.001, a root mean squared error of 0.022, a relative absolute error of 0.283% and a root relative squared error of 6.69%. The results provided a number of instances that were classified correctly, as well as those that were misclassified, the accuracy of each class also given in Table 5.29. Only 6 instances (of NF class) were predicted incorrectly as RL. Generally, the results showed that the J48 algorithm has an acceptable performance in terms of both the test's accuracy and quality.

Table 5.27 The accuracy of the classifier (J48)

Correctly Classified Instances	8262	**99.9%**
Incorrectly Classified Instances	6	0.073%
Kappa statistic	**0.99**	
Mean absolute error	0.001	
Root mean squared error	0.022	
Relative absolute error	0.283%	
Root relative squared error	6.69%	
Total Number of Instances	**8268**	

Table 5.28 shows the result of the performance of the J48 and the parameters used to quantify the quality of classification for the 53 OMU site. All those parameters were summarised in Table 5.28 and the confusion matrix in Table 5.29.

The results in Table 5.28 showed the best results in terms of precision, recall and f-measure, which present high values 1 or close to 1 (0.99). The correlation coefficient results also showed a high correlation between the predicted and actual classification of each class represented a perfect correlation (MCC of 0.99 to 1). ROC area and PRC area values of each class also showed perfect discrimination between predicted classes.

Table 5.28 Accuracy analysis on J48 classifier by class

	TP Rate	**FP Rate**	**Precision**	**Recall**	**F-Measure**	**MCC**	**ROC Area**	**PRC Area**	**Class**
	0.999	0.000	1	0.999	1	0.998	1	1	**NF**
	1	0.001	0.994	1	0.997	0.996	1	0.994	**RL**
	1	0.000	1	1	1	1	1	1	**PF**
Weighted Avg.	0.999	0.000	0.999	0.999	0.999	0.998	1	0.999	

Table 5.29 Confusion Matrix of the classifier (predictive model)

A	b	C	<-- classified as
6702	6	0	| a = NF
0	936	0	| b = RL
0	0	624	| c = PF

5.6 **Summary**

This chapter has presented the results obtained from applying the methodological approaches adopted in this study in order to examine the three objectives of this study further to the overarching research aim. The chapter showed the results of processing Landsat images and the production of LCLU maps of the study area that were used to address the first and second objectives. The changes in LULC of the study area were detected using the PCC technique, and the changes of LULC were detected, and the changes type was identified. The result of study the study area population impact on the natural vegetation cover has revealed that population has increased steadily over the years investigated and is associated with a pattern of decrease in the natural vegetation cover through the increase in classes AA, IN, BA, and NV. The results of the natural vegetation cover changes show different trends in the different landforms, with most of the studied sites showing a decrease in their vegetation cover. The results of the monthly average ANDVI time series from 2004 to 2016 in study area landforms showed a significant positive correlation with monthly rainfall, but a negative correlation with monthly temperature. The prediction model of the natural vegetation cover types using ‘J48’ algorithm results showed an acceptable, excellent degree of accuracy for classify and predict the natural vegetation type of the study area.

6 DISCUSSION

This chapter summarizes the main findings of the research. The sections of this chapter present in sequence clear statements of the results addressing directly the research question. Also presented are the limitations noted of the study.

This chapter discusses the key findings of this study, discussed and organised according to the research hypotheses and the questions presented in Section 1.4 and 1.5, respectively, as follows.

6.1 The status of the natural vegetation cover of the Al Jabal Al Akhdar results

The results discussed here address the first question of the research *'Has the natural vegetation cover of the Al Jabal Al Akhdar changed over the period 2004 to 2016, and if so, how?'*.

The results reveal how 7.10% of the total study area (71,543 ha) of natural vegetation cover types (NF and RL) have been changed to other LULC classes (PF, agricultural areas (AA) infrastructure (IN), Built-up areas (BA)) over the study period. These results confirm the changes observed in the LULC maps (Figure 5.2 to Figure 5.7) with >94% of overall classification accuracy for the years investigated.

Comparison with prior studies on the LULC changes at different places using this approach, image classification, such as Al-fares (2013) in Euphrates River Basin in Syria, detected a decrease of 11.93 % of the total natural vegetation area over 32 years (1975 -2007) associated with the increase in agricultural expansion and NV areas. Results of a study carried out by Hassan et al. (2016) in Pakistan showed a decrease in NF and NV area over the period from 1992-2012. Furthermore, Alsoul (2016) studied the deforestation in Jefara Plain-Libya, the results showed that an area of 27% of the total forest area was

cleared over the period 1986- 2010, and increased to 35% over the period from 2011-2013, Ahwaidi (2017) studied the changes in land cover in the Al Jabal Al Akhdar-Libya over 42 years. The result showed a decrease in forest 128.9 km^2 (12,890 ha) in 1972 to 35 km^2 (3,500 ha) in 2014.

Although there are misclassification pixels (>9%-<17%) related to overlapping between the agricultural area (AA) and natural forest (NF) classes, and non-vegetated area classes, the >94% classification accuracies of the maps do confirm the benefit of using the classes separability approach in the classification processes and have produced a viable and useful classification for monitoring environmental change.

The results indicate the “from-to” change trajectory of LULC in the study area, explaining the transition path and the amount of loss and the gain in areas between the classes (Figure 5.9, Figure 5.11, Figure 5.13, Figure 5.15 and Figure 5.17 and Appendix Table G.1.1 and Table G.1.2). One striking result is with class AA, which in some areas of the study area, has been converted to urban areas or tourist resorts (agricultural contraction); this result highlights the impact of human activities not just on natural vegetation cover but on agricultural areas as well. Moreover, another result related to AA changes is agriculture construction, that AA has been converted to NF, PF, RL area, and degradation, that AA converted to NV area, this could attribute to the seasonal variation which affects the classification process This could also be an attribute of the spectral similarity between NF, RL classes and AA. The results of the transition changes are also confirmed also in maps that present the spatial distribution of areas that had converted under a transition group. A number of previous studies detection changes in the LULC using the post-classification comparison technique. Fan (2008) studied the changes in land use of Guangzhou from 1998-2003, he found that a decrease in the forest, dry land and orchard which transitioned to urban, non-vegetated area and cropland. Alphan et al. (2009) detected the change in land use in Turkey; the results confirmed that the major causes of LC conversions were urbanisation and agricultural expansion. Teferi et al. (2013) studied the transition system in Blue

Nile River in Ethiopia over 52 years (1957-2009), the result showed 46% of the area have been changed, and the significant transition was from RL to AA followed by the degradation of natural forest and marshland to RL. Haque and Basak (2017) also detected the land cover change from 1980-2010 in Bangladesh; he concluded that 40% of the land cover of the total study area moreover, been changed over 30 years. The finding showed that forest and the vegetation despread rapidly during with increase in BA and AA areas.

6.2 The impact of human activities on the natural vegetation cover of the Al Jabal Al Akhdar results

This section discusses the results for the impacts of human activities on the natural vegetation cover in the study area of the period of study. This discussion addresses the second question of the research: *'Has human activities influenced the natural vegetation cover of the Al Jabal Al Akhdar?'*.

The results of population growth (Section 5.3) show that the population in the study area increased by 21.7% from 410,61 capita in 2004 to 499,85 capita in 2016 (Table 5.6). These results imply that the more land is needed to meet the population's demand for housing, thus the increase in built-up areasand to expanding lands for the agricultur or gazing the livestock. Therefore, an area 71,543 ha or (7.10% of the total studyarea) of the NF and RL cover have changed to the other classes. The NF and RL areas were changed to NV areas by 78% of the total decreased areas, converted to AA, IN and BA areas by 10%, 8.5% and 3.7 of the total decreased areas, respectively, in addition to a tiny change for an area of 0.16% of the total decreased to PF area partically from RL areas. The transition group results also show the increase in agricultural expansion, urbanisation and distrubted lands (i.e. the transition of the AA, NF, RL and PF classes to NV class), these indicate that the significant transition of natural vegetation cover in the study area is due to human activities (Table 5.5).

The results also reveal an increase in built-up and infrastructural areas because of urbanisation as a result of the increase in population. The regerssion analysis results show the increase trend in population density and built-up and

infrastructural areas (R^2= 0.976, 0.885 and 0.713, respectively), . The agricultural areas also have increased with the increase of population (R^2= 0.271 for AA). Furthermore, the non-vegetated areas have an invreasing trend (R^2= 0.630) with increase in the population density. This increase in the non-vegetated areas represents the negative impact of human activities, reflecting the land degradation situation. This degradation can be occurred as a result of overgrazing, cutting down the trees and shrubs, collecting wood fuel, over-collecting the medical plants or experiencing fire (El-Barasi and Saaed, 2013; Zatout, 2014; Ahwaidi, 2017), taking into account the other factors such as growing season, crops types, soil moisture storage and seasonal variation impacts such as Landsat imagery date in this study.

The results conclude that human activities, mainly, urbanisation and agricultural expansion, have a direct impact on the natural vegetation cover changes in Al Jabal Al Akhdar, considering natural factors such as climate and fire, which can also influence these changes. This result agreed with a number of previous studies that considered the impact of population increase and human activity on land use/ land cover changes. Showqi et al. (2014) found that the decrease in forest cover and agriculture land in the Doodhganga watershed of Jhelum Basin in Kashmir Himalayas had resulted from human activities and highlighted how population growth had been a major driving force for these changes. Mhawish and Saba (2016) linked the changes in land use/land cover in Wadi Ziqlab catchment in Jordan during the period 1953-2008 to the population growth. In Libya, El Shatshat (2015) and Ahwaidi (2017) suggested that urbanisation and human activities play a critical role in changes in vegetation cover in Al Jabal Al Akhdar.

6.3 Impact of climate on the natural vegetation cover of the Al Jabal Al Akhdar results

Section 5.4 showed the result of the climate impacts on the natural vegetation cover in the study area. This section discusses the results of the statistical analysis between climatic factors and the average Normalized Difference Vegetation Index (ANDVI) in seven landforms to address the third question of

the research: *'Is there any discernible impact of climate on natural vegetation cover in the Al Jabal Al Akhdar region over the period from 2004-2016?'*.

The results of the monthly temperature and rainfall trends analysis for 13 study years (2004-2016) show a slight increase in both temperature and rainfall for all study area landforms. With the increase in rainfall regime, an increase in natural vegetation cover in all study area landforms is expected. However, circa 85% of the sample sites show a negligible decrease in the ANDVI over the same period (Figure 5.22, Figure 5.23, Figure 5.25, Figure 5.26, Figure 5.28 to Figure 5.33 and Figure 5.35). These results indicate that the negligible increase in rainfall observed over the study period has had an insignificant impact on the variation in the natural vegetation cover of Al Jabal Al Akhdar. Seasonal variations in rainfall have a far greater influence in natural vegetation cover. A study by Faour et al. (2016) in North Morocco (29°N –36°N) reported a decrease in vegetation cover while the rainfall had increased by 37% over the period from1999 to 2012.

The slight increase in temperature noted could affect the availability of water for the plants through increased evapotranspiration. This is influenced by the long dry and hot summer period across all the study area landforms, which varies depending on the location, elevation and soil physical properties of the sites (see Appendix Table B.3.1). The response of the natural vegetation cover to the increase of temperature varies according to the type of the plants' root systems and the environmental requirement of the plant species. Drought conditions and plant drought stress, particularly those resulting from the increase in temperature and water shortage, affect plants negatively. Such conditions cause damage and plant death (Ali and El Shatshat, 2015).

In general, the Pearson correlation coefficients in all study area landforms over the 13 years study period (2004-2016), show a significant positive correlation between the monthly rainfall and monthly ANDVI, and a significant negative correlation between the monthly temperature and monthly ANDVI (Figure 5.36 to Figure 5.39 and Table 5.26). The results also show that the correlation coefficients values differ from a landform to another. This could be attributed to

the variation in topography and soil types of each landform (see Appendix Table C.1.1) affluence the natural vegetation cover type associated with each landform. Moreover, in this study, NF cover type is primarily associated with the Coastal Plain and the Al Jabal Al Akdar Top landforms; the three natural vegetation cover types (NF, RL and PF) are associated with Al Jabal Al Akhdar Backslope and Wadi Al Qattarah. PF and NF cover types are found on the Al Jabal Al Akhdar Shoulder, RL and NF cover types are in Al Jabal Al Akhdar Toeslope, and lastly RL cover type is in Wadi Al Muallaq. Each type of natural vegetation cover has plant communities which can differ in the specific species composition, but *Juniperus phoenicea* L. is the dominant species of 80% of the studied NF sites, *Pinus halepensis* Mill.is the dominant species of the planted forest, while RL is dominated by *Hammada scoparia* (Pomel) Iljin and *Thymus capitatus* Hoff. et Link. (33% of each) (Appendix Table B.2.1).

The moderately significant positive correlation between the monthly rainfall and monthly ANDVI ranged from 0.443 to 0.599, and a moderately to strongly significant positive correlation was found between the rainfall minus 1-month and ANDVI ranged from 0.521 to 0.762. The results of the rainfall minus 1-month (e.g. a one-month time response for vegetation to develop) offer a better explanation of the ANDVI variability than does the rainfall amount in the same month; this indicates the rainfall amount of the previous month will have a substantial impact on the ANDVI values of the next month.

The moderate to a strong significant negative correlation between the monthly temperature and monthly ANDVI ranged from -0.563 to -0.838, which decreased to -0.523 to -0.817 for the temperature minus 1-month. The results of the temperature show a better explanation of the ANDVI variability. The strong negative correlation indicates that the increase in temperature leads to worsening drought conditions (Wang et al., 2001), that will influence negatively on the natural vegetation.

The linear regression results between monthly ANDVI and rainfall minus 1-month show the coefficient of determination (R^2) values ranged from 0.271-0.581, and R^2 ranged from 0.371- 0.702 between monthly ANDVI and monthly

temperature. These results indicate that the variation in monthly ANDVI could be attributed to rainfall minus 1-month (R^2=27%-58%) or monthly temperature (R^2=37%-70%). For example, in Al Jabal Al Akhdar Backslope landform, the variation of natural vegetation cover (NF, PF and RL), could be attributed to rainfall minus 1-month (R^2 of 27%, n=2635) and the remaining variations could attribute to temperature (R^2 of 37%); thus, the remaining could account for the human activities (Figure 5.27 and Figure 5.35). With respect, this landform includes three sites of 17 sites showed an increase in the NF cover and RL cover types.

The overall results indicate that the climate, particularly the increase in temperature, coupled with the terrain, altitude, soil type and human activities, have an impact on the observable changes in the natural vegetation cover. This result agreed with a number of previous studies that considered the status of vegetation in Al Jabal Al Akhdar. Ali and El Shatshat (2015) reported that dry condition due to the increase in temperature, and human activity such as agriculture expansion, urbanisation and overgrazing affected the vegetation composition in Al Jabal Al Akhdar. Suleiman et al. (2016) highlighted the factors that caused the decline in Juniper in Al Jabal Al Akhdar, which included the topographical aspects, altitude, dust storms in addition to human activities. Ahwaidi (2017) also suggested the vegetation changes over 42 years in Al Jabal Al Akhdar could be effected by climate changes, especially in the southern region.

6.4 The ability to predict the natural vegetation cover type using "Machine learning"

This section discusses the results of the prediction of natural vegetation cover type classes by applying a decision tree approach using the 'J48' algorithm (Quinlan, 1993; Wu et al., 2008), in the Weka environment (Weka, 2019), in order to address the third question of the research: *'Is it possible to predict the natural vegetation cover type based on location properties using machine learning?'*.

This section discusses the results of the examination of a machine learning approach undertaken to classify the natural vegetation cover type of Al Jabal Al Akhdar to provide a result based on model training with remote sensing data, topographical data, and location attributes.

The Correlation-based Feature Subset (CFS) method was undertaken, selected to ‘evaluates the worth of a subset of attributes by considering the individual predictive ability of each feature along with the degree of redundancy between them’ (Weka, 2019; (Hall and Smith, 1998) (Figure 5.41). The CFS algorithm selects ANDVI, altitude, silt%, clay%, and available water%. These five attributes are the most informative subset of attributes that are related to natural vegetation cover in the study area, and of these ANDVI is the most significant discriminator.

Interestingly, the CFS method excludes landform from the most-informative attributes; this could be due to the different elevations’ present in each landform. Therefore, the elevations of the study sites (53 sites), is the more informative attribute to be chosen rather than landforms.

The result of the ‘natural vegetation type’ model undertaken using the J48 algorithm has resulted in a pruned classification tree with a size of 29, and with 15 leaves (Figure 5.42 and Figure 5.43). This result confirms the benefits of the use of the CFS method, where (Samardžić-Petrović et al., 2017) reported that the attributes selection aid in the reduction of the model complexity, the reduction of time for processing, and a consequent increase in model accuracy.

Evaluating the results shows that the J48 algorithm has excellent prediction performances (Table 5.27, Table 5.28 and Table 5.29), where the best algorithm provides a simple tree with high accuracy (Mohamed et al., 2012). Therefore, the overall result confirms that machine learning ‘J48’ has the ability to classify and predict the natural vegetation cover type in Al Jabal Al Akhdar. A similar conclusion was reached by Biswal et al. (2013) who produced a LULC map of Thane, a district of Maharashtra in India, with good overall accuracy (92%) and kappa (0.90) using the J48 decision algorithm.

6.5 **Limitations**

The main limitation of this study was the enforced inability to obtain real-time ground-truth vegetation cover data due to the volatile political and security situation in Libya, preventing systematic fieldwork. Therefore, an existing detailed vegetative survey for the study area, conducted by OMU during the spring and summer of 2003 and 2004 (OMU, 2005) was used for classified the Landsat imagery. It was also used to provide the base data for this study. A pragmatic approach was therefore undertaken to use the sample location to create ground-truthing based on personal knowledge and Google Earth interpretation. The results were near perfectly classified images with an overall accuracy of >94%. Biswal et al. (2013) emphasised that Google Earth is considered as the best online high-resolution imagery available for free.

Secondly, the scarcity of climate data. Due to the political situation in Libya, no meteorological data were recorded from 2011 to 2016. Furthermore, the number of meteorological stations in Al Jabal Al Akhdar remains inadequate for coverage of this substantive area (3 stations within the study area, in addition to Benghazi station), the freely available online Global Climate Monitor (GCMon), was used to obtain the climatic data. Even though climate studies reported that an increase in temperature and decline in rainfall was detected in north Libya (El-Tantawi, 2005; Zeleňáková et al., 2014), the study shows an increase in both climate factors in the study area (32°N-33°N). However, Faour et al. (2016) noted that TRMM Online Visualization and Analysis System showed an increase in rainfall in North Marrocco (29°N-36°N) and North Algeria and Tunisia (32°N-37°N) from 1999-2012.

Thirdly, population data, this study was based on census data of 1973, 1984, 1995 and 2006. no census was conducted after 2006, and the next census would be in 2020 (BSC-L, 2016). Also, data is unavailable for the numbers of immigrants passing to the coast from south and west Libya who settled in the study area during the war in the Libyan revolution (2011), and the war of Benghazi and Derna districts (2014 to the present). This issue influenced the accuracy of the relationship assessment between the increase of population

density and the natural vegetation cover changes. Moreover, the results confirmed that the increase in population density had exerted a negative impact on the natural vegetation cover due to the human activities on the LULC changes (i.e. the increase in urbanisation and agricultural expansion with the increase in population) .

Lastly, Landsat imagery, cloud-free Landsat imagery was used for this study. 2-Landsat scenes' images (path/row: 183/37, and 183/38) were used to achieve cover across the study area. The issue was in sourcing imagery from the same annual temporal period across the years of study that was cloud-free and permitted intercomparisons, where it was often limited to only one image per year (or not at all). The cloud-free Landsat imagery obtained was therefore only available from different months across the study years, potentially also from different seasons. That meant that vegetation could appear in different growth stages. Although this did not affect the classification process within the year, it did complicate inter-year comparisons. It is recommended to use imagery that is as temporally as close as possible. Mohajane et al. (2018), for example, used cloud-free Landsat imagery acquired between July and September, because in this period of the year in Morocco all plant species are at the stable full vegetative stage. Therefore, the seasonal variability did not affect the detection processes. The results of the current Libyan research show evidence of fluctuation between an increase and a decline in vegetation throughout the study period because of seasonal variability effects. Where in spring (Landsat imagery of the year 2010) and early summer (Landsat imagery of the year 2008 and 2016) the land considers as a full vegetated due to the growth of the annual plants, while it is less vegetated in summer (Landsat imagery of the year 2004, 2008 and 2014), particularly in August the dry, hottest months in the year.

Moreover, the temporal resolution of imagery, as typically only one cloud-free Landsat image was available in each given year it was not possible to fully examine the impact of climate on the natural vegetation cover using Landsat imagery, where time series data are required. Therefore, MCD43A4-NDVI

imagery was used for this purpose instead, which can be accessed through the use of the Google Earth Engine platform.

6.6 Summary

The key results of the research are presented in this chapter. The discussion organised in four subsections following the research questions listed in Chapter 0.

The research detected a 7.10% decrease in natural vegetation cover in the Al Jabal Al Akhdar area during the study period. The transitions of the classes indicate that human activities have impacted on the changes in natural vegetation cover by the increase in agricultural expansion, urbanisation and increase in non-vegetated areas. The research confirms that the climate has a secondary role in the natural vegetation cover changes in the Al Jabal Al Akhdar, where the increase in temperature is a contribution to the natural vegetation cover changes considering the topographical differences such as terrain, elevation and aspect and slopes. The research confirms the ability of machine learning to classify and predict the natural vegetation cover type in Al Jabal Al Akhdar. Lastly, with the political considerations in the study region, the chapter highlights some limitations of the approach, and the pragmatic approaches adopted to mitigate these issues.

7 CONCLUSIONS AND RECOMMENDATIONS

This chapter concludes the research and explains its findings and implications. The chapter also provides recommendations and suggestions for future work in terms of monitoring and predicting changes in the natural vegetation cover in Al Jabal AL Akhdar region.

7.1 Conclusions

The northern region of the Al Jabal Al Akhdar lies on the Mediterranean coast and has been an area of vital importance from ancient times to the present for local communities and communities from surrounding regions and wider Mediterranean countries. The vegetation cover in Al Jabal Al Akhdar has been subjected to many human and natural pressures, contributing to the deterioration and overall shrinking of the naturally vegetated area. Human activities such as the expansion of agriculture, grazing, charcoal production, collection of medicinal and aromatic plant species at a commercial scale, and increasing urbanisation, have all increased. Also, after the Libyan uprising in 2011 greater pressures have been placed on the land with little centralised management, hindered by widespread weapons abundance and the absence of authorities (El Shatshat, 2015). The latter factors have also impacted on the methodologies selected in this study. Overall, this study has sought to "*Assess and evaluate the changes in the natural vegetation of the Al Jabal Al Akhdar region following the 2011 Libyan uprising"*.

The following conclusions can be drawn from the current study listed according to the specific objectives of this study:

7.1.1 Objective 1

Assess and evaluate changes in natural vegetation cover over the period from 2004 to 2016

The results of the LULC changes confirmed that from 2004-2016, natural forest and rangelands combined decreased by 71,543 ha or 7.10% of the total area of the study area. This decrease was observed over the entire study area. Moreover, urbanisation and agricultural expansion were found to pose the most critical change to the natural vegetation cover, reflecting the direct role of human activities in effecting the observed changes. This was confirmed from the results of change detection and transition type. The degradation in natural vegetation cover also represents changes caused by natural factors including climate and/or fire (non-deliberate but through natural ignition). However, the primary impact appears to derive from human activities such as overgrazing, tree felling, and/or collection of medicinal plant species.

The results of this objective are valuable in highlighting the significant changes in natural vegetation in Al Jabal Al Akhdar and introducing the value of the post-classification comparison technique to fill part of the gap in previous Libyan studies with regards to LULC changes using remote sensing and

7.1.2 Objective 2

Identify and characterise the impacts of human activities on the natural vegetation cover in Al Jabal Al Akhdar

This work drew upon the results of LULC changes detection, and the Libyan population census in order to identify the impact of human activities on the natural vegetation cover changes in the study area. An increasing trend in , urbanisation and agricultural expansion assicated with the increasing trend in population. Additionally, and the increasing trend in disturbed lands of natural vegetation cover, reflecting the indirect impact of human activities natural vegetation cover concerning the natural factors such as on climate and fire.

-

7.1.3 Objective 3

Investigate and quantify the impact of climate on the natural vegetation cover in Al Jabal Al Akhdar

A key conclusion from this objective is that the observed increase in temperature has had a negative effect on the vegetation cover for 85% of the total investigated sites across the different landforms concerning both abiotic factors such as soil types and altitude, and biotic factors such as plant species and human activities.

7.1.4 Objective 4

Evaluate the ability of machine learning to predict the natural vegetation cover types in Al Jabal al Akhdar

The J48 decision tree algorithm implemented in the WEKA tool[1], was applied to the study datasets, with the results confirming the high capability of J48 with its excellent prediction performances in terms of accuracy and run time.The prediction model created can be applied elsewhere in Libya and can be used furthermore to classify satellites image data.

The machine learning approach adopted can handle big data over very short time periods and with a high accuracy making this approach useful for supporting decision-makers in managing forests and rangelands.

7.2 Recommendations

- According to the results of land use land cover changes detection, it is necessary to evaluate current and forecast values in future for change detection in natural vegetation cover in Al Jabal Al Akhdar through the use of other sources of satellite imagery with a high resolution. Furthermore, there is an urgent ongoing demand to put in action plans to manage and protect the natural vegetation cover in Al Jabal Al Akhdar.

[1] https://www.cs.waikato.ac.nz/ml/weka/

- For further studies, as the capabilities of earth observation sensors grow with time, it is recommended that these sensors and their data be integrated and utilised together with such validated ground-based observations as exist. A further recommendation is for the installation and of more meteorological stations in Libya.

- The likelihood of the negative impacts of temperature on the natural vegetation cover across the 53 sites leads to the recommendation for further extended spatio-temporal investigations covering the entire Al Jabal Al Akhdar area to permit exclusion of human activities impacts in the fragmented, distributed areas of small populations. This would permit forecasting of the impact of climate changes on the future natural vegetation cover as well.

- According the high accuracy of the J48 classifier (3 types of landcover class), develop the approaches further is recommended. By extending LULC classes including all the LULC in Al Jabal Al Akhdar which could be assessed using the J48 algorithm and the results applied for the resulting classification model to the process of image classification

7.3 **Research Contribution**

The contribution of this research work is in three parts:

- The techniques used here represent a powerful and novel application for environmental management in Libya, providing practical tools for managing this fragile landscape and predicting potential outcomes.

- The approach has been devised to use ‘appropriate technology’ to better ensure its uptake. The use of proprietary, and where possible, open-source software and data to seek to reduce costs and remain free from chargeable dat, that will ensure the future practicality of the approaches put forward.

- The method has sought to provide an approach of ‘reduced intervention’ (low effort) which can ultimately be fully automated, permitting an ongoing, semi-autonomous monitoring approach. The use of datasets such as satellite

observations can be integrated into automated workflows in future that will permit fine monitoring of the emergent changes in the region.

7.4 The dissertation in summary

Al Jabal Al Akhdar, historically, was an important region for many successive civilisations from the era of the Greeks and Romans to the Ottoman Empire and the Italian occupation, where those successive civilisations have exerted their impact on the natural vegetation cover. Nowadays the human activities impact has increased due to the developments in technology and population levels. Therefore, identifying the causes of current change in vegetation cover, and monitoring these changes is very important in mitigating the risk of vegetation and land degradation. The main aim of this dissertation, therefore, was “to establish and evaluate the changes in the natural vegetation cover of the Al Jabal Al Akhdar region following the 2011 Libyan uprising”. The research was conducted by the utilising of GIS, and remote sensing data and techniques its achieve the objectives, along with the ancillary data in 53 sites, the representative sites of Al Jabal Al Akhdar region.

The main finding identified a reduction in two types of natural vegetation cover: natural forest and rangelands types in several areas across the studied area over 13 years. The human activities have influenced the natural vegetation cover through the increase in human-related land use, where is there a positive relationship between the increase in population and agricultural expansion and urbanisation. The human activities also affected the natural vegetation cover negatively through the increase in the non-vegetated areas leading to land disturbance as results of overgrazing, cutting down the trees, and uprooting of plant species for use as fuel or for medicinal purposes. The climate has a negligible impact on the natural vegetation cover changes, particularly temperature, where the increase in temperature could affect the natural vegetation cover negatively due to the decline in water availability to plants. Looking for a fast and accurate measurement technique that aids the managers and decision makers with classifying the natural vegetation cover, the overall result confirms that machine learning ‘J48’ has the ability to classify and predict

the natural vegetation cover type in Al Jabal Al Akhdar. Machine learning ‘J48’ can also be used to classify the satellite imageries as well.

Finally, the research highlights the importance of evaluating the current and forecast for change detection in natural vegetation cover in Al Jabal Al Akhdar through the use of high-resolution satellite imagery and recommended it for the future work. Furthermore, there is an urgent ongoing demand to put in action plans to manage and protect the natural vegetation cover in Al Jabal Al Akhdar

REFERENCES

Abdalrahman, Y., Spence, K. and Rotherham, I. D. (2010) 'The main causes of direct human-induced land degradation in the Libyan Al Jabal Alakhdar region.' *In End of Tradition? Landscape Archaeology and Ecology*-, pp. 7–21.

Abdi, O. A., Glover, E. K. and Luukkanen, O. (2013) 'Causes and Impacts of Land Degradation and Desertification: Case Study of the Sudan.' *International Journal of Agriculture and Forestry*, 3(2) pp. 40–51.

Abusaief, H. M. A. (2013) 'Life forms and rangeland for many habitats of Jarjar oma in Al Jabal Al Akhdar on Mediterranean sea.' *Journal of American Science*, 9(5) pp. 236–249.

Abusaief, H. M. A. and Dakhil, A. H. (2013) 'The floristic composition of Rocky habitat of Al Mansora in Al Jabal Al Akhdar- Libya.' *New York Science Journal*, 6(5) pp. 34–45.

Abusaif, H. M. A. (2013) 'Habitats and plant diversity of Al Mansora and Jarjr-oma regions in Al Jabal Al Akhdar- Libya.' *Life Science Journal*, 10(2) pp. 659–692.

Adesuyi, A. S. and Munch, Z. (2015) 'Using Time-Series NDVI to Model Land Cover Change : A Case Study in the Berg River Catchment Area, Western Cape, South Africa.' *International Journal of Geological and Environmental Engineering*, 9(5) pp. 553–558.

Afhima, G. A., Badi, H. A. and Al Haddad, S. M. (2008) 'The role of environmental policy in vegetation cover conservation to achieve the concept of sustainable development (In Arabic).' *In Conference on Sustainable Development in Libya, 28-29/06.* Benghazi.

Ageena, I., Macdonald, N. and Morse, A. P. (2013) 'Variability of minimum temperature across Libya (1945-2009).' *International Journal of Climatology*, 33(3) pp. 641–653.

Ageena, I., Macdonald, N. and Morse, A. P. (2014) 'Variability of maximum and

mean average temperature across Libya (1945-2009).' *Theoretical and Applied Climatology*, 117(3–4) pp. 549–563.

Ahwaidi, G. M. A. (2017) *Factors Affecting Recent Vegetation Change in North-East Libya*. PhD thesis. School of Environment and Life Sciences. The University of Salford. The UK.

Al-Bakri, J. T. and Suleiman, A. A. (2004) 'NDVI response to rainfall in different ecological zones in Jordan.' *International Journal of Remote Sensing*, 25(19) pp. 3897–3912.

Al-fares, W. (2013) *Historical Land Use/Land Cover Classification Using Remote Sensing: A Case Study of the Euphrates River Basin in Syria*. Springer Cham Heidelberg New York Dordrecht London.

Al-idrissi, M., Sbeita, A., Jebriel, A., Zintani, A., Shreidi, A. and Ghawawi, H. (1996) *Libya: Country Report to the FAO International Technical Conference on Plant Genetic Resources Leipzig, Germany. Leipzig*. Leipzig.

Al-Sodany, Y. M., Shehata, M. N. and Shaltout, K. H. (2003) 'Vegetation along an elevation gradient in Al Jabal Al Akhdar, Libya.' *Ecologia Mediterraneaediterranea*, 29(2) p. 200.

Alaib, M. A., Sherif, I. E.- and Al-hamedi, R. I. (2017) 'Floristic and ecological investigation of Wadi Al Agar in Al Jabal Al Akhdar - Libya.' *Science & its applications, University of Benghazi*, 5(1) pp. 57–61.

Alex, E. C., Ramesh, K. V and Sridevi, H. (2017) 'Quantification and understanding the observed changes in land cover patterns in Bangalore.' *International Journal of Civil Engineering and Technology*, 8(4) pp. 597–603.

Ali, M. and El Shatshat, S. (2015) 'Ecological study of Juniperus phoenicea L. in Al Jabal Al Akhdar area, Libya.' *European Journal of Experimental Biology*, 5(7) pp. 71–76.

Alphan, H., Doygun, H. and Unlukaplan, Y. I. (2009) 'Post-classification comparison of land cover using multitemporal Landsat and ASTER imagery:

The case of Kahramanmaras, Turkey.' *Environmental Monitoring and Assessment*, 151(1–4) pp. 327–336.

Alsoul, A. H. K. (2016) *Deforestation in Jefara Plain, Libya: Socio-economic and Policy Drivers (Algarabulli District case study)*. PhD thesis. School of Environment, Natural Resources and Geography. Bangor University.

Apan, A., Kelly, R., Jensen, T., Butler, D., Strong, W. and Basnet, B. (2002) 'Spectral Discrimination And Separability Analysis Of Agricultural Crops And Soil Attributes Using Aster Imagery.' *Proc 11th Australasian Remote Sensing and Photogrammetry Conference (ARSPC), Brisbane/Australia*, 2 pp. 396–411.

Araya, Y. H. and Cabral, P. (2010) 'Analysis and modeling of urban land cover change in Setúbal and Sesimbra, Portugal.' *Remote Sensing*, 2(6) pp. 1549–1563.

Archibold, O. W. (1995) *Ecology of World Vegetations*. *Chapman and Hall*. Dordrecht: Springer Netherlands.

Ashraf, N. A. (2016) 'Major determinants of population growth.' *International Journal of Human Resource & Industrial Research*, 3(4) pp. 01–07.

Baartman, J. E. M., Van Lynden, G. W. J., Reed, M. S., Ritsema, C. J. and Hessel, R. (2007) *Desertification and land degradation: origins, processes and solutions -DESIR project.*

Bai, Z. G., Dent, D. L., Olsson, L. and Schaepman, M. E. (2008) 'Proxy global assessment of land degradation.' *Soil Use and Management* pp. 223–234.

Banko, G. (1998) *A review of assessing the accuracy of and of methods including remote sensing data in forest inventory*. *Interim Report IT-98-081*. Laxenburg, Austria.

Bannari, A., Morin, D., Bonn, F. and Huete, A. R. (1995) 'A Review of Vegetation Indices.' *Remote Sensing Reviews*, 13(1) pp. 95–120.

Barbati, A., Arianoutsou, M., Corona, P., de las Heras, J., Fernandes, P., Moreira, F., Papageorgiou, K., Vallejo, R. and Xanthopoulos, G. (2010) 'Post-

fire forest management in southern Europe: A COST action for gathering and disseminating scientific knowledge.' *IForest*, 3(JANUARY) pp. 5–7.

Bartsch, I., Wiencke, C. and Laepple, T. (1973) *Mediterranean Type Ecosystems*. di Castri, F. and Mooney, H. A. (eds). Berlin, Heidelberg: Springer Berlin Heidelberg (Ecological Studies).

Batanouny, K. H., Hammouda, F. M., Ismail, S. I., Abdel-Azim, N. S. and Shams, K. A. . (2005) 'A Guide to Medicinal Plants in North Africa' pp. 153–155.

Ben-Mahmoud, K. (1995) *Soils of Libya: Genesis, classification, properties and agricultural potentiality.* Tripoli: National Academy of Scientific Research.

Ben-Mahmoud, K. (2001) *Soil resources in Libya: National Report*. Submitted to FAO Sub – Regional Office for the North Africa. (Workshop on SOTER Database. Rebat, Morocco.12-16 November).

Bennington, A. L. (2008) *Application of Multi-Spectral Remote Sensing for Crop Discrimination in Afghanistan*. Cranfield University.

Benyon, R. G. and Lane, P. N. J. (2013) 'Ground and satellite-based assessments of wet eucalypt forest survival and regeneration for predicting long-term hydrological responses to a large wildfire.' *Forest Ecology and Management*, 294 pp. 197–207.

Betts, R., Sanderson, M. and Woodward, S. (2008) 'Effects of large-scale Amazon forest degradation on climate and air quality through fluxes of carbon dioxide, water, energy, mineral dust and isoprene.' *Philosophical Transactions of the Royal Society B-Biological Sciences*, 363(1498) pp. 1873–1880.

Bhandari, S., Phinn, S. and Gill, T. (2012) 'Preparing Landsat Image Time Series (LITS) for monitoring changes in vegetation phenology in Queensland, Australia.' *Remote Sensing*, 4(6) pp. 1856–1886.

Biswal, S., Ghosh, A., Sharma, R. and Joshi, P. K. (2013) 'Satellite Data Classification Using Open Source Support.' *Journal of the Indian Society of Remote Sensing*, 41(3) pp. 523–530.

Boko, M., Niang, I., Nyong, A., Vogel, C., Githeko, A., Medany, M., Osman-Elasha, B., Tabo, R. and Yanda, P. (2007) 'Real interpolation and transposition of certain function spaces.' *In* Parry, M. L., Canziani, O. F., Palutikof, J. P., van der Linden, P. J., and Hanson, C. E. (eds) *Contribution of Working Group II to the Fourth Assessment Report of the Intergovernmental Panel on Climate Change*. Cambridge UK: Cambridge University Press, pp. 433–467.

Bosch, J. M. and Hewlett, J. D. (1982) 'A review of catachment experiments to determine the effect of vegetation changes on water yield and evapotranspiration.' *Journal of Hydrology* pp. 3–23.

BSC-L (2006) *Census of 2006*. *Bureau of statistics and census. Libyan government*. Tripoli.

BSC-L (2010) 'Vital Statistics.' Tripoli, Libya.: General Authority for Information and Documentation, The Libyan Government.

BSC-L (2016) *Assessment of statistical system, Libya*. *UNFPA*. Paris.

Camarillo-Naranjo, J. M., Álvarez-Francoso, J. I., Limones-Rodríguez, N., Pita-López, M. F. and Aguilar-Alba, M. (2018) 'The global climate monitor system: from climate data-handling to knowledge dissemination.' *International Journal of Digital Earth*, 8947, January, pp. 1–21.

Carmel, Y. and Kadmon, R. (1999) 'Effects of Grazing and Topography on Long-Term Vegetation Changes in a Mediterranean Ecosystem in Israel.' *Plant Ecology*, 145 pp. 243–254.

Ceccato, P., Pietsch, V. and Chen, Y.-J. (2016) *Google Earth Engine: MODIS Normalized Difference Vegetation Index (NDVI) Training*. *IRI*.

Chauhan, Y. and Vania, J. (2013) 'J48 Classifier Approach to Detect Characteristic of Bt Cotton base on Soil Micro Nutrient.' *IEEE Access*, 5(6) pp. 305–309.

Chen, W., Moriya, K., Sakai, T., Koyama, L. and Cao, C. (2014) 'Monitoring of post-fire forest recovery under different restoration modes based on time series

Landsat data.' *European Journal of Remote Sensing*, 47(1) pp. 153–168.

CHRS RainShere (2016) *CHRS RainSphere info*. [Online] [Accessed on 20th October 2016] http://rainsphere.eng.uci.edu/RainSphere.html#.

Cook, B. I., Anchukaitis, K. J., Touchan, R., Meko, D. M. and Cook, E. R. (2016) 'Spatiotemporal drought variability in the Mediterranean over the last 900 years.' *Journal of Geophysical Research Atmospheres* pp. 2060–2074.

Cornelis, W. M., Araya, T., Wildemeersch, J., Banda, M. K. M.-, Waweru, G., Obia, A. and Verbist, K. (2012) 'Building resilience against drought: the soil-water perspective.' *In* De Boeve, M., Khlosi, M., Delbecque, N., Pue, J. De, Ryken, N., Verdoodt, A., Cornelis, W. M., and Gabriels, D. (eds) *Desertification and land degradation: processes and mitigation*. Belgium: UNESCO Chair of Eremology, Ghent University, Belgium The, pp. 118–127.

Corner, R. J., Dewan, A. M. and Chakma, S. (2014) 'Monitoring and Prediction of Land-Use and Land-Cover (LULC) Change.' *In* Dewan, A. and Corner, R. (eds) *Dhaka Megacity: Geospatial Perspectives on Urbanisation, Environment and Health*. Dordrecht: Springer Netherlands, pp. 75–97.

Crosti, R., Ladd, P. G., Dixon, K. W. and Piotto, B. (2006) 'Post-fire germination: The effect of smoke on seeds of selected species from the central Mediterranean basin.' *Forest Ecology and Management*, 221(1–3) pp. 306–312.

Czeglédi, L. and Radácsi, A. (2005) 'Overutilization of Pastures by Livestock.' *Grassland Studies*, 3 pp. 29–35.

Derneği, D. (2010) *Ecosystem Profile: Mediterranean Basin Biodiversity Hotspot*. *The CEPF Donor Council*.

Desanker, P., Magadza, C., Allali, A., Basalirwa, C., Boko, M., Dieudonne, G., Gowning, T. E., Dube, P. O., Githeko, A., Githendu, M., Gonzalez, P., Gwary, D., Jallow, B., Nwafor, J. and Sholes, R. (2001) *Africa*. Desanker, P., Magadza, C., Allali, A., Basalirwa, C., Boko, M., Dieudonne, G., Gowning, T. E., Dube, P. O., Githeko, A., Githendu, M., Gonzalez, P., Gwary, D., Jallow, B., Nwafor, J., and Sholes, R. (eds) *Climate Change 2001: Impacts, Adaptation and*

Vulnerability. The press syndicate of the University of Cambridge.

Di-Gregorio, A. (2005) 'Land Cover Classification System(LCCS), version2: Classification Concepts and User Manual.' Environment and Natural Resources Service Series, No. 8, FAO, Rome p. 208.

Di-Pasquale, G., Di Martino, P. and Mazzoleni, S. (2005) 'Forest History in the Mediterranean Region.' *In Recent Dynamics of the Mediterranean Vegetation and Landscape*. Chichester, UK: John Wiley & Sons, Ltd, pp. 13–20.

Dimkić, M., Brauch, H.-J. and Kavanaugh, M. (2008) *Groundwater Management in Large River Basins*. 1est ed., London: IWA Publishing.

Eckert, S., Hüsler, F., Liniger, H. and Hodel, E. (2015) 'Trend analysis of MODIS NDVI time series for detecting land degradation and regeneration in Mongolia.' *Journal of Arid Environments*. Elsevier Ltd, 113 pp. 16–28.

Eddenjal, A. S. (2015) *Dust/Sand Storms over Libya: Their Spatial Distribution, Frequency and Seasonality*. *Series: Sand and Dust Storm Warning Advisory and Assessment System (SDS- WAS) Regional Center for Northern Africa-Middle East-Europe (NAMEE). Technical Reports*. Barcelona.

El-Barasi, Y. M. M., Barrani, M. W. and Al Tajoury, O. R. (2013) 'Land Deterioration of a Semi-desert Grazing Area in the North-Eastern Zone of Libya (Cyrenaica).' *Journal of Environmental Science and Engineering B 2*, 2 pp. 357–373.

El-Barasi, Y. M. M. and Saaed, M. W. B. (2013) 'Threats to Plant Diversity in the North Eastern Part of Libya (Al Jabal Al Akhdar and Marmarica Plateau).' *Journal of Environmental Science and Engineering A*, 2 pp. 41–58.

El-Darier, S. M. and El-Mogaspi, F. M. (2009) 'Ethnobotany and Relative Importance of Some Endemic Plant Species at El-Jabal El-Akhdar Region (Libya).' *World Jounal of Agricultural Sciences*, 5(3) pp. 353–360.

El-Tantawi, A. M. M. (2005) *Climate Change in Libya and Desertification of Jifara Plain: Using Geographical Information System and Remote Sensing*

Techniques. Johannes Gutenberg-University, Mainz, German.

ELD Initiative and UNEP (2015) *The Economics of Land Degradation in Africa: Benefits of Action Outweigh the Costs.*

Elmahdy, S. I. and Mohamed, M. M. (2016) 'Factors controlling the changes and spatial variability of Junipers phoenicea in Al Jabal Al Akhdar, Libya, using remote sensing and GIS.' *Arabian Journal of Geosciences*. Arabian Journal of Geosciences, 9(6) p. 478.

El Shatshat, S. A. (2015) 'Increasing anthropogenic impacts on restricted-range taxa of Libya from 2011 to 2015.' *Archive of Applied Science Research*, 7(5) pp. 91–96.

Elshatshat, S. and Mansour, A. (2014) 'Disturbance of flora and vegetation composition of Libya by human impacts : Costal Region of Al Jabal Al Akhdar area as model.' *Advances in Applied Science Research*, 5(5) pp. 286–292.van Engelen, V. W. P. and Dijkshoorn, J. a. (2013) *Global and National Soils and Terrain Digital Databases (SOTER). Procedures Manual, Version 2.0*. *ISRIC – World Soil Information*. Wageningen.

ENVI version 4.7 (2009) 'Atmospheric Correction Module : QUAC and FLAASH User ' s Guide.' ITT Visual Information Solutions p. 44.

Fajji, N. G., Palamuleni, L. G. and Mlambo, V. (2018) 'A GIS Scheme for Forage Assessment and Determination of Rangeland Carrying Capacity.' *Journal of Remote Sensing & GIS*, 7(1) pp. 1–11.

Fan, F. (2008) 'Digital Change Detection by Post-Classification Comparison of RS Data in Land Use of Guangzhou.' *Journal of Computational Information*, 42 pp. 1–6.

FAO (2010) *Developing effective forest policy: A guide*. *FAO Firestry Paper-161*. Rome, Italy: FAO.

FAO (2011a) *Land degradation assessment in drylands (LADA) project (Final Draft)*. *FAO*. Rome.

FAO (2011b) ‘NDVI as indicator of degradation.’ *Unasylva*, 62(2) pp. 39–46.

FAO (2011c) *State of Mediterranean Forests (SoFMF), concept paper.* (Arid Zone Forests and Forestry Working Paper No.2, Rome).

FAO (2013) *Land Degradation Assessment in Drylands. Mapping Land Use Systems at Global and Regional Scales for Land Degradation Assessment Analysis.*

FAO and Plan Bleu (2013) *State of Mediterranean Forests 2013*. Rome.

Faour, G., Mhawej, M. and Fayad, A. (2016) ‘Detecting Changes in Vegetation Trends in the Middle East and North Africa (MENA) Region Using SPOT Vegetation.’ *Cybergeo: European Journal of Geography*, 779(April).

Fernández-Lugo, S., Arévalo, J. R., de Nascimento, L., Mata, J. and Bermejo, L. A. (2013) ‘Long-term vegetation responses to different goat grazing regimes in semi-natural ecosystems: a case study in Tenerife (Canary Islands).’ Prober, S. (ed.) *Applied Vegetation Science*, 16(1) pp. 74–83.

Fichera, C. R., Modica, G. and Pollino, M. (2012) ‘Land Cover classification and change-detection analysis using multi-temporal remote sensed imagery and landscape metrics.’ *European Journal of Remote Sensing*, 45(1) pp. 1–18.

Foley, J. a, Defries, R., Asner, G. P., Barford, C., Bonan, G., Carpenter, S. R., Chapin, F. S., Coe, M. T., Daily, G. C., Gibbs, H. K., Helkowski, J. H., Holloway, T., Howard, E. a, Kucharik, C. J., Monfreda, C., Patz, J. a, Prentice, I. C., Ramankutty, N. and Snyder, P. K. (2005) ‘Global consequences of land use.’ *Science (New York, N.Y.)*, 309(5734) pp. 570–4.

Franklin, S. E. (2001) *Remote sensing for sustainable forest management*. CRC Press LLC.

Galdi, P. and Tagliaferri, R. (2019) ‘Data Mining: Accuracy and Error Measures for Classification and Prediction.’ *Encyclopedia of Bioinformatics and Computational Biology*, (January) pp. 431–436.

Gallego, F. J. (2005) *Mapping rural/urban areas from population density grids*.

Institute for Environment and Sustainability, JRC. Ispra, Italy.

Gandhi, N., Armstrong, L. J., Petkar, O. and Tripathy, A. K. (2016) 'Rice crop yield prediction in India using support vector machines.' *In 3th International Joint Conference on Computer Science and Software Engineering (JCSSE)*. IEEE, pp. 1–5.

Gashaw, T., Tulu, T., Argaw, M. and Worqlul, A. W. (2017) 'Evaluation and prediction of land use/land cover changes in the Andassa watershed , Blue Nile Basin , Ethiopia.' *Environmental Systems Research*. Springer Berlin Heidelberg.

Gawhari, A. M. H., Jury, S. L. and Culham, A. (2018) 'Towards an updated checklist of the Libyan flora.' *Phytotaxa*, 338(1) pp. 1–16.

GCMon (2016) *Global Climate Monitor info*. [Online] [Accessed on 10th November 2016] http://alojamientosv.us.es/climatemonitor/gcm-info/.

Gebril, A. O. and Saeid, A. G. (2012) 'Importance of Pastoral Human Factor Overloading in Land Desertification : Case Studies in Northeastern Libya.' *World Academy of science, Engineering and Technology*, 6(10) pp. 1087–1092.

GEE (2017) *MODIS Combined 16-Day NDVI*. Google Earth Engine. [Online] [Accessed on 5th August 2018]

https://code.earthengine.google.com/datasets/MODIS/MCD43A4_NDVI.

GEE (2018) *Google Earth Engine API : Google Developers*. [Online] [Accessed on 14th June 2018] https://developers.google.com/earth-engine/.

van Genderen, J. L. (2011) *Advances in Environmental Remote Sensing: Sensors, Algorithms, and Applications*. *International Journal of Digital Earth*.

Gorelick, N., Hancher, M., Dixon, M., Ilyushchenko, S., Thau, D. and Moore, R. (2017) 'Google Earth Engine: Planetary-scale geospatial analysis for everyone.' *Remote Sensing of Environment*. The Author(s), 202 pp. 18–27.

Govaerts, B. and Verhulst, N. (2010) *The normalized difference vegetation index (NDVI) Greenseeker (TM) handheld sensor: toward the integrated evaluation of crop management. Part A-Concepts and case studies*. Mexico.

Hadi, S. J. and Tombul, M. (2017) ‘Conversion of CruTS 3.23 data and evaluation of precipitation and temperature variables in a local scale.’ *In MATEC Web of Conferences 120, 05007*.

Hadjimitsis, D. G., Papadavid, G., Agapiou, A., Themistocleous, K., Hadjimitsis, M. G. and Retalis, A. (2010) ‘Atmospheric correction for satellite remotely sensed data intended for agricultural applications : impact on vegetation indices.’ *Nat. Hazards Earth Syst. Sci.,* 10 pp. 89–95.

Hall, M. A. (1999) *Correlation-based Feature Selection for Machine Learning*. The University of Waikato. Hamilton, New Zealand.

Hall, M. A. and Smith, L. A. (1998) ‘Practical Feature Subset Selection for Machine.’ *In* C. McDonald (Ed.) (ed.) *Computer Science ’98 Proceedings of the 21st Australasian Computer Science Conference ACSC’98, Perth, 4-6 February, 1998*. Berlin: Springer, pp. 181–191.

Hamad, S. M. (2012) ‘Status of Groundwater Resource of Al Jabal Al Akhdar Region, North East Libya.’ *International journal of environment and water*, (1) pp. 68–78.

Han, C. (2008) ‘Overgrazing Behavior and Rationality: A Dynamic Perspective.’ *In Proceedings of the 2008 International Conference of the System Dynamics Society*.

Hao, P., Wang, L., Niu, Z., Aablikim, A., Huang, N., Xu, S. and Chen, F. (2014) ‘The Potential of Time Series Merged from Landsat-5 TM and HJ-1 CCD for Crop Classification: A Case Study for Bole and Manas Counties in Xinjiang, China.’ *Remote Sensing*, 6(8) pp. 7610–7631.

Haque, M. I. and Basak, R. (2017) ‘Land cover change detection using GIS and remote sensing techniques: A spatio-temporal study on Tanguar Haor, Sunamganj, Bangladesh.’ *The Egyptian Journal of Remote Sensing and Space Science*. National Authority for Remote Sensing and Space Sciences, 20(2) pp. 251–263.

HARRIS Geospatial Solution (2017a) *Classification*. [Online] [Accessed on 15th

January 2018]

https://www.harrisgeospatial.com/docs/Classification.html#ClassSupervised.

HARRIS Geospatial Solution (2017b) *Thematic Change*. [Online] [Accessed on 11th September 2017]

https://www.harrisgeospatial.com/docs/ThematicChange.html.

Hassan, Z., Shabbir, R., Ahmad, S. S., Malik, A. H., Aziz, N., Butt, A. and Erum, S. (2016) 'Dynamics of land use and land cover change (LULCC) using geospatial techniques: a case study of Islamabad Pakistan.' *SpringerPlus*. Springer International Publishing, 5(1).

Hegazy, A. K., Boulos, L., Kabiel, H. F. and Sharashy, O. S. (2011) 'Vegetation and Species Altitudinal Distribution in Al Jabal Al Akhdar Landscape, Libya.' *PAK.J.BOT.*, 43(4) pp. 1885–1898.

Herrmann, S. M., Anyamba, A. and Tucker, C. J. (2005) 'Recent trends in vegetation dynamics in the African Sahel and their relationship to climate.' *Global Environmental Change*, 15 pp. 394–404.

Hobohm, C. (2014) *Endemism in Vascular Plants*. Hobohm, C. (ed.). Dordrecht: Springer Netherlands (Plant and Vegetation).

Huang, X., Weng, C., Lu, Q., Feng, T. and Zhang, L. (2015) 'Automatic labelling and selection of training samples for high-resolution remote sensing image classification over urban areas.' *Remote Sensing*, 7(12) pp. 16024–16044.

Ibrahim, A. A. (2008) 'Using Remote Sensing Technique (NDVI) for Monitoring Vegetation Degradation in semi-arid lands and its relationship to precipitation: Case study from Libya.' *In The 3rd International Conference on Water Resources and Arid Environments (2008) and the 1st Arab Water Forum*.

Ibrahim, A. A. and Assayah, A. M. (2014) 'Using Remote Sensing Technique (NDVI) for Monitoring Vegetation Degradation in Al Jabal Al Akhdar - Libya.' *In The 8th edition of the international scientific Congress of GIS and geospace applications Geotunis 2014*, pp. 1–14.

Ioras, F., Bandara, I. and Kemp, C. (2014) ‘Introduction to climate change and land degradation.’ *In* Arraiza Bermúdez-Cañete, M. P., Santamarta Cerezal, J. C., Ioras, F., García Rodríguez, J. L., Abrudan, I. V., Korjus, H., and Gálos, B. (eds). Madrid: Colegio de Ingenieros de Montes, pp. 15–52.

Ismail, M. H. and Jusoff, K. (2008) ‘Satellite Data Classification Accuracy Assessment Based from Reference Dataset.’ *World Academy of Science, Engineering and Technology*, 15 pp. 527–533.

Jagtap, S. B. and Kodge, B. G. (2013) ‘Census Data Mining and Data Analysis using WEKA.’ *In International Conference in “Emerging Trends in Science, Technology and Management-2013*. Singapore, pp. 35–40.

James, G., Witten, D., Hastie, T. and Tibshirani, R. (2013) *An Introduction to Statistical Learning*. New York, NY: Springer New York (Springer Texts in Statistics).

Jiang, M., Tian, S., Zheng, Z., Zhan, Q. and He, Y. (2017) ‘Human activity influences on vegetation cover changes in Beijing, China, from 2000 to 2015.’ *Remote Sensing*, 9(3) pp. 1–19.

Johnson, D. L. and Lewis, L. A. (2007) *Land Degradation: Creation and Destruction*. 2ed ed., Rowman & Littlefield publisher ,Inc.

Kairis, O., Karavitis, C., Salvati, L., Kounalaki, A. and Kosmas, K. (2015) ‘Exploring the Impact of Overgrazing on Soil Erosion and Land Degradation in a Dry Mediterranean Agro-Forest Landscape (Crete, Greece).’ *Arid Land Research and Management*. UASR, 29(3) pp. 360–374.

Kassas, M. (1995) ‘Desertification: a general review.’ *Journal of Arid Environments*, 30(2) pp. 115–128.

Keblouti, M., Ouerdachi, L. and Boutaghane, H. (2012) ‘Spatial Interpolation of Annual Precipitation in Annaba- Algeria - Comparison and Evaluation of Methods.’ *Energy Procedia*, 18 pp. 468–475.

Keeley, J. E., Bond, W. J., Bradstock, R. A., Pausas, J. G. and Rundel, P. W.

(2012) *Fire in Mediterranean Ecosystems. Ecology, evolution and management*.

Knapp, R. (1974) *Vegetation Dynamics*. Knapp, R. (ed.) *Vegetation Dynamic*. Dordrecht: Springer Netherlands.

Kohavi, R. (1995) 'Cross validation number.pdf.' *In International Joint Conference on Artificial Intelligence, Montreal, QC, Canada, 20–25 August*.

Kuchler, A. W. (1988) 'Mapping dynamic vegetation.' *In* Kuchler, A. W. and Zonneveld, I. S. (eds) *Handbook of vegtation science: Vegetation mapping*. Cambridge: Kluwer academic publishers, pp. 321–330.

LGAI (2007) *Atlas of the final results of the agricultural census*. *The Libyan General Information Authority. The Libyan Government*. Tripoli, Libya (in Arabic).

Li, F., Zhang, S., Bu, K., Yang, J., Wang, Q. and Chang, L. (2015) 'The relationships between land use change and demographic dynamics in western Jilin province.' *Journal of Geographical Sciences*, 25(5) pp. 617–636.

Li, G., Lu, D., Moran, E. and Sant'Anna, S. J. S. (2012) 'Comparative analysis of classification algorithms and multiple sensor data for land use / land cover classification in the Brazilian Amazon.' *Journal of Applied Remote Sensing*, 6 pp. 061706-1–11.

Libyan Environment General Authority (2008) *National Biosafety Framework of Libyan Jamahiriya*.

Lillesand, T. M., Kiefer, R. W. and Chipman, J. W. (1989) *Remote Sensing and Image Interpretation*. *Journal of Chemical Information and Modeling*. 5th ed.

Liping, C., Yujun, S. and Saeed, S. (2018) 'Monitoring and predicting land use and land cover changes using remote sensing and GIS techniques — A case study of a hilly area ,.' *PloS one* pp. 1–23.

Liu, H., Zheng, L. and Yin, S. (2018) 'Multi-perspective analysis of vegetation cover changes and driving factors of long time series based on climate and terrain data in Hanjiang River Basin, China.' *Arabian Journal of Geosciences*.

Arabian Journal of Geosciences, 11(17).

Louhaichi, M., Salkini, A. K., Estita, H. E. and Belkhir, S. (2011) 'Initial assessment of medicinal plants across the Libyan Mediterranean coast.' *Advances in Environmental Biology*, 5(2) pp. 359–370.

Lu, D., Mausel, P., Brondízio, E. and Moran, E. (2004) 'Change detection techniques.' *International Journal of Remote Sensing*, 25(12) pp. 2365–2407.

Lu, D. and Weng, Q. (2007) 'A survey of image classification methods and techniques for improving classification performance.' *International Journal of Remote Sensing*, 28(5) pp. 823–870.

LUPA (2008) *Third generation planning project, Benghazi Region (Al Marj, Al Jabal Al Akhdar and Derna sub-regions): Master Report*. Libyan Urban Planning Agency.

LWGA and ACSAD (2005) *Libyan soils and terrain digital database (SOTER)*. *Libyan Water General Authority and The Arab Centre for the Studies of Arid Zones (In Arabic)*. Tripoli, Libya.

Mahmoodzadeh, H. (2007) 'Digital change detection using remotely sensed data for monitoring green space destruction in Tabriz.' *International Journal of Environmental Research*, 1(1) pp. 35–41.

Malkisnon, D., Wittenberg, L., Beeri, O. and Barzilai, R. (2011) 'Effects of Repeated Fires on the Structure, Composition, and Dynamics of Mediterranean Maquis: Short- and Long-Term Perspectives.' *Ecosystems*, 14(3) pp. 478–488.

Masoudi, M. (2014) 'Risk Assessment of Vegetation Degradation Using GIS.' *J.Agr.Sci.Tech.*, 16 pp. 1711–1722.

Masoudi, M. and Amiri, E. (2013) 'Hazard assessment of currrent stat of vegetation degradation using GIS, a case study.' *Journal of Ecology and Environment*, 36(1) pp. 49–56.

Matthews, E. (1983) 'Global Vegetation and Land Use: New High-Resolution Data Bases for Climate Studies.' *Journal of Climate and Applied Meteorology*,

22(3) pp. 474–487.

Mausel, P. W., Kramber, W. J. and Lee, J. K. (1990) ‘Optimum band selection for supervised classification of multispectral data.’ *Photogrammetric Engineering and Remote Sensing*, 56(1) pp. 55–60.

Maxwell, A. E., Warner, T. A. and Fang, F. (2018) ‘Implementation of machine-learning classification in remote sensing: An applied review.’ *International Journal of Remote Sensing*. Taylor & Francis, 39(9) pp. 2784–2817.

McGregor, H. V., Dupont, L., Stuut, J.-B. W. and Kuhlmann, H. (2009) ‘Vegetation change, goats, and religion: a 2000-year history of land use in southern Morocco.’ *Quaternary Science Reviews*. Elsevier Ltd, 28(15–16) pp. 1434–1448.

Megahed, Y., Cabral, P., Silva, J. and Caetano, M. (2015) ‘Land Cover Mapping Analysis and Urban Growth Modelling Using Remote Sensing Techniques in Greater Cairo Region—Egypt.’ *ISPRS International Journal of Geo-Information*, 4(3) pp. 1750–1769.

Meyer, W. B. and Turner II, B. L. (1992) ‘Human population growth and global land use/land cover change.’ *Annual Review of Ecology and Systematics*, (23) pp. 39–61.

Mhawish, Y. M. and Saba, M. (2016) ‘Impact of Population Growth on Land Use Changes in Wadi Ziqlab of Jordan between 1952 and 2008.’ *International Journal of Applied Sociology*, 6(1) pp. 7–14.

Milas, A. Š., Rupasinghe, P. and Balenović, I. (2015) ‘Assessment of Forest Damage in Croatia using Landsat-8 OLI Images.’ *South-east European forestry*, 6(2) pp. 159–169.

Mishra, A. K. and Singh, V. P. (2010) ‘A review of drought concepts.’ *Journal of Hydrology*. Elsevier B.V., 391(1–2) pp. 202–216.

Mohajane, M., Essahlaoui, A., Oudija, F., El Hafyani, M., Hmaidi, A. El, El Ouali, A., Randazzo, G. and Teodoro, A. C. (2018) ‘Land Use/Land Cover (LULC)

Using Landsat Data Series (MSS, TM, ETM+ and OLI) in Azrou Forest, in the Central Middle Atlas of Morocco.' *Environments*, 5(12) p. 131.

Mohamed, W. N. H. W., Salleh, M. N. M. and Omar, A. H. (2012) 'A comparative study of Reduced Error Pruning method in decision tree algorithms.' *In IEEE International Conference on Control System, Computing and Engineering, ICCSCE , Penang - Malaysia 23-25 Nov.2012*, pp. 392–397.

Mulder, V. L., de Bruin, S., Schaepman, M. E. and Mayr, T. R. (2011) 'The use of remote sensing in soil and terrain mapping — A review.' *Geoderma*. Elsevier B.V., 162(1–2) pp. 1–19.

Mundia, C. N. and Aniya, M. (2005) 'Analysis of land use/cover changes and urban expansion of Nairobi city using remote sensing and GIS.' *International Journal of Remote Sensing*, 26(13) pp. 2831–2849.

Murakami, T., Ogawa, S., Ishitsuka, N., Kumagai, K., Saito, G., Ogawa, S., Ishitsuka, N., Kumagai, K. and Crop, G. S. (2001) 'Crop discrimination with multitemporal SPOT / HRV data in the Saga Plains , Japan.' *International Journal of Remote Sensing*, 22(7) pp. 1335–1348.

Niang, I., Ruppel, O. ., Abdrabo, M. A., Essel, A., Lennard, C., Padgham, J. and Urquhart, P. (2014) 'Africa.' *In* Barros, V. R., Field, C. B., Dokken, D. J., Mastrandrea, M. D., Mach, K. J., Bilir, T. E., Chatterjee, M., Ebi, K. L., Estrada, Y. O., Genova, R. C., Girma, B., Kissel, E. S., Levy, A. N., MacCracken, S., Mastrandrea, P. R., and White, L. L. (eds) *Climate Change 2014: Impacts, Adaptation, and Vulnerability. Part B: Regional Aspects. Contribution of Working Group II to the Fifth Assessment Report of the Intergovernmental Panel on Climate Change*. Cambridge University Press, pp. 1199–1265.

NIC (2009) *North Africa: The Impact of Climate Change to 2030 (selected Countries)*. *National Intelligence Council*.

Niel, T. G. Van, Mcvicar, T. R. and Datt, B. (2005) 'On the relationship between training sample size and data dimensionality : Monte Carlo analysis of broadband multi-temporal classification.' *Remote Sensing of Environment*, 98

pp. 468–480.

Noss, R. F., Franklin, J. F., Baker, W. L., Schoennagel, T. and Moyle, P. B. (2006) ‘Managing fire-prone forests in the western United States.’ *Frontiers in Ecology and the Environment*, 4(9) pp. 481–487.

Nwer, B. (2013) ‘Soil Resources of Libya.’ *In* Yigini, Y., Panagos, P., and Montanarella, L. (eds) *Soil Resources of Mediterranean and Caucasus Countries*. Office for Official Publications of the European Communities, Luxembourg, pp. 174–188.

OMU (2005) *Studying and evaluating the natural vegetation in Al Jabal Al Akhdar area*. *Omer Al-Mukhtar University*. Al Bieda, Libya. (In Arabic).

Pausas, J. G. (1999) ‘Mediterranean vegetation dynamics: modelling problems and functional types.’ *Plant Ecology*, 140(1) pp. 27–39.

Penny, G., Daniels, K. E. and Thompson, S. E. (2013) ‘Local properties of patterned vegetation: quantifying endogenous and exogenous effects.’ *Philosophical Transactions of the Royal Society A*, 371(1984) pp. 1–27.

Pignatti, S. (1978) ‘Evolutionary trends in Mediterranean flora and vegetation.’ *Vegetatio*, 37(3) pp. 175–185.

Pourabdollah, A., Leibovici, D. G., Simms, D. M., Tempel, P., Hallett, S. H. and Jackson, M. J. (2012) ‘Towards a standard for soil and terrain data exchange: SoTerML.’ *Computers & Geosciences*, 45, August, pp. 270–283.

Price, R. (2017) *Climate change and stability in North Africa*. *The K4D helpdesk*.

Quinlan, J. R. (1993) *C4.5: Programs For Machine Learning*. *Machine Learning*. San Mateo, California: Morgan Kaufmann Publishers.

Radford, E., Catullo, G. and de Montmollin, B. (2011) *Important Plant Areas of the South and East Mediterranean Region: Priority Sites for Conservation*. *IUCN, Plant Life, WWF*. IUCN, Gland, Switzerland and Málaga, Spain.

Richards, J. A. (2013) *Remote Sensing Digital Image Analysis: An Introduction*.

5th ed, Springer Berlin Heidelberg.

Rowntree, K., Duma, M., Kakembo, V. and Thornes, J. (2004) 'Debunking the Myth of Overgrazing and Soil Erosion.' *Land Degradation & Development*, 15 pp. 203–214.

Saad, A. M. A., Shariff, N. M. and Gairola, S. (2011) 'Nature and causes of land degradation and desertification in Libya: Need for sustainable land management.' *African Journal of Biotechnology*, 10(63) pp. 13680–13687.

Sah, A. K., Sah, B. P., Honji, K., Kubo, N., Senthil, S., Cover, L., Detection, C. and Infrared, N. (2012) 'Semi-Automated Cloud/Shadow Removal and Land Cover Change Detection Using Satellite Imagery.' *In International Archives of the Photogrammetry, Remote Sensing and Spatial Information Science*. Melbourne, Australia, Vol.XXXIX-Part B7, pp. 335–340.

Samardžić-Petrović, M., Dragićević, S., Kovačević, M. and Bajat, B. (2016) 'Modeling Urban Land Use Changes Using Support Vector Machines.' *Transactions in GIS*, 20(5) pp. 718–734.

Samardžić-Petrović, M., Kovačević, M., Bajat, B. and Dragićević, S. (2017) 'Machine Learning Techniques for Modelling Short Term Land-Use Change.' *ISPRS International Journal of Geo-Information*, 6(12) p. 387.

Sathyaraj, R. and Prabu, S. (2015) 'An Approach for Software Fault Prediction to Measure the Quality of Different Prediction Methodologies using Software Metrics.' *Indian Journal of Science and Technology*, 8(35).

Schmid, J. (2017) *Using Google Earth Engine for Landsat NDVI status of forest stands Using Google Earth Engine for Landsat NDVI time series analysis to indicate the present status of forest stands*. Georg-August Universitat.

Schowengerdt, R. A. (2007) *Remote Sensing: Models and Methods for Image Processing*. Third Edit, Academic Press is an imprint of Elsevier.

SELKHOZPROMEXPORT (1980) *Soil Studies in the Eastern Zone of The Socialist People*. *Agricultural Reclamation and Land Development, SPLAJ*.

Tripoli, Libya.

Shaw, G. A. and Burke, H. K. (2003) ‘Spectral imaging for remote sensing.’ *LINCOLN LABORATORY JOURNAL*, 14(1) pp. 3–28.

Shen, Y., Wang, Y., Lv, H. and Qian, J. (2015) ‘Removal of thin clouds in Landsat-8 OLI data with independent component analysis.’ *Remote Sensing*, 7(9) pp. 11481–11500.

Showqi, I., Rashid, I. and Romshoo, S. A. (2014) ‘Land use land cover dynamics as a function of changing demography and hydrology.’ *GeoJournal*, 79(3) pp. 297–307.

da Silva, E. C., Carmo, R. S., Gomes, L. E. de O. and Barros, F. (2017) ‘Should we still talk about balance of nature in ecology ? Contributions of marine ecology and bioinvasion.’ *Filosofia e História da Biologia*, 12(1) pp. 39–63.

Singh, A. (1989) ‘Review Article: Digital change detection techniques using remotely-sensed data.’ *International Journal of Remote Sensing*, 10(6) pp. 989–1003.

Sivakumar, M. V. K. (2007) ‘Interactions between climate and desertification.’ *Agricultural and Forest Meteorology*, 142(2–4) pp. 143–155.

Story, M. and Congalton, R. (1986) ‘Accuracy Assessment: A User’s Perspective.’ *Photogrammetric Engineering and Remote Sensing*, 52(3) pp. 397–399.

Stroosnijder, L. (2003) ‘Technologies for improving green water use efficiency in West Africa.’ *In Water conservation technologies for sustainable dryland agriculture in Sub-Saharan Africa, symposium and workshop, Bloemfontein, South Africa.*

Stroosnijder, L. (2007) *Rainfall and land degradation*. *Environmental Science and Engineering (Subseries: Environmental Science)*.

Suleiman, B. M., Elmehdy, S. I., Mohamed, M., Hamad, S., Alhendaw, R., Sciences, E. and Baydah, A. (2014) ‘Infrared Spectral Measurements in

Remotes Sensing and GIS to asses factors controlling Flora diseases in Al Jabal Al Akhdar , Libya.' *In* Breton, J. G. C., Quartieri, J., Guida, M., Guida, D., and Guarnaccia, C. (eds) *Latest Trends in Energy, Environment and Development*. Salerno, Italy: WSEAS Press, pp. 385–392.

Suleiman, B. M., Mohamed, M., Hamad, S. and Elmehdy, S. (2016) 'Assessment of Forest and Juniperus Phoenicea Decline in Al Jabal Al Akhdar Using NDVI-Remote Sensing and GIS Data (2006-2013).' *International Journal of Remote Sensing Applications*, 6(0) p. 159.

Sundseth, K. (2009) *Natura 2000 in the Mediterranean Region*. *European Commission Environment Directorate General*. Belgium.

Teferi, E., Bewket, W., Uhlenbrook, S. and Wenninger, J. (2013) 'Understanding recent land use and land cover dynamics in the source region of the Upper Blue Nile, Ethiopia: Spatially explicit statistical modelling of systematic transitions.' *Agriculture, Ecosystems and Environment*. Elsevier B.V., 165 pp. 98–117.

Terink, W., Immerzeel, W. W. and Droogers, P. (2013) 'Climate change projections of precipitation and reference evapotranspiration for the Middle East and Northern Africa until 2050.' *International Journal of Climatology*, 33(14) pp. 3055–3072.

UNCCD (1994) 'Elaboration of an international convention to combat desertification in countries experiencing serious drought and/or desertification, particularly in Africa' pp. 1–58.

UNEP, ISSS, ISRIC and FAO (1995) *Global and national soils and terrain digital databases (SOTER): procedures manual*. *World Soil Resources Reports, 74 Rev.1*. FAO.

USDA (2015) 'Glossary of Soil Survey Terms.' *In National Soil Survey Handbook*. United State Department of Agriculture, p. 45.

USGS (2017) *Landsat Processing Details*. United States Geological Survey (USGS). [Online] [Accessed on 1st May 2017] http://landsat.usgs.gov/Landsat Processing Details.php.

Uttara, S., Bhuvandas, N. and Aggarwal, V. (2012) ‘Impacts of urbanisation on streams.’ *International Journal of Research in Engineering & Applied Sciences (IJRES)*, 2(2) pp. 1637–1645.

Vargas, P. (2003) ‘Molecular evidence for multiple diversification patterns of alpine plants in Mediterranean Europe.’ *Taxon*, 52(3) pp. 463–476.

Vicente-Serrano, S. M., Zouber, A., Lasanta, T. and Pueyo, Y. (2012) ‘Dryness is accelerating degradation of vulnerable shrublands in semiarid mediterranean environments.’ *Ecological Monographs*, 82(4) pp. 407–428.

Vitousek, P. M., Mooney, H. A., Lubchenco, J. and Melillo, J. M. (1997) ‘Human Domination of Earth’s Ecosystems.’ *Science*, 277(5325) pp. 494–499.

Vitti, A. and Bezzi, M. (2004) ‘A GRASS-DataMining integrated procedure for land cover classification.’ *In Geomatics Workbooks Vol. 4 - 5th Italian GRASS users meeting proceedings, 5-6 February*. Padova, Italy, p. 13.

Vogiatzakis, I. N., Mannion, a M. and Griffiths, G. H. (2006) ‘Mediterranean ecosystems: problems and tools for conservation.’ *Progress in Physical Geography*, 30(2) pp. 175–200.

Wang, A., Price, D. T. and Arora, V. (2006) ‘Estimating changes in global vegetation cover (1850-2100) for use in climate models.’ *Global Biogeochemical Cycles*, 20, GB3028, September.

Wang, J., Price, K. P. and Rich, P. M. (2001) ‘Spatial patterns of NDVI in response to precipitation and temperature in the central Great Plains.’ *International Journal of Remote Sensing*, 22(18) pp. 3827–3844.

Wang, Q. (2014) ‘Impact of Overgrazing on Semiarid Ecosystem Soil Properties: A Case Study of the Eastern Hovsgol Lake Area, Mongolia.’ *Journal of Ecosystem & Ecography*, 04(01) pp. 1–7.

Weka (2019) *Weka 3 - Data Mining with Open Source Machine Learning Software in Java*. [Online] [Accessed on 25th January 2019] https://www.cs.waikato.ac.nz/~ml/weka/.

Wingate, V., Phinn, S., Kuhn, N., Bloemertz, L. and Dhanjal-Adams, K. (2016) ‘Mapping Decadal Land Cover Changes in the Woodlands of North Eastern Namibia from 1975 to 2014 Using the Landsat Satellite Archived Data.’ *Remote Sensing*, 8(8) p. 681.

WMO (2005) *Climate and Land Degradation*. *World Meteorlogical Organization*.

Wu, X., Kumar, V., Quinlan, J. R., Ghosh, J., Yang, Q., Motoda, H., Mclachlan, G. J., Ng, A., Liu, B., Yu, P. S., Michael, Z. Z., David, S. and Dan, J. H. (2008) ‘Top 10 algorithms in data mining.’ *Knowl Inf Syst*, 14 pp. 1–37.

Xiao, J., Bai, X., Zhou, D., Qian, Q., Zeng, C. and Chen, F. (2018) ‘Spatial-temporal Evolution of Vegetation Coverage and Analysis of it’s Future Trends in Wujiang River Basin.’ *IOP Conference Series: Earth and Environmental Science*, 108(4).

Xie, Y., Sha, Z. and Yu, M. (2008) ‘Remote sensing imagery in vegetation mapping: a review.’ *Journal of Plant Ecology*, 1(1) pp. 9–23.

Yang, X. and Lo, C. P. (2000) ‘Relative radiometric normalization performance for change detection from multi-date satellite images.’ *Photogrammetric Engineering and Remote Sensing*, 66(August) pp. 967–980.

Yengoh, G. T., Dent, D., Olsson, L., Tengberg, A. E. and Tucker, C. J. (2014) *The use of the Normalized Difference Vegetation Index (NDVI) to assess land degradation at multiple scales: a review of the current status, future trends, and practical considerations*. Lund, Sweden.

Yeom, J., Han, Y. and Kim, Y. (2013) ‘Separability Analysis and Classification of Rice Fields using KOMPSAT-2 High Resolution Satellite Imagery.’ *Classification, Rice field, Separability analysis, High resolution satellite image, KOMPSAT-2.*, 17(12).

Zahran, M. A. (2010) *Climate-Vegetation, Afro-Asian Mediterranean and Red Sea Coastal Lands*. Gilbert, F. (ed.). Dordrecht: Springer Netherlands (Plant and Vegetation).

Zaidi, S. M., Akbari, A., Abu Samah, A., Kong, N. and Gisen, J. (2017) 'Landsat-5 Time Series Analysis for Land Use/Land Cover Change Detection Using NDVI and Semi-Supervised Classification Techniques.' *Polish Journal of Environmental Studies*, 26(6) pp. 2833–2840.

Zatout, M. M. (2011) *The Roles of Exotic and Native Tree Species in Preventing Desertification and Enhancing Degraded Land Restoration in the North East of Libya*. The University of Bradford.

Zatout, M. M. M. (2014) 'Effect of negative human activities on plant diversity in the Jabal Akhdar pastures.' *International Journal of Bioassays*, 3(09) pp. 3324–3328.

Zatout, M. M. M. and Soliman, A. M. S. (2014) 'Impact of Overgrazing and Burning on Plant Diversity in the Ras Al-Hilal Region in the North East of Libya.' *International Journal of Advances in Agricultural & Environmental Engineering*, 1(1) pp. 135–138.

Zavala, L. M. and Celis, R. D. E. (2014) 'How Wildfires Affect Soil Properties. A Brief Review.' *Cuadernos de Investigación Geográfica*, 40(2) pp. 311–331.

Zeleňáková, M., Purcz, P. and Kuzevičová, Ž. (2014) 'Statistical and Geographical Analysis of Precipitation and Temperatures of Libya,' 22(72).

Zhao, F. F., Zhang, L. and Xu, Z. X. (2009) 'Effects of vegetation cover change on streamflow at a range of spatial scales.' *18th World IMACS/MODSIM Congress*, (July) pp. 3591–3597.

Zhao, P., Lu, D., Wang, G., Wu, C. and Huang, Y. (2016) 'Examining Spectral Reflectance Saturation in Landsat Imagery and Corresponding Solutions to Improve Forest Aboveground Biomass Estimation.' *Remote Sensing*, 8(6).

Zhou, Q., Wei, X., Zhou, X., Cai, M. and Xu, Y. (2019) 'Vegetation coverage change and its response to topography in a typical karst region: the Lianjiang River Basin in Southwest China.' *Environmental Earth Sciences*. Springer Berlin Heidelberg, 78(6) pp. 1–10.

Zhu, X. (Earth scientist) (2016) *GIS for environmental applications : a practical approach*. London: Routledge.

Zunni, S. A. (1977) *The Forests of Jabal el Akdar, Libya*. Colorado State University.

APPENDICES

Appendix A Historical Maps

A.1 storiacl Maps of the study area

Historical maps the coastal region of Al Jabal Al Akhdar shows the old cities that have established during Greek and Roman eras. Figure A.1.1 shows the landform of the north-east Libya and Figure A.1.2 is a northern Africa map during the Roman era shows the ancient cities.

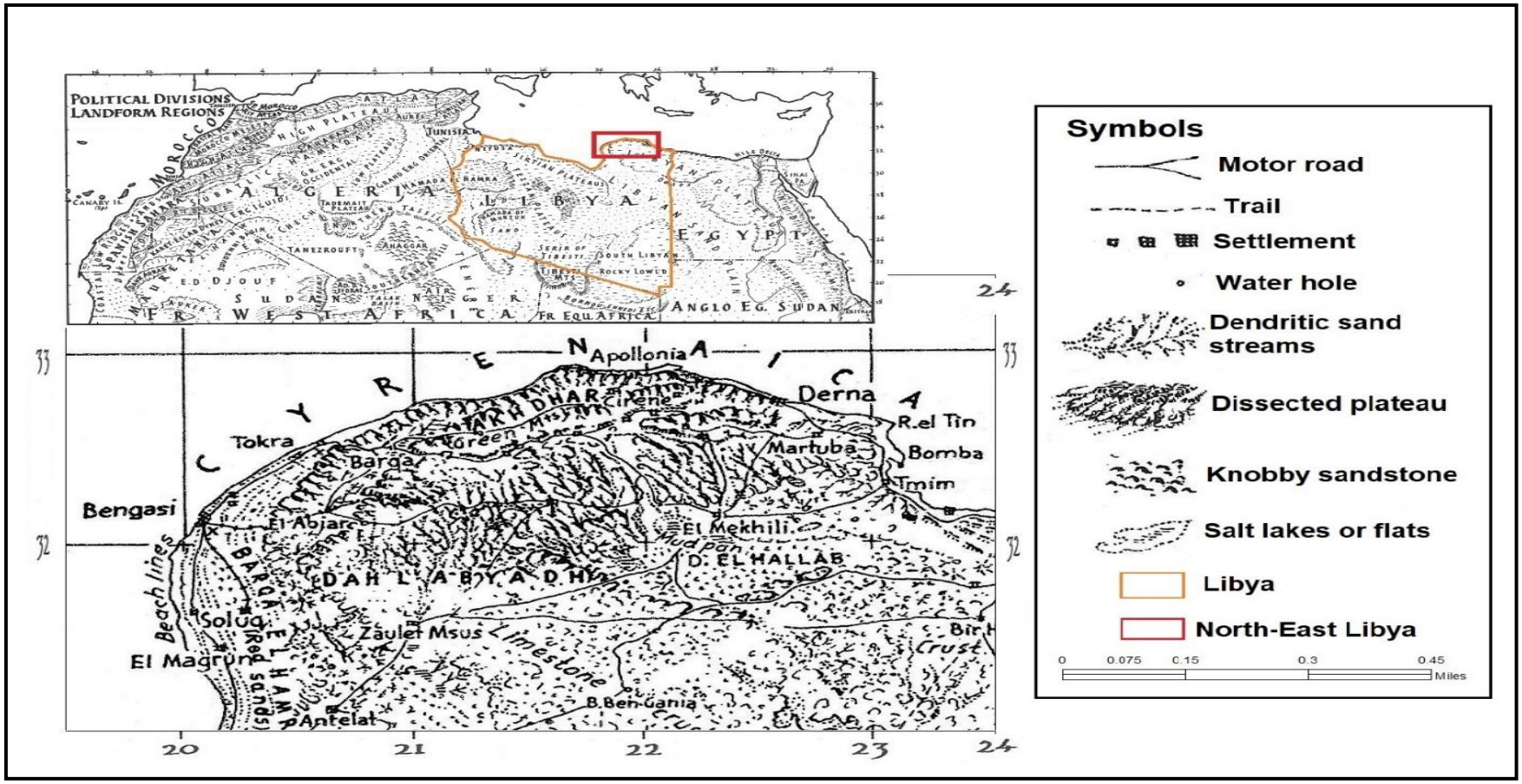

Figure A.1.1 Landform map of North- East Libya (source Landform map of North Africa by Raisz (1952))

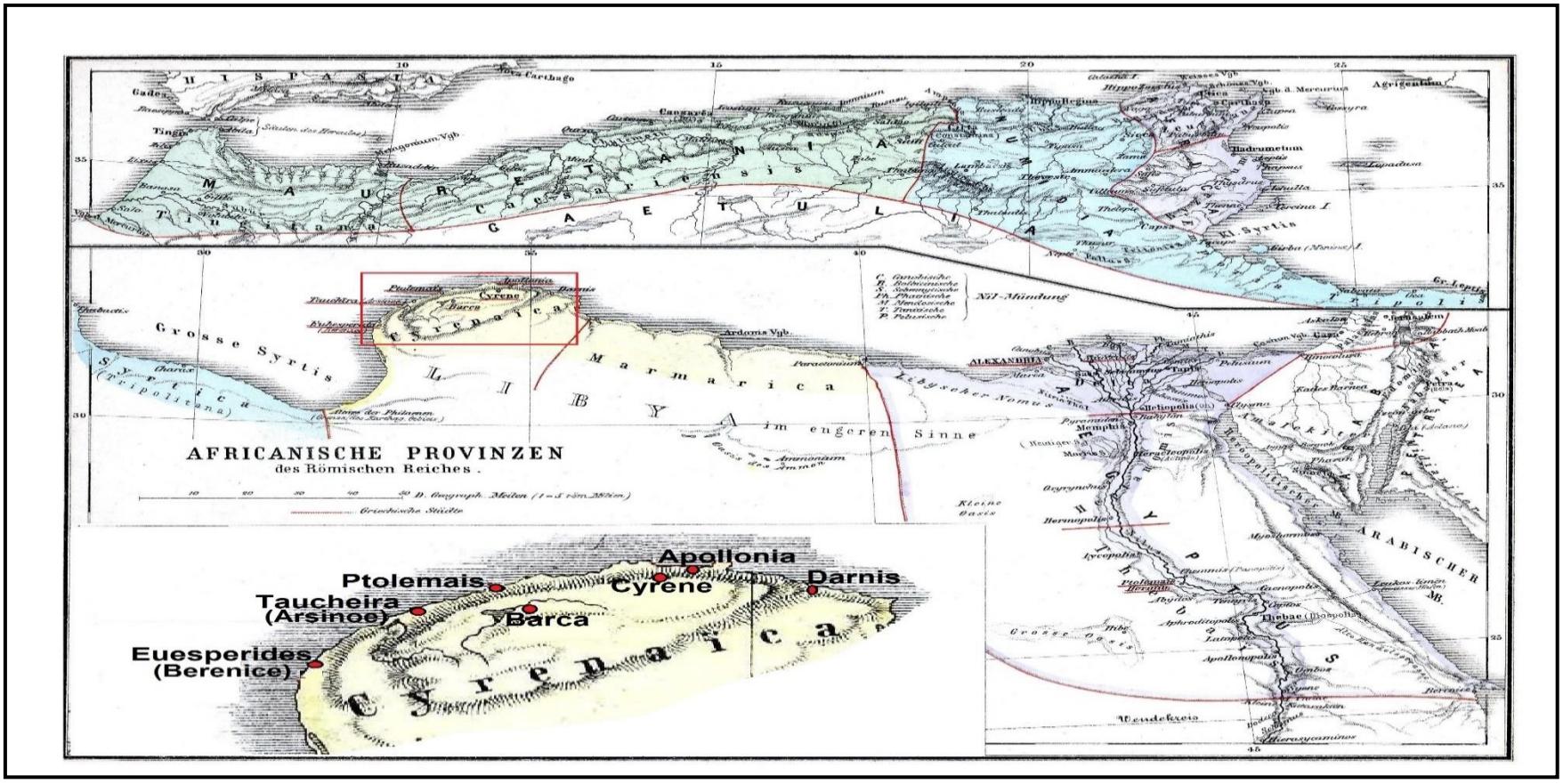

Figure A.1.2 Northern Africa under Roman rule map by Kiepert (1879)

The smaller map in th low lift shows a part of Cyrenaica 'Barqa' where Al Jabal Al Akhdar, the study area of this research, is located. The Small map also shows ancient cities: Euesperides (Berenice)= Benghazi, Taucheira (Arsinoe)= Tocra, Ptolemais= Tolmeitha, Barca= Al Marj, Cyrene= Shahhat, Apollonia= Susa and Darnis= Derna

Appendix B Omer Al-Mukhtar University Survey (2005)

The following Appendix presents the results of a biogeophysical survey undertaken by Omer Al-Mukhtar University (OMU) in 2005. This survey data has been used in this thesis as a source of primary data.

B.1 Sampling Sites

The sampling sites of the OMU (2005), the sites comprise six sites located within Rangelands (RL) and 43 sites within Natural Forest (NF) areas, and four sites in Planted Forest (PF) areas. Table B.1.1 shows the data associated with each sample site, its name, position, elevation (m.a.s.l.), area (ha) and the type of natural vegetation cover (NVT).

Table B.1.1 the sites location, position, area and natural vegetation cover type (source: OMU (2005))

ID	Site Name	Abbreviation	Longitude (DD)	Latitude (DD)	Terrace	Altitude (m)	Area (ha)	NVT
1	Karsa	Krs	22.41815	32.83752	1	90	12.69	NF
2	Alaslab	Aslb	22.14310	32.92413	1	63	325	NF
3	Wadi El Mahbool	WMah	22.09442	32.91598	1	30	87.12	NF
4	Wadi Bo annidi	WBA	21.77325	32.91755	1	34	588.32	NF
5	RasAmer	RMR	21.69875	32.92947	1	44	882.77	NF
6	Alhamama-RasAmer	HRMR	21.63917	32.91885	1	38	265.30	NF
7	Bo Traba	BTB	20.82748	32.63833	1	52	265.50	NF
8	Mirad Massoad (the Coast)	MMC	21.26328	32.75567	2	198	144.70	NF
9	Wadi El Mogawah	WMog	21.41622	32.62143	2	420	79.00	NF
10	Wadi Alakki	Waki	21.17308	32.51553	2	420	271.60	NF
11	Al Hejab	Hjb	21.51887	32.62848	2	430	325.00	NF
12	Sattia	Sati	21.92538	32.84093	2	403	356.00	NF
13	Arqoob Sidi Hamad	AqSH	22.35992	32.81017	2	420	245.00	NF
14	Sidi Khaled	SKh	22.44107	32.76147	2	385	319.00	NF
15	Wadi Margos	Wmarg	22.23662	32.86983	2	378	94.20	NF

ID	Site Name	Abbreviation	Longitude (DD)	Latitude (DD)	Terrace	Altitude (m)	Area (ha)	NVT
16	Ghot Maibara	GMb	21.66055	32.87532	2	226	277.70	NF
17	Qandafora	Qand	21.72690	32.89260	2	280	124.00	NF
18	Sidi Al Qarib	SQrib	21.17570	32.57058	2	355	189.60	NF
19	Mirad Massoad	MM	21.25225	32.73797	2	221	774.30	NF
20	Mirad Massoad (Roman's dams)	MMD	21.26985	32.68848	2	275	436.70	NF
21	Mirad Massoad (Terraces)	MMT	21.28415	32.57058	2	416	620.70	NF
22	Wadi Al-Sudan	Wsu	21.43002	32.68273	2	415	412.00	NF
23	Wadi Al Zawia	WZw	21.41007	32.65717	2	451	350.00	NF
24	Wadi El Kuf stream	WkufS	21.59900	32.69657	2	360	29.10	NF
25	Tolmitha - Sidi Erhoma	T-Roh	20.94065	32.65850	2	294	298.70	NF
26	Eqfanta	Eqf	21.56787	32.78345	2	282	80.30	NF
27	El Mansoura - El Dabadeb	Mans	21.80492	32.83315	2	336	174.00	NF
28	Al Wasita-Salion	Wast	21.65290	32.78923	2	360	60.20	NF
29	El Nador - El Mekhili	Nd-Mekh	22.29428	32.46425	2	414	1070.00	RL
30	Lamloda – Ras El Helal	Lam-Hel	22.16050	32.81010	3	684	100.60	NF
31	Kashaf Forest	Kash	21.11937	32.51450	3	465	65.60	PF

ID	Site Name	Abbreviation	Longitude (DD)	Latitude (DD)	Terrace	Altitude (m)	Area (ha)	NVT
32	El Daher El Hammer	DaHa	22.44205	32.68223	3	450	572.00	NF
33	Argoob Al Abiad	AqAb	22.16077	32.85328	3	540	79.50	NF
34	Marawah - Quasser Libya	Mar-QL	21.41210	32.58090	3	558	497.80	NF
35	Quasser Libya - El Bayada (Qud Khalil)	QL-Bd	21.29560	32.52713	3	465	619.70	NF
36	Al Ghriqa -Ras ATrab	Gh-Trb	21.81963	32.73053	3	669	148.00	NF
37	Wadi Al Mahja – Kholan	WMhj-Kh	22.09913	32.58078	3	620	383.20	RL
38	Azzrada	Zrda	22.12068	32.78863	3	680	4225.00	NF
39	Alquasser Alromani	Qrom	21.57038	32.61918	3	659	153.50	NF
40	Wadi El Kuf	WKuf	21.64607	32.69058	3	600	115.00	NF
41	Wadi El kuf (Cyperss Forest)	WkufCF	21.65477	32.67677	3	660	129.00	NF
42	Zawat Alqsoor-Jardas	ZQ-Jrd	20.91552	32.32938	3	550	271.00	NF
43	Madwer El Zaitoon (Plantation)	MadZF	21.27637	32.45023	3	520	456.00	PF
44	Marawah Forest	MarF	21.40350	32.48397	3	490	19.00	PF
45	Sidi El Homari Forest	SHF	21.80273	32.63977	3	830	107.76	PF
46	Shnaishnn Forest	ShnF	21.92915	32.60820	3	780	950.26	NF
47	El Hesha	Hesh	22.29635	32.60750	3	470	2907.50	RL

ID	Site Name	Abbreviation	Longitude (DD)	Latitude (DD)	Terrace	Altitude (m)	Area (ha)	NVT
48	Bo Draa	BoDr	22.14208	32.69650	3	660	62.75	RL
49	Jerdas Al Abeed	Jrd	20.93280	32.41270	3	464	70.40	NF
50	Bo Querawa	BoQrw	21.11282	32.53493	3	458	217.60	NF
51	Jerdas - Jabanet Sidi Saad	Jrd-JSS	21.01090	32.29595	3	600	1512.00	NF
52	Taknis - El Caroba	Tak-Crob	21.18225	32.40980	3	460	1980.00	RL
53	Madwer El Zaitoon	MadzR	21.24205	32.43812	3	440	1080.00	RL

B.2 Plant species of OMU (2005)

Presented here are the data for plant species based on the OMU survey. This appendix section is divided into two subsections. The first subsection shows the dominant perennial species for each site, while the second subsection lists the plant species that were recorded within each of the plots across the 53 sample sites.

B.2.1 Dominant perennial species of each OMU sampling sites

The dominant perennial species of each site was identified based on % relative coverage of the plant species within the plant community scale. Table B.2.1 shows the area (ha), natural vegetation cover type (NVT), dominant species of perennial plants (DPS), % bare soil (BS), % vegetation cover (VC) and % species coverage (SC) at the total area (TA) and plant community levels (PCL) in each site.

Table B.2.1 DPS of OMU (2005) sites, NVT, % BS, % VC and % SC

ID	Site Name	Area (ha)	Terrace	NVT	DPS	% BS	% VC	% SC	
								At TA	At PCL
1	Karsa	12.69	1	NF	*Juniperus phoenicea* L.	82.16	17.84	10.5	58.86
2	Alaslab	325	1	NF	*Juniperus phoenicea* L.	55.02	44.98	32.13	73.54
3	Wadi El Mahbool	87.12	1	NF	*Cupressus sempervirens* L.	21.904	78.096	43.27	63.45
4	Wadi Bo annidi	588.32	1	NF	*Pistacia lentiscus* L.	67.03	32.97	14.41	44.05
5	RasAmer	882.77	1	NF	*Juniperus phoenicea* L.	67.1	32.9	9.61	29.14
6	Alhamama-RasAmer	265.3	1	NF	*Juniperus phoenicea* L.	0	100	77.55	60.87
7	Bo Traba	265.5	1	NF	*Juniperus phoenicea* L.	73.38	26.62	13.1	49.21
8	Mirad Massoad (the Coast)	144.7	2	NF	*Juniperus phoenicea* L.	76.85	23.15	20.12	85.1
9	Wadi El Mogawah	79	2	NF	*Juniperus phoenicea* L.	59.8	40.2	30.98	77.06
10	Wadi Alakki	271.6	2	NF	*Juniperus phoenicea* L.	31.18	68.82	62.09	90.22

ID	Site Name	Area (ha)	Terrace	NVT	DPS	% BS	% VC	% SC	
								At TA	At PCL
11	Al Hejab	325	2	NF	*Juniperus phoenicea* L.	54.16	45.84	27.18	59.29
12	Sattia	356	2	NF	*Juniperus phoenicea* L.	65.4	34.6	21.89	63.26
13	Arqoob Sidi Hamad	245	2	NF	*Juniperus phoenicea* L.	70.61	29.39	13.89	47.26
14	Sidi Khaled	319	2	NF	*Juniperus phoenicea* L.	70.69	29.31	17.72	60.45
15	Wadi Margos	94.2	2	NF	*Juniperus phoenicea* L.	44.89	55.11	16.51	29.42
16	Ghot Maibara	277.7	2	NF	*Juniperus phoenicea* L.	80.18	19.82	11.77	59.38
17	Qandafora	124	2	NF	*Quercus coccifera* L.	72.55	27.45	7.51	27.35
18	Sidi Al Qarib	189.6	2	NF	*Juniperus phoenicea* L.	65.3	34.7	25.78	74.29
19	Mirad Massoad	774.3	2	NF	*Juniperus phoenicea* L.	69.63	30.37	21	69.14
20	Mirad Massoad (Roman’s dams)	436.7	2	NF	*Juniperus phoenicea* L.	74.5	25.5	15.87	62.23

ID	Site Name	Area (ha)	Terrace	NVT	DPS	% BS	% VC	% SC	
								At TA	At PCL
21	Mirad Massoad (Terraces)	620.7	2	NF	*Cistus* spp.	84.53	15.47	7.41	47.89
22	Wadi Al-Sudan	412	2	NF	*Juniperus phoenicea* L.	55.59	44.41	31.41	70.72
23	Wadi Al Zawia	350	2	NF	*Juniperus phoenicea* L.	51.79	48.21	21.33	43.91
24	Wadi El Kuf stream	29.1	2	NF	*Juniperus phoenicea* L.	47.51	52.49	32.53	62.55
25	Tolmitha - Sidi Erhoma	298.7	2	NF	*Juniperus phoenicea* L.	51.7	48.3	22.2	45.96
26	Eqfanta	80.3	2	NF	*Juniperus phoenicea* L.	13.31	86.69	69.28	79.92
27	El Mansoura - El Dabadeb	174	2	NF	*Juniperus phoenicea* L.	44.17	55.83	19.59	35.08
28	Al Wasita-Salion	60.2	2	NF	*Juniperus phoenicea* L.	39.95	60.05	46.37	77.21
29	El Nador - El Mekhili	1070	2	RL	*Hammada scoparia* (Pomel) Iljin	50.82	49.18	3.64	27.5
30	Lamloda – Ras El Helal	100.6	3	NF	*Arbutus pavarii* Pamp.	50.82	49.18	15.52	40.56

ID	Site Name	Area (ha)	Terrace	NVT	DPS	% BS	% VC	% SC	
								At TA	At PCL
31	Kashaf Forest	65.6	3	PF	*Pinus halepensis* Mill.	67.84	32.16	27.98	87
32	El Daher El Hammer	572	3	NF	*Juniperus phoenicea* L.	97.11	2.89	2.16	74.74
33	Argoob Al Abiad	79.5	3	NF	*Juniperus phoenicea* L.	50.34	49.66	16.01	31.6
34	Marawah - Quasser Libya	497.8	3	NF	*Juniperus phoenicea* L.	90.15	9.85	1.75	72.86
35	Quasser Libya - El Bayada (Qud Khalil)	619.7	3	NF	*Juniperus phoenicea* L.	57.88	42.12	36.68	87.08
36	Al Ghriqa -Ras ATrab	148	3	NF	*Arbutus pavarii* Pamp.	48.91	51.09	16.89	33.07
37	Wadi Al Mahja – Kholan	383.2	3	RL	*Hammada scoparia* (Pomel) Iljin	77.72	22.28	19.8	88.89
38	Azzrada	4225	3	NF	*Pistacia lentiscus* L.	49.51	50.49	12.55	24.72
39	Alquasser Alromani	153.5	3	NF	*Juniperus phoenicea* L.	56.94	43.06	27.47	63.79

ID	Site Name	Area (ha)	Terrace	NVT	DPS	% BS	% VC	% SC	
								At TA	At PCL
40	Wadi El Kuf	115	3	NF	*Pistacia lentiscus* L.	61.9	38.1	14.36	37.69
41	Wadi El kuf (Cyperss Forest)	129	3	NF	*Cupressus sempervirens* L.	35	65	42.65	65.61
42	Zawat Alqsoor-Jardas	271	3	NF	*Juniperus phoenicea* L.	90.187	9.81	9.56	97.45
43	Madwer El Zaitoon (Plantation)	456	3	PF	*Pinus halepensis* Mill.	/	/	/	/
44	Marawah Forest	19	3	PF	*Pinus halepensis* Mill.	/	/	/	/
45	Sidi El Homari Forest	107.76	3	PF	*Pinus halepensis* Mill.	/	/	/	/
46	Shnaishnn Forest	950.26	3	NF	*Juniperus phoenicea* L.	78.34	21.66	21.3	98.33
47	El Hesha	2907.5	3	RL	*Hammada scoparia* (Pomel) Iljin	79.55	20.45	8.23	40.24
48	Bo Draa	62.75	3	RL	*Viburnum tinus* L.	94.5	5.5	3.5	5.74

ID	Site Name	Area (ha)	Terrace	NVT	DPS	% BS	% VC	% SC	
								At TA	At PCL
49	Jerdas Al Abeed	70.4	3	NF	*Juniperus phoenicea* L.	/	/	/	/
50	Bo Querawa	217.6	3	NF	*Pistacia lentiscus* L.	75.05	24.95	10.74	43.01
51	Jerdas - Jabanet Sidi Saad	1512	3	NF	*Thymus capitatus* Hoff. et Link.	97.08	2.92	1.48	50.51
52	Taknis - El Caroba	1980	3	RL	*Thymus capitatus* Hoff. et Link.	87.88	12.12	3.93	31.89
53	Madwer El Zaitoon	1080	3	RL	*Stipa capensis* Thunb.	22.67	77.33	47.78	91.51

B.2.2 Plant species names and uses

Table B.2.2 shows the plant species that were included in the OMU study (2005). The table illustrates the botanical name of the species, common name, family, life span, Natural vegetation cover type (NVT) in which the species grows, as well as the uses (included use and indicator) of species as listed in Batanouny et al. (2005), OMU (2005), El-Darier and El-Mogasapi (2009) and Louhaichi et al. (2011). Natural vegetation cover is classified here as Natural Forest (NF), Planted Forest (PF) and Rangelands (RL).

Table B.2.2 Plant species, Family Common name, Life Span, VCT and uses of botanical survey plots (OMU, 2005)

Species	Family	Common Name	Life Span	NVT	Uses
Acacia cyanophylla Lindl.	Fabaceae	Blue-Leafed Wattle	Perennial	PF	WB / AFFP
Allium ursinum L.	Amaryllidaceae	/	Annual	NF	/
Anabasis articulata (Forssk.) Moq.	Chenopodiaceae	Jointed Anabasis	Perennial	RL	/
Arbutus pavarii Pamp.	Ericaceae	Libyan Strawberry-Tree	Perennial	NF	BP/MP/HF/IP (tanning)
Artemisia herba-alba Asso.	Asteraceae	Wormwood	Perennial	RL	AF/MP /FP/AP
Arum cyrenaicum Hruby	Araceae	Arum Lilies	Annual	NF	PS
Asparagus aphyllus L.	Asparagaceae	Prickly Asparagus	Perennial	NF	MP
Asphodelus microcarpus Salzm. & Viv.	Asparagaceae	Common Asphodel	Annual	NF / RL	DEIN / PS / NP
Atractylis cancellata L.	Asteraceae	Cardo Enrejado	Annual	NF / RL	AF (Camel)
Atriplex halimus L.	Chenopodiaceae	Saltbush	Perennial	RL	AF / HF / SF / HP / EC
Avena alba Vahl.	Poaceae (Gramineae)	Barbed Oat	Annual	NF / RL	AF
Avena spp.	Poaceae (Gramineae)	Common Wild Oat	Annual	NF / RL	AF
Brachypodium distachyum (L.) Beauv.	Poaceae	Purple or Spiky False-Brome	Annual	NF	/

Species	Family	Common Name	Life Span	NVT	Uses
Brumus rubens L.	Poaceae	Red Brome	Annual	NF	NP
Calicotome rigida (Viv.) Maire & Weiller	Fabaceae	Hairy Thorny Broom and Spiny Broom	Perennial	NF	DEIN / NP
Ceratonia siliqua L.	Fabaceae	Carob	Perennial	NF	AF / MP / FP / IP / SHP / BP / HF
Chamomilla aurea (Loefl.) Coss. & Kralik	Compositae	Golden Chamomile	Annual	NF	MP
Cistus spp.	Cistaceae	/	Perennial	NF	OP/ IP (essential oil)
Crepis vesicaria L.	Asteraceae	Hawk's-Beard.	Annual	NF / RL	AF
Cupressus sempervirens L.	Asteraceae	Mediterranean Cypress	Perennial	NF	MP/ WB/IP (oils) / Clmx
Cynara cornigera Lindl.	Asteraceae	/	Annual	NF	AF (Camel) / MP
Cynara cyrenaica (L.) Brett.	Asteraceae	/	Annual	NF / RL	MP/ BP /HF
Echinops polyceras Boiss	Asteraceae	/	Annual	NF / RL	AF
Erica multiflora L.	Ericaceae	/	Perennial	NF	/
Eryngium campestre L.	Apiaceae	Sea Holly	Perennial	NF	AF/MP
Eucalyptus camaldulensis Dehnh.	Myrtaceae	Red River Gum	Perennial	PF	AFFP / MP

Species	Family	Common Name	Life Span	NVT	Uses
Euphorbia dendroides L.	Euphorbiaceae	Tree Spurge	Perennial	NF	DEIN / PS / OP
Gaudinia fragilis (L.) Beauv	Poaceae (Gramineae)	Avena Fragilis L.	Annual	NF / RL	AF
Genista acanthoclada DC.	Papilionaceae	Genista	Perennial	NF	/
Globularia alypum L.	Globulariaceae	Zoreka	Perennial	NF	MP / NP / DEIN
Hammada scoparia (Pomel) Iljin	Chenopodiaceae	Haloxylon Articulatum (Cav.) Bunge	Perennial	NF / RL	FP
Haplophyllum tuberculatum (Forssk.) Juss	Rutaceae	Kheisa, Mesaika, Sazab, Zeita	Perennial herb	NF / RL	MP / IR / FP
Helichrysum stoechas (L.) Moench.	Compositae	Manzanilla Bastarda	Annual	NF / RL	MP
Hordeum spp.	Poaceae (Gramineae)	Barley	Annual	NF / RL	AF
Juniperus phoenicea L.	Cupressaceae	Phoenician Juniper	Perennial	NF	Clmx / MP / AP / IP (cosetic uses, essential oil)
Laguius ovatus (C.) L.	Poaceae (Gramineae)	Hare's Tail Grass	Annual	NF	AF
Limonsiatrum monopetalum (L.) Boiss	Plumbaginaceae	Limonsiatrum	Annual	NF	AF (camel) / FP / IS
Lygeum spartum Loefl. ex L.	Solanaceae	Lygeum	Perennial	NF	AF

Species	Family	Common Name	Life Span	NVT	Uses
Malva sylvestris L.	Malvaceae	/	Annual	NF	AF / MP
Marrubium vulgare L.	Lamiaceae	Horehound	Perennial	NF / RL	BP / MP / FAA / OP
Mesembryanthemum crystallinum L.	Aizoaceae	Crystalline Ice Plant	Perennial	NF / RL	NP
Myrtus communis L.	Myrtaceae	Common Myrtle	Perennial	NF	MP/OP/AP/FP
Olea europaea var. oleaster (Hoffmannsegg & Link) Negodi	Oleaceae	Wild Olive	Perennial	NF	MP/GS/IP
Onopordon espinae Coss.	Asteraceae	Cotton Thistle	Annual	NF	AF (Camel)
Onopordum cyrenaicum Maire & Weiller	Asteraceae	/	Perennial	NF	/
Periploca laevigata Ait.	Apocynaceae	Periploca of the Woods	Perennial	NF	AF / MP/ OP
Phagnalon rupestre (L.) DC.	Compositae	Rock Phangnalon	Annual	NF	MP
Phillyrea angustifolia L.	Oleaceae	False Olive	Perennial	NF	AF / OP / AP
Phlomis floccosa D. Don	Lamiaceae	Jerusalem Sage	Perennial	NF / RL	MP / SD / DEIN
Pinus halepensis Mill.	Pinaceae	Aleppo Pine	Perennial	NF / PF	MP / AFFP
Pistacia lentiscus L.	Anacardiaceae	Mastic Tree	Perennial	NF	AF / MP / FP/ IP (gum/resin)
Pistacia terebinthus L.	Anacardiaceae	/	Perennial	NF	MP
Pituranthus tortuosus (Desf.) Benth. & Hook.	Apiaceae	Pituranthos	Perennial	RL	AF / MP

Species	Family	Common Name	Life Span	NVT	Uses
Polygonum equisetofome Sm.	Polygonaceae	Horse-Tail Khotweed	Annual	RL	AF / MP
Quercus coccifera L.	Fagaceae	Kermes Oak	Perennial	NF	MP
Rhamnus oleoides Lam.	Rhamnaceae	Blue-Leafed Wattle	Perennial	NF	AF
Rhus tripartita (Ucria) Grande	Anacardiaceae	Syrian Sumach	Perennial	NF	MP
Rosmarinus officinalis L.	Lamiaceae	Rosmary	Perennial	NF	MP
Salvia fruticosa Mill.	Lamiaceae	Greek Sage	Perennial	NF	AP/ MP/ IP (essential oil) / HF
Sarcopoterium spinosum (L.) Spach	Rhamnaceae	Thorny Burnet	Perennial	NF	MP / HP / FP / DEIN
Satureja thymbra L.	Lamiaceae	Pink Savory	Perennial	NF	MP/ AP/ BP
Sinapis pubescens L.	Brassicaceae	/	Annual	NF	/
Smilax aspera L.	Solanaceae	Common Smilax, Rough Bindweed	Perennial	NF	HF / MP / IP (dye)
Stipa capensis Thunb.	Poaceae Gramineae)	Cape Rice Grass	Annual	NF / RL	AF
Stipa pennata L.	Poaceae (Gramineae)	European Feather Grass	Annual	RL	AF
Suaeda pruinosa Lange.	Chenopodiaceae	Risultati Della Ricerca	Perennial	NF	IS

Species	Family	Common Name	Life Span	NVT	Uses
Teucrium polium L.	Lamiaceae	Poley	Perennial	NF	AF / MP
Thapsia garganica L.	Apiaceae	Deadly Carrots	Annual	NF	NP /MP
Thymelaea hirsuta (L.) Endl.	Thymelaeaceae	Hairy Thymelaea	Perennial	RL	SF / MP /IP (fibre)
Thymus capitatus (L.) Hoffmanns. & Link	Lamiaceae	Conehead-Thyme	Perennial	NF / RL	AF / MP/ HF/ BP/ EC
Trifolium spp	Fabaceae	/	Annual	NF	AF / ISF
Urginea maritima (L.) Baker.	Hyacinthace	/	Annual	NF	DEIN /MP / PS / NP
Viburnum tinus L.	Caprifoliaceae	Laurustinus Viburnum	Perennial	NF / RL	HP
Vicia sativa (L.) Guss	Fabaceae	/	Annual	NF	AF

Abbreviations:

AF = Animal Feed
SHP = Shade Plant
IP = Industry Plant
EC = Erosion Control
IS = Indicator of Soil Salinity
NP=Non-palatable
HF = Human Food
FP = Fuel Plant
AP = Aromatic Plant
OP = Ornamental Plant
SD = Sensitive to drought
MP = Medicinal Plant
BP = Bee Plant
AFFP = Afforestation
HP = Hedge Plant
DEIN = Degradation Indicator
WB = Wind Break
GS = Graft Stock
SF = Sand Fixation
Clmx = Climax Species
PS = Poisonous species

B.3 Soil properties of OMU sampling sites

This section presents the data of soil property analysis obtained from the OMU survey (2005). The appendix section is divided into two subsections, with the first subsection showing the physical properties, and the second subsection displaying the chemical properties of each of the 53-sample sites.

B.3.1 Soil physical properties

Data of soil physical properties for each site of OMU (2005) samples are listed in Table B.3.1. Table B.3.1 shows the soil type, soil separates, including %sand, %silt, and %clay. The table also shows the soil moisture content, including % field moisture, % field capacity, % wilting point and %available water, erodibility ability number (K) and the bulk density for each site.

Table B.3.1 Soil physical properties of 53-sample sites (source: OMU,2005)

ID	Site Name	Soil Type	Soil Separates (%)			% Soil Moisture Content				Erodibility Ability No. (K)	Bulk Density (gm cm $^{-3}$)
			Sand	Silt	Clay	Field moisture	Field capacity	Wilting point	Available water		
1	Karsa	Clay Loam	23.39	40.59	36.02	12.23	35.82	20.17	15.64	0.26	-
2	Alaslab	Clay	14.71	31.37	53.92	8.77	25.35	19.02	6.33	0.25	1.11
3	Wadi El Mahbool	Sandy Loam	60.75	29.90	9.35	5.79	28.26	16.94	11.32	-	-
4	Wadi Bo annidi	Silty Clay Loam	19.07	46.33	34.60	7.87	28.24	16.04	12.20	0.33	1.24
5	RasAmer	Clay	16.00	38.19	45.81	7.07	27.50	16.58	10.92	0.32	1.33
6	Alhamama-RasAmer	Clay	12.27	37.59	50.14	8.25	23.96	17.58	6.38	0.31	1.26
7	Bo Traba	Clay Loam	30.19	36.79	33.02	5.15	22.56	12.30	10.26	0.39	1.32
8	Mirad Massoad (the Coast)	Clay	20.00	36.19	43.81	8.39	26.64	14.24	12.40	0.29	1.35
9	Wadi El Mogawah	Loam	33.01	44.66	22.33	11.29	35.56	18.75	15.31	0.28	-
10	Wadi Alakki	Loam	36.19	40.00	23.81	5.03	21.63	14.78	6.85	0.35	1.18
11	Al Hejab	Clay	19.05	33.33	47.62	10.67	27.40	16.27	11.13	0.27	1.32

ID	Site Name	Soil Type	Soil Separates (%)			% Soil Moisture Content				Erodibility Ability No. (K)	Bulk Density (gm cm $^{-3}$)
			Sand	Silt	Clay	Field moisture	Field capacity	Wilting point	Available water		
12	Sattia	Clay	20.00	26.67	53.33	13.29	29.51	18.21	11.23	0.26	1.30
13	Arqoob Sidi Hamad	Clay	21.15	31.73	47.12	5.69	29.77	17.27	12.50	0.34	-
14	Sidi Khaled	Clay	24.04	30.77	45.19	8.24	26.51	14.99	11.52	0.36	1.26
15	Wadi Margos	Loam	38.89	38.89	22.22	4.14	22.66	9.21	13.45	0.29	1.22
16	Ghot Maibara	Clay Loam	29.52	38.10	32.38	12.67	21.47	12.62	8.85	0.43	1.30
17	Qandafora	Clay	14.29	35.23	50.48	8.49	27.68	15.98	11.70	0.18	1.26
18	Sidi Al Qarib	Loam	29.88	43.58	25.72	10.00	36.43	18.73	17.02	0.28	-
19	Mirad Massoad	Clay	20.19	36.00	43.81	8.40	26.63	14.23	12.39	0.28	1.34
20	Mirad Massoad (Roman's dams)	Clay	18.87	37.73	43.40	6.89	27.56	14.99	12.57	0.35	1.34
21	Mirad Massoad (Terraces)	Clay Loam	32.31	27.61	40.08	10.77	31.91	15.98	15.93	0.24	-
22	Wadi Al-Sudan	Clay	20.59	34.31	45.10	16.36	24.19	18.88	5.31	0.30	1.30
23	Wadi Al Zawia	Clay Loam	25.00	38.46	36.54	8.54	21.15	17.27	3.88	0.26	1.32
24	Wadi El Kuf stream	Silty Clay	17.31	40.38	42.31	10.46	22.76	14.74	8.02	0.30	1.08

ID	Site Name	Soil Type	Soil Separates (%)			% Soil Moisture Content				Erodibility Ability No. (K)	Bulk Density (gm cm $^{-3}$)
			Sand	Silt	Clay	Field moisture	Field capacity	Wilting point	Available water		
25	Tolmitha - Sidi Erhoma	Silty Loam	26.79	49.81	23.40	7.65	42.09	17.35	24.73	0.34	-
26	Eqfanta	Clay	18.10	28.57	53.33	11.87	29.04	16.09	12.95	0.07	1.33
27	El Mansoura - El Dabadeb	Clay Loam	24.27	37.87	37.86	13.92	23.19	18.13	5.06	0.24	1.22
28	Al Wasita-Salion	Loam	48.15	33.33	18.52	6.31	22.39	5.88	16.51	0.35	1.24
29	El Nador - El Mekhili	Loam	39.62	34.91	25.47	5.69	19.99	11.91	8.08	0.44	1.33
30	Lamloda – Ras El Helal	Silty Clay loam	18.86	42.50	38.46	8.28	30.11	17.00	13.10	0.36	-
31	Kashaf Forest	Clay Loam	23.53	42.16	34.31	11.01	28.46	24.47	3.99	0.30	1.03
32	El Daher El Hammer	Clay Loam	26.92	39.43	33.65	7.09	21.10	12.09	9.01	0.35	1.24
33	Argoob Al Abiad	Clay	10.68	31.07	58.26	13.30	25.98	21.10	4.88	0.14	1.14
34	Marawah - Quasser Libya	Clay Loam	28.85	40.38	30.77	6.90	22.38	16.59	5.79	0.29	1.24
35	Quasser Libya - El Bayada (Qud Khalil)	Clay Loam	23.08	46.15	30.77	6.69	30.00	16.57	13.43	0.32	-

ID	Site Name	Soil Type	Soil Separates (%)			% Soil Moisture Content				Erodibility Ability No. (K)	Bulk Density (gm cm $^{-3}$)
			Sand	Silt	Clay	Field moisture	Field capacity	Wilting point	Available water		
36	Al Ghriqa -Ras ATrab	Clay	15.38	30.77	53.58	10.90	28.12	8.15	19.97	0.21	1.39
37	Wadi Al Mahja – Kholan	Loam	35.81	41.45	22.99	4.85	30.65	12.19	18.45	0.31	-
38	Azzrada	Clay	19.23	29.81	50.96	11.92	24.39	17.46	6.93	0.29	1.30
39	Alquasser Alromani	Clay Loam	26.17	42.09	31.78	8.90	24.52	10.29	14.23	0.26	1.21
40	Wadi El Kuf	Clay	47.17	31.13	21.70	7.59	25.19	13.79	11.40	0.20	1.29
41	Wadi El kuf (Cyperss Forest)	Clay Loam	26.21	38.84	34.95	9.57	28.11	17.27	10.84	0.18	1.25
42	Zawat Alqsoor-Jardas	Sandy Clay Loam	50.94	18.87	30.19	4.33	21.33	10.84	10.49	0.26	1.34
43	Madwer El Zaitoon (Plantation)	Silty Clay Loam	17.31	47.11	35.58	5.64	23.72	15.06	8.66	0.25	1.24
44	Marawah Forest	Clay Loam	26.42	45.22	28.30	6.94	23.42	12.50	10.92	0.30	1.34
45	Sidi El Homari Forest	Clay loam	33.33	35.30	31.37	9.21	68.15	13.23	54.92	0.26	-
46	Shnaishnn Forest	Clay loam	37.74	32.07	30.19	6.31	26.38	12.77	13.61	0.20	1.28

ID	Site Name	Soil Type	Soil Separates (%)			% Soil Moisture Content				Erodibility Ability No. (K)	Bulk Density (gm cm $^{-3}$)
			Sand	Silt	Clay	Field moisture	Field capacity	Wilting point	Available water		
47	El Hesha	Clay	37.74	36.79	25.47	4.84	20.54	10.47	10.07	0.38	1.30
48	Bo Draa	Loam	36.76	41.21	22.03	5.81	32.42	12.45	19.96	0.34	-
49	Jerdas Al Abeed	Silty Clay Loam	21.30	43.78	34.92	6.93	33.90	17.37	16.54	0.30	-
50	Bo Querawa	Clay Loam	23.16	42.53	34.31	11.00	28.45	24.46	3.98	0.29	1.01
51	Jerdas - Jabanet Sidi Saad	Clay loam	25.96	35.58	38.46	7.99	22.61	14.21	8.40	0.25	1.23
52	Taknis - El Caroba	Clay loam	24.76	44.76	30.48	5.08	19.93	11.89	8.04	0.31	1.40
53	Madwer El Zaitoon	Clay loam	30.19	40.56	29.25	5.96	22.07	12.53	9.54	0.28	1.26

B.3.2 Soil chemical properties

Data for the soil chemical properties were measured for each site of OMU (2005) samples and are presented in this subsection. Table B.3.2 shows the organic matter % (OM), calcium carbonate % ($CaCO_3$), exchangeable cations (meq/100gm) that included the measurement of Ca^{+2}, Mg^{+2}, Na^{+1} and K^{+1}, pH, cation exchange capacity (CEC) (meq/100gm), electrical conductivity (EC) ($mmhos^{-cm}$) and the available phosphorus (P) (ppm). The table also shows the exchangeable sodium percentage (ESP), sodium adsorption ratio (SAR) and mean EC_e those calculated by the author for each site.

Table B.3.2 Soil chemical properties of 53-sample sites (source: OMU, 2005)

ID	Site Name	OM (%)	$CaCO_3$ (%)	Exchangeable Cations (meq / 100gm)				ESP*	SAR*	pH	CEC (meq / 100 gm)	EC (mmhos $^{-cm}$)	Mean Ece*	Available P (ppm)
				Ca^{+2}	Mg^{+2}	Na^{+1}	K^{+1}							
1	Karsa	8.21	1.07	23.82	3.04	2.68	2.83	9.03	0.73	8.21	32.28	0.461	2.994	3.97
2	Alaslab	5.54	0.15	13.10	1.45	0.68	3.52	3.76	0.25	7.90	18.75	0.221	1.437	3.40
3	Wadi El Mahbool	2.00	62.50	43.25	3.45	0.62	0.93	1.30	0.13	8.16	10.00	0.423	2.750	10.70
4	Wadi Bo annidi	3.92	0.12	9.12	3.87	0.63	2.90	3.96	0.25	8.04	16.52	0.188	1.222	0.10
5	RasAmer	4.05	0.08	9.07	1.17	0.76	3.48	5.54	0.34	7.74	14.48	0.137	0.891	4.40
6	Alhamama-RasAmer	3.62	0.08	16.00	2.35	0.56	2.09	2.74	0.18	7.38	19.84	1.683	10.940	19.80
7	Bo Traba	3.00	28.00	9.40	4.75	0.33	2.24	2.01	0.12	8.24	16.72	0.510	3.315	1.80
8	Mirad Massoad (the Coast)	3.96	0.10	7.90	3.74	0.74	2.01	5.42	0.31	7.55	14.39	0.268	1.742	1.30
9	Wadi El Mogawah	8.06	21.95	20.18	2.01	0.68	1.50	2.87	0.20	7.81	24.38	0.281	1.823	2.45
10	Wadi Alakki	6.36	47.50	18.19	6.32	0.45	1.61	1.72	0.13	7.75	27.57	0.266	1.729	10.80
11	Al Hejab	1.08	7.20	10.55	0.72	0.16	2.87	1.13	0.07	8.18	14.20	8.18	53.170	4.20

ID	Site Name	OM (%)	$CaCO_3$ (%)	Exchangeable Cations (meq / 100gm)				ESP*	SAR*	pH	CEC (meq / 100 gm)	EC (mmhos $^{-cm}$)	Mean Ece*	Available P (ppm)
				Ca^{+2}	Mg^{+2}	Na^{+1}	K^{+1}							
12	Sattia	5.30	0.92	11.52	1.55	0.58	1.66	3.94	0.23	7.65	13.31	0.126	0.819	1.90
13	Arqoob Sidi Hamad	3.30	0.09	8.72	6.29	0.52	2.27	3.01	0.19	7.75	17.80	0.294	1.911	0.60
14	Sidi Khaled	3.42	0.15	7.89	6.77	0.45	2.67	2.60	0.17	7.46	17.76	0.137	0.891	0.20
15	Wadi Margos	1.92	64.50	11.27	1.40	0.39	0.98	2.86	0.15	7.65	14.03	0.402	2.613	6.50
16	Ghot Maibara	10.14	0.07	7.91	3.14	0.64	1.38	5.15	0.27	8.07	13.07	0.173	1.125	25.50
17	Qandafora	4.38	0.12	9.95	2.35	0.93	0.51	7.26	0.38	7.33	13.74	0.141	0.917	2.00
18	Sidi Al Qarib	5.70	25.97	20.79	4.52	0.72	2.65	2.57	0.20	7.52	28.70	0.344	2.233	22.90
19	Mirad Massoad	3.95	0.09	7.88	3.72	0.73	2.02	5.36	0.30	7.56	14.38	0.267	1.736	1.29
20	Mirad Massoad (Roman's dams)	4.20	0.10	9.53	1.07	0.92	1.38	7.68	0.40	7.96	12.90	0.215	1.398	2.80
21	Mirad Massoad (Terraces)	5.31	34.30	20.32	3.12	0.54	2.24	2.08	0.16	7.65	26.31	0.215	1.398	1.00
22	Wadi Al-Sudan	4.08	5.10	21.04	4.60	0.43	2.38	1.53	0.12	7.78	28.49	0.188	1.222	1.10
23	Wadi Al Zawia	6.60	5.70	19.37	0.79	0.50	2.02	2.25	0.16	7.85	22.68	0.205	1.333	2.30
24	Wadi El Kuf stream	3.18	3.20	17.43	4.75	0.47	1.64	1.97	0.14	7.65	24.30	0.169	1.099	0.10

ID	Site Name	OM (%)	$CaCO_3$ (%)	Exchangeable Cations (meq / 100gm)				ESP*	SAR*	pH	CEC (meq / 100 gm)	EC (mmhos $^{-cm}$)	Mean Ece*	Available P (ppm)
				Ca^{+2}	Mg^{+2}	Na^{+1}	K^{+1}							
25	Tolmitha - Sidi Erhoma	8.40	53.22	14.41	2.11	1.21	1.36	6.78	0.42	7.90	19.09	0.502	3.263	9.75
26	Eqfanta	4.92	0.92	9.09	1.56	0.66	0.99	5.67	0.29	7.90	12.30	0.167	1.086	16.30
27	El Mansoura - El Dabadeb	6.80	0.13	23.90	0.75	0.72	0.70	2.84	0.21	8.05	26.06	0.359	2.334	3.70
28	Al Wasita-Salion	4.20	70.47	19.51	3.44	0.33	0.29	1.42	0.10	8.48	23.58	0.190	1.235	5.60
29	El Nador - El Mekhili	2.70	33.50	22.17	2.73	0.63	4.80	2.12	0.18	9.28	30.33	0.448	2.912	9.60
30	Lamloda - Ras El Helal	3.04	0.28	12.46	3.00	0.63	1.44	3.74	0.23	7.54	17.54	0.257	1.672	7.50
31	Kashaf Forest	5.30	6.00	20.25	6.20	0.72	3.85	2.38	0.20	7.38	31.02	0.353	2.295	4.40
32	El Daher El Hammer	2.70	2.00	11.85	3.18	0.52	2.66	2.94	0.19	7.09	18.20	0.228	1.482	1.00
33	Argoob Al Abiad	3.79	0.15	11.37	3.12	0.80	1.88	4.89	0.30	7.30	15.89	0.227	1.476	3.10
34	Marawah - Quasser Libya	4.47	8.00	27.82	0.35	0.42	1.76	1.40	0.11	7.61	30.36	0.253	1.645	2.30
35	Quasser Libya - El Bayada (Qud Khalil)	7.38	4.50	23.01	1.06	0.56	1.63	2.18	0.16	7.36	26.27	0.260	1.690	18.30

ID	Site Name	OM (%)	$CaCO_3$ (%)	Exchangeable Cations (meq / 100gm)				ESP*	SAR*	pH	CEC (meq / 100 gm)	EC (mmhos $^{-cm}$)	Mean Ece*	Available P (ppm)
				Ca^{+2}	Mg^{+2}	Na^{+1}	K^{+1}							
36	Al Ghriqa -Ras ATrab	2.70	0.19	10.32	3.95	0.41	2.14	2.50	0.15	8.60	16.84	0.220	1.430	4.30
37	Wadi Al Mahja – Kholan	3.48	27.33	13.10	1.45	2.20	2.09	13.25	0.82	7.55	28.24	0.890	5.785	3.97
38	Azzrada	9.00	0.14	8.24	4.72	0.42	1.63	2.88	0.16	7.04	15.01	0.195	1.268	0.60
39	Alquasser Alromani	10.80	61.90	39.08	1.12	0.52	1.12	1.26	0.12	8.02	41.84	0.184	1.196	5.30
40	Wadi El Kuf	5.22	46.19	26.60	9.80	0.14	0.88	0.38	0.03	7.64	37.13	0.207	1.346	1.60
41	Wadi El kuf (Cyperss Forest)	4.26	23.80	39.48	3.52	0.50	1.74	1.12	0.11	7.74	45.24	0.215	1.398	0.60
42	Zawat Alqsoor-Jardas	2.40	52.95	22.31	2.39	0.41	1.50	1.56	0.12	8.12	23.61	0.203	1.320	3.70
43	Madwer El Zaitoon (Plantation)	4.95	1.04	18.20	5.88	0.27	2.90	1.00	0.08	7.88	27.24	0.366	2.379	1.20
44	Marawah Forest	1.65	15.09	25.39	3.56	0.43	2.06	1.37	0.11	7.60	31.44	0.240	1.560	12.80
45	Sidi El Homari Forest	8.10	0.11	20.94	3.78	0.23	2.41	0.85	0.07	7.30	26.90	0.837	5.441	7.60
46	Shnaishnn Forest	1.81	19.04	32.20	7.15	0.57	1.64	1.39	0.13	8.05	41.56	0.196	1.274	3.00

ID	Site Name	OM (%)	$CaCO_3$ (%)	Exchangeable Cations (meq / 100gm)				ESP*	SAR*	pH	CEC (meq / 100 gm)	EC (mmhos $^{-cm}$)	Mean Ece*	Available P (ppm)
				Ca^{+2}	Mg^{+2}	Na^{+1}	K^{+1}							
47	El Hesha (Rangeland)	1.98	22.50	5.75	5.97	2.96	2.77	20.43	1.22	7.93	17.45	0.486	3.159	3.50
48	Bo Draa	3.78	37.57	14.44	1.66	0.48	0.55	2.86	0.17	7.65	17.10	0.305	1.984	11.00
49	Jerdas Al Abeed	4.44	0.26	11.16	5.43	0.52	3.16	2.63	0.18	7.73	20.27	0.399	2.594	8.65
50	Bo Querawa	5.00	5.98	20.23	6.18	0.71	3.84	2.35	0.20	7.38	31.01	0.352	2.288	4.38
51	Jerdas - Jabanet Sidi Saad	4.68	29.33	15.44	9.51	0.73	2.76	2.63	0.21	8.29	28.44	0.213	1.385	3.90
52	Taknis - El Caroba	8.60	0.40	13.45	3.00	0.73	3.14	3.73	0.25	8.24	20.32	0.267	1.736	3.50
53	Madwer El Zaitoon	3.45	1.37	36.73	3.08	0.66	2.62	1.56	0.15	7.52	43.09	0.160	1.040	2.50

* Calculated by the author

Appendix C Soil Terrain Digital Database (SOTER)

C.1 Al Jabal Al Akhdar and Benghazi regions landforms

Landform classes data of the Al Jabal Al Akhdar and Benghazi regions those extracted from Libyan soil terrain digital database (L-SOTER) illustrated in this section. Table C.1.1 shows the landforms of each landscape within AL Jabal Al Akhdar and Benghazi regions and the dominant soils associated with each landform, including soil order, suborder and soil great group based in WGA and ACSAD (2005).

Table C.1.1 SOTER of Al Jabal Al Akhdar and Benghazi Regions (source: (LWGA and ACSAD, 2005)**)**

Soil Formation				
Landscape	**Landform/ Relief**	**Dominate Soils**		
		Order	**Suborder**	**Great Group**
North Eastern Mountain Area (M1)	Al Jabal Al Akhdar Top (M11)	Mollisols	Rendolls	*Haprendolls*
		Inceptisols	Xerepts	*Haploxerepts, Calcixerepts*
	Al Jabal Al Akhdar Shoulder (M12)	Inceptisols	Xerepts	*Calcixerepts*
		Mollisols	Rendolls	*Haprendolls*
	Al Jabal Al Akhdar Backslope (M13)	Mollisols	Rendolls	*Haprendolls*
		Inceptisols	Xerepts	*Haploxerepts, Calcixerepts*
		Alfisols	Xeralfs	*Rhodoxeralfs*
		Vertisols	Xererts	Haploxererts
	Al Jabal Al Akhdar Fall Face (M14)	Entisols	Orthents	*Torriorthents*
	Al Jabal Al Akhdar Toeslope (M15)	Inceptisols	Xerepts	*Calcixerepts, Haploxerepts*
		Mollisols	Rendolls	*Haprendolls*
		Alfisols	Xeralfs	*Rhodoxeralfs*
		Entisols	Orthents	*Xerorthents*

Soil Formation				
Landscape	**Landform/ Relief**	**Dominate Soils**		
		Order	**Suborder**	**Great Group**
North Eastern Plain Area (Pl1)	Benghazi Plain Relatively High Lands (Pl11)	Aridisols	Cambids	*Haplocambids*
			Argids	*Haplargids*
		Entisols	Fluvents	*Xerofluvents*
	Benghazi Plain Moderately High Lands (Pl12)	Aridisols	Argids	*Haplargids*
		Entisols	Orthents	*Xerorthents*
	Benghazi Plain Relatively Low Lands (Pl13)	Aridisols	Cambids	*Haplocambids*
			Argids	*Haplargids*
		Entisols	Fluvents	*Xerofluvents*
North Eastern Plateau Area (Pt1)	North Eastern Plateau Summit (Pt11)	Aridisols	Gypsids	*Petrogypsids*
	North Eastern Plateau Escarpment (Pt12)			
	North Eastern Plateau Pediment (Pt13)		Calcids	*Petrocalcids*
North Eastern Terrace Area (T1)	North Eastern Terrace 1 (T11)	Entisols	Orthents	*Torriorthents*
	North Eastern Terrace 3 (T13)	Entisols	Orthents	*Torriorthents*

Soil Formation				
Landscape	**Landform/ Relief**	**Dominate Soils**		
		Order	**Suborder**	**Great Group**
Depression Areas (De)	Wadies and alluvial plains (De2) Wadi Al Muallaq Wadi Al Qattarah Wadi Ar Ramlah	Entisols	Orthents	*Torriorthents*
			Fluvents	*Torrifluvents, Xerofluvents*
	Benghazi Sabkha (De4)	Aridisols	Salids	*Haplosalids, Aquisalids*
Non-Soil Formation				
Cs	Coastal Plain (Cs)			

Appendix D Landform-Soil-Dominant Species and Climate of the study area Sites

D.1 Landform, soil type, dominant species and dominant plant species of study area Sites

Data of Landform class soil type and dominant plant species (DPS) and the number of climatic grids (Climate No.) associated with each site of OMU (2005).is shown in Table D.1.1. The landform class based on LSOTER (LWGA and ACSAD, 2005), soil type and DPS based on OMU (2005) and Climate No. based on numbering the climate grids of the Global Climate Monitor (GCMon) where the sites are located.

Table D.1.1 Landform classes, soil type, DPS and Climate No. of the study areasamples sites

ID	Site name	Abbreviation	Landform class	Soil Type	DPS	Climate No.
1	Karsa	Krs	Coastal Plain	Clay Loam	*Juniperus phoenicea* L.	C 6
2	Alaslab	Aslb	Coastal Plain	Clay	*Juniperus phoenicea* L.	C 6
3	Wadi El Mahbool	WMah	Coastal Plain	Sandy Loam	*Cupressus sempervirens* L.	C 6
4	Wadi Bo annidi	WBA	Coastal Plain	Silty Clay Loam	*Pistacia lentiscus* L.	C 5
5	RasAmer	RMR	Coastal Plain	Clay	*Juniperus phoenicea* L.	C 5
6	Alhamama-RasAmer	HRMR	Coastal Plain	Clay	*Juniperus phoenicea* L.	C 5
7	Bo Traba	BTB	Coastal Plain	Clay Loam	*Juniperus phoenicea* L.	C 1
8	Mirad Massoad (the Coast)	MMC	Coastal Plain	Clay	*Juniperus phoenicea* L.	C 4
9	Wadi El Mogawah	WMog	Al Jabal Al Akhdar Top	Loam	*Juniperus phoenicea* L.	C 4
10	Wadi Alakki	Waki	Wadi Al Qattarah	Loam	*Juniperus phoenicea* L.	C 4
11	Al Hejab	Hjb	Al Jabal Al Akhdar Top	Clay	*Juniperus phoenicea* L.	C 5

ID	Site name	Abbreviation	Landform class	Soil Type	DPS	Climate No.
12	Sattia	Sati	Coastal Plain	Clay	*Juniperus phoenicea* L.	C 5
13	Arqoob Sidi Hamad	AqSH	Al Jabal Al Akhdar Backslope	Clay	*Juniperus phoenicea* L.	C 6
14	Sidi Khaled	SKh	Al Jabal Al Akhdar Backslope	Clay	*Juniperus phoenicea* L.	C 6
15	Wadi Margos	Wmarg	Coastal Plain	Loam	*Juniperus phoenicea* L.	C 6
16	Ghot Maibara	GMb	Al Jabal Al Akhdar Backslope	Clay Loam	*Juniperus phoenicea* L.	C 5
17	Qandafora	Qand	Al Jabal Al Akhdar Backslope	Clay	*Quercus coccifera* L.	C 5
18	Sidi Al Qarib	SQrib	Al Jabal Al Akhdar Backslope	Loam	*Juniperus phoenicea* L.	C 4
19	Mirad Massoad	MM	Coastal Plain	Clay	*Juniperus phoenicea* L.	C 4
20	Mirad Massoad (Roman's dams)	MMD	Coastal Plain	Clay	*Juniperus phoenicea* L.	C 4
21	Mirad Massoad (Terraces)	MMT	Al Jabal Al Akhdar Shoulder	Clay Loam	*Cistus* spp.	C 4
22	Wadi Al-Sudan	Wsu	Al Jabal Al Akhdar Top	Clay	*Juniperus phoenicea* L.	C 4

ID	Site name	Abbreviation	Landform class	Soil Type	DPS	Climate No.
23	Wadi Al Zawia	WZw	Al Jabal Al Akhdar Top	Clay Loam	*Juniperus phoenicea* L.	C 4
24	Wadi El Kuf stream	WkufS	Al Jabal Al Akhdar Top	Silty Clay	*Juniperus phoenicea* L.	C 5
25	Tolmitha - Sidi Erhoma	T-Roh	Coastal Plain	Silty Loam	*Juniperus phoenicea* L.	C 1
26	Eqfanta	Eqf	Al Jabal Al Akhdar Backslope	Clay	*Juniperus phoenicea* L.	C 5
27	El Mansoura - El Dabadeb	Mans	Al Jabal Al Akhdar Shoulder	Clay Loam	*Juniperus phoenicea* L.	C 5
28	Al Wasita-Salion	Wast	Al Jabal Al Akhdar Backslope	Loam	*Juniperus phoenicea* L.	C 5
29	El Nador - El Mekhili	Nd-Mekh	Al Jabal Al Akhdar Backslope	Loam	*Hammada scoparia* (Pomel) Iljin	C 7
30	Lamloda – Ras El Helal	Lam-Hel	Al Jabal Al Akhdar Backslope	Silty Clay loam	*Arbutus pavarii* Pamp.	C 6
31	Kashaf Forest	Kash	Wadi Al Qattarah	Clay Loam	*Pinus halepensis* Mill.	C 4
32	El Daher El Hammer	DaHa	Al Jabal Al Akhdar Toeslope	Clay Loam	*Juniperus phoenicea* L.	C 6
33	Argoob Al Abiad	AqAb	Coastal Plain	Clay	*Juniperus phoenicea* L.	C 6

ID	Site name	Abbreviation	Landform class	Soil Type	DPS	Climate No.
34	Marawah - Quasser Libya	Mar-QL	Al Jabal Al Akhdar Shoulder	Clay Loam	*Juniperus phoenicea* L.	C 4
36	Quasser Libya - El Bayada (Qud Khalil)	QL-Bd	Al Jabal Al Akhdar Top	Clay	*Arbutus pavarii* Pamp.	C 5
37	Al Ghriqa -Ras ATrab	Gh-Trb	Wadi Al Muallaq	Loam	*Hammada scoparia* (Pomel) Iljin	C 6
38	Wadi Al Mahja – Kholan	WMhj-Kh	Al Jabal Al Akhdar Backslope	Clay	*Pistacia lentiscus* L.	C 6
39	Azzrada	Zrda	Al Jabal Al Akhdar Top	Clay Loam	*Juniperus phoenicea* L.	C 5
40	Alquasser Alromani	Qrom	Al Jabal Al Akhdar Top	Clay	*Pistacia lentiscus* L.	C 5
41	Wadi El Kuf	WKuf	Al Jabal Al Akhdar Top	Clay Loam	Cupressus *sempervirens* L.	C 5
42	Wadi El kuf (Cyperss Forest)	WkufCF	Wadi Al Qattarah	Sandy Clay Loam	*Juniperus phoenicea* L.	C 2
43	Zawat Alqsoor-Jardas	ZQ-Jrd	Wadi Al Qattarah	Silty Clay Loam	*Pinus halepensis* Mill.	C 3
44	Madwer El Zaitoon (Plantation)	MadZF	Al Jabal Al Akhdar Backslope	Clay Loam	*Pinus halepensis* Mill.	C 3

ID	Site name	Abbreviation	Landform class	Soil Type	DPS	Climate No.
45	Sidi El Homari Forest	SHF	Al Jabal Al Akhdar Shoulder	Clay loam	*Pinus halepensis* Mill.	C 5
46	Shnaishnn Forest	ShnF	Al Jabal Al Akhdar Backslope	Clay loam	*Juniperus phoenicea* L.	C 5
47	El Hesha	Hesh	Wadi Al Muallaq	Clay	*Hammada scoparia* (Pomel) Iljin	C 6
48	Bo Draa	BoDr	Al Jabal Al Akhdar Toeslope	Loam	*Viburnum* tinus L.	C 6
49	Jerdas Al Abeed	Jrdsh	Al Jabal Al Akhdar Backslope	Silty Clay Loam	*Juniperus phoenicea L.*	C 2
50	Bo Querawa	BoQrw	Al Jabal Al Akhdar Backslope	Clay Loam	*Pistacia lentiscus* L.	C 4
51	Jerdas - Jabanet Sidi Saad	Jed-JSS	Al Jabal Al Akhdar Backslope	Clay loam	*Thymus capitatus* Hoff. et Link.	C 3
52	Taknis - El Caroba	Tak-Crob	Al Jabal Al Akhdar Backslope	Clay loam	*Thymus capitatus* Hoff. et Link.	C 3
53	Madwer El Zaitoon	MadzR	Wadi Al Qattarah	Clay loam	*Stipa capensis* Thunb.	C 3

Appendix E LULC Python Script

E.1 Transition types of LULC classes

A Python script was developed to group transition types (Figure E.1.1), applied using the ‘field calculator’ tool in GIS software. The LULC classes that changed to the same ‘new class’ were grouped together under a transition group. Those Transition types used to visualise the transition map.

```
def Recode (class_t1, class_t2):
  if (class_t2=="Agricultural Areas"):
     if (class_t1=="Agricultural Areas"):
        return "Agricultural Areas"
  if (class_t2=="Natural Forest"):
     if (class_t1=="Natural Forest"):
        return "Natural Forest"
  if (class_t2=="Planted Forest"):
     if (class_t1=="Planted Forest"):
        return "Planted Forest"
  if (class_t2=="Rangelands"):
     if (class_t1=="Rangelands"):
        return "Rangelands"
  if (class_t2=="Built-up Areas"):
     if (class_t1=="Built-up Areas"):
        return "Built-up Areas"
  if (class_t2=="Infrastructure"):
     if (class_t1=="Infrastructure"):
        return "Infrastructure"
```

```
 if (class_t2==" Non-Vegetated areas"):

    if (class_t1==" Non-Vegetated areas"):

       return "Non-Vegetated Areas"

 if (class_t2=="Rangelands"):

    if (class_t1=="Natural Forest" or class_t1=="Planted Forest" or class_t1==" Non-
Vegetated areas " or class_t1=="Built-up Areas" or class_t1=="Infrastructure"):

       return "Rangelands Expansion"

 if (class_t2==" Non-Vegetated areas"):

    if (class_t1=="Natural Forest" or class_t1=="Agriculture Areas" or class_t1=="Planted
Forest" or class_t1=="Rangelands" or class_t1=="Built-up Areas" or
class_t1=="Infrastructure"):

       return " Disturbed Lands"

 if (class_t2=="Planted Forest"):

    if (class_t1=="Natural Forest" or class_t1==" Non-Vegetated areas" or
class_t1=="Rangelands" or class_t1=="Built-up Areas" or class_t1=="Infrastructure"):

       return "Reforestation"

 if (class_t2=="Natural Forest"):

    if (class_t1==" Non-Vegetated areas" or class_t1=="Planted Forest" or
class_t1=="Rangelands" or class_t1=="Built-up Areas" or class_t1=="Infrastructure"):

       return "Reforestation"

 if (class_t2=="Built-up Areas"):

    if (class_t1=="Natural Forest" or class_t1=="Planted Forest" or
class_t1=="Rangelands" or class_t1==" Non-Vegetated areas" or
class_t1=="Infrastructure"):

       return "Urbanisation"

 if (class_t2=="Infrastructure"):

    if (class_t1=="Natural Forest" or class_t1=="Planted Forest" or
class_t1=="Rangelands" or class_t1==" Non-Vegetated areas" or class_t1=="Built-up
Areas"):
```

```
        return "Urbanisation"
  if (class_t2=="Agricultural Areas"):
     if (class_t1=="Natural Forest" or class_t1=="Planted Forest" or
class_t1=="Rangelands" or class_t1==" Non-Vegetated areas" or class_t1=="Built-up
Areas" or class_t1=="Infrastructure"):
        return "Agricultural Expansion"
  if (class_t2=="Natural Forest" or class_t2=="Planted Forest" or class_t2=="Rangelands"
or class_t2==" Non-Vegetated areas" or class_t2=="Built-up Areas" or
class_t2=="Infrastructure"):
     if (class_t1=="Agricultural Areas"):
        return "Agricultural Recession"
     else:
        return "unclassified"
  else:
      return "unclassified_t2"
```

Figure E.1.1 Transition group Python script

Appendix F Imagae Classifucation

This appendix section divided to two parts, the first defines the Jeffreys-Matusita (JM) distance method and the second is for the accuracy assessment.

F.1 The JM distance

The JM distance, which is a statistical measure of the distance between pairs of spectral class signatures (i.e. two features), was used. The spectral signatures of training samples were collected for each LULC class, referred to as the ROI in ENVI, and JM distance is computed as follows (Yeom et al., 2013):

$$JM_{ij} = \sqrt{2(1 - e^{-B})} \qquad \textbf{F.1.1}$$

and

$$B = \frac{1}{8}(\mu_i - \mu_j)^T \left(\frac{C_i + C_j}{2}\right)^{-1} (\mu_i - \mu_j) + \frac{1}{2}\ln\left(\frac{\frac{1}{2}|C_i + C_j|}{\sqrt{|C_i| \times |C_j|}}\right) \qquad \textbf{F.1.2}$$

Where:

i *and* j *= the two classes being compared*

μ_i *and* μ_j*= the mean vectors of* μ_i *and* μ_j*, respectively*

C_i *and* C_j*= the covariance matrices*

$|C_i|$ *and* $|C_j|$*= the determinants of the covariance matrices classes* i *and* j*, respectively*

F.2 Classification Accuracy Assessment

Accuracy assessment is an essential part of any image classification process that aims to define quantitatively how pixels are assigned into feature classes in the area under investigation (Banko, 1998; Ismail and Jusoff, 2008; Araya and Cabral, 2010). A confusion matrix, sometimes called a contingency table or a classification error matrix, is the typical way of expressing classification

accuracy (Story and Congalton, 1986; Lillesand et al., 1989; Araya and Cabral, 2010; Richards, 2013). This matrix compares the relationship between ground truth (reference data) which is represented by the columns of the matrix and the equivalent results of automated classification (classified data) which are represented by the rows (Story and Congalton, 1986). The confusion matrix also provides calculation methods for overall accuracy, producer's accuracy, user's accuracy, and Kappa Coefficient (Lu and Weng, 2007; van Genderen, 2011). The overall accuracy is calculated following Equation F.2.1 (Story and Congalton, 1986; Al-fares, 2013; Gashaw et al., 2017), which represents the accuracy of the entire product. Likewise, the accuracies of individual categories are calculated following Equation F.2.2 and Equation F.2.3 which are termed as the producer accuracy and user accuracy, respectively (Story and Congalton, 1986; Lillesand et al., 1989; Al-fares, 2013). Where, producer's accuracy indicates the probability that a ground sample will be correctly classified, and user's accuracy indicates the probability that a pixel classified into a given class really represents that class on the ground.

$$Overall\ accuracy = \frac{\sum_{i=1}^{M} n_{ii}}{N} \times 100 \qquad \textbf{F.2.1}$$

$$Producer\ accuracy = \frac{n_{ii}}{n_{+i}} \times 100 \qquad \textbf{F.2.2}$$

$$User\ accuracy = \frac{n_{ii}}{n_{i+}} \times 100 \qquad \textbf{F.2.3}$$

Richards (2013) described the Kappa Coefficient as "a measure of classifier performance derived from the error matrix but which, purportedly, is free of any bias resulting from the chance agreement between the classifier output and the reference data". It is estimated as represented in Equation F.2.4 (Banko, 1998; Richards, 2013) and Table F.2.1 shows the ranges of the Kappa coefficient as listed by Richards (2013):

$$k = \frac{N\sum_{i=1}^{M} n_{ii} - \sum_{i=1}^{M} n_{i+}n_{+i}}{N^2 - \sum_{i=1}^{M} n_i + n_{+i}} \qquad \textbf{F.2.4}$$

Where:

M *= Number of rows / columns (classes) in the confusion matrix*

n_{ii} *= Number of observations in the major diagonal in row* i *and column* i *(the number of correct classifications*)

n_{i+} *= Total number of rows* i

n_{+i} *= Total number of columns* i

N *= the total number of reference data (validation set) samples.*

Table F.2.1 Interpretation of Kappa (Richards, 2013)

Kappa Coefficient	Classification can be regarded as
Below 0.4	Poor
0.41- 0.60	Moderate
0.61- 0.75	Good
0.76 – 0.80	Excellent
0.81 and above	Almost perfect

Appendix G Study area land use land cover change detection

The folloing Appenndix presents the result of Post-Classification Comparision techniues (PCC). By comparing two classified images from different date. The result presents in coress-tabulation matrics were generated using statistical report data for the years investigated.

G.1 LULC changes detection

The cross-tabulation matrix for the three periods, from 2004 to 2006, from 2006 to 2008 and from 2008 to 2010 (before the 2011 Libyan uprising) is presented in Table G.1.1; and for the two time periods, from 2010 to 2014, and from 2014 to 2016 (after the 2011 Libyan uprising) is presented in Table G.1.2.

Table G.1.1 Cross-tabulation matrix for the periods: 2004 to 2006 (A), 2006 to 2008 (B) and 2008 to 2010 (C) showing gains, losses, and net changes (ha) in the study area

(A) 2004-2006	NF	PF	RL	AA	BA	IN	NV	Total 2004	Loss
NF	305,811	0.00	672	10,825	26.2	112	5,555	323,001	17,190
PF	0.00	679	0.00	0.00	0.00	0.00	0.00	679	0.00
RL	37.3	0.00	395,699	6,792	9.72	36.2	4,681	407,256	11,557
AA	12,648	0.00	15,904	173,925	64.3	110	8,49	211,141	37,216
BA	0.00	0.00	0.00	0.00	2,637	0.00	0.00	2,637	0.00
IN	37.3	0.00	14	64.3	0.00	5,783	0.00	5,899	116
NV	2,613	0.00	4,750	5,158	169	62.5	43,795	56,547	12,752
Total 2006	321,146	679	417,038	196,765	2,906	6,104	62,522		
Gain	15,335	0.00	21,339	22,839	269	321	18,726		
Net change	-1,845	0.00	9,782	-1,4376	269	205	5,975		
(B) 2006-2008	NF	PF	RL	AA	BA	IN	NV	Total 2006	Loss
NF	316,644	0.00	1,443	5,153	0.00	58.8	1,467	324,766	8,122
PF	0.00	673	0.00	0.00	0.00	0.00	0.00	673	0.00
RL	542	0.00	399,006	14,388	0.00	45.7	4,182	418,164	19,158
AA	23,549	0.00	6,832	159,182	2.34	49.7	3,605	193,221	34,039
BA	0.00	0.00	0.00	0.00	2,991	0.00	0.00	2,991	0.00
IN	152	0.00	84.8	82.8	0.00	5,290	11.5	5,621	331
NV	13,342	0.00	1,0732	11,635	20.1	0.00	25,931	61,661	35,730
Total 2008	354,230	673	418,098	190,442	3,013	5,444	35,198		
Gain	37,586	0.00	1,9092	31,259	22.4	154	9,267		
Net change	29,463	0.00	-66.4	-2,779	22	-177	-26,462		

Table G.1.1 (continued)

(C) 2008-2010	NF	PF	RL	AA	BA	IN	NV	Total 2008	Loss
NF	307,148	0.00	1,023	42,600	54.0	315	6,319	357,459	50,311
PF	0.00	658	0.00	0.00	0.00	0.00	0.00	658	0.00
RL	16,118	84.9	345,248	13,467	26.3	171	41,200	416,314	71,067
AA	19,304	10.8	17,119	146,237	177	59.5	5,783	188,690	42,454
BA	0.00	0.00	0.00	0.00	3,025	2.70	0.00	3,028	2.70
IN	129	0.00	67.4	66	2.43	5,174	7.74	5,446	273
NV	2,796	8.91	3,476	6,950	185	3.51	22,299	35,719	13,420
Total 2010	345,495	763	366,933	209,320	3,470	5,727	75,609		
Gain	38,348	105	21,685	63,083	445	552	53,310		
Net change	-11,963	105	-49,381	20,629	442	279	39,889		

Table G.1.2 Cross-tabulation matrix for the periods: 2010 to 2014 (A) and 2014 to 2016 (B) showing gains, losses, and net changes (ha) in the study area

(A) 2010-2014	NF	PF	RL	AA	BA	IN	NV	Total 2010	Loss
NF	278,748	0.00	8,573	38,592	145	1,003	17,141	344,201	65,454
PF	0.00	795	0.00	0.00	0.00	0.00	0.00	795	0.00
RL	2,188	0.00	314,452	30,549	84.2	431	19,369	367,073	52,621
AA	3,2316	0.00	4,192	144,631	401	1,129	27,364	210,033	65,403
BA	0.00	0.00	0.00	0.00	3,549	52.6	0.00	3,602	52.6
IN	163	0.00	18.6	38.2	2.34	5,997	6.30	6,225	228
NV	2,877	0.00	10,896	3924	673	255	56,835	75,460	18,625
Total 2014	316,290	795	338,132	217,734	4,855	8867	120,716		
Gain	37,543	0.00	23,680	73,103	1,306	2,871	63,881		
Net change	-27,910	0.00	-28,941	7,700	1,253	2,642	45,255		
(B) 2014-2016	NF	PF	RL	AA	BA	IN	NV	Total 2014	Loss
NF	293,234	0.00	2,266	16,621	3.24	331	4,496	316,952	23,718
PF	0.00	792	0.00	4.14	0.00	0.00	0.00	796	4.14
RL	2,371	0.00	313,604	9,842	13.6	47.9	11,647	337,526	23,922
AA	19,804	0.00	11,169	171,974	37.6	500	11,006	214,492	42,518
BA	0.00	0.00	0.00	0.00	5,126	32.8	0.00	5,159	32.8
IN	177	0.00	47	0.00	0.00	10966	0.00	11190	224
NV	5,002	0.00	11,040	20,059	111	362	84,942	121,516	36,574
Total 2016	320,588	792	33,8125	218,501	5291	12,240	112,093		
Gain	27,354	0.00	24,522	46,526	165	1,274	27,151		
Net change	3,636	-4.14	599	4,008	132	1050	-9,423		

GLOSSARY

Association: A plant community of definite floristic composition, dominated by particular species and grown under uniform habitat condition.

Chamaephyte: A woody plant in Raunkiaer's life-form classification with perennating buds located 0-25 cm above the soil surface.

Cryptophyte or Geophytes: A plant in Raunkiaer's life-form classification with perennating buds below the surface of the ground.

Desert: a region of an arid or hyper-arid climate inhabited by species adapted to aridity and having large contiguous areas with bare soil and low vegetation cover.

Desertification: the emergent outcome of a suite of social and biophysical causal factors, with pathways of change that are specific in time and place.

Drylands: a climatic attribute defines the only ecosystems that by definition, are prone to desertification – their water input or gain is much lower than the potential output or loss (the ratio of precipitation to potential evapotranspiration; i.e. the "aridity index", is lower than 0.65, which means that the potential loss from the soil surface and through its vegetation cover is at least one and a half time higher than the precipitation).

Floristic diversity: The number of plant species that occur in a community or area.

Formation: A regionally extensive assemblage of natural vegetation with a recurring physiognomy determined by its dominant life form.

Formation-type: A group of geographically widespread plant formations of similar physiognomy and occurring under similar environmental conditions.

Garrigue: An open shrubby vegetation of dry Mediterranean regions, consisting of spiny or aromatic dwarf shrubs interspersed with colourful ephemeral species.

Halophyte: A plant that grows naturally in a saline environment.

Hemicryptophyte: A herbaceous plant in Raunkiaer's life-form classification with perennating buds located at the soil surface, often protected by dead tissues.

Plant Life form: the characteristic form or appearance of a species at maturity.

Maquis: a shrubland biome in the Mediterranean region, typically consisting of densely growing evergreen shrubs.

Phanerophyte: A woody plant in Raunkiaer's life-form classification with perennating buds located more than 25 cm above ground, especially trees and shrubs.

Phrygana (Batha): Steppe is short, open treeless vegetation, with various proportions of bare ground, physiognomically dominated by perennial species. It also is the typical vegetation type of the Arid Zone of North Africa and extends into the Desert Zone.

Phytosociology: a branch of vegetation science that deals with current plant assemblages (communities) at a spatial grain size of vegetation stands.

Rangeland: Land on which the indigenous vegetation (climax or sub-climax) is predominantly grasses, grass-like plants, forbs or shrubs that are grazed or have the potential to be grazed, and which used as a natural ecosystem for the production of grazing livestock and wildlife. Rangelands may include natural grasslands, savannas, shrublands, many deserts, steppes, tundras, alpine communities and marshes.

Sabakha: are flat and very saline areas of sand or silt lying just above the water-table and often containing soft nodules and enterolithic veins of gypsum or anhydrite.

Therophyte: An herbaceous annual plant in Raunkiaer's life-form classification which survives unfavourable periods as seeds.

Wadi: A steep-sided, flat-floored stream channel in arid regions.

Xerophyte: A plant adapted to grow in arid places.